Clinical Applications of Neuromonitoring Following Acute Brain Injury

Leanne Alexis Calviello, B.A. M.Sc.

This dissertation is submitted for the degree of

Doctor of Philosophy

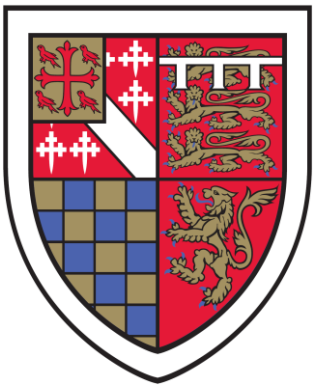

Supervised by Prof. Marek Czosnyka and Dr. Peter Smielewski

St. Edmund's College

University of Cambridge

July 2019

Preface

This dissertation is the result of my own work and includes nothing which is the outcome of work done in collaboration except as declared in the Preface and specified in the text.

It is not substantially the same as any that I have submitted, or, is being concurrently submitted for a degree or diploma or other qualification at the University of Cambridge or any other University or similar institution except as declared in the Preface and specified in the text. I further state that no substantial part of my dissertation has already been submitted, or, is being concurrently submitted for any such degree, diploma, or other qualification at the University of Cambridge or any other University or similar institution except as declared in the Preface and specified in the text.

It does not exceed the prescribed word limit for the relevant Degree Committee (60,000 words).

Leanne Alexis Calviello,

October 2019

Acknowledgements

This Ph.D. thesis is dedicated to my family, both living and no longer with us for the time being – I would never have imagined that I would have achieved any of this without your constant support, generosity, and love felt from thousands of miles away. You have encouraged me to pursue my passions in whichever order they appeared, expected me to challenge myself, and reminded me that there is always some grace to be found in making mistakes and asking for help. I am endlessly proud to be yours. I love you.

It would have been impossible for me to reach this point without having had the lifelong opportunity to surround myself with so many brilliant, talented, and inspiring friends. There is no greater joy than to watch you succeed. I cannot put into words just how much it means to me to be able to stand by your side, from any amount of physical distance. Your kind words, humor, wisdom, and continuous presence make me feel less alone wherever I choose to wander.

I would especially like to express my gratitude towards my supervisors, Professor Marek Czosnyka and Dr. Peter Smielewski, for their unlimited supply of personal and academic guidance during my time at Cambridge. To all of my Brain Physics and Neurosurgery colleagues, collaborators, and co-conspirators – your depth of expertise, patience, friendship, and enthusiasm for research are invaluable. Thank you for making me a part of your family.

Abbreviations

- **ABI** – Acute Brain Injury
- **ABP** – Arterial Blood Pressure
- **ABPd** – Diastolic ABP
- **AMP** – Fundamental Amplitude of ICP
- **ARI** – Autoregulation Index
- **a.u.** – Arbitrary Units
- **AUC** – Area Under the Curve
- **A_1** – Fundamental Amplitude of ABP
- **BRS** – Baroreflex Sensitivity
- **CA** – Cerebral Autoregulation
- **Ca** – Compliance of the Cerebral Arterial Bed
- **CaBV** – Cerebral Arterial Blood Volume
- **CBF** – Cerebral Blood Flow
- **CBFV/FV** – Cerebral Blood Flow Volume Velocity
- **CBV** – Cerebral Blood Volume
- **CFF** – Continuous Flow Forward
- **Ci** – Compliance of the Cerebrospinal Space
- **cm/s** – Centimeters Per Second
- **$CMRO_2$** – Global Cerebral Metabolic Rate of Oxygen
- **CNS** – Central Nervous System
- **CO_2** – Carbon Dioxide
- **COx** – Cerebral Oximetry Index
- **CrCP** – Critical Closing Pressure
- **CSF** – Cerebrospinal Fluid
- **CPC** – Cerebral Performance Category
- **CPP** – Cerebral Perfusion Pressure
- **CPP** – Mean CPP
- **CPP_{OPT}** – Optimal Cerebral Perfusion Pressure
- **CT** – Computed Tomography
- **CVR** – Cerebrovascular Resistance
- **DCM** – Diastolic Closing Margin
- **Dx** – Diastolic Component of the FV Waveform
- **EEG** – Electroencephalography

- **$EtCO_2$** – End-Tidal Carbon Dioxide
- **EVD** – External Ventricular Drain
- **F1** – Fundamental Frequency of CBFV
- **FVd** – Diastolic Flow Velocity
- **FVm** – Mean Flow Velocity
- **FVs** – Systolic Flow Velocity
- **GCS** – Glasgow Coma Scale
- **GOS** – Glasgow Outcome Score
- **HR** – Heart Rate
- **HRV** – Heart Rate Variability
- **Hz** - Hertz
- **ICP** – Intracranial Pressure
- **ICPm** – Mean ICP
- **kPa** - Kilopascal
- **MAP** – Mean Arterial Pressure
- **MCA** – Middle Cerebral Artery
- **mm Hg** – Millimeters of Mercury
- **MRI** – Magnetic Resonance Imaging
- **Mx** – Mean Flow Index
- **Mx_a** – Mean Flow Index Calculated with ABP
- **nCPP** – Non-Invasive Cerebral Perfusion Pressure
- **nICP** – Non-Invasive Intracranial Pressure
- **nPAx** – Non-Invasive Pulse Amplitude Index
- **nPRx** – Non-Invasive Pressure Reactivity Index
- **NIRS** – Near-Infrared Spectroscopy
- **ORx** – Oxygen Reactivity Index
- **$PaCO_2$** – Partial Pressure of CO_2 in Arterial Blood
- **PAx** – Pulse Amplitude Index
- **$PbtO_2$** – Brain Tissue Oxygenation
- **PET** – Positron Emission Tomography
- **PFF** – Pulsatile Flow Forward
- **PI/gPI** – Pulsatility Index
- **PRx** – Pressure Reactivity Index
- **RAC** – Autoregulation Index Derived from AMP and CPP Correlation

- **RAP** –Compensatory Reserve Index (Amplitude and Pressure Correlation)
- **ROC** – Receiver Operating Characteristic
- **s** – Time in Seconds
- **SAH** – Subarachnoid Hemorrhage
- **sPI** – Spectral Pulsatility Index
- **Sx** – Systolic Component of the FV Waveform/Systolic Flow Index
- **Sx_a** - Linear Correlation Coefficient between FVs and ABP
- **TAU/τ** – Cerebrovascular Time Constant
- **TBI** – Traumatic Brain Injury
- **TCD** – Transcranial Doppler Ultrasonography
- **THI** – Total Hemoglobin Index
- **TOI** – Total Oxygenation Index
- **WeightedICP** – Compensatory-Reserve-Weighted ICP
- **WT** – Vascular Wall Tension

Table of Contents

List of Tables

List of Figures

Summary

Various invasive and non-invasive cranial monitoring techniques can be applied clinically to describe the extent to which cerebral hemodynamics and subsequently, patient outcome, have been impacted following acute brain injury (ABI).

This Ph.D. thesis examines both prospective and retrospective patient data in both neurocritical and general intensive care patients. Thirty neurotrauma patients and forty general intensive care patients with neurological complications were prospectively monitored after ABI. Retrospective patient data was harvested from a database of 1,023 traumatic brain injury (TBI) patients with invasive intracranial pressure (ICP), arterial blood pressure (ABP), and transcranial Doppler ultrasonography (TCD) recordings. Data analysis focused on ICP microsensor accuracy, compensatory reserve, the pulsatility of brain signals (ICP and TCD), and cerebral arterial blood volume (CaBV) based on TCD. The main results are summarized below:

I. Intracranial hypertension has a profound negative influence on cerebrovascular parameters and patient outcome.
II. ICP microsensor accuracy is limited, with an average error of approximately ± 6.0 mm Hg.
III. ICP weighted with the compensatory reserve better predicts outcome than mean ICP alone.
IV. ICP and TCD pulsatility are functions of mean ICP and cerebral perfusion pressure (CPP).
V. Continuous blood flow forward (CFF) and pulsatile blood flow forward (PFF) models can approximate CaBV with derived TCD signals; CFF best models TCD pulsatility.
VI. The pressure reactivity index (PRx) and the pulse amplitude index (PAx) can be estimated non-invasively using slow waves of TCD estimated by CaBV with similar outcome-predictive power.

VII. Multi-parametric TCD-based monitoring of general intensive care patients is clinically feasible; the joint estimation of autoregulation, dysautonomia, non-invasive ICP, and critical closing pressure is possible.

The culmination of these projects should have an impact on current monitoring practices in ABI patients, emphasizing the continued validation and refinement of TCD methodology in clinical neurosciences.

Chapter 1

Working Hypotheses

The preservation of cerebral autoregulation is of critical interest to patients suffering from traumatic brain injury (TBI). TBI affects the balanced relationship between cerebral pressures and flows, often leading to complications such as intracranial hypertension or cerebral ischemia that may prove fatal if left untreated. Non-invasive cranial monitoring techniques can be applied clinically to describe the extent to which the injury has impacted cerebral hemodynamics and subsequently, patient outcome.

Transcranial Doppler ultrasonography (TCD) is considered to be a reliable "stethoscope" for the brain that is uniquely suitable to monitor cerebral hemodynamics in both acute vascular conditions and neurological disorders. Although TCD data is classically associated with the estimation of cerebral blood flow velocity, it can be further analyzed and adapted with the aid of dedicated neuromonitoring software to provide additional derived parameters that are of immediate clinical value in the prediction of patient mortality. Among these, five groups of parameters are of particular interest within the scope of this Ph.D. thesis: 1) cerebral autoregulation as described by the pressure reactivity index and the mean flow index, PRx and Mx, respectively; 2) non-invasive estimators of intracranial pressure (ICP) and cerebral perfusion pressure (CPP); 3) cerebral arterial blood volume (CaBV); 4) spectral pulsatility index (sPI); and 5) critical closing pressure (CrCP), wall tension (WT), and the diastolic closing margin (DCM).

Each of the above parameters expresses the likelihood of mortality following TBI, but their outcome-predictive power increases exponentially when used in conjunction to create a more complete cerebral hemodynamic profile for each patient. The body of this Ph.D. thesis applies a continuous multi-parametric approach to TCD monitoring in

neurocritical care, with a focus on the continued validation and refinement of this methodology in clinical neurosciences.

The three major aims of this thesis form the backbone of each of the three chapters outlining results (Chapters 4-6):

1. Describe the clinical indications of elevated intracranial pressure after traumatic brain injury.
2. Develop and understand new mathematical models that explore pulsatile cerebral hemodynamics in terms of cerebrovascular resistance and cerebral blood volume in both the time and frequency domains.
3. Apply non-invasive neuromonitoring techniques such as transcranial Doppler ultrasonography to both create alternatives to invasive monitoring and expand neuromonitoring principles to broader patient populations.

A review of contemporary literature is presented in Chapter 2, followed by an outline of the methodologies (Chapter 3) common to each of the seven studies relating to the aims of this thesis (Chapters 4-6). The final chapter (Chapter 7) provides a summary of the previous results chapters and identifies future directions for the research in this field.

1.1. Clinical Consequences of Elevated ICP

Intracranial pressure (ICP) monitoring is a crucial informative tool in neurocritical care. ICP is a reference pressure for cerebral blood flow (CBF). Intracranial hypertension and adequacy of brain blood flow are two main concerns following traumatic brain injury (TBI) It is well documented that elevated ICP (>20 mm Hg) after TBI increases the risk of poor outcome, independent of low cerebral perfusion pressure (CPP) or the severity of primary injury. However, all ICP sensors, irrespective of design, are subject to systematic and random measurement inaccuracies that can affect patient care if overlooked or disregarded. "Compensatory-reserve-weighted intracranial pressure (ICP)", named "weightedICP" for brevity, is introduced as a variable that may better describe changes leading to mortality after TBI over the standard mean ICP displayed by traditional sensors.

Hypotheses

- Elevated ICP affects cerebral autoregulation as assessed by both the pressure reactivity (PRx) and mean flow (Mx) indices. Elevated ICP will associate with a higher risk of mortality, as it exposes the brain to ischemic insults whenever CPP falls.
- All ICP sensors will be subject to measurement inaccuracies. In theory, the sensors with the most "acceptable" long-term measurement errors will be the ones incorporated into routine ICP management protocols.
- "WeightedICP" will be significantly associated with mortality after TBI, perhaps more so than mean ICP. This variable will be sensitive to both the rising absolute ICP and to the critical deterioration of pressure-volume compensation.

1.2. Modeling Pulsatile Cerebral Hemodynamics

The pulsatility index (PI) is suggested to describe various hemodynamic mechanisms, such as ICP and CPP modulation, as a function of cerebrovascular resistance. The determination of relationships between the TCD-based spectral pulsatility index (sPI) and pulse amplitude (AMP) of intracranial pressure in severe TBI patients exhibiting extreme physiology will support a previously-proposed model of TCD-based pulsatility. Mathematical modeling can further explain the underlying pulsatile component of cerebral arterial blood volume (CaBV). Data can be analyzed with either the continuous flow forward (CFF, moderately pulsatile blood inflow and steady blood outflow) or pulsatile flow forward through regulating arterioles (PFF, both blood inflow and outflow are pulsatile) modeling approaches to estimate the pulse component of CaBV. This way, clinical monitoring of changes in cerebral compartmental compliances becomes possible.

Hypotheses

- sPI will closely approximate both ICP and AMP, and will also signal to clinicians when a patient's CPP is approaching the lower limit of autoregulation. The sPI equation can be applied with confidence to extreme physiological conditions such as ICP plateau waves and unstable mean arterial pressure (MAP).
- TCD-based estimation of CaBV pulsations will appear feasible when employing the CFF modeling approach. Optimal CaBV estimation will properly outline the blood volume component of ICP, which may allow the implementation of targeted therapies for particular intracranial components contributing to elevated ICP.

1.3. Non-Invasive Neuromonitoring Applications

The advancement of non-invasive approximations of "traditional" invasive estimators of cerebral autoregulation (i.e. nPRx and PRx, nICP and ICP, nCPP and CPP, etc.) offers the potential to expand continuous neuromonitoring both within and outside of neurocritical care. These parameters can be calculated in real time on the basis of non-invasive TCD waveform analysis to predict patient outcome. TCD can also be utilized in conjunction with routine electroencephalography (EEG); joint consideration of cerebral electrical and circulatory activity is presumed to provide more thorough insight into brain health than isolated monitoring modalities. Multi-modal monitoring can potentially detect and track the evolution of secondary complications in a large variety of patients.

Hypotheses

- CaBV modeling principles can be expanded to the derivation of non-invasive equivalents of the outcome-predictive pressure reactivity index (PRx) and the pulse amplitude index PAx with slow waves of mean CaBV and its pulse amplitude (yielding nPRx and nPAx models).
- TCD-based monitoring analyses will return information about ICP (calculated non-invasively) and CPP that would otherwise be unavailable. For example, the application of Mx_a to general intensive care patients will generate models of cerebral autoregulation and outcome prediction

Chapter 2

A Practical Introduction to Neuromonitoring Following Acute TBI

The following publications formed the basis of this chapter:

- Calviello LA, Donnelly J, Zeiler FA, Thelin EP, Smielewski P, Czosnyka M. Cerebral autoregulation monitoring in acute traumatic brain injury: what's the evidence? *Minerva Anestesiologica*. 2017 Aug;83(8):844.
- Calviello LA and Czosnyka M. Neurocritical Care Monitoring in ICU: Measurement of the Cerebral Autoregulation by TCD. *NESCC Project*. 2018 September.
- Calviello LA, Zeiler FA, Donnelly J, Smielewski P, Czigler A, Lavinio A, Hutchinson PJ, and Czosnyka M. Cerebrovascular Consequences of Elevated Intracranial Pressure after Traumatic Brain Injury. *Neurocritical Care. In Review.*

Cerebral autoregulation is considered to be the vascular self-regulatory mechanism that maintains a constant balance between cerebral blood flow and variations in blood pressure. Governed by interactions between various biophysical processes, autoregulation functions as a shield from the potential damages caused by unexpected fluctuations in pressures and/or flows. Autoregulation may be compromised following acute or traumatic brain injuries (ABI or TBI), potentially leading to an unfavorable outcome for the patient if left untreated.

Despite its complexity, autoregulation can be quantified non-invasively with the aid of transcranial Doppler ultrasonography (TCD) or interpreted as mathematically-

derived indices based on commonly-monitored input signals such as arterial blood pressure (ABP) and intracranial pressure (ICP) that yield outcome-predictive indices such as the pressure reactivity index (PRx). Although these autoregulatory indices are primarily surrogate markers of cerebral hemodynamic activity, they have been robustly correlated with patient outcomes.

This chapter seeks to explain the methodology behind the calculations of various measures of autoregulation, and how these indices affect clinical outcome prediction modeling. A comparison of relevant methods of the assessment of autoregulation and their respective relationships with outcome are listed in Table 2.1, with: PRx, mean flow index (Mx), NIRS-based spatially-resolved indices, and brain tissue oxygenation ($PbtO_2$) -based oxygen reactivity index (ORx) highlighted. Finally, the advantages and disadvantages of each parent monitoring device are outlined in Table 2.2.

2.1. Overview of Cerebral Autoregulation

Cerebral autoregulation is the inherent capability of the brain to regulate cerebral blood flow across a range of blood pressures within the cranial cavity[1]. It is a protective mechanism for the brain that enables it to withstand dynamic changes; however, TBI often disrupts this process and leaves the brain in a state of "dysautoregulation" that can prove fatal if left untreated[2].TBI is commonly attributed to events such as blunt force, falls, or motor vehicle accidents that result in a decrease or loss in consciousness, memory deficit, or neurological and/or mental state alterations such as weakness or disorientation[3]. However, the appearance of injury severity is not the decisive factor in determining the ability of the brain to recover its disposition towards this protective mechanism[1]. Moderate to severe TBI cases (i.e. cerebral hemorrhages or contusions) are generally easier to diagnose with imaging techniques such as magnetic resonance imaging (MRI) and computed tomography (CT) than are mild TBI cases, but standard scoring criteria for both cannot be determined as absolute predictors of the damage sustained by the cerebral autoregulatory reserve following the initial insult[4].

2.1.1. Physiological Drivers of Cerebral Autoregulation

The loss of autoregulation is theorized to be a multifactorial event process. Cerebral structural integrity can be compromised by injury, leading to the scrambled communication between metabolic demand and delivery pathways to the brain via blood vessels, or this can occur in the reverse order[1]. Autoregulation has previously been described as a delicate balancing act between vasoconstriction and vasodilation as the resistance of the cerebrovascular bed adapts[5,6] to both sudden and slow dynamic changes in cerebral perfusion pressure (CPP), a product of the difference between ABP and ICP.

Arterial Blood Pressure

Cerebrovascular tone has long been observed to fluctuate along with changes in ABP; cerebral vessels constrict as ABP rises, and dilate when ABP drops[7]. The quantity of blood flowing through the cerebral arteries is thus directly affected by any changes in ABP. In acute brain injury, the homeostatic mechanism governing cerebral autoregulation can become disturbed. In order for cerebral autoregulation to be considered "intact", ABP must be independent of the cerebral circulation and at a value that is neither too high (predisposing the patient to edema or hemorrhage) nor too low (predisposing the patient to cerebral ischemia)[8,9]. In Figure 2.1 (below), autoregulation is preserved at mean arterial pressures (MAP) of 50-150 mm Hg, and CBF at about 50 ml/100 g brain tissue/minute[8]. In hypertensive patients, this range moves towards higher values, with the placement of the curve shifting towards the right, whereas the converse occurs in hypotensive patients[10]. A passive relationship between ABP and cerebral blood flow (CBF) is indicative of poor prognosis.

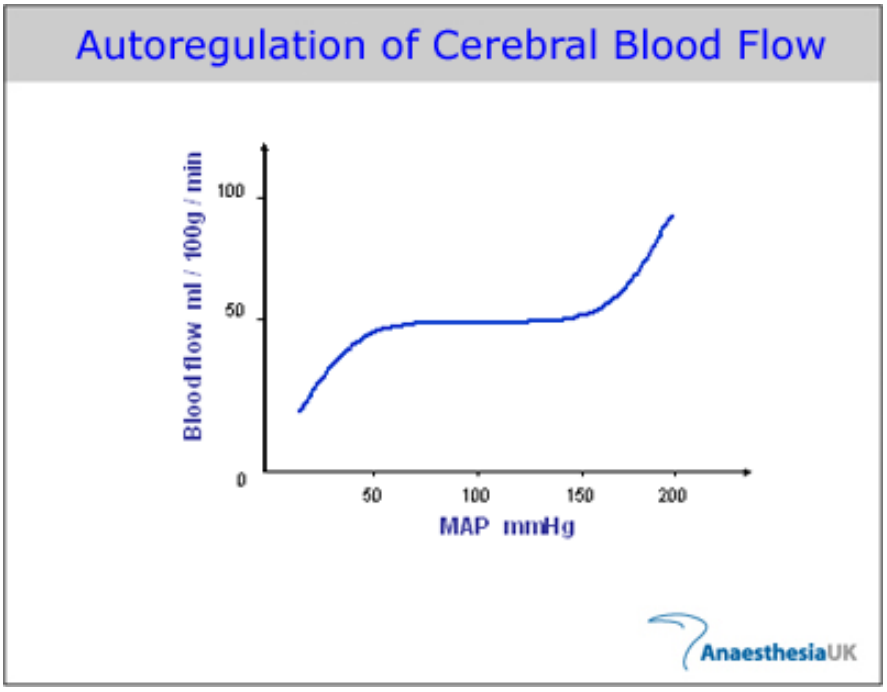

Figure 2.1. **Autoregulation of Cerebral Blood Flow**. Cerebral autoregulation is preserved at (MAP) or 50-150 mm Hg, and CBF at about 50 ml/100 g brain tissue/minute.

Intracranial Pressure

Perhaps the greatest risk factor for poor patient outcome is sustained, high values of intracranial pressure (ICP), which dangerously strain cranial volumetric capacity and can produce irreversible damage[11]. According to the Monro-Kellie doctrine, ICP is comprised of four separate components: arterial blood inflow and venous blood outflow (both of which contribute to cerebral blood volume, CBV), cerebrospinal fluid (CSF), and a fixed brain volume[12]; in a healthy system, when one component increases, the others should decrease to accommodate for this change in order to maintain a constant value. In TBI patients, ICP is often abnormally elevated, requiring aggressive clinical intervention to maintain perfusion and prevent brain herniation. These interventions include the use of sedative agents and vasopressors, head positioning, CSF drainage,

osmotherapy, surgical evacuation or decompression, and targeted temperature management[11].

Intracranial compliance is characteristically reduced in patients with intracranial hypertension, meaning that patients with elevated ICP are at risk of further significant spikes in ICP even in response to minor volume changes of intracranial blood and CSF or brain swelling. Low CPP inversely correlates with increased ICP, predisposing the injured brain to hypoxia until it triggers the ultimately deadly trifecta of "mechanical compression, displacement, and herniation of brain tissue"[13]. Invasive ICP monitors are essential to the diagnosis and treatment of high ICP; however, initial values of ICP (determined on admission) are poor predictors of outcome, particularly in those with mass lesions[14]. There is a bilateral, causal relationship between brain damage and high ICP. Intracranial hypertension (sustained values of ICP >20 mm Hg) unfolding over a period of days can progressively alter the brain's ability to adapt its cerebral structural and volumetric reserves[15] to maintain a reasonable degree of function. In survivors, the long-term effects of persistent neuroinflammation and chronic structural degeneration can dramatically increase the risks of depression, susceptibility to cognitive loss and dementia, or accelerated rates of brain atrophy[3].

2.1.2. Systemic Regulation of Vessel Caliber

Additionally, metabolic, endothelial, myogenic, and neurogenic factors have each been theorized to lead the regulation of vessel caliber. To date, it is unclear which of these mechanisms predominate in the control of cerebral arterial vessel caliber[16]. The metabolic theory postulates that byproducts of cerebral metabolism lead to alterations in vessel diameter. However, the changes in extra-cellular metabolic byproducts is relatively slow in relation to the rapid response of the cerebral vasculature, thus it may not be integral in autoregulatory control[16].

Endothelial factors, such as nitric oxide synthase (NOS) and endothelin (ET), are expressed as a function of the flow-related stresses encountered by the endothelium. It

is plausible to consider these endothelial mediators as potential key players in preserved and deranged autoregulatory states[16].

Myogenic autoregulatory theories revolve around the concept of flow-related stress on the vascular smooth muscle, leading to reflexive changes in vessel diameter secondary to varied smooth muscle tone[16]. Both myogenic and endothelial mechanisms probably overlap, forming one reflex, known as autoregulation: CBF remaining independent despite changes in cerebral perfusion pressure[1].

Finally, the neurogenic hypothesis focuses on neurotransmitter-mediated changes in vascular tone, which are believed to stem from fluctuations in sympathetic or parasympathetic output to the tunica media[16]. One or more of these mechanisms may be the driver(s) of autoregulatory control, and are likely subject to derangements depending on the individual host response to injury during various neuropathologic conditions[1,16].

2.2. Clinical Applications of Cerebral Autoregulation

To provide the greatest and the most reliable amount of clinical information, neurocritical care professionals have increasingly been focusing their attention on non-invasive, bedside multi-modal brain monitoring in conjunction with traditional imaging techniques. Prediction of patient outcome in adult TBI is difficult; primarily correlational assessment methods of surrogate markers are relied upon for investigation into autoregulation (i.e., pressure reactivity index (PRx), mean flow velocity (Mx), oxygen pressure reactivity index (ORx), etc.). One of, if not the most, popular methods of non-invasively assessing cerebral autoregulation comes in the form of TCD, which can detect irregularities in cerebral blood flow[2], providing diagnostic value for secondary insults like cerebral vasospasm. TCD is applied to the middle cerebral artery (MCA), which is considered the primary conduit for the cerebral circulatory system and is assumed to have a constant diameter[1]. Ultrasonic penetration of the MCA returns a pulse wave spectrum that can be immediately visually classified as either normal or

abnormal (i.e. vasospastic[17], and can be further analyzed to provide more in-depth information about the state of cerebral autoregulation.

Residual autoregulatory capacity is then described by TCD as "either the speed or the direction of changes" of flow velocity in the face of fluctuations in arterial blood pressure[17]. Figures 2.2A and 2.2B demonstrate the effects of variable ABP and ICP on blood flow velocity in animal models using TCD[11,18].

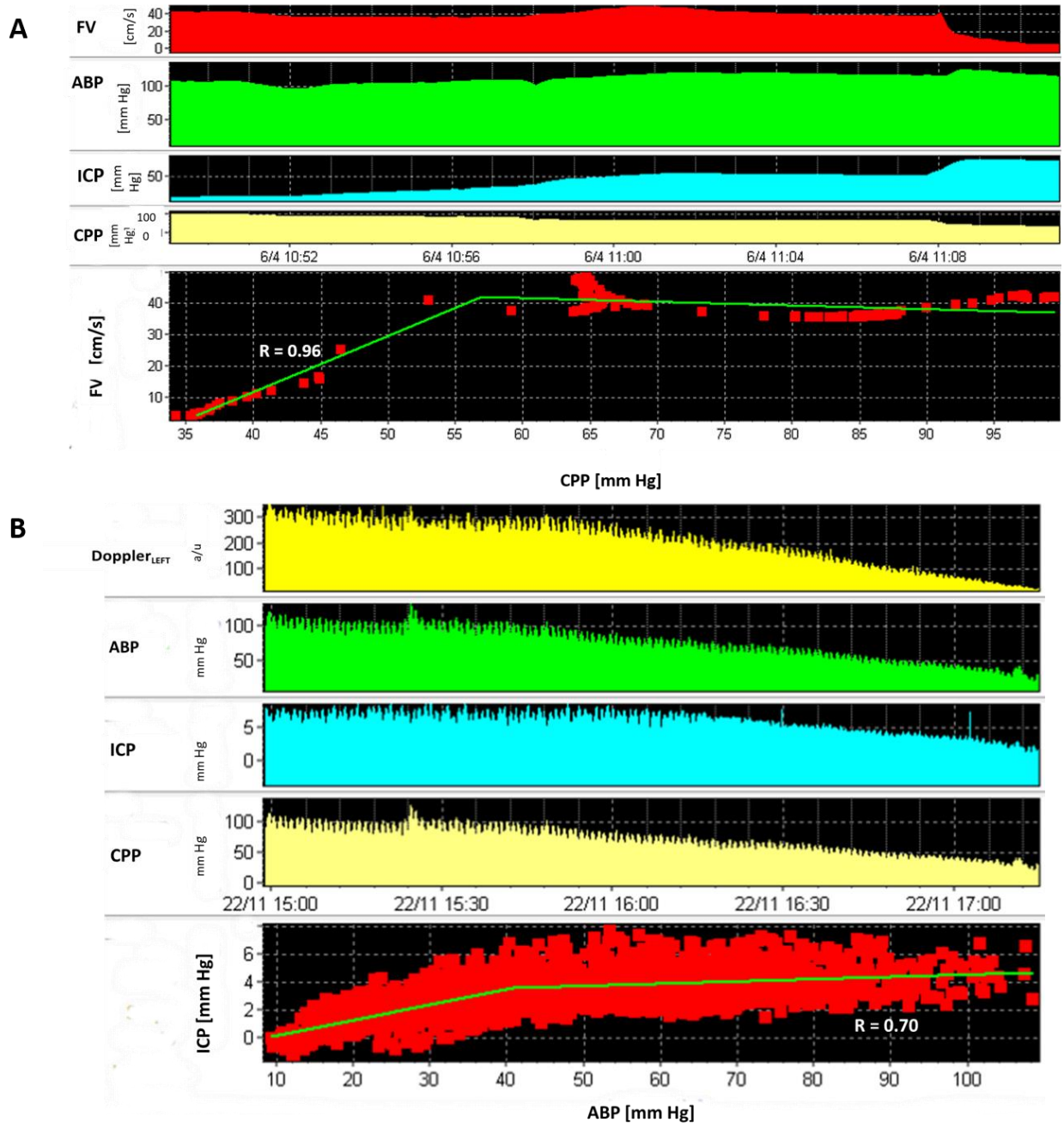

Figure 2.2. **Graphs over time highlighting (top to bottom) pressure-passivity of the cerebrovascular bed in animal models**. A) FVx, ABP, ICP and CPP over a 20-minute recording period in New Zealand white rabbits being subjected to intracranial hypertension. There is a robust correlation (R=0.96) between FVx and CPP below the lower limit of autoregulation[11]; B) Doppler flow, ABP, ICP, and CPP during a 2-hour recording period in piglets with induced arterial hypotension. ICP and ABP are strongly-correlated below the lower limit of autoregulation (R=0.70), again demonstrating pressure-passivity with decreasing ABP accompanied by decreasing ICP[19].

FVx: middle cerebral arterial flow velocity; ABP: arterial blood pressure; ICP: intracranial pressure; CPP: cerebral perfusion pressure; mm Hg: millimeters of Mercury.

2.2.1. Transcranial Doppler as a Technique

TCD is the most-validated technique for non-invasively measuring the velocity of the blood flowing through cerebral arteries; Doppler ultrasonography reflects the rate of change in the frequency of sound waves perceived by an observer moving relative to the wave source [1,20–27]. The "traditional" TCD instrument used in neurocritical care centers (such as the Multi Dop X4, DWL Elektronische Systeme, Sipplingen, Germany) features a headframe that is inserted into the patient's ears, supporting bilateral 2 MHz probes that are fixed onto the temporal window (located above the zygomatic arch) in order to insonate the MCA[28] (Figure 2.3). Once in place, a high-frequency ultrasonic beam is transmitted that penetrates the skull, commonly at a depth of 50-60 mm, to return the Doppler spectra from the artery on accompanying software[29] (Figure 2.3). This waveform demonstrates the systolic, mean, and diastolic values of the cerebral blood flow velocity (FV), which can be further examined individually in detailed studies of outcome prediction[27]. FV in healthy subjects has been previously determined to perfuse at a rate of 62 ± 12 cm/s, and was found to be nearly symmetrical between the left and the right branches of the MCA[29].

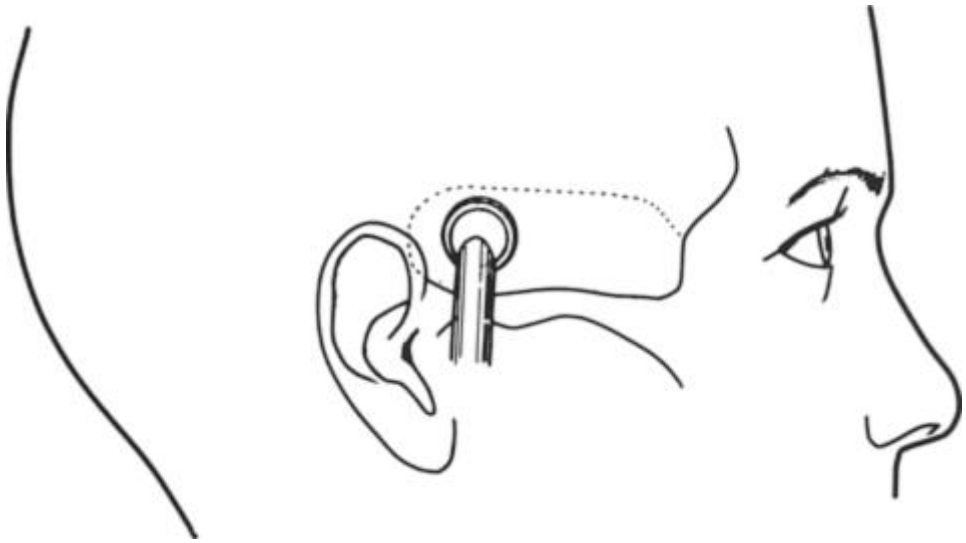

Figure 2.3. **Transcranial Doppler Device Operation**. Diagram of the area (dotted line) where Doppler signals from intracranial arteries were obtained[29]. The zygomatic arch is indicated. The most likely location to obtain signals is shown by the position of the probe.

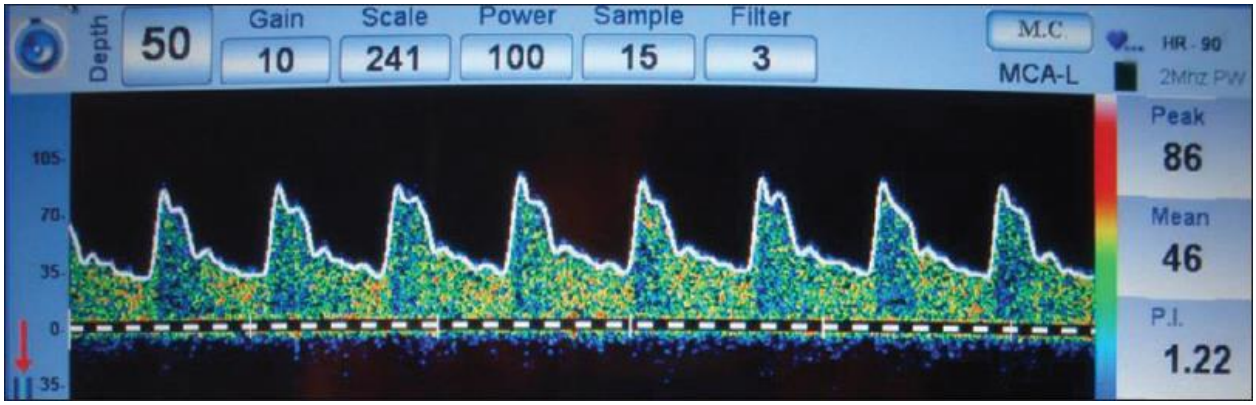

Figure 2.4. **Transcranial Doppler Signal Acquisition**. The transcranial Doppler waveform showing [the] middle cerebral artery, identified by the characteristic tracing in [the] upward direction[30].

TCD can be highly instrumental in the prediction of secondary insults and/or complications of TBI. For example, TCD-based FV can be indicative of vasospasm (the narrowing of a vessel accompanied by MCA flow >120 cm/s) following subarachnoid hemorrhage (SAH)[17]. Routine monitoring sessions are undertaken daily for an average duration of about 30 minutes. TCD devices can be connected to bedside monitors that provide invasively-quantified clinical information, such as ABP, ICP, and CPP. Employing dedicated neuromonitoring software such as ICM+™ (Cambridge Enterprise, Ltd.), day-to-day comparisons of FV are often utilized alongside these parameters to assess both short- and long-term trends with respect to the patient's autoregulatory status (Figure 2.4)[1,2].

2.2.2. Transcranial Doppler as a Clinical Informant

In addition to FV, TCD yields several descriptive parameters that paint a broader picture of cerebral autoregulation. The pulsatility index (PI), a measure of distal cerebrovascular resistance to flow[28], can be calculated as the difference between systolic and diastolic FV divided by mean FV over one cardiac cycle. TCD-based FV can also be compared against readily-available clinical information from bedside monitors (i.e. ABP, ICP, CPP, etc.) to provide distinctive correlational assessments of surrogate markers of cerebral autoregulation, such as the pressure reactivity index (PRx) or the mean flow index (Mx) within ICM+™ (Figure 2.5, below)[1]. The dynamic autoregulation index (ARI) demonstrates the interactions between non-invasive TCD and standard invasively-quantified measurements to produce a graded score of cerebral autoregulation. Analyses of these parameters are increasingly becoming a part of clinical practice and represent the patient's autoregulatory reserve at any observed timepoint [2].

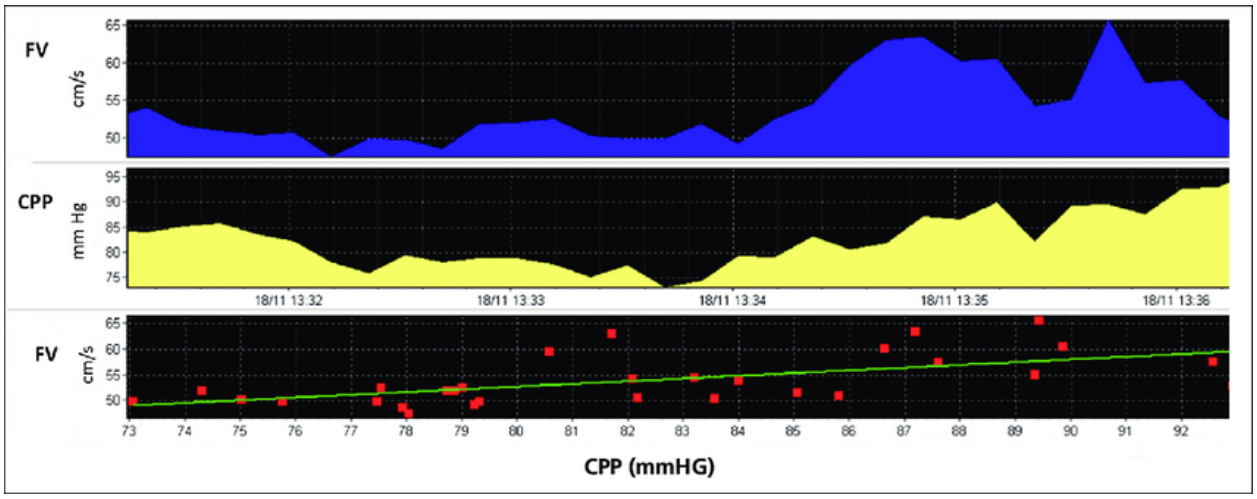

Figure 2.5. **Dynamic Changes in Flow Velocity and Cerebral Perfusion Pressure**. Captured during a transcranial Doppler recording for a single TBI patient over 5 minutes. Cerebral autoregulation can be approximated by a calculation of Mx from the correlation coefficient between mean FV and CPP, here the Mx value is positive (0.73), denoting disturbed autoregulation).

MCA: middle cerebral artery; FV: flow velocity; CPP: cerebral perfusion pressure; Mx: mean flow index; mmHg: millimeters of Mercury.

Autoregulation Index (ARI)

The concept of creating a holistic TCD-based autoregulatory index was first developed by Aaslid et al.[32] to assess the dynamic changes in cerebral autoregulation that occur following step-changes in CPP. By manipulating ABP in decrements of 20 mm Hg via thigh-cuff deflation, the rapid physiological response (or lack thereof) of the cerebral blood supply to these fluctuations in ABP is examined as a predictor of autoregulatory capacity. This experimental setup was revisited by Tiecks et al.[33], who collected FV and ABP values following the thigh-cuff release to calculate a graded reference index (ARI – the index of autoregulation) that would describe the

cerebrovascular resistance (CVR) as a function of ABP. ARI effectively answers the question of whether cerebral blood flow moderates itself appropriately when ABP

varies[2]. Plotting FV against the elapsed time from the initial thigh-cuff release, a series of 10 best-fit template models is generated through transfer function analysis[34,35]; increased steepness in these curves highlights a greater reservoir of cerebral autoregulation, where an ARI of 0 indicates pressure-passivity and an ARI of 9 indicates optimal autoregulation (Figure 2.6). In patients suffering from TBI or other cerebrovascular diseases such as stroke, ARI is lower than it would be in a healthy population (ARI <5)[35].However, this primarily visual assessment method is susceptible to bias, as strict observer standards are not in place and the quality of curve-fitting can vary[34].

The validity of ARI to mirror dynamic changes in cerebral autoregulation was further examined by Panerai et al.[34] via Monte Carlo simulations that mimed random input and output signals of both FV and ABP over a 5-minute interval. As transfer function analysis is crucial to the calculation of ARI, the strength of the index is tied to its spectral components[34,36]. ARI's utility to gauge patient outcome is limited if the recorded signals have a low signal-to-noise ratio. For each harmonic, the amount of output power that can be linearly explained by the input power is expressed by the squared coherence function. A coherence of 1 for pure, univariate systems is indicative of a high signal-to-noise ratio, whereas a coherence at or near 0 represents the latter[34,36] The phase shift between the Fourier components of both the input and the output signals reflects the "interdependence" of FV and ABP, with a positive phase shift (optimally 90°) revealing the presence of an intact, non-passive autoregulatory reserve[36–38]. When applied to the Glasgow Outcome Score (GOS), a lower ARI is compatible with GOS 1 or 2 (unfavorable outcome), whereas a higher ARI implies the converse, GOS 3-5 (favorable outcome)[36]. However, ARI is less sensitive when discriminating scores along the lower end of its 0-9 scale, and is largely dependent on how accurately the template model[33,39] matches the individual physiological events captured by TCD and ABP monitors.

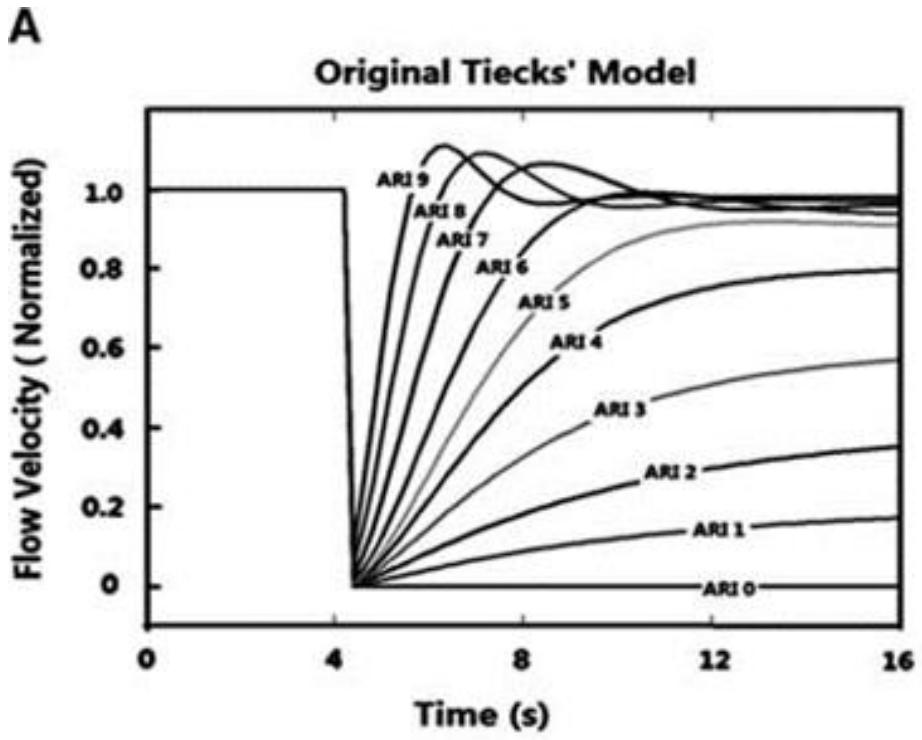

Figure 2.6. **Tiecks' Model of Autoregulation.** An example[36] of Tiecks' model, demonstrating the ARI curves scaled from 0-9. An ARI score of 9 is indicative of optimal cerebral autoregulation.

Mean Flow Index (Mx)

The mean flow index (Mx) is derived from the linear correlation coefficient between mean FV and CPP[40,41]; this marker of cerebral autoregulation is fundamentally dependent on non-invasive TCD monitoring data as opposed to invasive parameters (i.e. ABP and ICP). A central tenet to the success of Mx as a surrogate for the autoregulatory reserve is the assumption that the diameter of the MCA remains constant, which has yet to be either proven or disproven[41]. As the first 48 hours of admission are crucial to the recovery of autoregulation after TBI[1], TCD and

subsequently Mx can assess this rather easily; values of Mx less than or equal to 0 are representative of an intact autoregulatory reserve in which FV actively responds to changes in CPP, whereas positive Mx trends state the opposite[40]. Overall patient outcome (dichotomized into "favorable" and "unfavorable" outcomes) appeared to be largely affected by positive values of Mx within this timeframe, regardless of whether Mx "recovered" to negative values during the patient's course of stay. Figure 2.5, above, provides an example of a patient with disturbed autoregulation, as assessed with Mx.

Lang et al.[26] used Mx with TCD to gauge autoregulation in a cohort of TBI patients. Recalling that Mx is a continuous measure of slow, spontaneous changes in CPP and cerebral blood flow volume (CBFV) applied for the examination of MCA blood flow regularity[26], this research group attempted to produce the same results with Mx values derived from each of the separate input signals of ABP and CPP. Despite revealing a non-significant difference between the discriminatory powers of these two input signals, Lang et al.[26] cautioned that Mx as a function of CPP necessitates invasive ICP data collection to produce CPP calculations, whereas Mx as a function of ABP does not. As non-invasive measures of autoregulatory status are prioritized, it seems much more likely for Mx derived from ABP as the input to become a routine TCD index than would its counterpart when invasive monitoring is undesirable. However, in a more recent study in a larger cohort of patients (n=288), Liu et al.[36] compared Mx derived from both ABP and CPP in outcome prediction, finding CPP to be the superior input signal.

However, the time-domain calculation of Mx itself does not rely entirely on non-invasive data collection to express autoregulatory reserve; once again, CPP is the difference between ABP and ICP, making Mx somewhat dependent on ICP fluctuations as a result. Lang et al.[26] attempted to attain Mx with two separate input signals: CPP and ABP, the latter rendering the parameter to be quantifiable with non-invasive measures. Although possible to use, Mx determined from ABP is not as sensitive as Mx determined from CPP[36]. Continuing the search for an entirely non-invasive Mx function, Budohoski et al.[27] cited correlations between the systolic (Sx), diastolic (Dx), and mean (Mx) components of the FV waveform when using the input signals of either ABP or CPP. Separate analyses yielded the same result: Mx calculated with CPP is the superior predictor of functional patient outcome[1,27].

2.2.3. Benefits and Limitations of Transcranial Doppler

TCD is an important tool to have in neuro-critical care units. It is inexpensive, portable, and relatively simple to use once trained in how to do so. TCD examinations are as accurate as magnetic resonance imaging (MRI) when assessing vascular pathology[42] and do not require patients to be moved to imaging suites. Additionally, TCD devices can be paired with clinical monitoring software such as ICM+™ (Cambridge Enterprise, Ltd.) to return pertinent information about a TBI patient that cannot be gleaned from bedside monitors. Without TCD and dedicated analytical platforms such as ICM+™, mortality and functional outcome could not be determined on the basis of one or two functions (ARI is a more robust predictor of mortality than Mx, but the latter is more sensitive to functional outcome[36,40,43]). The benefit of both ARI and Mx is that they assign scalar value to cerebral autoregulation to the "weighted spatial averages as seen from the aspect of the MCA"[44] when employing the TCD monitoring technique.

Additionally, although PRx and Mx have both been used to describe different components of the autoregulatory mechanism and it has been suggested that Mx is a better predictor of functional outcome than of mortality[43,45], PRx is more discriminatory for survival versus mortality); however, both demonstrate U-shaped curves when plotted against CPP and are directly responsive to alterations of ICP[46]. High values of Mx and PRx insinuate the inability of the cerebral vasculature to regulate cerebral blood flow as measured by either of these parameters[47].

Although there is a shortage of "autoregulation markers"[20], the above surrogates (ARI, Mx, PRx) can technically be monitored continuously, as their respective values can be repeatedly calculated over any specified time period during the patient's neuro-intensive care stay. The utility of TCD was further affirmed by Panerai et al.[42], who compared the quality of the measurement to the sensitivity of gradient-echo MRI sequences as a marker of blood flow velocity changes attributable to injury and pathology in patients suffering from acute ischemic stroke. Therefore, they can be reported in the same fashion as ABP and ICP.

Despite this important point, TCD, and thus its derived parameters, are only intermittently affixed to the patients (<1 hour) due to the relative "clumsiness" and potential disruptiveness of the instrument to routine nursing interventions (i.e. turning the patient, preparing the patient for an x-ray or scan, etc.). TCD is primarily viewed as a research tool and is treated as an accessory to the patient; for example, it is nearly impossible to retain a stable probe position if a patient is being re-positioned or examined, as nurses are not obligated to be vigilant over the TCD recording session itself. TCD's time dependence only permits clinicians to receive "snapshots" of cerebral hemodynamic activity[1]. Another drawback of TCD is its reliance on operator validity[25]; even experienced technicians may not agree on the probe placement, depth of the MCA, etc. The relative strengths and limitations of TCD-based assessments are detailed further in Table 2.2. If the diameter of the MCA was ever to be proven variant, the core of TCD monitoring technology and thus its credibility would be undermined.

2.2.4. Invasive Alternative Techniques to TCD

PRx, and subsequently, outcome, is affected by interrelationships between such parameters as MAP, ICP, and CPP[46] that cannot be described non-invasively with TCD. These components need to be controlled to drive minimal values of PRx, as appropriate vessel diameter modifications spurred by vascular smooth muscle cells ensure the protection of the brain[45,47]. However, emerging evidence indicates that PRx may be affected by many other factors including red blood cell transfusion[48], alterations in temperature[49], or arterial glucose concentration[50].

In addition to PRx, near-infrared spectroscopy (NIRS) and brain tissue oxygenation ($PbtO_2$) are common alternatives to operator and time-dependent TCD recordings. Although invasive in nature, these techniques can be utilized outside of dedicated research environments, and thus are perhaps more likely to become clinically-accepted descriptors of cerebral autoregulation.

Pressure Reactivity Index (PRx)

The PRx is calculated as the moving linear correlation coefficient between MAP and ICP, from 30 consecutive samples binned into 10-second data windows[40]. PRx values at or below 0 reflect intact autoregulatory reserves. PRx values above 0 indicate the increasing passivity of the cerebrovascular bed, in which variations in arterial blood pressure directly influence increases or decreases in ICP. This inability of the brain to discriminate the ABP and ICP input, and to mediate vasoconstriction or vasodilation accordingly, is a predictor of poor outcome. Ideally, in the attempt to preserve cerebral autoregulation, these indices

should not be co-dependent, as cerebrovascular passivity intimates a global autoregulatory disturbance. The utilization of computerized ABP and ICP monitoring to produce the PRx as a correlation coefficient has shown to be a robust predictor of outcome following rises in ICP. Sorrentino et al.[21] described critical values of PRx that maximized the difference between patients who died (PRx =0.25) and those with a more favorable outcome (PRx =0.05).

The inherent capacity for this neuroprotective mechanism deteriorates with age[51], but is especially compounded by TBI[40]. The age of patients may serve as a predisposition to secondary insults, with natural aging processes affecting the reactivity of the cerebrovascular bed[51]. The impaired state of the brain after injury makes it even more vulnerable to and uncompromising with sudden changes in ICP and CPP[52]. For example, large reductions in CPP lead to arteriolar dilations, which in turn decrease cerebrovascular resistance, and vice versa[53]. Therefore, the elderly TBI population may be more vulnerable to secondary brain injuries caused by reductions in CPP.

Interactions of PRx with Cerebral Metabolic Factors

In combination with CPP, $PbtO_2$ is theorized to act as a surrogate marker of cerebral blood flow, taking tissue oxygenation pressure into account[54]. Disturbances in cerebral blood flow after severe head injury directly contribute to the brain's inability to adjust vessel diameter in response to transmural pressure demands. Microdialysis can aid in the detection of TBI-mediated cerebral metabolic changes. Common markers include glucose, lactate, pyruvate, glutamate, glycerol, and the lactate/pyruvate ratio. The relative concentrations of these parameters are associated with outcome. For instance, Timofeev et al.[55] quantified the lactate/pyruvate ratio as a surrogate marker of cerebral metabolism, showing that higher values (>25) reflect an independent association with patient mortality attributable to either mitochondrial dysfunction or a lack of oxygen supply in the brain.

Further assessment of these additional factors' effects on PRx can be useful in outcome prediction. Steiner et al.[56] questioned the role of cerebral metabolic dysfunction in suboptimal PRx, and subsequently, outcome. The global cerebral metabolic rate of oxygen ($CMRO_2$) was hypothesized to play a role in the incidence of dysautoregulation explained by PRx that could prime patients for secondary insults to the brain (i.e. ischemia, hyperemia, etc.). Ang et al.[57], posited similar oxygen disturbances in lesioned tissue as evidence of autoregulatory failure. An inverse relationship between $CMRO_2$ and PRx was determined, but the effects of the two could not pinpoint the underlying causes of poor

outcome, or the dynamics and concentrations of blood in the lesioned part of the brain. Autoregulatory status is important for neuro-intensive care management. Autoregulation depends on CPP to balance cerebral blood flow and cerebral metabolism[56]. Elevated CPP can predispose patients to cerebral metabolic failure (demonstrated by decreased $CMRO_2$), and thus can potentially drive autoregulatory failure. However, there is currently no data available to firmly suggest that changing local metabolics would lead to improved autoregulation, although support for the theory that metabolic derangements are associated with unfavorable PRx is leant by the work of Timofeev et al.[55]. It remains to be proven that cerebral metabolic alterations will influence patient outcome; for example, $CMRO_2$ signal decreases may be a downstream consequence of autoregulatory failure [56].

Application of PRx toThe Monitoring of Optimal Cerebral Perfusion Pressure (CPP_{OPT})

The autoregulatory response to CPP changes has been demonstrated within the physiological boundaries of 50-100 mm Hg, with some studies showing evidence of CPP values above this upper bound[22,58]. Drastic CPP variations after TBI can greatly affect a patient's chances of survival, and additionally, functional outcome[5]. The progressive failure of autoregulation with falling CPP can predict the incidence of secondary, potentially intractable insults to the brain such as delayed cerebral ischemia, vasospasm, etc. However, increasing CPP past a "safe" range could lead to hyper-perfusion (current guidelines stipulate that CPP should rest between 60-70 mm Hg) which has been associated
with risk of edema or leakages through the blood-brain barrier, as well as potential cardiac or respiratory distress[59].

To simplify cerebral vasoreactivity as a direct measure of pressure and flow, it is perhaps best to explain it by its relationship with CPP[60]. PRx is the regression between ICP and MAP, and CPP is the difference between arterial blood pressure and ICP. PRx has been used to derive an optimal CPP (CPP_{OPT}) in traumatic brain-injured patients[5]. CPP_{OPT} is determined from the lowest PRx value plotted against all of the CPP values

within a recorded period (usually 4 hours). This often results in a simple-to-comprehend U-shaped curve in which CPP_{OPT} is the minimum value found at the base of the curve (Figure 2.7). On the further suggestion of Steiner et al.[61] with CPP_{OPT} determined as the lowest-measured plotted average of PRx trends, it may be sensible to continually direct patient management towards 0 or negative values in accordance with CPP_{OPT} treatment protocols based on pressure autoregulatory capacity[53,54,62].

Yet, individualized CPP_{OPT} values may not be contained within the boundaries of 60-70 mm Hg, as evidenced by Figure 2.7, which features a CPP_{OPT} value at 91.14 mm Hg. Some patients may achieve a more stable PRx at CPP_{OPT} above or below the advised "safe" range, an observation which has led research to examine the benefits of CPP_{OPT} therapies that are separately tailored to each patient, to reduce incidences of secondary injuries across the board[17,23,53,56]. A recent systematic review conducted by Needham et al.[5] reaffirms the importance of safeguarding against mortality by treating each patient in accordance with his or her individually-determined target CPP_{OPT} to maximize cerebrovascular reactivity.

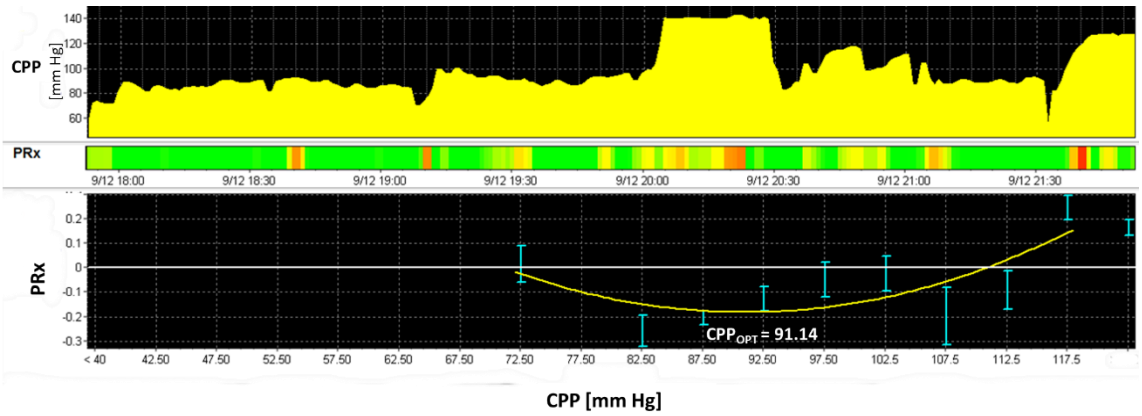

Figure 2.7. **Determination of CPP_{OPT}**. An example[1] of CPP derived from PRx obtained from a single patient over a monitoring period of approximately 4 hours. The green, yellow, orange, and red bars of PRx respectively represent a spectrum of favorable to unfavorable PRx during the observation. These values of PRx are plotted against CPP, with the minimum value of the curve declared CPP_{OPT}. In this particular patient, CPP_{OPT} is equivalent to 91.14 mm Hg.

PRx: Pressure Reactivity Index; CPP: cerebral perfusion pressure; mm Hg: millimeters of Mercury.

Criticisms of PRx

The original definition of PRx functions as a descriptor of "graded loss of autoregulation"[61], raising the question of whether it is possible to incorporate PRx into CPP management protocols, yielding an autoregulatory therapy (perhaps indexed as PRx_{OPT}). Steiner et al.[61] assessed the effect of time on PRx and posited that disturbed PRx (reported as PRx >0.2) for a period of six hours was a strong predictor of patient mortality. Corresponding CPP values during these observations were analyzed for deviations from calculated CPP_{OPT}, however, CPP_{OPT} was unable to be defined in some cases, demonstrating that autoregulation-oriented therapy is difficult to implement because it is nearly impossible to guarantee the consistency of curve-fitting between surrogate measures of autoregulation. CPP_{OPT} fundamentally requires an index of vascular reactivity for its calculation, in addition to high-frequency data examined every four hours to create time points[63]. Table 2.2 provides an in-depth description of the strengths and limitations of PRx and other continuous autoregulatory indices.

Aries et al.[64] similarly found an obstacle to the design of PRx-guided therapy, stating that the fundamental calculation of PRx as a function of arterial blood pressure and intracranial pressure assumes that the vacillations of cerebrovascular resistance are coupled with those of cerebral blood volume, inducing the direction of ICP towards higher values when intracranial compliance is low, and vice versa. The necessity of this pairing is problematic for independent models of PRx-guided therapy protocols, as PRx is a "noisy" derived index requiring a higher signal-to-noise ratio and time-domain analysis[64]. To counter this, Aries et al.[64] put forth the proposition of PAx (the index of the intracranial pressure waveform amplitude) as a modification of PRx that is "potentially independent" of ICP fluxes that could affect the validity of PRx as a true measure of autoregulation[65].

Finally, the plot showing the distribution of PRx along various CPP values contains many intrinsic calculations. It is PRx: the correlation of ABP and ICP, versus the difference: ABP minus ICP. It may be possible that the U-shape of this relationship may be derived from the nature of mathematical transformations, rather than a physiological relationship[66].

Near-Infrared Spectroscopy (NIRS)

Near-infrared spectroscopy (NIRS) provides a continuous, dynamic measure of cerebral autoregulation through the calculation of the tissue oxygenation index TOx (used interchangeably with the cerebral oximetry index, COx[67]), the moving correlation coefficient between invasive ABP and regional oxygen saturation (rSO_2) over 30 consecutive samples averaged over 10 seconds[68]. Cerebral oxygenation is obtained non-invasively by affixing optodes to a patient's forehead, which capture the light emitted from a single laser diode in the near-infrared spectrum that penetrates the superficial cerebral tissues[67]. rSO_2 is displayed by NIRS as the tissue oxygenation index, a compilation of the concentrations of oxygenated, deoxygenated, and total hemoglobin in region, parameters which can be further dissociated by their absorption spectra[69–71]. NIRS has been verified as an alternative technique through which to describe autoregulation in TBI patients when ICP monitors are declared unfeasible by the nature of pathology. Additionally, NIRS is not operator-dependent like TCD, which makes it more accessible to clinicians. However, NIRS can be confounded by factors such as the presence of frontal contusions, which can complicate optode placement[69].

TOx is invasive, requiring an arterial catheter for the ABP input signal[68]. Similar to the acquisition of CPP_{OPT} by PRx, recorded ABP values can be plotted against TOx, producing a curve-fitted "ABP_{OPT}" as the lowest-associated TOx[68,69]. Highton et al.[72] applied ICP, TCD, and NIRS to compare the agreements between PRx, Mx, and TOx in predicting autoregulatory failure. They found that both PRx and Mx were significantly correlated with TOx, although there was incomplete agreement between the reactivity indices[72]. The NIRS-derived total hemoglobin reactivity index (THx), the correlation coefficient between the total hemoglobin index (THI = oxygenated + deoxygenated blood) and ABP, has been suggested as analogous to PRx[73]. THI used in this calculation is described by Diedler et al.[73] as "a normalized measure of [total] hemoglobin concentration and thereby provides a tracer of cerebral blood volume". NIRS-based THx has been suggested as a non-invasive substitute for PRx, supporting the PRx-THx association reported by Zweifel et al.[69], who posited that ABP can provide a "reasonable approximation" of CPP. Later work by Dias et al.[74] examined the calculation of CPP_{OPT}

with TOx instead of PRx, although the results of that single-center study have yet to be confirmed as evidence of the influence of NIRS for CPP_{OPT} determination. Further details on the relative strengths and limitations of the application of NIRS for autoregulatory assessment are available in Table 2.2.

Oxygen Reactivity Index (ORx)

Collating analog MAP, ICP, CPP, and $PbtO_2$ data from double-lumen skull bolts (Licox IM2, Integra NeuroSciences Inc.) inserted in the right frontal region of the brain, Jaeger et al.[75] calculated the oxygen pressure reactivity index (ORx) as a moving correlation coefficient between CPP and the invasively-quantified $PbtO_2$. They discovered parallels between the scoring of ORx and that of PRx to measure whether a patient is capable of autoregulating. (Table 2.2 compares ORx to PRx as has been documented within the existing body of literature). Similar to PRx, ORx values range between -1 and 1, with a positive, passive relationship between $PbtO_2$ and CPP indicating impaired autoregulation. Figure 2.8 describes this relationship.

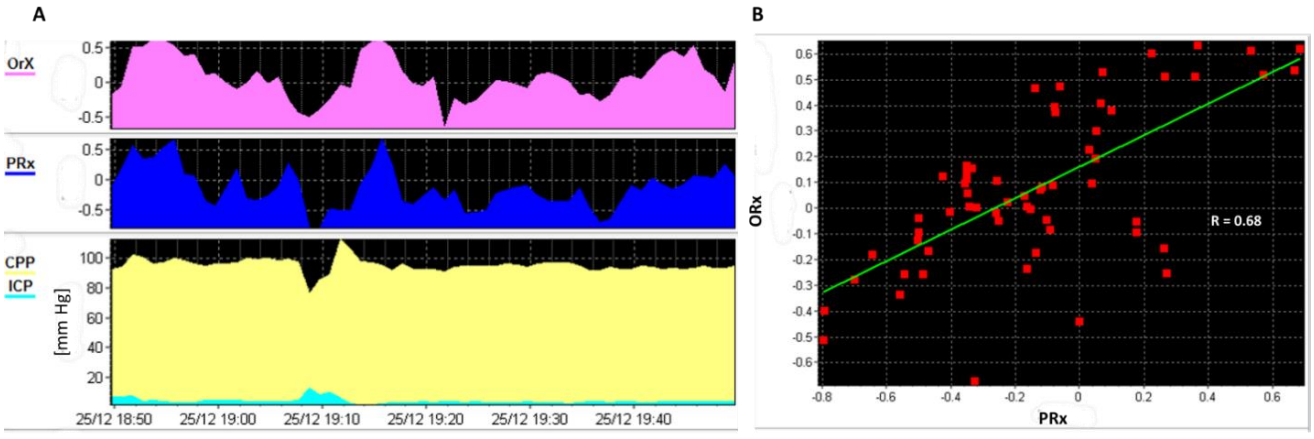

Figure 2.8. **Comparison of ORx and PRx**. A) An example[1] of a 50-minute time-trend of ORx derived from PbtO2 plotted against PRx obtained from a single patient to demonstrate the similarities in scoring between the indices; B) Although this ORx-PRx plot suggests a robust correlation between ORx and PRx (R=0.68), it should be noted that PbtO2 can be mechanically altered, whereas ICP is only subject to natural fluctuations within the brain - therefore, PRx values cannot change while ABP or ICP remain the same.

ORx: Oxygen Pressure Reactivity Index; PbtO2: brain tissue oxygenation; PRx: pressure reactivity index; CPP: cerebral perfusion pressure; ICP: intracranial pressure; mm Hg: millimeters of Mercury.

2.3.1. Factual Tables Based on Literature

Cerebral autoregulation is not fully elucidated, but it is widely agreed-upon that disturbed autoregulation directly influences outcome following TBI. This selective review of the existing body of literature confirms that the concept of autoregulation is difficult to model, and even more so to mediate. Intricate relationships between blood flow and blood pressure govern calculations of derived indices of autoregulation, such as that of PRx and Mx, which are suitable for continuous monitoring. Assessments of autoregulation, heavily reliant on non-invasive transcranial Doppler analysis of blood flow within the middle cerebral artery, can provide deeper insight into autoregulation, although this notion is challenged by both mechanical and data-driven criticism of TCD monitoring. Near-infrared spectroscopy can be considered as promising technology, but is still awaiting strong proofs. Despite the absence of a true marker of autoregulatory capacity, the control of this mechanism is a central feature of neuro-critical care management plans, whether treating patients in accordance with either ICP- or CPP-oriented protocols.

Table 2.1. Autoregulation Index Characteristics and Summary of Available Core Literature in TBI. *AMP = fundamental amplitude of ICP, Dx = diastolic flow index, CPP = cerebral perfusion pressure, FVm = mean flow velocity, FVd = diastolic flow velocity, FVs = systolic flow velocity, GOS = Glasgow Outcome Scale, ICP = intracranial pressure, MAP = mean arterial pressure, MCA = middle cerebral artery, NIRS = near infrared spectroscopy, ORx = oxygen reactivity index, $PbtO_2$ = brain tissue oxygenation, PAx = pulse amplitude index, PRx = pressure reactivity index, Sx = systolic flow index, TCD = transcranial Doppler, THI = total hemoglobin index, TOI = total oxygenation index. *This total number of patients for PRx and Mx studies is inflated given many studies have arisen from a small number of centers, yielding overlap between patient populations reported in various studies. Thus, the total number of unique patients reported is substantially less. **Only spatially resolved signals and indices are described, given the design of spatially resolved NIRS is to remove signal contamination from skin based extra-cranial circulation. Many "other" non-spatially resolved indices exist and are not covered in this table.*

Parent Signal Acquisition	**Commonly Derived Autoregulatory Indices**	**Calculation Technique**	**Approximate # of Papers in the Literature**	**Number of Patients Described**	**Core Evidence**	**Summary of Evidence**
Invasive ICP monitoring	1. ***PRx*** – correlation between ICP and MAP 2. ***PAx*** – correlation between AMP and MAP	-Pearson correlation coefficients between 10-second averaged signals (ICP, AMP, MAP) over a 5-minute window. -Typically updated every 60 seconds	1. PRx - 28 with core focus on patient outcome 2. Many more documenting relationships between PRx and other indices (ie. PAx, etc.) and other physiologic signals	Outcome Studies -4690 total (mean 168 per study)*	1. PRx is more positive in those patients with fatal outcome ($p<0.0002$)[76,77] 2. PRx threshold for mortality prediction at 6months is ~+0.25.[21] 3. PRx threshold for morbidity prediction at 6-	1. Positive PRx is positively correlated to mortality and poor functional outcome at 6 months. 2. PRx above +0.25 is positively correlated with mortality. 3. PRx above 0.05 is positively

					months is ~0.05.[21] 4. PRx tends to display positive correlations with Mx (r=0.58; p<0.001)[47]. 5. PRx and PAx display positive correlations (r=0.68; p<0.001); with PAx potentially being a better predictor of outcome in those with low ICP (ie. 15 mm Hg or less)[64].	correlated with morbidity. 4. Unclear if PAx (or other ICP derived indices) may prove superior in outcome prediction for certain subpopulations of TBI patients.
TCD flow velocity derived - from MCA (typically)	1. ***Mx*** – correlation between FVm and mean CPP 2. ***Sx*** – correlation between FVs and mean CPP 3. ***Dx*** – correlation between FVd and mean CPP	-Pearson correlation coefficients between 10-second averaged signals (FVm, FVs, FVd, CPP/MAP) over a 5-minute window. -Typically updated every 60 seconds.	1. Mx – 17 main studies (with 50 or more patients) documenting association with patient outcome. 2. Many more smaller studies evaluating Mx/Sx/Dx and patient outcome or	Outcome studies (>50 patients/study) – 3606 total (mean 212 patients/study)*	1. Mx is negatively correlated with mortality and morbidity at 6 months (p=0.018 and p=0.002)[78]. 2. Mx is superior to Mx_a (and Sx_a/Dx_a) in outcome prediction[19,79].	1. Positive Mx values are correlated to morbidity and mortality at 6 months. 2. A threshold for poor outcome may be +0.3 for Mx.

	*Note: Mx/Sx/Dx can be derived non-invasively from MAP, instead of CPP. These "MAP" versions are denoted in literature with "-a" suffix typically.		physiologic outcomes.		3. A threshold of +0.3 for Mx is associated with mortality and morbidity[21].	
*NIRS derived – bifrontal signal acquisition***	1. ***TOx*** (also known as COx)– correlation between TOI and CPP 2. ***THx*** (also known as HVx) – correlation between THI and CPP *Note: TOx/THx can be derived non-invasively from MAP, instead of CPP. These "MAP" versions are denoted with "-a" suffix typically.	-Pearson correlation coefficients between 10-second averaged signals (TOI, THI, CPP/MAP) over a 5-minute window. -Typically updated every 60 seconds.	9 main studies documenting NIRS based moving correlation coefficient for autoregulatory assessment	Total of 187 patients (mean 21 patients/study)	1. THx and TOx are positively correlated with PRx (r=0.63 and r=0.40 respectively; p<0.05)[72]. 2. Non-spatially resolved indices may be influence by skin-related artifacts, thus are not strongly correlated with PRx[70]. 3. Mx appear to be more correlated with TOx (r=0.61, p=0.004) than THx (r=0.26, p=0.28)[72].	1. Spatially-resolved TOx and THx are moderately correlated with PRx. 2. Varying degrees of correlation between TOx/THx exist with Mx. 3. Non-spatially derived indices may be subject to skin blood flow contamination and should be interpreted with caution.

Brain Tissue Oxygen ($PbtO_2$) derived	1. ***ORx*** – correlation between the $PbtO_2$ signal and CPP	Varied calculation methods: -Strongest evidence from Jaeger et al. in TBI[31] -Typically 30-second signal averages ($PbtO_2$ and CPP) -Pearson coefficient calculated over various windows: 30 minutes, 60 minutes, 120 minutes. -updated every 60 seconds *Note: other variations within the literature exist.	10 studies in the literature describe ORx calculation	Total of 159 patients (mean: 18 patient/study)	1. ORx and PRx are positively correlated ($r=0.55$, $p<0.01$)[(75)]. 2. ORx displays a negative correlation with 6-month GOS ($r=-0.62$, $p<0.01$)[(75)]. 3. ORx does not appear to rapidly respond to extreme physiologic conditions, such as plateau waves[(80)].	1. ORx displays a positive correlation with PRx. 2. High ORx values are correlated with worse 6-month outcome.

Table 2.2. Advantages and Disadvantages of Continuous Autoregulatory Indices. *ABP = arterial blood pressure, AMP = fundamental amplitude of ICP, CBF = cerebral blood flow, CBFV = cerebral blood flow velocity, CBV = cerebral blood volume, Dx = diastolic flow index, FiO_2 = fraction of inspired oxygen, ICP = intra-cranial pressure, ICU = intensive care unit, MAP = mean arterial pressure, MCA = middle cerebral artery, Mx = mean flow index, NIRS = near infrared spectroscopy, ORx = oxygen reactivity index, PAx = index derived from correlation between AMP and MAP, $PbtO_2$ = brain tissue oxygen, PRx = pressure reactivity index, TCD = transcranial Doppler, THI = total hemoglobin index, TOI = total oxygenation index.*

Monitoring Device	Invasiveness of Monitor	Autoregulatory Indices Derived	Advantages	Disadvantages
ICP monitor (Parenchymal based strain-gauge/fiber-optic OR ventriculostomy based)	Invasive	***1. PRx*** ***2. PAx***	1. Based on commonly measured physiological variables in the ICU (ICP and MAP). 2. Many studies documenting association with patient outcome. 3. Thresholds for outcome prediction available for PRx. 4. Responsive during extremes of physiology (ie. plateau waves and ABP fluctuations).	1. Invasive ICP monitoring required 2. Subject to signal "noise" and changes in parent signal phase shift - impacting the correlation coefficient. Thus, averaging of PRx values over 30 minutes of steady state is recommended. 3. PRx may be unreliable post craniectomy 4. PRx and PAx are "global" assessments of autoregulatory capacity, thus symmetry of autoregulation cannot be commented on.
TCD	Invasive OR Non-invasive	***1. Mx*** ***2. Sx***	1. Can be conducted completely non-invasively (ie. using MAP in the calculation)	1. Operator dependent on acquisition of MCA flow velocities.

		3. Dx *And MAP derivatives: (Mx-a, Sx-a, Dx-a)	2. Studies documenting association with patient outcome. 3. Thresholds for outcome prediction are available for Mx. 4. Can use the technique for non-invasive follow-up on ward or in clinic. 5. Asymmetry in autoregulation can be assessed via bilateral CBFV acquisition.	2. Limited duration of signal acquisition (ie. as long as the probe can be held in position). 3. Labor intensive for acquisition of long recordings in large populations. 4. Non-invasive indices (Mx_a, Sx_a, Dx_a) are not as strongly associated with patient outcome as the CPP-derived ones. 5. Limited data on Sx and Dx.
NIRS (Spatially Resolved) (Obtained via transcutaneous bifrontal optode)	Invasive OR Non-invasive	***1. TOx*** ***2. THx*** *And MAP derivatives: (TOx-a, THx-a)	1. Ease of application of bifrontal adherent optode. 2. Long recording possible. 3. Can obtain non-invasive version of indices (ie. using MAP in the calculation). 4. Can be used in follow-up on the ward or in clinic. 5. Spatially resolved NIRS signals (TOI and THI)	1. Non-spatially resolved NIRS signals are subject to contamination of extracranial blood flow within the skin. 2. NIRS signals are not pulse responsive waveforms, thus linking to pulsatile signals such as ICP and ABP can be difficult. 3. Unclear aspect of cerebral physiology measured by NIRS. Thought to stem from cortical CBF/CBV, signals may represent more of the venous component of the cerebral vascular system.

			theoretically have skin based extra-cranial blood flow contamination removed. 6. Theoretically can assess symmetry of autoregulation, given bifrontal signal acquisition.	4. NIRS based oxy-/deoxy-hemoglobin signals may be influenced by systemic factors (ie. cardiorespiratory complications, hemoglobin levels and oxygen carrying capacity) 5. Available literature for NIRS based autoregulatory indices is limited. With mixed correlations with ICP and TCD derived indices. 6. Association between NIRS indices and patient outcome is currently not clear.
Brain Tissue Oxygenation ($PbtO_2$)	Invasive	***1. ORx***	1. Provides unique physiologic variable (local brain tissue oxygenation). 2. Once the $PbtO_2$ probe is placed, it can obtain continuous measures of local oxygen levels. 3. Some data to suggest association of ORx with patient outcome. 4. Some data to suggest moderate correlation with PRx.	1. Invasive parenchymal monitor. 2. $PbtO_2$ signal is slowly responsive, hence ORx indices need to be derived over long period of recording (ie. 30 min up to 2 hours; or longer). 3. $PbtO_2$ signal is influenced by many factors (ie. FiO_2, cardiovascular status, pulmonary gas exchange, hemoglobin level, cerebral capillary oxygen diffusion, etc.). 4. $PbtO_2$ signal may be influenced by probe location, with intra-/peri-contusional location yielding different results from "healthy"/non-lesional locations. 5. Given the $PbtO_2$ signal is focally obtained from the parenchyma surrounding the probe

	tip, it is unclear if ORx is a focal versus global measure of autoregulatory capacity. 6. Cannot comment on symmetry of autoregulation, given focal nature of $PbtO_2$ probe. 7. ORx literature is very limited.

Chapter 3

Methodology

There are substantial similarities among the methodological aspects of the seven studies presented in this thesis. Five of the seven studies retrospectively examined an established database of adult TBI patients to provide novel insight related to: 1) the consequences of intracranial hypertension, 2) the cerebral compensatory reserve and ICP, 3) the spectral pulsatility index, 4) mathematical modeling of cerebral arterial blood volume, and 5) non-invasive estimators of PRx and the pulse amplitude index (PAx). One prospective study applied TCD monitoring for the first time to a population of adult general intensive care patients, and the final study was performed as a topical literature review on ICP measurement accuracy. Common methods across the six adult patient studies are described below; additionally, each study is detailed separately within its respective chapter (Table 3.1, below).

3.1 Patients

Retrospective Data

The retrospectively-collected data that was utilized in five of the studies comprising this thesis was harvested in subsections from a database of 1,023 adult TBI patients admitted to the Addenbrooke's Hospital Neurosciences Critical Care Unit (NCCU) between 1992 and 2013. Each patient exhibited a clinical need for ICP monitoring; ICP and additional computerized bedside signal recordings are contained within this database, the collection of which was reviewed and approved by the local and institutional ethics committee at Addenbrooke's Hospital (NHS Trust, Cambridge, United Kingdom), the University of Cambridge and the NCCU Users' Group (30 REC

97/291). Inclusion criteria for these studies were: adult TBI, at least 12 hours of invasive ICP and ABP monitoring, the availability of admission Glasgow Coma Scale (GCS) score, and an inverted six-month Glasgow Outcome Score (GOS) outcome data (1= dead, 2= vegetative state, 3= severe disability, 4= moderate disability, and 5=good recovery).

All patients were sedated with a mixture of propofol, fentanyl, and midazolam before being intubated and mechanically ventilated. Prior to 1994, TBI patients were managed by the Department of Neurosurgery and general Intensive Care Unit (ICU) if they required further ventilatory or organ support. The present NCCU was first opened in 1994 with 12 beds, and fully expanded in 2011 into a 23-bed major trauma unit. During this timeframe, patients were treated in accordance with a protocol aiming to maintain ICP below 20 mm Hg and CPP above 70 mm Hg. In particular, ICP was controlled using a step-wise approach of positioning, sedation, ventriculostomy drainage, hypothermia, and finally barbiturate-induced burst suppression of electroencephalography (EEG) and decompressive craniectomy as rescue therapies. CPP was modulated by intravenous fluids, inotropes, and vasopressors.

Later, additional monitoring modalities (cerebral autoregulation as assessed by PRx (1999), microdialysis (2002), and brain tissue oxygenation ($PbtO_2$, 2004) were introduced into patient care standards. By 2003, CPP thresholds had been modified to a value above 60 mm Hg (previously 70 mm Hg), with additional restrictions on hyperventilation put in place (acceptable end-tidal carbon dioxide ($EtCO_2$) becoming scaled from 4.5-5 kPa instead of 4-4.5 kPa). Since 2012, individualized CPP targets based on autoregulation have become available to clinicians seeking to optimize patient management.

Prospective Data

The prospectively-collected data that was utilized and presented in this thesis is part of a new database of 40 adult patients who were admitted to either the NCCU at Addenbrooke's Hospital or the John Farman Intensive Care Unit (JFICU), also located at Addenbrooke's Hospital, between March 2017 and March 2019. Patients who failed to awaken appropriately after resuscitation from cardiac arrest, meningitis, seizure, sepsis, metabolic encephalopathies, overdose, or organ failure/transplant were referred by staff

members for inclusion in this study (IRAS Project ID: 165207). All patients received invasive ABP and non-invasive TCD (Rimed Digi- Lite™, Rimed Ltd., Israel). and EEG recordings (Nihon Kohden CerebAir, Shinjuku, Japan). Six-month outcome data (GOS) was also collected for each patient.

Patients were excluded from the study if they were: under the age of 18, lacking pre-existing mental capacity to consent, expressing wishes to not participate in research, or were unable to safely undergo transcutaneous monitoring due to skin infections, known allergies, etc. Prior to study enrollment, informed consent was obtained following consultation with the patients' next of kin/legal representative or professional clinical consultee.

Table 3.1. Description of Clinical Thesis Material. *CPC – Cerebral Performance Category (CPC 1: normal cerebral function and normal living; CPC 2: cerebral disability but sufficient function for activities of daily living; CPC 3: severe disability, limited cognition, inability to carry out independent existence; CPC 4: coma; CPC 5: brain death), GCS – Glasgow Coma Scale, GOS - Glasgow Outcome Score (1= dead, 2= vegetative state, 3= severe disability, 4= moderate disability, and 5=good recovery).*

Chapter	**Full Title of Study**	**Patient Demographics**	**Condition Studied**	**Retrospective or Prospective**
4	*Cerebrovascular Consequences of Elevated Intracranial Pressure after Traumatic Brain Injury*	1023 patients (Age Range: 18.5-56.2 years; Admission GCS: 3.3-10.4; Median GOS: 1-4).	TBI	Retrospective
4	*Measurement Accuracy for Intracranial Pressure Monitoring*	Variable	TBI	Literature Review
4	*Compensatory-Reserve-Weighted Intracranial Pressure and its Association with Outcome after Traumatic Brain Injury*	1023 patients (Age Range: 15.0-85.0 years; Admission GCS: 4-9; Median GOS: 1-5).	TBI	Retrospective
5	*Relationship Between Brain Pulsatility and Cerebral Perfusion Pressure*	20 patients (Age Range: 15.0-60.0 years; GCS: 3-7; Median GOS: 2-5).	TBI	Retrospective
5	*Estimation of Pulsatile Cerebral Arterial Blood Volume based on*	52 patients (Age Range: 17.0-70.0 years; GCS: 1-12;	TBI	Retrospective

	Transcranial Doppler Signals	Median GOS: 1-5).		
6	*Validation of Non-Invasive Cerebrovascular Pressure Reactivity and Pulse Amplitude Reactivity Indices in Traumatic Brain Injury*	273 patients (Age Range: 3.0-77.0 years; GCS: 1-15; Median GOS: 1-5).	TBI	Retrospective
6	*Feasibility of Non-Invasive Multimodal Brain Monitoring in Intensive Care Patients*	40 patients (Age Range: 20.4-69.73 years, Median CPC: 1-5).	Cardiac arrest, meningitis, seizure, sepsis, metabolic encephalopathies, overdose, or organ failure/transplant	Prospective

3.2 Data Acquisition and Processing

ABP was continuously monitored invasively [from the either the radial or the femoral artery using a pressure monitoring kit (Baxter Healthcare C.A., U.S.A.; Sidcup, U.K.)] in both the retrospective and prospective studies. In the five subsets of TBI patients, ICP was monitored using an intraparenchymal probe with strain gauge sensors (Codman & Shurtleff, M.A., U.S.A. or Camino Laboratories, C.A., U.S.A.). Prior to 1996, one-minute data time averages were collected by computerized software that was developed in-house. From 1996-2002, all data trends were sampled at 100 Hz and stored as one-minute trends with the dedicated monitoring software system ICM. From 2002 onward, all data trends were collected and integrated with ICM+© software (licensed by Cambridge Enterprise, Cambridge, U.K.: http://www.neurosurg.cam.ac.uk/icmplus). Cerebral autoregulation as expressed by PRx was calculated as the linear Pearson correlation coefficient between 30 consecutive 10-second averaged values of ABP and ICP (continuous PRx values were generated by a 300-second moving window). CPP was calculated as the difference between ABP and ICP. Post-processing, minute-by-minute data for each patient was exported into comma-separated-value (CSV) files for later analysis in Microsoft Excel, Statgraphics (Statpoint Technologies, Inc., V.A., U.S.A.), IBM SPSS Statistics 23, or R software (R Core Team [2017]; R: a language and environment for statistical computing. R Foundation for Statistical Computing, Vienna, Austria. URL https://www.R-project.org/).

Table 3.2. Neuromonitoring Modalities Utilized for Data Capture and Analysis. *ABP – arterial blood pressure, AMP – amplitude of the ICP waveform, CaBV – cerebral arterial blood volume, CrCP – critical closing pressure, CPP – cerebral perfusion pressure (ABP-ICP), DCM – diastolic closing margin, FV – cerebral blood flow velocity, ICP – intracranial pressure, Mx – mean flow index (correlation between FV and CPP), Mx_a – mean flow index calculated with ABP, PAx – pulse amplitude index (correlation between AMP and mean ABP), PI – pulsatility index, PRx – pressure reactivity index (correlation between ABP and ICP), RAP – resistance area product (linear regression analysis of ABP and FV waveforms over one cardiac cycle), and sPI – spectral pulsatility index.*

Modality	**Invasive or Non-Invasive**	**Transducer**	**Monitoring**	**Software**	**Secondary Parameters**
Intracranial Pressure	Invasive	Codman MICROSENSOR intraparenchymal probe (Codman & Shurtleff, M.A., U.S.A.)	GE Marquette Solar System (GE Healthcare, Chicago, I.L., U.S.A.)	ICM+™	Mean ICP CPP AMP PRx RAP PAx
Cerebral Blood Flow Velocity	Non-Invasive	Rimed 2 MHz probe (Rimed Digi-Lite™, Rimed Ltd., Israel), DWL 2MHz	None	ICM+™	Mean FV Mx Pulsatile CaBV

		probe (Multi Dop X4, DWL Elektronische Systeme, Sipplingen, Germany)			PI sPI CrCP DCM
Arterial Blood Pressure	Invasive	Taken from the radial or the femoral artery using a standard pressure monitoring kit (Baxter Healthcare C.A., U.S.A.; Sidcup, U.K.)]	GE CARESCAPE B850 (GE Healthcare, Chicago, I.L., U.S.A.)	ICM+™	Mean ABP CPP Mx_a

Chapter 4

Clinical Implications of Intracranial Pressure in Brain Injury

The following publications formed the basis of this chapter:

- Calviello LA, Zeiler FA, Donnelly J, Smielewski P, Czigler A, Lavinio A, Hutchinson PJ, and Czosnyka M. Cerebrovascular Consequences of Elevated Intracranial Pressure after Traumatic Brain Injury. *Neurocritical Care. In Review.*
- Calviello LA, Forcht Dagi T, Czosnyka Z, and Czosnyka M. Measurement Accuracy for Intracranial Pressure Monitoring. *Neurosurgery. In Review.*
- Calviello LA, Donnelly J, Cardim D, Robba C, Zeiler FA, Smielewski P, Czosnyka M. Compensatory-reserve-weighted Intracranial Pressure and its association with outcome after Traumatic Brain Injury. *Neurocritical Care*. 2018 Apr 1;28(2):212-20.

4.1 Cerebrovascular Consequences of Elevated ICP after TBI

4.1.1 Introduction

TBI commonly results from external blunt force applied to the cranium during such adverse events as falls, motor vehicle accidents, assaults, and sporting injuries[3]. Cerebral autoregulation is a complex intrinsic protective mechanism for the brain that is strongly dependent on the maintenance of clinically-appropriate levels of ABP, ICP, and CPP (the difference between ABP and ICP)[1]. Complications of TBI often manifest in the first two days after admission[40] in the form of worsening cerebral autoregulation. However, this does not exclude other reasons for dysautoregulation such as endothelial dysfunction, metabolic failure, hyperemia, etc.

Perhaps the greatest risk factor for poor patient outcome is sustained, high values of ICP, which dangerously strain cranial volumetric capacity and can produce irreversible damage[11]. According to the Monro-Kellie doctrine, ICP is comprised of four separate components: arterial blood inflow and venous blood outflow (both of which contribute to cerebral blood volume, CBV), cerebrospinal fluid (CSF), and a fixed brain volume[12]; in a healthy system, when one component increases, the others should decrease to accommodate for this change in order to maintain a constant value. In TBI patients, ICP is often abnormally elevated, requiring aggressive clinical intervention to maintain perfusion and prevent brain herniation. These interventions include the use of sedative agents and vasopressors, head positioning, CSF drainage, osmotherapy, surgical evacuation or decompression, and targeted temperature management[11].

Intracranial compliance is characteristically reduced in patients with intracranial hypertension, meaning that patients with elevated ICP are at risk of further significant spikes in ICP even in response to minor volume changes of intracranial blood and CSF or brain swelling. High CPP inversely correlates with ICP, predisposing the injured brain to hypoxia by increasing the compartmental volume load until it triggers the ultimately deadly trifecta of "mechanical compression, displacement, and herniation of brain tissue"[13]. Invasive ICP monitors are essential to the diagnosis and treatment of

high ICP; however, initial values of ICP (determined on admission to NCCU) are poor predictors of outcome, particularly in those with mass lesions[14]. There is a bilateral, causal relationship between brain damage and high ICP; intracranial hypertension (sustained values of ICP >20 mm Hg) unfolding over a period of days can progressively alter the brain's ability to adapt its cerebral structural and volumetric reserves[15] to maintain a reasonable degree of function. In survivors, the long-term effects of persistent neuroinflammation and chronic structural degeneration can dramatically increase the risks of depression, susceptibility to cognitive loss and dementia, or accelerated rates of brain atrophy[3].

In neurocritical care centers, outcome following TBI cannot be predicted on the basis of ICP alone. ICP interacts with a variety of other parameters (both "traditional" and derived) to influence the tactics of individual management[9,81–87]. In conjunction with invasive ICP, ABP, and cerebral tissue oxygenation monitoring (yielding $PbtO_2$, brain tissue oxygen partial pressure), non-invasive methods such as TCD can strengthen clinical efforts to predict outcome. With this bedside tool, cerebral blood flow velocity (CBFV) from the middle cerebral artery, the waystation for cerebral circulation, can be measured and analyzed as a surrogate descriptor of global cerebral blood flow[81]. Although CBFV in TBI cannot be correlated with CBF because of the variable cross-sectional area of the investigated vessels, multiple indices of CBF based on TCD have been proposed. TCD monitoring also returns the pulsatility index (PI), that has been suggested to alert clinicans to high ICP[88,89]. Important clinical indices such as the invasively-quantified PRx (based on the analysis of slow vasogenic waves in ABP and ICP) and the non-invasive cerebral autoregulation index based on TCD (Mx – the linear correlation coefficient between CBFV and CPP) can also be displayed at the bedside; both indices are interpreted in the same fashion, with negative values of each suggesting preserved cerebral autoregulation and increasingly positive values indicating the opposite effect[1].

This study examines the consequences of increasing ICP on cerebral autoregulation and their implications for TBI patients. It aims to provide clear description of the differences in both physiological and cerebral hemodynamic activities in a large population of TBI patients and their correlation with favorable or unfavorable outcome.

4.1.2 Methods

Patients

Patient data were retrospectively acquired from a database of patients subjected to continuous recording of ICP and ABP signals. These recordings were taken over the patients' entire stay on the neurocritical care unit (NCCU) at Addenbrooke's Hospital, Cambridge, U.K. from 1992-2013 (anywhere between 1 day to 4 weeks in duration, *n*= 1,023). In an indicated further number of patients, brain tissue oxygenation was monitored. Some of these patients had TCD recordings (*n*=325) and TCD-related parameters were calculated. Six-month outcome data has been documented during the period between 1992-2015. Each cohort (intermittent TCD and long-term ICP/ABP/ $PbtO_2$) was further separated into groups of patients with either normal ICP (<15 mm Hg) or elevated ICP (>23 mm Hg). All patients received continuous monitoring with ICM+™ software (Cambridge Enterprise Ltd., Cambridge, U.K., http://www.neurosurg.cam.ac.uk/icmplus) recorded together with continuous invasive ICP and ABP to provide a visualization of the pathophysiological effects of TBI. All patients were sedated with a mixture of propofol, fentanyl, and midazolam and were mechanically ventilated. 75% of patients presented with an admission GCS <9 and were treated with a graded management protocol aiming CPP above 60-70 mm Hg and ICP <20 mm Hg[36].

Monitoring

All patients underwent invasive ABP, ICP, and $PbtO_2$ monitoring. A subset of 325 patients also received non-invasive monitoring of TCD-based CBFV. Raw data signals from select monitoring devices were captured and digitally archived using WREC software (Warsaw University of Technology) or ICM+™ software (Cambridge Enterprise, Ltd. -contemporary to WREC software). ABP was continuously monitored invasively from the radial artery via pressure monitoring kits (Baxter Healthcare, C.A., U.S.A.; Sidcup, U.K.). ICP was also monitored continuously with invasive intraparenchymal probes equipped with strain gauge sensors (Codman & Shurtleff,

M.A., U.S.A. or Camino Laboratories, C.A., U.S.A.) inserted predominantly in the right frontal lobe. Mean cerebral blood flow velocity (CBFVm) was recorded from the middle cerebral artery (MCA) with a 2 MHz TCD probe (Multi Dop X4, DWL Elektronische Systeme, Sipplingen, Germany), on the side of the ICP microtransducer placement, or the opposite side if the TCD signal window was better. Data were processed through a 16-bit, 100kHz analog-to-digital converter (DT9803 USB Data Acquisition (DAQ) Module, Measurement Computing Corporation, Norton, M.A., U.S.A.).

Ethics

All described monitoring modalities are routinely employed as standard care practice on NCCU, complete with an anonymized database of physiological parameters. Identifiable patient information such as age, injury severity, and clinical status at hospital discharge were recorded during monitoring periods; clinical records were not revisited for additional analytical purposes. At the time of data extraction from the hospital records, each archived monitoring session was fully anonymized so that obtaining formal patient or proxy consent for access was not required.

Since all data was extracted from the hospital records and fully anonymized, no data on patient identifiers were available, and need for formal patient or proxy consent was waived. Within our institution, patient data may be collected with waiver of formal consent, as long as it remains fully anonymized, with no method of tracing this back to an individual patient. Patient physiologic, demographic, and outcome data was collected by the clinicians involved with patient care, and subsequently recorded in an anonymous format. This anonymous data is then provided for future research purposes. Such data curation remains within compliance for research integrity as outlined in the UK Department of Health - Governance Arrangements for Research Ethics Committees (GAfREC), September 2011 guidelines, section 6.0.[90]

Data Processing

Raw data signals were supported and processed by ICM+™ software (Cambridge Enterprise, Cambridge, U.K., http://www.neurosurg.cam.ac.uk/icmplus). Signal

artifacts were manually removed by internal signal cropping tools within ICM+™. CPP was calculated as the difference between the raw ABP and ICP signals.

In the primary analysis phase, time-averaged mean values for ABP, CBFV, CPP, and ICP were calculated for each patient over 10-second time windows, updated every 10 seconds to eliminate overlap. Mean CBFV was calculated from the raw CBFV signals. Next, in the intermittent TCD cohort, multi-parametric measures of autoregulation such as: Mx (mean flow index, the correlation between CBFV and CPP)[36], CrCP (critical closing pressure, the plotted comparison between ABP and CBFV where CBFV = 0)[91], DCM (diastolic closing margin, the difference between diastolic ABP and CrCP)[85], sPI[28] (spectral pulsatility index), F1/CBFVm (with F1 the fundamental frequency of CBFV), and ARI (autoregulation index, a graded reference index of cerebral autoregulation) were also calculated[36]. In the long-term ICP/ABP/$PbtO_2$ cohort, PRx (pressure reactivity index, the correlation between ABP and ICP)[92], HR (heart rate), AMP (the fundamental frequency of ICP, 20-second time windows updated every 10 seconds), SLOW (slow waves of ICP, yielded through low-pass spectral filtration of raw ICP signals), PbtO2 (brain tissue oxygenation), PAx (pulse amplitude index, the correlation between AMP and mean ABP), and RAC (an autoregulation index determined by the correlation between AMP and CPP) were calculated in addition to the primary parameters[93]. In all patients, age, admission GCS (Glasgow Coma Scale, assessing consciousness from scores of 3-15, with 15 representing the highest level of consciousness), and GOS (Glasgow Outcome Scale, ranging from 1-5, with 1 representing death and 5 a good outcome) were included as additional demographic data to identify long-term outcome trends.

Final data processing involved the comparison of the above hemodynamic parameters between the two ICP groups (normal vs. elevated) within each cohort (intermittent TCD vs. long-term ICP/ABP/$PbtO_2$). All data post-processing were exported from each patient to separate comma-separated variable (CSV) files for further statistical analysis.

Statistics

All statistical analyses were conducted using STATISTCA data analysis software. Post-processing data, exported as CSV files, were compiled into two large CSV documents (intermittent TCD and long-term ICP/ABP/$PBtO_2$ cohorts) containing all of the above recorded signals for each patient. Data for each cohort was then filtered by ICP level (normal ICP <15 mm Hg, and elevated ICP >23 mm Hg). The value of 23 is a critical level of ICP from the point of view of differentiation between survival and mortality[36], whereas 15 mm Hg is a consensus -accepted threshold of value for normal ICP. Statistical significance for invasively-monitored variables and non-invasively derived variables (based on TCD) was determined both within and between each subset of patients via the Mann-Whitney U-test with an alpha of 0.05 assigned to entries with *p*-values below this threshold. Given that this analysis is an exploration into multi-modal defined cerebrovascular parameters during normal ICP and intracranial hypertension (i.e. ICP >23 mmHg), we elected to not correct for multiple comparisons, in keeping with other physiologic exploratory studies.

In the TCD cohort, the relationships between CBFVdiastolic/CBFVm, Mx, CrCP, DCM, sPI, and ARI were compared between the normal and elevated ICP patient subgroups. In the long-term cohorts, the effects of "normal" versus "elevated" ICP were similarly compared to outcome with respect to the following variables: age, admission GCS, GOS, PRx, CPP, ABP, HR, AMP, SLOW, $PbtO_2$, PAx, and RAC.

4.1.3 Results

Examples of selected recorded vascular variables are provided in Figures 4.1-3. They include the short-term elevation of ICP provoked by cerebrovascular relaxation, causing a temporary increase in ICP – a plateau wave (Figure 4.1). The second example features refractory intracranial hypertension associated with malignant brain edema (Figure 4.2). The third presents a temporary rise in ICP driven by an increase in CBFV; this may be attributable to an increase in either $PaCO_2$ or brain metabolism (Figure 4.3).

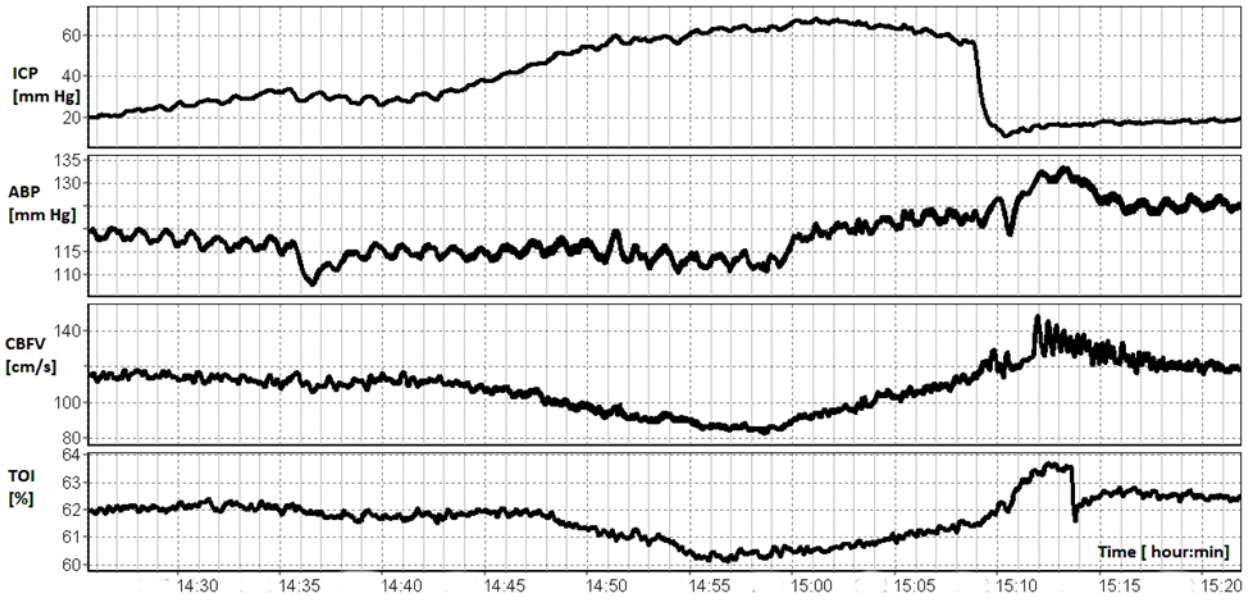

Figure 4.1. **Plateau Wave of ICP**. This is an example of when CBFV decreases due to failing autoregulation. Brain oxygen saturation yielded from near-infrared spectroscopy (TOI) decreases, indicating a similar response in cerebral blood flow. This elevation in ICP occurred over 15 minutes and was managed by nursing intervention (vasoconstriction via Ambu-bag short-term hyperventilation).

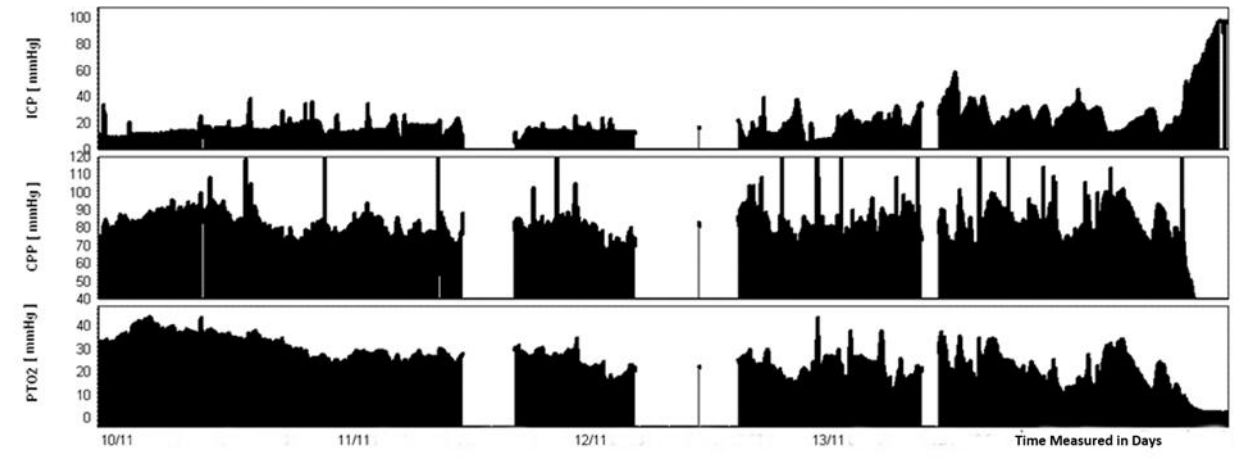

Figure 4.2. **Refractory Intracranial Hypertension**. After a few days of stable ICP (around or below 20 mm Hg) and CPP, dynamics of the signal increased. Finally, ICP increased to 90 mm Hg over a period of several hours, CPP decreased to below 40 mm Hg, and brain tissue oxygenation fell to below 10 mm Hg.

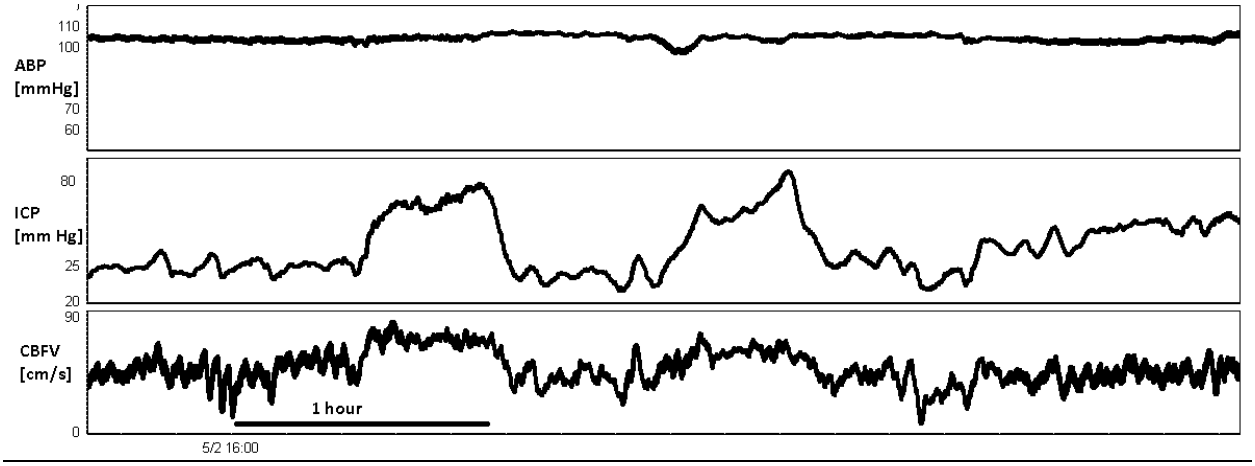

Figure 4.3. **Effects of ICP on Cerebral Blood Flow.** Deep ICP waves related to the increase in cerebral blood flow and therefore cerebral blood volume. This effect can be observed quite frequently after TBI. Note that the change in CBFV is not caused by intracranial hypertension, but that intracranial hypertension is secondary to the rise in cerebral blood volume.

Table 4.1 summarizes the mean values and standard deviations of each parameter compared against either normal or elevated levels of ICP; summary statistics data for each patient cohort are also featured in this table. Significance levels are reported at the bottom of the table. The results of the presented analyses indicated that irrespective of the patient cohort, elevated levels of ICP significantly affect cerebrovascular function, and subsequently, patient outcome after TBI.

	Normal ICP (<15 mm Hg)	**Elevated ICP (>23 mm Hg)**	***p*-value**[◊]
Age [Years]	39.0 (±17.2) *n* = 419	34.0 (±15.5) *n* = 115	*p*=0.0065 **
Median GCS	7.0 *n* = 396	6.0 n = 104	*p*=0.089
Median GOS	4.0 n = 401	1.0 n = 116	p<0.00001 ****
ICP [mm Hg]	10.504 (±3.21) *n* = 401	31.1(±9.22) *n* =116	*p*<0.0001 ***
CPP [mm Hg]	80.52 (±10.2) *n* = 401	66.9 (±13.9) *n* = 116	*p*=0 ****
ABP [mm Hg]	91.3 (±10.1) *n* = 401	97.6 (±12.2) *n* = 116	*p*<0.001 **
HR [bpm]	80.6 (±16.1) *n* = 413	83.7 (±16.0) *n* = 105	*p*=0.16
$PbtO_2$ [mm Hg]	30.14 (±19.8) *n* = 99	24.9 (±45.0) *n* = 10	*p*=0.15
PRx	0.07 (±0.15) *n* = 334	0.2 (±0.24) *n* = 66	*p*<0.001 ***
PAx	-0.12 (±0.17) *n* = 69	0.41 (±0.17) *n* = 6	*p*<0.0001 ***
RAC	-0.252 (±0.24) *n* = 223	-0.118 (±0.26) *n* = 38	*p*=0.0076 **
AMP [mm Hg]	1.44 (±0.86) *n* = 394	2.63 (±1.6) *n* = 110	*p*=0 ****
SLOW [mm Hg]	1.28 (±2.52) *n* = 63	1.13 (±1.28) *n* = 85	p=0.63
CBFVdiastolic/CBFVm	0.61 (±0.067) *n* = 127	0.57 (±0.089) *n* = 66	*p*=0.0056 **
Mx	-0.015 (±0.29) *n* = 127	0.13 (±0.31) *n* = 66	*p*=0.0019 **
ARI	4.36 (±1.51) *n* = 101	3.44 (±1.36) *n* = 52	*p*<0.0001 ***
CrCP [mm Hg]	36.8 (±8.32) *n* = 109	53.7 (±9.8) *n* = 56	*p*=0 ****
DCM [mm Hg]	28.0 (±6.5) *n* = 109	19.5 (±7.4) *n* = 56	*p*<0.0001 ***
sPI	0.3 (±0.08) *n* =127	0.36 (±0.096) *n* = 66	p=0.0014 **

Table 4.1. Comparison of cerebral hemodynamics with both normal and elevated levels of intracranial pressure in both the intermittent and long-term ICP/ABP/ $PbtO_2$ cohorts [mean values unless otherwise reported]. *ABP – arterial blood pressure, Age – age measured in years, AMP – amplitude of the intracranial pressure wave, ARI – autoregulation index, bpm – beats per minute, CBFVdiastolic/CBFVm – the quotient of*

*diastolic cerebral blood flow velocity and mean cerebral blood flow, CPP – cerebral perfusion pressure, CrCP – critical closing pressure, DCM – diastolic closing margin, GCS - Glasgow Coma Scale, GOS – Glasgow Outcome Score, HR – heart rate, ICP – intracranial pressure, mm Hg – millimeters of mercury, Mx – mean flow velocity index, PAx – pulse amplitude index, $PbtO_2$ – brain tissue oxygenation partial pressure, PRx – pressure reactivity index, RAC – the correlation coefficient between the pulse amplitude of intracranial pressure and cerebral perfusion pressure, SLOW – slow waves of intracranial pressure, and sPI – spectral pulsatility index. * – significant, ** – very significant, *** – very highly significant, and **** – extremely significant.*

◊Statistical significance) was determined via the Mann-Whitney U-test with an alpha of 0.05 assigned to entries with p-values below this threshold.

4.1.4 Discussion

The main finding of this study is that elevated ICP significantly affects healthy cerebrovascular dynamic function. Both directly invasively-quantified parameters (i.e. mean values of CPP, $PbtO_2$, etc.) and non-invasive, TCD-based derived parameters (i.e. CBFV, Mx, etc.) reflect physiological variability, with respect to patient subgroup.

In patients with intact autoregulatory capacity, ABP and ICP are inversely related. However, in those patients with failing autoregulatory capacity, this pressure/volume relationship becomes pressure-passive. ABP was determined to be higher in patients with elevated ICP, the result of either natural fluctuations in cerebral blood volume (CBV) attributable to vasodilation or to the administration of vasopressors to stabilize TBI patients[94] (additionally, more severely-injured patients had lower admission GCS scores and overall higher ICP[95]. By treating dysautoregulation by altering either ABP or ICP to constrain CBV, the likelihood of pressure-passivity decreases[94]. The pressure reactivity index (PRx), the linear correlation coefficient between mean ABP and mean ICP, was also determined to be higher in those with elevated ICP[95]. As ABP becomes pressure-passive to rising ICP, the value of PRx increases from negative values to either approach or exceed 0. Patients with high ICP and high PRx are more likely to have poor long-term outcomes after TBI[1,21,90,95,96]

CPP is classically recognized as the cerebrovascular pressure gradient[91], the calculated difference between ABP and ICP; values of CPP ranging from 55-105 mm Hg

are considered to be within the limits of normal cerebral autoregulation. Increasing ICP, and thus ICP wave amplitude (AMP), as a result of TBI is inversely related to the brain's ability to maintain an appropriate level of CPP; continuous decrements of CPP can predispose patients towards ischemia[14]. Our findings are consistent with this general knowledge of CPP. Furthermore, when plotting CBFV against CPP, yielding the non-invasive, TCD-based parameter Mx, patients with intact autoregulation have values of Mx that are either negative or close to 0; conversely, it is expected that a dysautoregulating patient with high ICP and therefore low CPP, would have a higher Mx[9], a trend echoed by our analyses. Non-linear regression analysis of sPI (spectral pulsatility index) versus CPP also reveals worsening autoregulation, as the value of sPI increases with falling CPP[89]. This parameter is also associated with the prediction of CPP reaching its lower bound, likely resultant of high ICP in susceptible patients[89].

Mean CBFV in the MCA is significantly affected by ICP. The flow velocity waveform is dampened in patients with intracranial hypertension, particularly in the diastolic portion of the raw wave signals extracted from TCD recordings[85]. This effect can be attributed to the interaction between low CPP resultant of high ICP and the acceleration of global cerebral blood flow towards pressure-passivity, characteristic of dysautoregulation, which can be monitored by identifying the critical closing pressure (CrCP) for each patient, the value of ABP at which cerebral blood flow ceases. CrCP is defined as the sum of ICP and vascular wall tension, and calculated by correlating pulsatile CBFV and ABP and extrapolating the ABP value at which CBFV equals zero. CrCP can demonstrate CPP below its "safe" lower bound and can predict pressure-passive responses to cerebral blood flow[28,84,85,92]. Our results agree, as patients with elevated ICP would by definition have a higher threshold for CrCP[84]; when the brain is no longer able to compensate for declining CPP via vasodilation over repeated cardiac cycles, this absence of diastolic flow precludes "imminent" hypoxia and brain death[85]. The diastolic closing margin (DCM), the difference between diastolic ABP and CrCP, describes the local point at which diastolic cerebral blood flow ceases, coupled with pressure-passivity and likely microvascular collapse when approaching 0 or negative values[85]. Patients in the elevated ICP subgroups for both TCD monitoring and long-term ICP/ABP/ $PbtO_2$ exhibited lower DCM, which is consistent with the observed

trends of high ICP coupled with both dysautoregulation and poor outcome, in the wider body of literature.

Dysautoregulation can also be described by interactions between high ICP and the derived ARI, which quantifies dynamic changes in cerebral autoregulation after step-changes in CPP (by manipulating ABP via thigh-cuff release), and is a graded reference index that assesses appropriate cerebral blood flow moderation to ABP variability. When plotting CBFV against the elapsed time from the thigh-cuff release, a series of 10 best-fit template models emerges through transfer function analysis, with increasing steepness of these models reflecting better cerebral autoregulation (ARI=9), and more gradually-sloped models reflecting the latter (ARI=0)[93]. ARI is compatible with outcome prediction scoring methods such as GOS, displaying higher values with GOS categories of 3-5 (severe disability, moderate disability, and good recovery, respectively), and lower values for GOS scores of 1 (dead) or 2 (vegetative state).

The continuous, ICP-based indices of autoregulation PAx (pulse amplitude index, the correlation between AMP and mean ABP) and RAC (the correlation between AMP and CPP) can also identify the effects of ICP on cerebral hemodynamics. Both indices are closely related to PRx[86], and are similarly scored, with the exception of RAC of 0 indicating worsening autoregulation as ICP increases. Patients with elevated ICP had significantly higher PAx (due to increased AMP and ABP) and RAC (due to low CPP) than those with normal levels of ICP. As RAC in particular is sensitive to ICP and CPP, plotting it against CPP produces a parabolic relationship between the parameters, suggestive of RAC's potential use in the determination of individual values of optimal cerebral perfusion pressure[87].

Limitations

The predictive value of each of the above trends is directly related to the calculation methods required to yield each parameter, and how reliably each parameter represents true physiology. This being said, there is an established difficulty with the identification of a "universal, 'normal' value of ICP"[91], as ICP is strongly dependent on age, body position, and pathology; our study is limited by our arbitrary categorization of "normal" versus "elevated" ICP thresholds on the basis of grand mean values of ICP,

and the potential ramifications of this effect on our statistical reporting when assigning our patients into subgroups. These thresholds may explain the counter-intuitive relationships between ICP, age, and median GOS identified in our results (younger patients with lower ICP generally have a higher GOS score[9], as the number of patients assigned to each ICP group for comparison was uneven). Additionally, the amount of patient data available for multi-parametric autoregulation analysis varied according to different selection criteria necessary for the calculation of each parameter[9,36].

It is of note that TCD monitoring is only a surrogate descriptor of cerebral autoregulation, and is fundamentally limited by both inter- and intra-operator variability; MCA flow velocity recordings may differ on the basis of probe position and return inconsistent measurements, or natural differences in patient skull thickness can affect the observed strength of the TCD signal. Although invasive measurement techniques are considered "gold standards", they are flawed; ICP and ABP pressure transducers may not sample from the most reliable positions, potentially skewing values that then form the bases of derived parameters, such as CPP, which are increasingly becoming relied upon for clinical management[82]. To minimize these effects and reduce the risk of infection, non-invasive ICP (nICP) monitoring derived from CBFV and ABP waveforms introduces temporally-sensitive reference data that bolsters reliability when predicting outcome[1,90]; however, nICP protocols are not yet widely implemented in neurocritical care.

4.1.5 Conclusions

Elevated ICP after TBI directly contributes to decrements in cerebral blood flow. Significant alterations in cerebral hemodynamics are the result of the combined effects of high ICP, described by positive values of PRx and Mx, which signifies failing cerebral autoregulation and leads to more than two-fold increase in mortality.

4.2 Measurement Accuracy for Intracranial Pressure Monitoring

4.2.1 Introduction

A variety of ICP sensors have been utilized to measure ICP and guide treatment. Lundberg is widely credited with establishing the clinical paradigm for continuous ICP monitoring in the 1960s[97]. External ventricular drains (EVDs) are placed within the ventricle, measuring ICP pressure directly, and can be used to drain excess CSF and lower ICP. They are often characterized as the "gold standard" of ICP measurement. Other types of fluid-coupled systems, such as the Richmond bolt™, also measure pressure in the CSF but cannot effectively reduce it. ICP measurement devices have also been designed around fiberoptic, piezoelectric strain gauge, and pneumatic microsensor technologies. Depending on the specific design, they can be inserted into the parenchyma, ventricle, or the subarachnoid, subdural, or epidural spaces. While they cannot drain CSF, they are easier to implant correctly and carry lower risks of infection and complications than EVDs. ICP measurement is utilized routinely when there is concern about pressure elevation and there are no contraindications[98–101].

Accuracy can be elusive when measuring ICP. The problem derives both from the physiology of ICP and the limitations of existing instrumentation[102]. Two FDA-approved devices of the same type by the same manufacturer can yield different measurements when put in two different regions of the brain. Almost every ICP measurement device may drift; some types may be recalibrated, but not all. This paper reviews the concepts and factors that bear on the accuracy of ICP measurements including the reliability of the existing ICP measuring technologies.

4.2.2 Intracranial Pressure Sensor Technology

ICP can be monitored continuously by means of devices implanted in the ventricle, the parenchyma, the subarachnoid space, the epidural space, the skull (but open to the

subarachnoid space), the cervical cistern, or the lumbar subarachnoid space. Devices in the ventricle, the cervical cistern, and the lumbar subarachnoid space can be designed to drain CSF and measure ICP. Those implanted elsewhere are capable only of ICP measurement.

Pressure measurement requires either a manometer to which the fluid-filled catheter is connected, or some kind of pressure transducer. A manometer is the classical instrument for pressure measurement. It displays a column of fluid, generally CSF but alternatively mercury, whose height corresponds to the pressure. This simple instrument gives rise to direct pressure readings taking the form "centimeters of H_2o" or "mm of Hg", with both conventions accepted. A pressure transducer, in contrast, is a device with an elastic or moveable component which deforms or moves when subjected to pressure, and generates a signal. The signal is typically electrical and correlates with the pressure. CSF pressure is traditionally expressed in "centimeters of H_2o" or "mm of Hg" just as it would be on a manometer.

The three most common types of pressure transducers are: piezoelectric, fiberoptic, and pneumatic. Piezoelectric sensors change their internal electrical resistance and produce electric signals when subjected to mechanical forces such as ICP[103]. Fiberoptic sensors incorporate a calibrated mirror which changes position in response to pressure[104]. Reflected light is transmitted fiber-optically to a photoelectric device that generates electrical signals[104]. Pneumatic sensors typically consist of a small air-pouch balloon which changes volume with pressure. These changes are translated into ICP measurements[103,104]. As already noted, pressure transducers can take many forms and can be implanted in various locations. One simple and particularly successful system is connected to a hollow bolt threaded into the calvaria and open to the subarachnoid space. This straightforward ICP monitor describes the original or modified Richmond subarachnoid screw[105,106] or the commonly-used Licox™ bolt (Integra Life Sciences, Plainsboro Township, N.J., U.S.A.). Transducer-based devices are quicker to place and less technically demanding than catheter-based devices. Although both device families are relatively safe, either can be complicated by blockage, infection, and hemorrhage[107].

Catheter systems can be calibrated or zeroed *in-vivo*. Pressure transducers, in contrast, must be calibrated before implantation with one exception: the Gaeltec™

epidural system, which was designed to allow *in-vivo* calibration[108] (Gaeltec, Dunvegan, Isle of Skye, Scotland). Monitors that can be recalibrated (or zeroed) in-situ to overcome drift and to optimize measurement accuracy are often characterized as "gold standards" in ICP measurement[104,109,110].

4.2.3 Rationale for Continuous ICP Monitoring

ICP is monitored to help prevent secondary injury after a neurological event. Historically, the study of ICP has been pursued most intensively in TBI. Head-injured patients often exhibit abnormal ICP dynamics; elevated ICP interferes with cerebral blood flow, cerebral perfusion and cerebral compliance (Figure 4.4, below)[111–113]. Very high levels of ICP can result in cerebral ischemia, herniation of the temporal lobe, or trans-tentorial brainstem herniation[111].

The American Brain Trauma Foundation suggests ICP monitoring for all cases of TBI with GCS between 3-8 and abnormal CT scans[49], and for older patients with GCS 3-8, with either uni- or bilateral motor posturing or with systolic blood pressure below 90 mm Hg despite a normal scan[109]. Some investigators have observed that invasive ICP monitoring correlates with improved patient outcomes, independently of intervention[104,114–119].

However, the risks associated with ventriculostomy, which are shared by cervical and lumbar drains, include: infection, CSF leak, interference from air bubbles, clots and debris, secondary injury and hemorrhage from improper insertion, and other complications of prolonged monitoring such as (for ventricular catheters) slit ventricles[109,120–124]. Intraparenchymal ICP sensors, typically implanted through a burr hole to a depth of about 2 centimeters, carry a lower risk of complications and correlate closely with intra-ventricular pressure[104,121].

Overall, intraparenchymal placement of contemporary ICP sensors is regarded as safe, with low risk of hemorrhage (<0.04%)[122]. The disadvantages of intraparenchymal monitoring are linked to the fact that they measure vectors of force within the parenchyma rather than actual CSF pressures. These measurements are subject to distortion by several factors, including the direction of the vectors of force

exerted on the sensor. As already noted, they can neither drain excess CSF, nor be recalibrated following insertion[104,121]. In the event that both an EVD and an intraparenchymal sensor are implanted at the same time in the same patient, the EVD must be closed for measurements to be comparable (Figure 4.5).

The reliability of intraparenchymal catheters is dependent on pressure sampling and distribution, even if the instruments operate as intended. Pressure throughout the central nervous system (CNS) follows Pascal's law: it is equally distributed throughout the CNS except in the case of rare stoppages or "hard blocks" in the circulation of CSF, although pressure differences are often small[125]. Thus, in non-communicating hydrocephalus, the pressure gradient between the ventricles and subarachnoid space has been reported to be on the order of 1-2 mm Hg or less[125]. Even though the correlation between two microsensors reporting simultaneously may vary over time and in terms of absolute value (Figure 4.6), intraparenchymal ICP measurements ought to be reliable.

4.2.4 Thresholds for Clinical Intervention

The threshold for intervention remains under study. Interventions including ventricular drainage, sedation, osmotic diuresis, hypothermia and decompressive craniectomy are generally recommended for ICP above 15-25 mm Hg[112]. These guidelines are based primarily on historical outcome studies focused on survival. Large-scale studies emphasizing functional outcomes are currently underway[126–131] and may reach different conclusions. Outcome-based guidelines for monitoring in childhood and for other conditions are also under consideration[132–138].

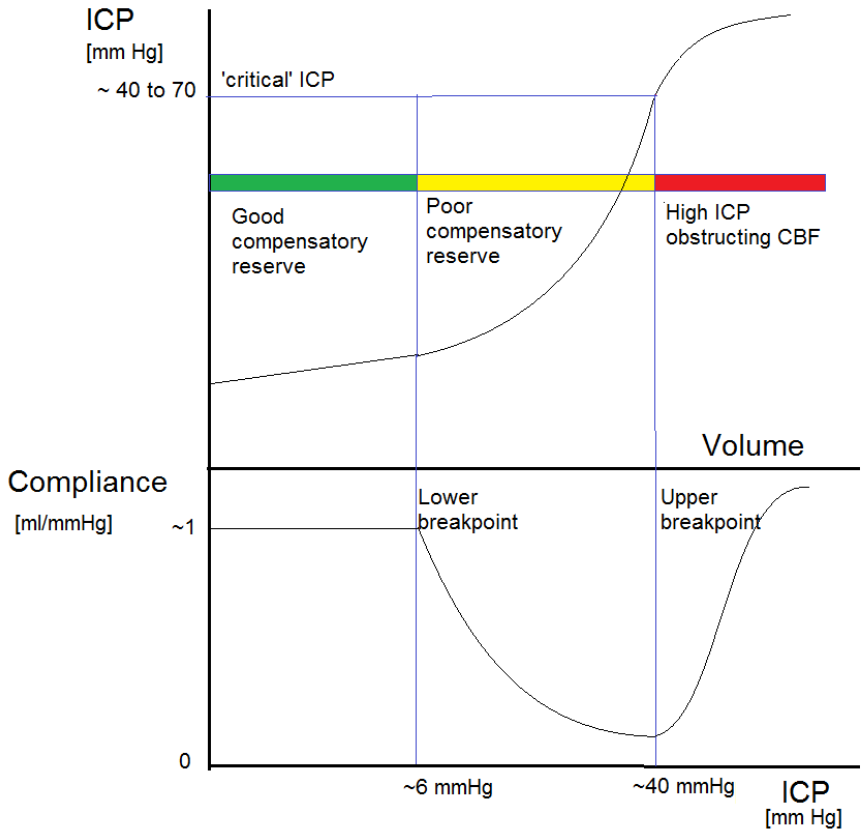

Figure 4.4. **The Pressure-Volume Curve and Brain Compliance.** The general shape of the pressure-volume curve (upper panel) and related brain compliance (lower panel). When extra volume is loaded, ICP first increases linearly, until it reaches the "lower breakpoint". In this zone of good compensatory reserve, brain compliance is independent of ICP (note: numerical values on this graph are given for orientation; individual limits may be variable). With a further volume load, the shape of the pressure-volume curve becomes exponential, and compliance decreases inversely to further ICP elevations to a state of poor compensatory reserve. Further, when ICP reaches a very high level ("critical" ICP), the arterial bed starts to become compressed, with usually observed decreases in cerebral blood flow – there is a threat of brain ischemia in this state. The pressure-volume curve deflects to the right and brain compliance increases. The shapes of curves and levels of all demarcation points are individual; they may be affected by many factors such as cerebral perfusion pressure, $PaCO_2$, level of anesthesia, medication, etc. This graph is a compilation of many previous works, starting from Löfgren and Zwetnow[139], through Marmarou et al.(140), and many more contemporary authors[111].

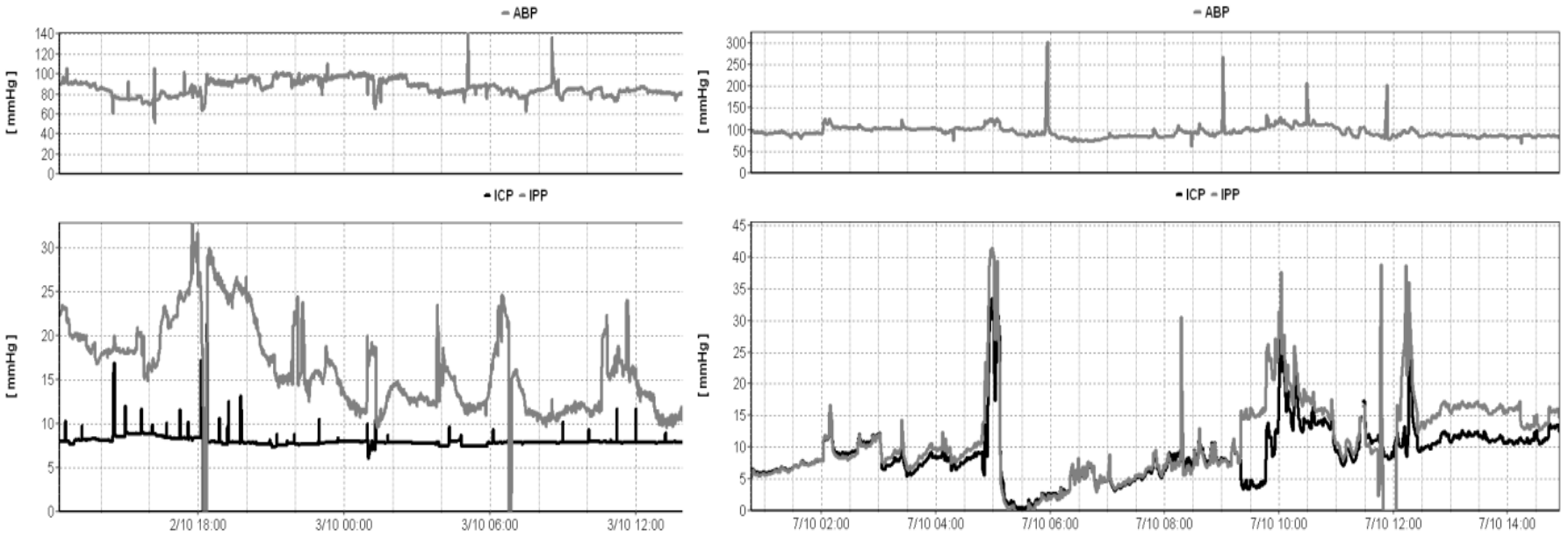

Figure 4.5. **Monitoring with an External Ventricular Drain**. A recording featuring arterial blood pressure (ABP) and intraparenchymal pressure (IPP- bottom panel, grey line) together with EVD pressure (ICP- bottom panel, black line) using an external transducer in a patient after poor grade subarachnoid hemorrhage. The left panel demonstrates the results with the drain opened, whereas the right panel demonstrates results with the drain closed. With an open EVD, the two pressure readings failed to correlate. EVD pressure is held constant at a value representing the calibrated level of the drain above the heart. With a closed EVD (right panel), the two measured pressure values correlate over time.

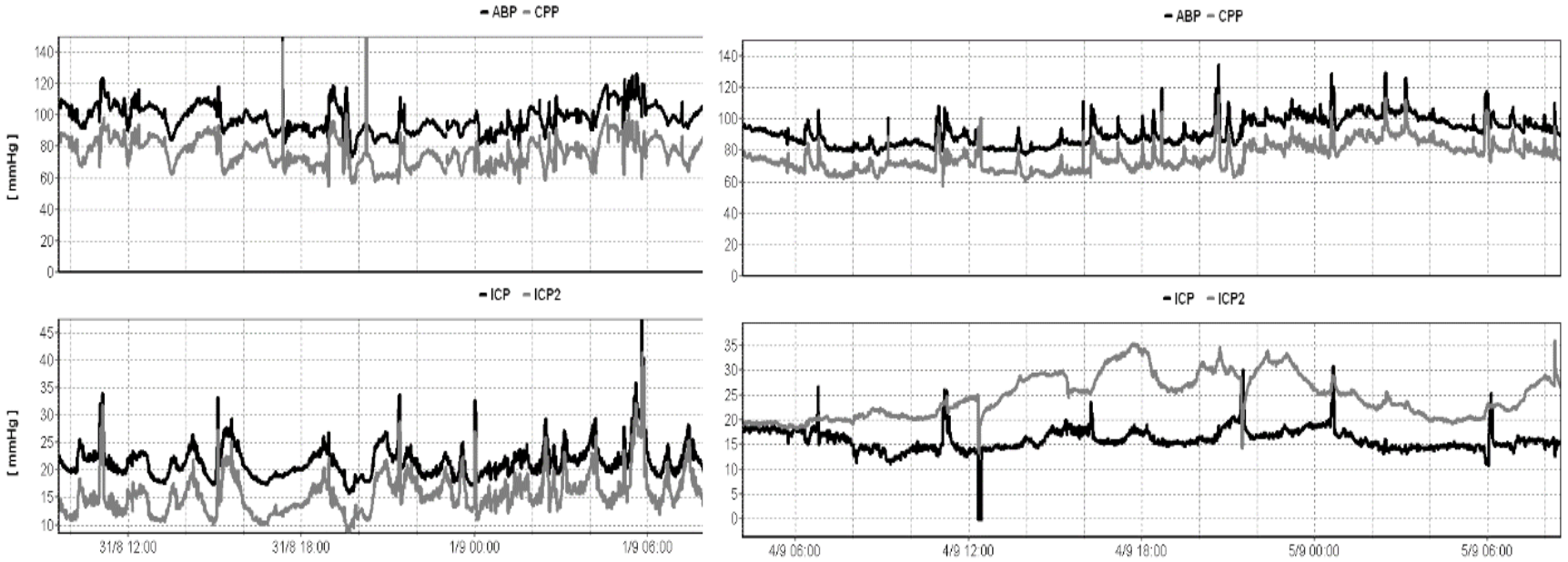

Figure 4.6. **ICP Sensor Discrepancies**. A contradictory presentation of ICP recorded in one patient after TBI. ICP was recorded using two intraparenchymal microsensors (ICP- left hemisphere, ICP2- right hemisphere). In the left panel, the two pressures are very well-correlated in time, even though around 6 mm Hg of constant difference between the two readings is observed. In the right panel, in contrast, the difference is seen to have increased to 20 mm Hg three days later. This patient suffered from diffuse brain injury, without midline shift. The reason for the difference in readings was elusive. The true value of the ICP cannot be determined from these sensors.

As illustrated in Figure 4.6, ICP is not uniformly distributed within the cranial cavity. The ICP sensor can only report the value that is locally available[121]. In the brain parenchyma, these values are in fact not ICP (the pressure of the CSF fluid) but values of the tensor of forces in the parenchyma. Discrepancies between recorded intraparenchymal ICP values appear to be unavoidable with the current monitoring techniques. Treatment is quickly administered especially where protocols to this effect have been initiated. While pressure spikes might command more interest than low ICP, falsely low and normal values may be the result of ICP sensor dysfunction and must be evaluated in accordance with the specifics of the clinical context[124,141].

4.2.5 Comparison of ICP Sensor Performance with Laboratory Bench Testing

Prior to regulatory approval, most ICP sensors undergo routine laboratory "bench testing" to confirm their performance relative to manufacturing specifications for zero drift standards and overall measurement accuracy. The Cambridge experimental bench test procedure mimics CSF and physiological compliance[142]. A bottle is filled with deionized water, leaving 20 mL of air to be removed during dynamic catheter testing. The bottle is then submerged horizontally in a water bath at a constant temperature of 35°C. Static pressure on the bottle (representing pressure detected by ICP catheters) and reference static pressure (representing true ventricular pressure) are compared by changing the height of a water column in a 1.5 m graded vertical tube. Static pressure is released in intervals by allowing the water to flow out of an opened stopcock; conversely, pressure is increased by infusing fluid into the tubing[143,144] (Figure 4.7, below).

Maximal zero drift measurements for a variety of ICP sensors were collected from the existing body of literature. They are presented in Table 4.2 (below). Tables 4.3 and 4.4 (below) display literature-based comparisons of ICP sensors to each other and to CSF reference pressure, respectively.

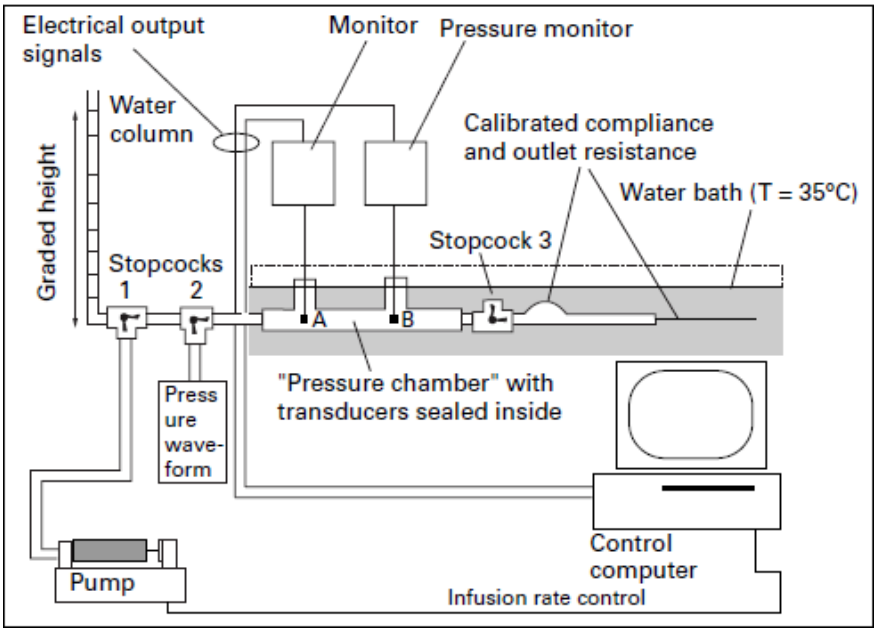

Figure 4.7. **Bench Test Procedure**. A sophisticated, computer-controlled rig was used to assess the compliance of ICP sensors and responsiveness to increased pressure loads. A detailed description can be found in Czosnyka et al.[142].

Table 4.2. Comparison of Zero Drift Among Different ICP Sensors. Zero drift refers to a drift in device calibration that can be remedied by resetting the zero point. ICP sensors that cannot be recalibrated *in-situ* (fiberoptic or piezoelectric strain gauge sensors) and even those that can be (pneumatic sensors) often present inaccurate assessments of ICP to clinicians that can misinform treatment proceedings. Each sensor is susceptible to zero drift, with comparative observations presented here. *mm Hg – millimeters of mercury*.

Reference	**Sensor**	**Sensor Type**	**Maximal Drift (mm Hg/day)**	**Comments**
Allin et al. (2008)[143]	Sophysa Pressio	Piezoelectric Strain Gauge	<0.05	Over a 7-day period
Allin et al. (2008)[143]	Codman MicroSensor	Piezoelectric Strain Gauge	<0.05	Over a 7-day period
Al-Tamimi et al. (2009)[145]	Codman MicroSensor	Piezoelectric Strain Gauge	2.0	Median value; 108 *in-situ* hours (median); drift was found to increase over time (Spearman's correlation coefficient = 0.342; p= 0.001); drift ≥ 5.0 mm Hg found in 20% of sensors
Citerio et al. (2004)[146]	Raumedic Neurovent-P	Piezoelectric Strain Gauge	0-2.0	Overall drift past 5 days; precise measurements for long-term, continuous recording
Citerio et al. (2008)[147]	Raumedic Neurovent-P	Piezoelectric Strain Gauge	±3.0	Clinical application of Citerio et al. (2004)[51]; 12-17% failure of sensor to accurately measure ICP (n=99)
Czosnyka et al. (1996)[144]	Camino 110-4B	Fiberoptic	<0.8	24-hour period
Czosnyka et al. (1996)[144]	Codman MicroSensor	Piezoelectric Strain Gauge	<0.8	24-hour period
Czosnyka et al. (1996)[148]	InnerSpace Medical ICP	Spectral Frequency	<0.8	24-hour period; zero drift <0.4 mm

	Monitoring Catheter Kit (OPD-SX)			Hg measured at a static pressure of 0 mm Hg
Czosnyka et al. (1997)[142]	Camino 110-4B	Fiberoptic	<0.7	24-hour period
Czosnyka et al. (1997)[142]	Spiegelberg	Pneumatic	<0.7	24-hour period; hourly adjustments to zero produced <0.3 mm Hg drift
Gelabert-González et al. (2006)[149]	Camino 110-4B	Fiberoptic	7.3 ±5.1	Mean value; clinical assessment of 1000 sensors: 79 sensors (12.6%) showed no zero drift on removal; mean monitoring time of 58.4 ±8.6 hours
Gray et al. (1996)[150]	Codman MicroSensor	Piezoelectric Strain Gauge	0-1.0	24-hour period; sensors inserted in both parenchymal (mean zero drift: 0.312 mm Hg) and subdural (mean zero drift: 0.475 mm Hg) locations
Koskinen et al. (2005)[151]	Codman MicroSensor	Piezoelectric Strain Gauge	0.9±0.2	Zero drift not correlated with duration of monitoring (analysis of data recorded over 7.2 ± 0.4 days; p= 0.9, Pearson R=0.002)
Lang et al. (2003)[152]	Spiegelberg	Pneumatic	≥±2.0	Average monitoring time of 10 days; sensors inserted in both intraparenchymal and subdural locations
Lilja et al. (2014)[153]	Raumedic Neurovent-P	Piezoelectric Strain Gauge	±2.0	Assessment of hydrocephalus patients (n=21); median duration

				of sensor implantation was 288 days; poor compatibility with ICP curve visualization software
Martínez-Mañas et al. (2000)[154]	Camino 110-4B	Fiberoptic	0±2.0 in the first 24 hours, then <±1.0 per day	56 probes tested to confirm manufacturer specifications; 60.71% complied with zero drift standards, 39.28% drifted to positive or negative values; no observed correlation between monitoring duration and zero drift (p=0.27)
Morgalla et al. (1999)[155]	Camino 110-4B	Fiberoptic	1.0-2.0	Microsensor accuracy was reported: 24-hour period (0.80 mm Hg drift), measurements binned at 5 mm Hg pressure intervals between 0-80 mm Hg; 10-day drift measured at the same intervals (8.0 mm Hg)
Morgalla et al. (1999)[155]	Codman MicroSensor	Piezoelectric Strain Gauge	4.0≥	Microsensor accuracy was reported: discrepancies observed at pressures ≥60 mm Hg; 24-hour period (0.95 mm Hg drift), measurements

				binned at 5 mm Hg pressure intervals between 0-80 mm Hg; 10-day drift measured at the same intervals (2.0 mm Hg)
Morgalla et al. (1999)[155]	Epidyn	Epidural	>8.0	Microsensor accuracy was reported: underestimated ICP, especially at higher pressures; 24-hour period (1.20 mm Hg drift), measurements binned at 5 mm Hg pressure intervals between 0-80 mm Hg; 10-day drift measured at the same intervals (15.0 mm Hg)
Morgalla et al. (1999)[155]	Gaeltec ICT/B	Epidural	4.0≥	Microsensor accuracy was reported: 24-hour period (1.5 mm Hg drift), measurements binned at 5 mm Hg pressure intervals between 0-80 mm Hg; 10-day drift measured at the same intervals (10 mm Hg)
Morgalla et al. (1999)[155]	HanniSet	External Ventricular Drain	1.0-3.0	Microsensor accuracy was reported: 24-hour period (0.2 mm Hg drift), measurements binned at 5 mm

				Hg pressure intervals between 0-80 mm Hg; 10-day drift measured at the same intervals (1.0 mm Hg)
Morgalla et al. (1999)[155]	Medex	External Ventricular Drain	2.0-4.0	Microsensor accuracy was reported: 24-hour period (1.8 mm Hg drift), measurements binned at 5 mm Hg pressure intervals between 0-80 mm Hg; 10-day drift measured at the same intervals (3.5 mm Hg)
Morgalla et al. (1999)[155]	Spiegelberg	Pnematic	<4.0 at pressures >50mm Hg; ≤6.0 at pressures >60 mm Hg	Microsensor accuracy was reported: 24-hour period (2.1 mm Hg drift), measurements binned at 5 mm Hg pressure intervals between 0-80 mm Hg; 10-day drift measured at the same intervals (7.0 mm Hg)
Morgalla et al. (2002)[156]	Camino 110-4B	Fiberoptic	2.9	Median values for mean absolute pressure changes; 10-day drift: 4.0 mm Hg (transducers tested at 0-50 mm Hg)
Morgalla et al. (2002)[156]	Gaeltec ICT/B	Epidural	5.2	Median values for mean absolute pressure changes; 10-day drift: 9.0

				mm Hg (transducers tested at 0-50 mm Hg)
Morgalla et al. (2002)[156]	HanniSet	External Ventricular Drain	0	Median values for mean absolute pressure changes; 10-day drift: 0 mm Hg (transducers tested at 0-50 mm Hg)
Morgalla et al. (2002)[156]	Spiegelberg	Pneumatic	2.4	Median values for mean absolute pressure changes; 10-day drift: 2.0 mm Hg (transducers tested at 0-50 mm Hg)
Norager et al. (2018)[124]	Raumedic Neurovent-P	Piezoelectric Strain Gauge	2.5	Median baseline drift in 19 sensors (median implantation time of 241 days)
Piper et al. (2001)[157]	Camino 110-4B	Fiberoptic	-0.67	Mean zero drift (3-day median implantation time); median drift reported at -1 mm Hg; more than 50% of the catheters had an observed drift >±3 mm Hg

Table 4.3. Agreement Between Intraparenchymal ICP Sensors. This table highlights the main differences in measurement capacity found between popular intraparenchymal ICP sensors in laboratory* and clinical** studies of TBI patients; these results may influence the decision to introduce one sensor over another in clinical practice. *ICP – intracranial pressure, mm Hg – millimeters of mercury.*

Reference	**Sensor 1**	**Sensor 2**	**Agreement**	**Comments**
*Allin et al. (2008)[143]	Codman MicroSensor	Sophysa Pressio	Excellent agreement (reported Pearson *R*= 0.999)	Codman devices require additional bridge amplifiers to connect to computerized data streaming
**Banister et al. (2000)[158]	Camino 110-4B	Codman MicroSensor	ICP measured within 10 mm Hg in 11 patients; >10 mm Hg disparity in 6 patients	Small sample size (*n*=17); Codman was "misleading" in 18% of patients; preference for Camino sensors to register clinical events
*Czosnyka et al. (1996)[144]	Camino 110-4B	Codman MicroSensor	No significant differences in zero drift at a static pressure of 20 mm Hg; comparable for pulsatile pressure measurement; Camino temperature drift (0.27 mm Hg/◦C) significantly higher than Codman; <0.3 mm Hg static error (Camino) vs. <2 mm Hg static error	Codman is preferred for clinical use; also bench tested InnerSpace Medical's ICP Monitoring Catheter Kit (OPX-SD), which had the lowest 24-hour zero drift compared with both Codman and Camino sensors, but otherwise did not perform as well

			(Codman); very good frequency detection for both (bandwidth >30 Hz)	
*Czosnyka et al. (1997)[142]	Camino 110-4B	Spiegelberg	Camino temperature drift recorded at 0.27 mm Hg/◦C; excellent agreement between transducers at pressures 0-100 mm Hg over 20 minutes (reported Pearson *R*=0.99); static error <1 mm Hg up to pressures of 40 mm Hg that increased to 5 mm Hg at 100 mm Hg (Spiegelberg) vs. static error <0.7 mm Hg (Camino)	Spiegelberg devices are less expensive, but are "limited by low frequency response and non-linear distortion as amplitude underestimation increases [with] mean pressure"
**Eide (2006)[159]	Camino 110-4B	Codman MicroSensor	Differences >5 mm Hg observed in 13% of ICP recordings	Extremely small sample size (*n*=3); discrepancies attributed to differing baseline pressures
**Eide & Bakken (2011)[160]	Codman MicroSensor	Raumedic Neurovent-P	Differences in baseline pressure ≥2 mm Hg in 96% of Codman sensors and 53% of Raumedic sensors observed as a result of electrostatic	Discrepancies in baseline pressures (either sudden or gradual shifts) ≥10 mm Hg can significantly affect ICP management

	discharges (0.5-5kV)

Table 4.4. Agreement Between Intraparenchymal Sensors and CSF Pressure Measurement in Clinical Studies. Sensors that most accurately reflect reference pressures within the CSF demonstrate a clear advantage in ICP monitoring. It is worth noting that although each sensor sacrifices measurement accuracy to inherent differences between atmospheric and cranial compartment pressures, technical issues related to either surgical insertion or sensor composition can influence discrepancies between "real" and measured pressures. *CSF – cerebrospinal fluid, ICP – intracranial pressure, and mm Hg – millimeters of mercury.*

Reference	Sensor	Differences from CSF Pressure	Comments
Brean et al. (2006)[161]	Codman MicroSensor	Mean difference between Codman and ventricular reference pressure reported at -0.71 ± 6.8 mm Hg	Data obtained from a case study; measurements from single wave parameters
Bruder et al. (1995)[162]	Camino 110-4B	Camino underestimated ventricular pressure by about 9 mm Hg	95% confidence interval of bias: -9.8 to 27.8 mm Hg; small sample size (n=10), male patients only
Chambers et al. (1993)[163]	Camino 110-4B	Reads an average of 1.15 mm Hg higher than ventricular pressure	
Chambers et al. (2001)[164]	Spiegelberg	Mean ICP differences >±1.5 mm Hg between Spiegelberg and ventricular pressure	Reported results obtained from 10 patients; small overall sample size (n=11)
Childs & Shen (2015)[165]	Raumedic Neurovent-P	Mean difference between intraparenchymal and ventricular pressure measured at –0.832 mm Hg	Tissue pressure is reported to be marginally lower than ventricular pressure (p=0.379); temperature also did not vary significantly between local pressure sites (p=0.92); small sample size (n=17)

Crutchfield et al. (1990)[166]	Camino Model 420	Camino estimated ventricular pressure within ±3 mm Hg over a 0-30-mm Hg pressure range; robust correlation of 0.977	Study conducted in dogs
Eide et al. (2012)[167]	Codman MicroSensor, Edward's fluid sensor connected to an external ventricular drain (Truwave PX-600 F Pressure Monitoring Set, Edwards Life sciences LLC, Irvine, C.A., U.S.A.), and Spiegelberg	Significant differences in mean ICP reported >5 mm Hg between ventricular pressure and each sensor type	Comparison of solid strain gauge sensors with either fluid or air-pouch sensors; "simultaneous monitoring of ICP using two solid sensors may show marked differences in static ICP but close to identity in dynamic ICP waveforms"; solid ICP sensors exhibit less disparity from "true" ICP and are preferred for clinical use; small sample size (n=17)
Gopinath et al. (1995)[168]	Codman MicroSensor	Mean difference between Codman and ventricular pressure measured at 0.5 ± 2.6 mm Hg	Small sample size (n=25)
Koskinen et al. (2005)[151]	Codman MicroSensor	Strong agreement between the Codman and ventricular pressure (p<0.0001, Pearson R= 0.79)	Mean ICP in the ventricles measured at 18.3 ±0.3 mm Hg vs. 19.0 ±0.2 mm Hg measured by Codman (n=128)
Lang et al. (2003)[152]	Spiegelberg	Absolute difference between Spiegelberg and intraventricular pressure >±3 mm Hg in 99.6% of paired readings and >±2	Average Bland Altman bias of 0.5, with 10% lower Spiegelberg readings with ICP >25 mm Hg (n=87)

		mm Hg in 91.3% of paired readings	
Lenfeldt et al. (2007)[169]	Codman MicroSensor	Measured differences between Codman and lumbar pressure observed at -0.75 ±2.10 mm Hg	Agreement between intracranial and lumbar pressure assessed patients with normal pressure hydrocephalus (*n*=10)
Schickner & Young (1992)[170]	Camino 110-4B	Mean ICP difference between the Camino and the ventricular catheter of 9.2 ±7.8 mm Hg	ICP recorded for up to 118 hours; small sample size (*n*=10)

4.2.6 Discussion

Two ICP microsensors implanted in the same brain do not necessarily show the same pressure readings. On the basis of the known literature and of our own measurements, one can estimate the average 95% confidence limit of agreement to be around 6 mm Hg – this should be taken as the inherent accuracy of ICP measuring microsensors after implantation. While *in-vitro* bench-test studies demonstrate much better accuracy, accuracy decreases *in-vivo*.

To illustrate this point, we performed the following experiment. An animal brain was submerged in a sealed jar and two microsensors were placed at the same depth beneath the top of the water column; one microsensor was inside the brain tissue and the other was in the surrounding water. When the jar was pressurized, the transducer in the water exhibited a pressure that was 20 mm Hg higher than that in the brain. This constant difference was maintained over several hours (Fig 4.8). In the living brain, there are still cerebral blood microcirculation pressure differences, but at a much lower rate (microsensor tips are in a semi-liquid extravascular environment).

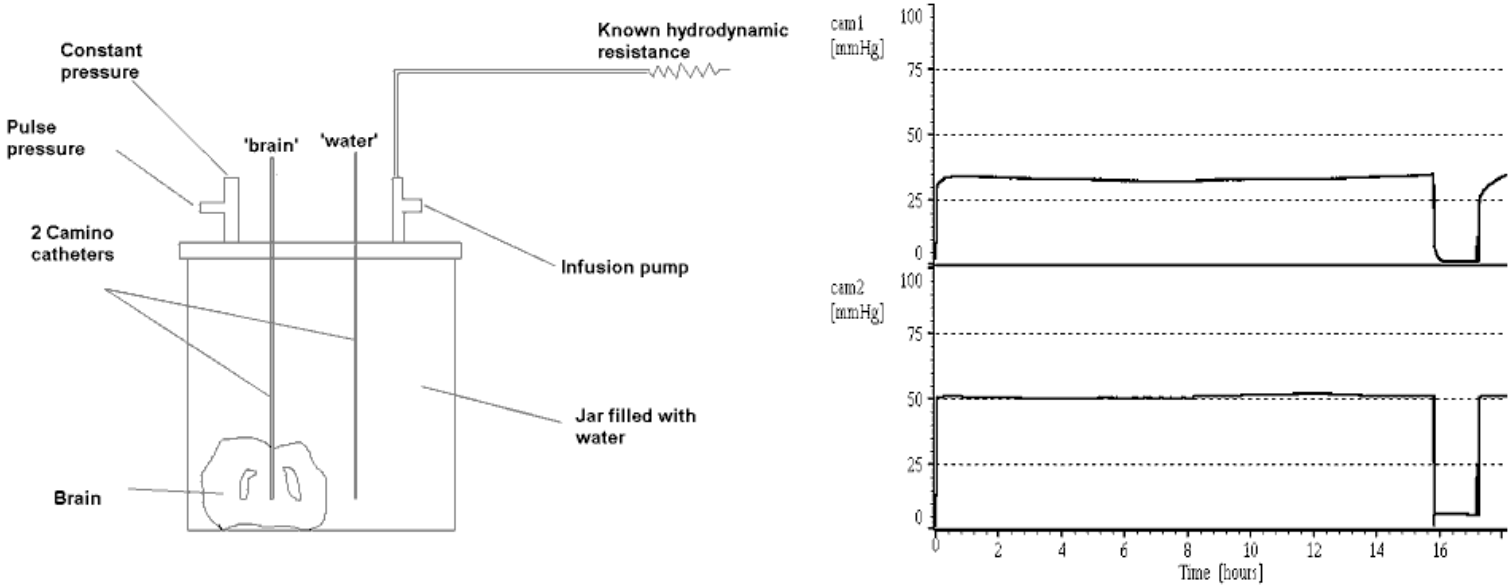

Figure 4.8. The "dead brain" in a jar (pressurized externally). The microsensor in the brain tissue shows a pressure measured at nearly 20 mm Hg higher than that of the water. This difference remained unchanged over a long period.

Comparison of Intraparenchymal Fiberoptic vs. Piezoelectric Strain Gauge Sensors

Intraparenchymal ICP probes, particularly the fiberoptic Camino 110-4B sensor, and strain gauge probes, particularly the Codman MicroSensor, are very popular among neurocritical care centers for TBI management. In a laboratory bench test[144], both the Camino and Codman sensors exhibited zero drift <0.8 mm Hg over 24 hours at a static pressure of 20 mm Hg. In comparison, the Camino sensors were found to have significantly higher temperature drift than the Codman sensors[142]. In a later paired comparison of clinical ICP recordings from the Camino and Codman sensors, however, the Codman was observed to be deviating by as much as 10 mm Hg in 18% of patients[158]. Another clinical assessment of the two sensors suggested >5 mm Hg differences in 13% of paired ICP recordings[159].

Paired measurements from Codman MicroSensor and the Sophysa Pressio sensor have been reported to be in excellent agreement in a laboratory bench test setting with a 7-day zero drift <0.05 mm Hg and static accuracy >0.5 mm Hg. over the tested range of 0-100 mm Hg[143]. Clinical testing has yet to be completed.

A paired comparison of the Codman MicroSensor and the Raumedic Neurovent-P sensor revealed significant differences between baseline pressures (≥2 mm Hg in 96% of the Codman sensors and in 53% of the Raumedic sensors) due to either sudden or gradual shifts in baseline pressure. These measurement discrepancies were attributed to electrostatic discharges (0.5-5.0kV)[160]

Comparison of Intraparenchymal versus Pneumatic Sensors

Pneumatic sensors can be recalibrated to atmospheric pressure following implantation, unlike other intraparenchymal systems. Czosnyka et al.[142] compared the zero drift accuracy of the fiberoptic Camino 110-4B model to the Spiegelberg ICP Monitoring System sensor. Both sensors reported zero drift <0.7 mm Hg in a 24-hour period. The Spiegelberg's automatic hourly adjustments contributed 0.3 mm Hg (42.9%) to the overall measurement drift. Morgalla et al.[155] compared the Speigelberg device to competitors and concluded that it exhibited less zero drift over a 10-day period[155,156]. In contrast, the Spiegelberg device showed greater error than the Camino and Codman

sensors at pressures >60 mm Hg, and tended to underestimate pressures in bench testing as dynamic pressure loads increased[142].

Overall Accuracy of ICP Sensors with Respect to CSF Reference Pressure

The efficacy of an ICP sensor for clinical use is dependent on its competence to accurately reflect ventricular CSF pressure. In one report, ICP readings from the fiberoptic Camino 110-4B sensor seemed to exceed true ventricular pressure by 1.15 mm Hg[163]. Another indicated the mean differences to be as high as 9.2±7.8 mm Hg[170].

The literature tends to be more supportive of the accuracy of piezoelectric strain gauge sensors. Koskinen et al.[151] observed strong agreement between mean ventricular ICP and the Codman probe (18.3±0.3 mm Hg vs. 19.0±0.2 mm Hg, respectively) in a population of 128 neuro-critically ill patients. The Codman MicroSensor was also found to approximate lumbar CSF pressure in hydrocephalus patients, with measured differences of -0.75±2.10 mm Hg[169]. The Spiegelberg pneumatic sensor exhibited an absolute difference of 3 mm Hg between the transducer and intraventricular pressure. Spiegelberg was also reported to produce ICP values 10% lower than the reference pressure, especially when ICP >25 mm Hg[152].

Current evaluations of ICP measurement accuracy for intraparenchymal sensors provide an average error of ±6.0 mm Hg, due to the fact that intraparenchymal pressure is not defined as a global value and can exhibit local pressure differences. Although zero drift remains a significant issue, ICP pulse waveforms are satisfactorily recorded by contemporary sensors, with good frequency properties (i.e. recorded pulse waveforms are not distorted).

4.2.7 Limitations and Future Design Considerations

This portion of this chapter is primarily a narrative review, although factual tables were provided. There is a vast heterogeneity in the methods, error presentations, and measurement protocols (both in-vitro and in-vivo) which made any attempt to perform a formal metanalysis impossible.

To improve resistance to infection following sensor insertion, future devices should function without cable connections to main monitors. Although the first implantable sensors are available (Raumedic, Miethke), accuracy and sampling frequency are unsatisfactory; these selective telemetric systems are additionally challenged to maintain a reliable power supply and to stream undistorted signal transmission to external recording units[171]. Although telemetric sensors cannot provide detailed ICP pulse waveform information, they can be useful in the determination of the pressure reactivity index (PRx) and optimal cerebral perfusion pressure (CPP_{opt}) in acute care settings[172].

4.2.8 Conclusions

Precise ICP monitoring is a key tenet of neurocritical care. Intraparenchymal piezoelectric strain gauge sensors are commonly implanted to monitor ICP. However, measured intraparenchymal pressure is not always equal to real ICP (the pressure measured in the CSF) – the average discrepancy may be ± 6 mm Hg. Accounting for zero drift is vital. Laboratory bench testing reveals the shortcomings of current ICP sensors, although the results from bench tests may not always compare to *in-vivo* observations. It is important to continually revisit the performance of ICP monitors to optimize sensor and monitoring recommendations as ICP monitoring technology evolves[149,152,153,156,173]. Despite awareness of ICP measurement inaccuracies, mean ICP values reported by these sensors are still routinely incorporated into and relied upon in current neurocritical care practices. The following section of this chapter seeks to account for ICP sensor drift by exploring the role of the compensatory reserve in the creation of a new, potentially more accurate ICP metric.

4.3 Compensatory Reserve-Weighted

Intracranial Pressure and its Association with Outcome after Traumatic Brain Injury

4.3.1 Introduction

ICP is an essential monitoring modality that can provide feedback needed for appropriate and timely management of patients following TBI. High ICP has been associated with fatal outcome as a result of TBI[174]. From this point of view, it is reasonable to monitor and to avoid high ICP during the intensive care period. Although the monitoring of ICP per se cannot improve outcome[175], a combination of monitoring with efficient management can assist in the prevention of mortality[176].

Efficient management of raised ICP requires an understanding of intracranial pressure–volume relationships. An increase in ICP is associated with a change in volume of any of the four essential intracerebral compartments: arterial and venous blood, CSF, and the volume of brain tissue including any space-occupying lesions (i.e., hematomas, tumors, abscesses)[177]. It is important to distinguish between different causes of raised ICP, as clinical strategies to fight intracranial hypertension depend upon which component is elevated. For example, changes in transmural pressure and thus cerebral arterial blood volume may elevate ICP to very high levels in a matter of tens of seconds (these events are known as plateau waves), secondary to massive, intrinsic arterial dilatation[178]. These extreme fluctuations in ICP that affect the pressure-volume balance are influenced by a patient's autoregulatory status; if cerebral autoregulation is disturbed, high ICP cannot be mitigated by adjustments in ABP or excess CSF drainage[94]. Rapid, short-term hyperventilation usually reduces ICP in such cases. The cerebrospinal fluid circulatory component may elevate ICP in acute hydrocephalus[179], in which external ventricular drainage is helpful. Venous outflow obstruction may also elevate ICP, and can be combated with proper head positioning or investigation of possible venous thrombosis. Finally, if ICP is elevated due to brain edema or a space-occupying lesion, osmotherapy or surgical intervention (including decompressive craniectomy) may be recruited, as the arterial bed would collapse at very high ICP and prohibit blood flow at a designated critical closing pressure (CrCP)[85]. This

phenomenon, first described by Burton in 1951[180] as the sum of ICP and vascular wall tension (WT), may also explain the vascular mechanics of failing autoregulation when patients exhibit intracranial hypertension[85].

Harnessing the additional information contained in the ICP signal could be an operable way to determine whether elevated ICP requires aggressive management or a more conservative approach. While ICP above 20–25 mm Hg increases the risk of mortality more than twofold, a more exact threshold in a large patient cohort has been demonstrated at 23 mm Hg[21]. It has also been stressed that this threshold may be variable between patients (and perhaps even within a patient), in the same way that has been proposed for CPP[61]. In a retrospective survey, Lazaridis[181] combined ICP with a measure of cerebrovascular pressure reactivity, and observed that the threshold for ICP associated with the loss of cerebral pressure reactivity can vary from 18 to 35 mm Hg. Additionally, this study demonstrated that these variable ICP thresholds can be further individually-tailored to patients when based on PRx, a strong predictor of outcome[1] rather than on the fixed Brain Trauma Foundation guidelines of 20 mm Hg and 25 mm Hg[182]. If clinicians strictly adhere to these values only when revisiting ICP management protocols, some patients may not receive life-saving treatment if their ICP is not "objectively" worrisome.

The cerebrospinal pressure–volume compensatory reserve can be illustrated by an exponential pressure–volume curve. However, at both extremes of the pressure–volume curve, the relationship may not be exponential. With a low intracranial volume, increases in volume are linearly associated with an increase in ICP. With further increases in intracranial volume, a classical exponential relationship occurs between increases in volume and pressure, in which the value of one component rises rapidly as a result of incremental increases in the other. Finally, at extreme levels of intracranial volume, further increases in volume are weakly transmitted to ICP, and the curve deflects to the right. This occurs at CPP values well below the lower limit of autoregulation, where the deflection to the right is due to the hypothetical collapse of cerebral arterial vessels (Fig. 4.9) as cerebral blood flow becomes pressure-passive[85]. This phenomenon has been described by Lofgren et al.[139] through direct observations

of pressure during the experimental inflation of a subdural balloon and has also been demonstrated as an increase in the pressure–volume index at very high levels of ICP[183].

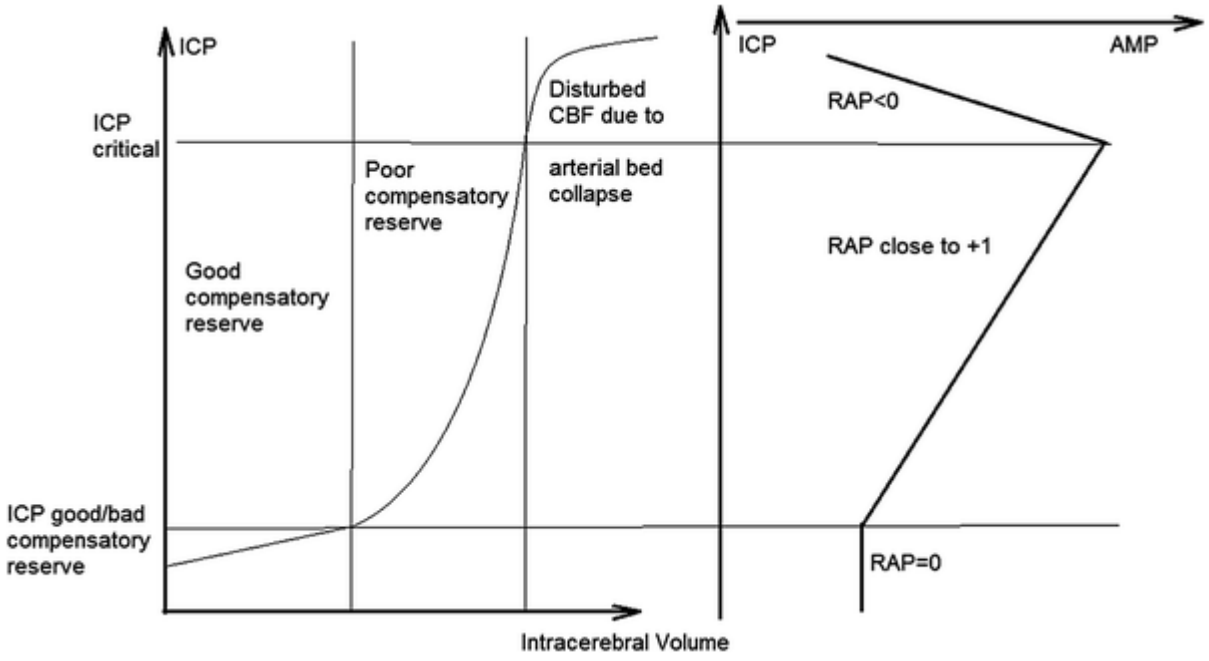

Figure 4.9. **Relationship Between RAP and ICP.** Schematic diagrams showing the foundation of the model behind the general relationship between the RAP (R—correlation, A—amplitude, and P—pressure) index and mean intracranial pressure (ICP) [139,140,184,185]. *Left*: The extended shape of the pressure–volume (P/V) curve showing three zones: good compensatory reserve when the P/V relationship is linear, poor compensatory reserve when the P/V curve is exponential, and the zone of disturbed CBF due to arterial bed collapse. Along the *y*-axis, there are two ICP thresholds: the first between the linear and the exponential zones, delineating good versus affected compensatory reserve. Almost all patients after TBI (exception—those after craniotomy) have poor compensatory reserve. The second threshold is: 'critical ICP,' above which the curve deflects to right and the system gains some extra compensatory reserve due to the collapse of cerebral microvasculature. This is associated with the discontinuity of CBF. *Right*: The associated relationship between the pulse amplitude of ICP (AMP) and mean ICP. In the zone of good compensatory reserve, AMP does not depend upon mean ICP. In the exponential zone (poor compensatory reserve), AMP increases with increasing mean ICP. For ICP above the 'critical threshold,' AMP decreases when ICP increases further. The RAP index is zero within the zone of good compensatory reserve, +1 with poor compensatory reserve, and negative above the 'critical ICP' level.

The shape of the pressure–volume curve described, according to the classical interpretation of Marmarou[140], has implications for the relationship between the changes in mean ICP and the changes in the amplitude of ICP pulsations (AMP). When plotting these pulsations against the incoming cerebral blood volume load (modeled by the height of the AMP signal), an exponential pressure-volume curve appears when mean ICP rapidly increases as a function of small volumetric step-increases[185]. However, these changes in volume may be affected by fluctuations in arterial CO_2 (a potent vasodilator), ABP, and underlying arterial pulse pressure[185].

In the linear zone, where pressure–volume compensation is good, AMP is not correlated with mean ICP. In the exponential zone, AMP is positively correlated with increasing mean ICP. Above a critical level of ICP, at the point of rightward deflection of the pressure–volume curve, AMP starts to decrease with rising ICP, resulting in a negative correlation (Fig. 4.9, right panel). Thus, the moving correlation coefficient between AMP and ICP (10-second averages) calculated over a 5-min period has been termed RAP (R—correlation, A—amplitude, and P—pressure) and described[184] as an index of compensatory reserve. It is 0 in the linear zone (good compensatory reserve), +1 in the exponential zone (poor compensatory reserve), and negative at very high ICP levels—indicative of crossing the threshold for "critical ICP".

Incorporating both the potential detrimental effects of position on the pressure–volume curve and the mean ICP, a "compensatory-reserve-weighted ICP" metric can be created as the product of mean ICP and (1–RAP)[186]:

- If the compensatory reserve is good (RAP=0) at low ICP, ICP*(1–RAP) remains low.
- If the compensatory reserve is exhausted (RAP=1) at a medium ICP (which is often the case after TBI, due to brain swelling), ICP*(1–RAP) stays low.
- Conversely, if ICP crosses the "critical threshold", RAP becomes negative and ICP*(1–RAP) increases abruptly—see samples in Fig.4.10a, b.

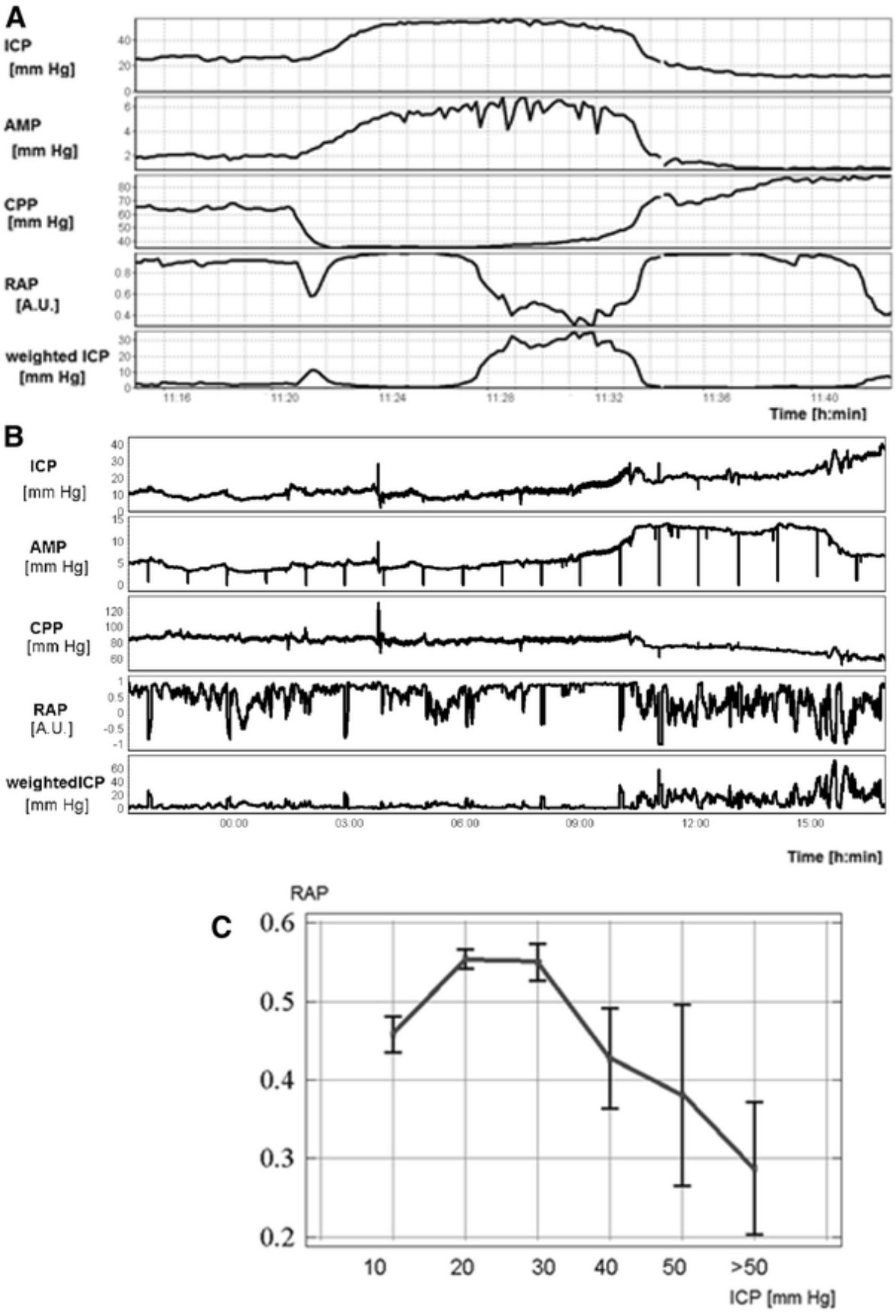

Figure 4.10. **Monitoring "WeightedICP", Mean ICP, AMP, and RAP:** Example of the monitoring of weightedICP, mean ICP, the pulse amplitude of ICP (AMP), the index of

compensatory reserve (RAP), and the statistical relationship between RAP and mean ICP in the whole cohort of analyzed cases**.** *A*) During a plateau wave of ICP, the correlation between AMP and ICP shows a dip at the beginning of the plateau wave—RAP decreases to negative values and weightedICP increases, suggesting that the rise of ICP is associated with cerebrovascular deterioration. *B*) Example of nearly 20 hours of monitoring of a patient with a closed-head injury who gradually developed intracranial hypertension up to 35 mm Hg (starting from a baseline of 12 mm Hg). CPP remained above 60 mm Hg for the whole monitoring period. Gradually-increasing ICP was followed by an increase in pulse amplitude (AMP) and values of RAP close to +1. WeightedICP was below 5 mm Hg in this period. When ICP increased above 25 mm Hg, AMP stabilized and then started to decrease with further increases in ICP. RAP decreased down to zero and even negative values, indicative of reaching a 'critical' value for ICP. WeightedICP started to increase at this point. *C*) Empirical regression of RAP versus mean ICP in a cohort of patients. It indicates that RAP is low with low ICP levels, increases for ICP 20–30 mm Hg, and decreases for ICP above 30 mm Hg. Results of averaging in a large cohort of patients make RAP never ideally equal to 0, +1, or a negative value. However, the general classification is similar (Fig. 4.9). Below 20 mm Hg: good compensatory reserve, between 20-30 mm Hg: poor compensatory reserve, and above 40 mm Hg: intracranial hypertension is interfering with cerebral blood flow. The vertical bars show 95% confidence intervals for mean values, with the red line connecting mean values in each category along the x-axis.

Our current aim is to investigate the metric which translates the absolute mean ICP value to a variable which expresses both the absolute level of intracranial hypertension and the state of the cerebrospinal compensatory reserve.

4.3.2 Methods

Clinical Material

Computer-assisted ICP monitoring has been used in patients receiving critical care after TBI since 1992[187]. Over a nearly 25-year period, we accumulated computer recordings from 1023 patients. Patients were admitted to the Addenbrooke's Hospital Neurosurgical Neuro-Rehabilitation Annex between 1992 and 1995, and from 1995 onward, the Neurocritical Care Unit (NCCU). All patients suffered from TBI, with initial GCS less than 9 (75%) or above 8 who deteriorated later and required intensive care

(25%). The average patient age was 37 years (range: 15–85 years old), and the male/female ratio was 3:5.

Over this period, patients were treated in accordance with various rules ranging from no formal protocol (1992–1994), classical CPP-oriented therapy with a fixed threshold of 70 mm Hg (1994–1996), to a mixed CPP–ICP protocol[184] (from 1997) with a gradually-decreasing threshold of CPP (65, 60 mm Hg). Later, additional monitoring modalities (autoregulation, brain oxygenation, microdialysis, etc.) were introduced into patient assessment [188].

Patients were sedated, intubated, and mechanically ventilated. Interventions were aimed at keeping ICP <20 mm Hg using a step-wise approach of positioning, sedation, ventriculostomy drainage, hypothermia, and finally barbiturate-induced burst suppression of electroencephalography and decompressive craniectomy as rescue therapies. ICP monitoring was conducted over this period as an element of standard clinical care. The use of computer-recorded data was approved by the NCCU Users' Committee and conducted before 1997 as a part of an anonymous clinical audit. After 1997, national ethical approval was obtained (30 REC 97/291).

Monitoring and Computations

ICP was monitored with an intraparenchymal sensor inserted into the frontal cortex (Codman ICP Micro-Sensor, Codman & Shurtleff, Raynham, M.A., U.S.A.) via a burr hole. Data were sampled at 100 Hz with proprietary data acquisition software, which was also used to calculate the RAP index in real time with ICM[140] (pre-2003) and ICM+™ onward[189]. (http://www.neurosurg.cam.ac.uk/icmplus, Cambridge Enterprise, Cambridge, U.K.). All of these signals were then stored digitally for retrospective analysis.

The pulse amplitude of ICP (AMP) was calculated using spectral analysis, which is defined by the detection of fundamental frequencies and the conversion of power associated with a peak at a particular frequency equal to that of heart rate, to the value of AMP updated every 10 seconds. Mean ICP was also averaged within 10-second windows. RAP was calculated as the Pearson correlation coefficient of 30 consecutive values of AMP and ICP, also averaged within 10-second windows. Values were averaged

every 60 seconds. For statistical purposes, patients were characterized by grand averages of mean ICP, AMP, RAP, and "weightedICP" expressed as ICP*(1–RAP). It should be emphasized that RAP and weightedICP calculations are not software-specific. Not only ICM+™ can be used, but also simple macro written for Excel, script for MATLAB, or any homemade code.

Statistical Analysis

Statistical analysis was performed using Statgraphics software. Empirical regression was used to show the non-linear relationships between ICP and RAP, and ICP, weightedICP, and mortality rate. Analysis of variance was used to visualize the differences between variables such as ICP, ICP*(1–RAP), and different outcome categories, with a Kruskal–Wallis statistics number (K) assigned to compare which parameter most strongly differentiated outcome groups. ROC analysis with (AUC) was performed to compare the abilities of weightedICP or ICP to predict mortality.

4.3.3 Results

The distributions of age, sex, GCS, outcome, and mean values of blood pressure, ICP, CPP, and the RAP index are listed in Table 4.5. None of these variables were different between males and females, with the exception of CPP (females: 75 ±12 mm Hg; males: 78 ± 9 mm Hg; $p<0.001$)

Table 4.5. Distribution of outcome plus mean value/standard deviations of monitored parameters *(*R—*correlation,* A—*amplitude, and* P—*pressure).*

Outcome	Mean	SD
Good	22%	
Moderate Disability	25%	
Severe Disability	28%	
Vegetative State	2%	
Dead	23%	
Female/Male Ratio	2:7	
Age	37	16
Glasgow Coma Score (median; 〈25%,75% quartiles)	6; 〈4;9〉	–
Arterial Blood Pressure (mm Hg)	93.3	9.46
Intracranial Pressure (mm Hg)	16.3	8.98
Cerebral Perfusion Pressure (mm Hg)	77.3	10.56
Compensatory Reserve Index RAP (a.u.)	0.53	0.22

Examples of individual recordings during plateau waves of ICP and in patients who died from refractory intracranial hypertension are given in Fig. 4.10A, and 4.10B. In both cases, RAP became negative at increased ICP levels. In the case of refractory intracranial hypertension, it was at the level of 84 mm Hg; with respect to plateau waves, it was at 47 mm Hg. We can expect that these "critical ICP" levels (84 and 47 mm Hg as in the examples in Fig. 4.10 A, 4.10B) change from patient to patient, and may also remain different in various scenarios of ICP elevation (like plateau waves–spikes in ICP of vasogenic origin, and refractory intracranial hypertension, which in most instances is caused by rapidly-evolving brain edema).

The distribution of the RAP coefficient along the variable of ICP presented an inverse U-shaped curve (Fig. 4.10C). Mean ICP is related to mortality after TBI; the distribution of ICP in different outcome groups suggests that in patients who died, ICP is significantly higher ($p<0.05$) than in patients who survived, without a difference between outcome categories among survivors. The multiple range test, Fig.4.11, shows that ICP values for the outcomes of disability (good, moderate, and severe) and vegetative state are homogenous, and ICP for patients who died is greater at $p<0.05$. Compensatory reserve, as described with the RAP index, is best in patients with good outcome and moderate disability, and worsens in patients with severe disability and non-survivors. Vegetative-state patients are underrepresented with only 18 cases in our database (Fig.4.11B). The multiple-range test shows that good and moderate disability form one homogenous group, severely disabled patients another, and patients who died yet another group, with the lowest RAP value ($p<0.05$).

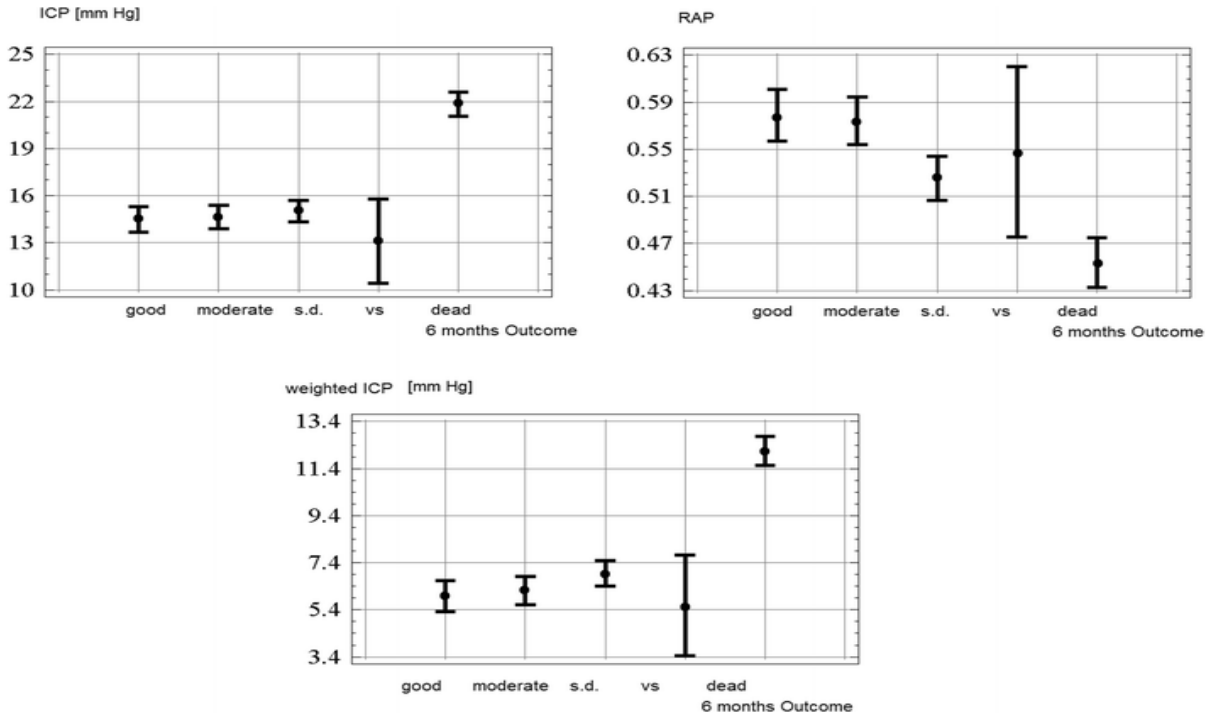

Figure 4.11. **Distribution of Mean ICP, RAP, and weightedICP Between Five Outcome Categories.** Vertical bars show 95% confidence intervals for mean values. Points indicate mean values in each category. WeightedICP (p<0.0001) differentiates between survival and death better than absolute ICP (p<0.0005) and RAP (p=0.002). However, RAP significantly differentiates between severe disability and favorable outcome groups (p=0.004), which is not the case for ICP and weightedICP.

"WeightedICP" only visually shows a more gradual rise of its value through worsening outcome categories than does absolute ICP (Fig.4.11c). A multiple-range test showed homogenous groups identical to those for ICP distribution (p<0.05). Relationships with outcome remained significant when weightedICP and mean ICP were corrected for known factors affecting outcome, such as age and GCS on admission.

Both weightedICP and mean ICP were also able to differentiate between favorable and unfavorable outcome (weightedICP: 6.1 ±4.1 vs. 9.1 ±8.4 mm Hg; p<0.0001 and mean ICP: 14.5 ± 5.3 vs 17.8 ± 10.6 mm Hg; p<0.0001; ANOVA, N=1023). Analysis of variance (Kruskal–Wallis statistics value K) showed higher values of test statistics for weightedICP (K=93) than ICP (K=64) in outcome categorization.

Additionally, ROC analysis indicated greater AUC for weightedICP (0.71) than mean ICP (0.67) for the prediction of mortality. However, these two parameters were not significantly different (De Long test; p=0.12). The best threshold (maximizing jointly sensitivity and specificity) for the mean ICP ROC curve is 19.5 mm Hg, and for weightedICP, 8 mm Hg. Finally, mortality rate depicted as a function of both mean ICP and weightedICP showed ascending distribution (Fig. 4.12). Mortality versus mean ICP showed abrupt increases for ICP between 20-30 mm Hg. For weightedICP, mortality increased more gradually for values between 10-30 mm Hg.

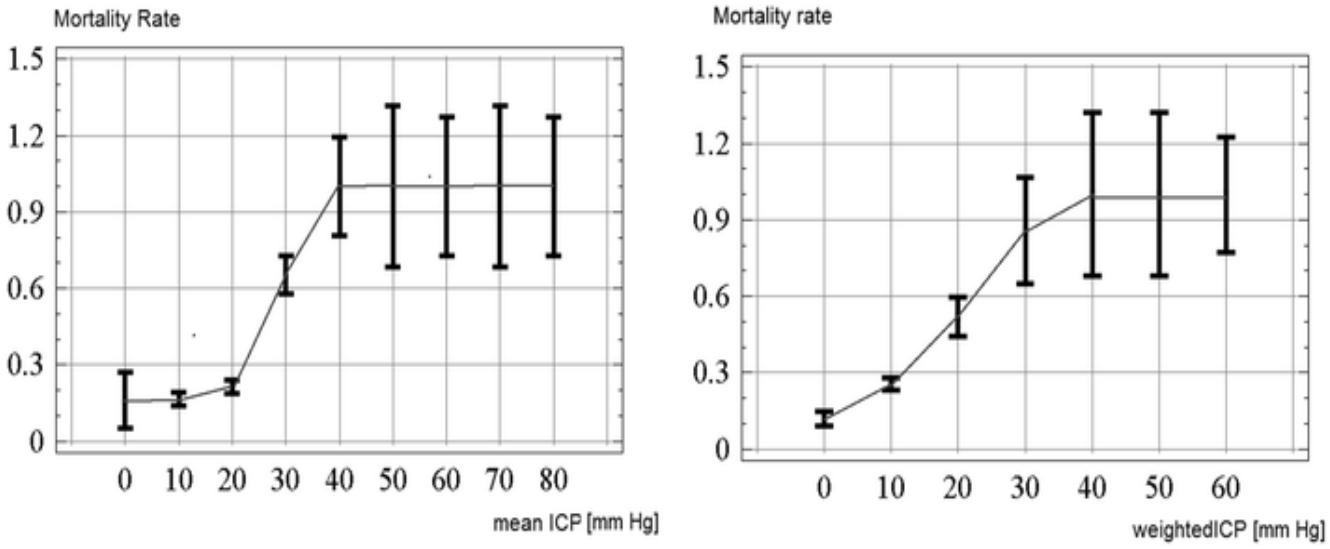

Figure 4.12**. Distribution of mortality rate versus mean intracranial pressure (ICP) and "weighted ICP"**. Vertical bars show 95% confidence intervals for mean values. The line connects mean values in each category along the x-axis.

4.3.4 Discussion

ICP discriminates between life and death in many clinical emergency situations. However, thresholds for increased and normal ICP may vary from patient to patient[85]. An alternative measure of ICP is proposed, which magnifies the state in which raised pressure obstructs cerebral blood flow—presuming that such a situation is detrimental for critically ill patients and is evaluated at the bedside. Hassler et al.[190] observed with TCD that intracranial circulatory arrest begins at the capillary bed, where blood flow stagnates in the distal-to-proximal direction if ICP reaches a terminally-high value. The resulting brain death can also be confirmed with TCD, and is characterized by absent or reversed diastolic flow, or small early systolic spikes in the flow velocity waveform[191]. Continuous monitoring of this "weightedICP" index has the potential to distinguish between situations where increased ICP is still tolerable, or is threatening a deficit of cerebral blood flow able to inflict irreversible brain damage. However, taking into account the retrospective character of this study, this effect should be investigated in a prospective manner. WeightedICP has previously been investigated [186] as "trueICP" in a limited group of patients.

The clinical value of ICP monitoring is still controversial[175]. The existing body of the literature states that since ICP can modulate cerebral blood flow through its direct impact on CPP, it should be monitored minutely to avoid ischemic insults as a component of an efficient management protocol. Short periods of critical rises in ICP (like plateau waves) can drag CPP below the lower limit of autoregulation and cause ischemia. If elevated ICP lasts longer, it starts to associate strongly with mortality[192]. A recent randomized trial was unable to show the clinical benefit of ICP monitoring on outcome following TBI, with patients separated into decompressive craniectomy or ongoing care groups if ICP exceeded 25 mm Hg. After 6 months, patients receiving decompressive craniectomies were found to have lower instances of mortality and disability than those receiving bedside ICP interventions[193]. However, some caveats need to be appreciated—the trial was underpowered, and the monitoring of ICP was not continuous; end-hour instant ICP values were taken for control of the treatment protocol.

There is an open debate over which value of ICP is a best as an input variable for any management protocol: mean ICP, a "dose of ICP"[194], complexity of ICP[195], or anything else. "WeightedICP" was proposed as a shorthand form of "compensatory-reserve-weighted ICP". RAP is an index of compensatory reserve that switches from positive to negative values at high ICP, hypothetically denoting the final deterioration of cerebral blood flow continuity, caused by extremely advanced intracranial hypertension[11]. The exact meaning of a "critical threshold" for ICP is still uncertain. One theory states that at the "critical threshold", diastolic blood pressure becomes equal to critical closing pressure (driven up by increasing ICP), and cerebral arterioles start to collapse during each cardiac cycle. This causes cerebral blood flow to be intermittently discontinued and aggravates ischemia as the lower limit of autoregulation is approached[85]. It also prevents proper transmission of intra-arterial pulsations to the cerebrospinal space due to a decrease in pulsating arterial blood volume, which disrupts the coupling between mean ICP and its pulse amplitude, thus driving RAP towards negative values. Such a situation is clinically rare and requires simultaneous monitoring of ABP, ICP, and TCD blood flow velocity; as TCD is primarily viewed as a research tool and is only applied intermittently, there is not much evidence to support the above hypothesis.

It is demonstrated that weightedICP shows greater values (>10 mm Hg) only if ICP increases above the individualized critical level (see Fig. 4.10). Its value correlates with worsening clinical outcome. WeightedICP is simple to calculate and is expressed as a time trend on the screen of bedside monitoring systems. It may be of assistance in making clinical decisions about the individual safety threshold for ICP in addition to the previously-described autoregulation-weighted ICP[181]. It may be true that weightedICP is a better indicator of ICP-related vascular obstruction, but this should be demonstrated by prospective study.

4.3.5 Limitations

This is a retrospective study utilizing clinical material that has been gathered for over 25 years. Different treatment protocols have been used during this period[188], and thus

different approaches to ICP management may have affected final outcome statistics. This study does not account for variable intensity of treatment. Outcome distribution is not representative for all TBI cases requiring NCCU treatment. Overall, it can be estimated that around 50% of cases over the years spanning from 1992 to 2015 were monitored using bedside computer systems (ICM and ICM+™ software). Also, in this statistical analysis, we did not take into account the potential difference between patients with closed-head injury and craniotomy.

The RAP index can be affected by local differences in compensatory reserve, as demonstrated by Eide and Sorteberg[196] using two different ICP sensors and revealing marked differences in RAP. Furthermore, Hall and O'Kane[197] emphasized its susceptibility to baseline error effects, which also could influence weightedICP. Approximately, 20% of patients underwent decompressive craniectomy in our cohort. Craniectomy on average reduces both ICP and RAP, therefore reducing weightedICP. However, the duration of monitoring after craniectomy is relatively short; therefore, if RAP and weightedICP are reduced, it does not "contaminate" overall results heavily.

Furthermore, our anonymized database does not contain information identifying which patients had infratentorial lesions. Hence, the possibility of calculating the "wrong ICP" and the "wrong RAP" using intraparenchymal frontal cortex sensors cannot be evaluated. In general, all ICP sensors, irrespective of design and manufacturer, are subject to systematic and random measurement inaccuracies that can adversely affect patient care. The ICP values that are streamed from bedside monitors may not be reflective of the patient's true condition, and can misinform essential outcome-predictive calculations such as weightedICP and PRx.

WeightedICP is also a "vasculo-centric" index characterizing the consequences of raised ICP and is exclusive of the additional neuronal mechanisms of TBI when exposed to high ICP, primarily the acute diffuse membrane perturbations that result in chronic neural loss over time[198]. This suggests that increases in ICP may have deleterious effects even in the absence of critical vascular obstruction [198].

Finally, the comparison of Fig. 4.10A–C may appear misleading. One should bear in mind that while in Fig.4.10 A and B we show two individual examples of when RAP becomes negative at two individual "critical ICP" levels, that the curve in Fig.4.10 C is an

effect of the averaging of 1023 individual cases. Given that "critical ICP" levels are different among patients, these averaged RAP values never cross the level of zero.

4.3.6 Conclusions

Compensatory-reserve-weighted ICP ("weightedICP") normally stays below 8 mm Hg. It increases above this threshold when ICP contributes to the final deterioration of patients after TBI.

Chapter 5

Understanding and Modeling of Cerebral Pulsatile Hemodynamics

The following publications formed the basis of this chapter:

- Calviello LA, de Riva N, Donnelly J, Czosnyka M, Smielewski P, Menon DK, Zeiler FA. Relationship Between Brain Pulsatility and Cerebral Perfusion Pressure: Replicated Validation Using Different Drivers of CPP Change. *Neurocritical Care*. 2017 May 25:1-9.
- Calviello LA, Zeiler FA, Donnelly J, Uryga A, de Riva N, Smielewski P, Czosnyka M. Estimation of pulsatile cerebral arterial blood volume based on transcranial doppler signals. *Medical Engineering & Physics*. 2019 Dec 1;74:23-32.

5.1. The Relationship Between Brain Pulsatility and CPP

5.1.1. Introduction

Multi-modal, high-resolution intracranial monitoring for critically-ill neurological patients is becoming standard in most high-volume neurocritical care units. Recent endorsement of multi-modal monitoring has come from a multitude of professional societies associated with the critical care management of these patients[199]. Worldwide interest in noninvasive measurement of various cranial hemodynamic indices has driven the application of TCD in a variety of scenarios, with the goal of correlating MCA flow velocity and pulsatility index (PI) to common invasive measures such as ICP and CPP, as documented within a recent systematic review[200].

The brain is extraordinarily fragile following TBI. Patients are at risk of increasing ICP, and of sudden changes in ABP or CPP that may require immediate clinical intervention. Low CPP is associated with potential instances of delayed cerebral ischemia; conversely, high CPP is associated with edema[28]. The pulsatility index, PI, has been found to be a complex descriptor of several "mutually interdependent" parameters within the brain[28]. In TBI, adequate cerebral circulation is essential for the maintenance of autoregulation. Elevated PI can signal rising ICP, decreasing ABP, low $PaCO_2$, and can additionally inform of both decreasing CPP and of increasing cerebrovascular resistance.

These correlations are particularly relevant to the study of plateau waves, phenomena characterized by unexpected elevations in ICP above 50 mm Hg accompanied by marked depletions of CPP for a duration of at least 5 minutes that either resolve on their own or through treatment with vasopressors. The resolution of plateau waves has been associated with relatively intact autoregulatory mechanisms, as the fluctuations in ICP are attributed to the redistribution of brain volume when CPP changes [178]. In addition to plateau waves, alterations of mean arterial pressure (MAP) can upset the balance of CPP in critically-ill neurological patients, due to the

fundamental nature of ABP within the CPP derivation. Clinical analysis of unstable, decreasing MAP can assist in the ongoing investigation of the relationships between various cerebral hemodynamic parameters.

To delineate the relationships between CPP, ICP, MAP, and TCD parameters, continuous data series through large ranges of CPP and ICP values are ideal. Difficulties with long-term, high-quality TCD signal acquisition have led to limited studies in humans correlating TCD measures to CPP, ICP, and MAP[201] , with some animal studies documenting the relationship[202] and others utilizing mathematical modeling[203] where PI had been found to increase in tandem with the amplitude of the FV waveform[202]. The components of the FV waveform can be further analyzed to provide more information about the underlying cerebral hemodynamic mechanisms of TBI[203]. Ideally, being able to correlate TCD-based PI with ICP pulse amplitude (AMP), MAP, and CPP could bolster the concept of reliable non-invasive measurement of these hemodynamic parameters. A previous study outlined the possibility of an inverse non-linear correlation between PI and CPP, utilizing "spectral" PI (sPI, defined as the first harmonic of the flow velocity (FV) pulse waveform divided by mean FV) in 51 patients with plateau waves and continuous TCD monitoring[202]. The following relationship between PI and CPP (Equation 5.1) was proposed within the supplementary portion of that same manuscript[28]:

$$PI = \frac{A_1}{CPPm} \times \sqrt{(CVR \times Ca)^2 HR^2 \times (2\pi)^2 + 1} \qquad [5.1]$$

In this equation, A_1 represents the fundamental harmonic of ABP, CPPm the calculated mean of recorded CPP values, CVR the cerebrovascular resistance, Ca the cerebral arterial compliance, and HR the heart rate.

It was hypothesized that the validation of relationships between CPP and indices of cerebrovascular pulsatility (defined using either sPI or AMP) would be strengthened by demonstrating similar relationships in clinical situations where the drivers of CPP change were different (either through the mitigation of high ICP in plateau waves, or as a direct result of unstable ABP). This study aimed to describe and compare the relationships between spectral PI (sPI) and various invasively-derived cerebral hemodynamic measures across two groups of TBI patients demonstrating either plateau waves or unstable MAP while recording FV with TCD. These patients were of interest given the continuous data recorded through a wide range of CPP values, allowing better insight into the relationship between TCD and invasively-monitored parameters. The following relationships are described for each cohort: ICP versus AMP, ICP versus sPI, AMP versus sPI, CPP versus AMP, and CPP versus sPI.

5.1.2. Methods

Patients

From a database of 1,023 head-injured patients with continuous ICM+™ (Intensive Care Monitoring) monitoring and TCD recordings of ABP and ICP, a retrospective review of recorded data was performed for patients exhibiting ICP plateau waves during the period from 1992 to 1998. This study primarily observed physiological effects in subsets of TBI patients, with plateau waves of special interest because they are relatively uncommon. Each recording lasted for a maximum of 15–30 minutes. These patients have previously been described within other published studies[202,204,205] and were selected to evaluate the relationship between CPP versus sPI and CPP versus AMP over a large range of CPP that was observed secondary to large fluctuations in ICP, as seen during plateau waves. 5,643 minute-by-minute data points for each variable were analyzed across all patients.

A second cohort of severe TBI patients with unstable MAP was retrospectively analyzed to determine the relationships between CPP versus sPI and CPP versus AMP during wide fluctuations in CPP secondary to unstable MAP. The definition of

"unstable MAP" describes mean ABP changing by a minimum of 15 mm Hg in either a monotonic or a fluctuating manner during recording. All patients in both cohorts suffered moderate–severe TBI and were admitted to the Neurosciences Critical Care Unit (NCCU) at Addenbrooke's Hospital, Cambridge. Patients were managed according to an ICP-oriented protocol which aimed to keep ICP below 20 mm Hg. Institutional ICP protocols were employed during the patients' NCCU stay, to provide homogeneity of care between patients. Of note, these patients were not treated via CPP-directed therapies, as this was not the standard of care within the NCCU at that time. Thus, fluctuations in CPP seen during plateau wave recordings are natural CPP responses, with no influence of vasoactive substances during recording. Patients within the unstable MAP cohort may have received vasopressors in an attempt to stabilize blood pressure; however, this was not titrated to CPP goals.

Monitoring

All patients underwent both invasive and noninvasive monitoring throughout admission. Raw data signals from select monitoring devices were recorded and electronically stored using WREC software (Warsaw University of Technology).

ABP was continuously monitored both invasively (from the radial artery using a pressure monitoring kit [Baxter Healthcare C.A., U.S.A.; Sidcup, U.K.]) and noninvasively. ICP was monitored using an intraparenchymal probe with strain gauge sensors (Codman & Shurtleff, M.A., U.S.A., or Camino Laboratories, C.A., U.S.A.). Mean and peak blood flow velocities (FVm and FVx, respectively) were monitored from the MCA with a 2 MHz probe.

Raw data recordings within the plateau wave cohort patients included only 20–40 minutes of continuous data, focusing on the immediate periods before, during, and after ICP plateau waves. Within the unstable MAP cohort, raw data recording occurred throughout the entire period of unstable blood pressures.

The monitoring of the above brain modalities was conducted as a part of standard NCCU patient care using an anonymized database of physiological monitoring variables in neurocritical care. Data on age, injury severity, and clinical status at hospital discharge were recorded at the time of monitoring on this database,

and no attempt was made to re-access clinical records for additional information. Since all data were extracted from the hospital records and fully anonymized, no data on long-term outcomes or patient identifiers were available, and formal patient or proxy consent was not sought.

Data Processing

Processing of raw data signals utilized ICM+™ software (Cambridge Enterprise, Cambridge, UK; http://www.neurosurg.cam.ac.uk/icmplus). Signal artifact removal was first conducted with signal cropping tools within ICM+™. CPP was determined from the difference between raw ABP and ICP signals.

Primary analysis involved the calculation of time-averaged mean values for ABP (MAP), ICP, cerebral blood FV, and CPP. These means were calculated during 10-seconds time windows and were updated every 10 seconds to eliminate overlap. Mean FV was calculated using the data from FV. In addition, we determined the amplitude of the fundamental frequency of FV (F1) and the amplitude of the fundamental frequency of ICP (AMP). Both fundamental amplitude calculations were done by applying a 20-second time window, updated every 10 seconds.

Final data processing involved the calculations of sPI over the course of each individual recording utilizing the equation: Mean F1/Mean FV. Mean F1 and FV were calculated utilizing a 10-second time window, updated every 10 seconds. All data post-processing was exported from each patient to separate comma-separated variable (CSV) files for further statistical analysis.

Statistics

All statistical analyses were conducted utilizing the XLSTAT (Addinsoft, New York, USA; https://www.xlstat.com/en/) add-on package to Microsoft Excel (Microsoft Office 15, Version 16.0.7369.1323) and IBM SPSS Statistics 23 software. Post-processing data of individual patients, as CSV documents, were compiled into one CSV document containing all patients and signals described previously. Statistical significance for measured and derived variables, both within and between the two

patient cohorts, was determined utilizing a two-tailed *t*-test, with an alpha set at 0.05. Various statistical techniques were employed to describe the following relationships in both patient cohorts: ICP versus AMP, ICP versus sPI, AMP versus sPI, CPP versus AMP, and CPP versus sPI. Relationships between ICP, AMP, and sPI were analyzed utilizing linear regression techniques. Goodness of fit was reported utilizing the Pearson correlation coefficient (r) and the determination coefficient (R^2). All R^2 values were reported. Statistical significance was assigned only if the p value was less than 0.05.

Analysis of the relationship between CPP, AMP, and sPI was conducted utilizing both linear and non-linear techniques, with goodness of fit reported via R^2. Non-linear regression involved the fitting of existing functions within the statistical programs, in addition to manual function fitting utilizing the non-linear inverse function: $y=a+(b/x)$.

5.1.3. Results

Patient Demographics

11 patients were eligible for inclusion within the plateau wave cohort of this study, with a total of 18 plateau waves recorded. 9 patients comprised the unstable MAP cohort, with 13 separate recordings of unstable blood pressure. Figure 5.1 displays an example of the ICP, CPP, and MAP recordings from individual patients during plateau waves (Figure 5.1A) and unstable blood pressure (Figure 5.1B). All available demographic details are listed in Table 5.1.

Table 5.2 summarizes the mean ICP, ABP, CPP, HR, FV, and sPI for both the plateau wave and unstable MAP cohorts. Data for the plateau wave cohort were split into measurements before the plateau wave (i.e., "baseline") and during the plateau wave, with comparison done via two-tailed *t*-test. Data for the unstable MAP cohort were split into the recorded variables during the "Lowest 10%" and "Highest 10%" of recorded arterial blood pressures, with comparison done via two-tailed *t*-test.

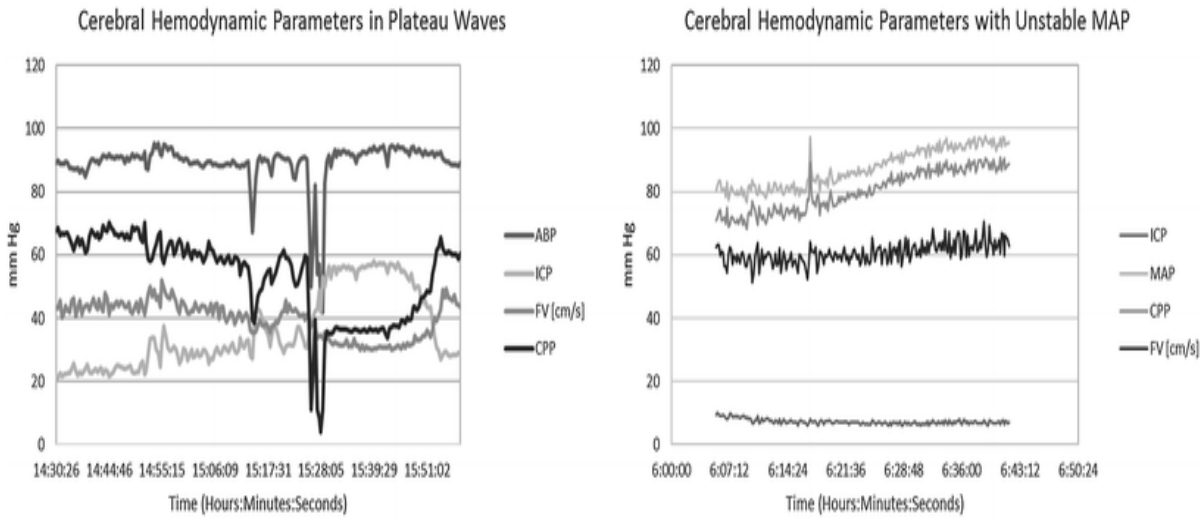

Figure 5.1. **ICP, CPP, and MAP Recordings in both Plateau Wave and Unstable MAP Patients**. In plateau waves, ABP, CPP, and FV decrease as ICP steeply increases during the plateau event. With unstable MAP, CPP increases along with MAP, while FV slightly increases and ICP is relatively constant.

ABP – arterial blood pressure, CPP – cerebral perfusion, FV – flow velocity, ICP – intracranial pressure, MAP – mean arterial pressure, and mm Hg – millimeters of mercury.

Table 5.1. Plateau Wave and Unstable MAP Patient Demographics. GOS utilized within this study is an inverted GOS, with 5=death and 1=good outcome. GCS – Glasgow *Coma Scale,* GOS– *Glasgow Outcome Scale*, #- *number,* MAP – *mean arterial pressure, and PVS – persistent vegetative state.*

Patient Cohort	**Number of Patients**	**Mean Age (Years)**	**Male:Female Ratio**	**Median Admission GCS**	**GOS at Discharge**	
Plateau Waves	11	27.2 (range: 17–76)	8:3	5 (range: 3–10)	GOS	# of patients
					Dead	2
					PVS	0
					Severe disability	5

Patient Cohort	**Number of Patients**	**Mean Age (Years)**	**Male:Female Ratio**	**Median Admission GCS**	**GOS at Discharge**	
					Moderate disability	4
					Good	0
Unstable MAP	9	25.1 (range: 17–60)	5:4	5 (range: 3–7)	GOS	# of patients
					Dead	2
					PVS	1

Patient Cohort	Number of Patients	Mean Age (Years)	Male:Female Ratio	Median Admission GCS	GOS at Discharge	
					Severe disability	5
					Moderate disability	1
					Good	0

Table 5.2. Measured and Derived Signals in the Plateau Waves and Unstable MAP Cohorts. *MAP – mean arterial pressure, CPP – cerebral perfusion pressure, ICP – intra-cranial pressure, AMP – fundamental amplitude of ICP, PI – pulsatility index, mm Hg – millimeters of Mercury, SD – standard deviation, and A1 – fundamental amplitude of arterial blood pressure.*

	Plateau Wave Recordings					**Unstable MAP Recordings**				
	Baseline		**Plateau**			**Lowest 10% of MAP**		**Highest 10% of MAP**		
	Mean	**SD**	**Mean**	**SD**	***p* value**	**Mean**	**SD**	**Mean**	**SD**	***p* value**◊
MAP (mm Hg)	96.93	10.12	95.06	8.39	0.52	71.96	15.96	103.65	20.05	0.0002
A1 (mm Hg)	16.41	2.32	15.96	2.25	0.53	15.61	3.76	19.10	5.30	0.07
ICP (mm Hg)	25.60	5.92	50.12	8.66	<0.0001	21.8	10.58	20.65	10.64	0.78

	Plateau Wave Recordings					**Unstable MAP Recordings**				
	Baseline		**Plateau**			**Lowest 10% of MAP**		**Highest 10% of MAP**		
	Mean	**SD**	**Mean**	**SD**	***p* value**	**Mean**	**SD**	**Mean**	**SD**	***p* value**[◊]
AMP (mm Hg)	2.23	0.73	6.41	1.64	<0.0001	2.51	2.16	1.71	1.15	0.25
CPP (mm Hg)	71.34	12.73	44.94	10.29	<0.0001	50.16	14.91	83.00	19.77	<0.0001
sPI (a.u.)	0.29	0.16	0.48	0.23	0.004	0.51	0.27	0.28	0.12	0.01

[◊]Statistical significance was determined via two-tailed *t*-test with an alpha of 0.05 assigned to entries with *p*-values below this threshold.

Relationships Between CPP, AMP, and sPI During Plateau Waves and Unstable MAP

Linear regression techniques failed to yield satisfactory relationships between CPP and AMP, or CPP and sPI. Their correlation coefficients were poor, and variance measures had large mean squared errors. As the scatterplots for each of these comparisons produced a non-linear pattern, non-linear regression analyses (with functions within XLSTAT and IBM SPSS Statistics 23 software) were utilized to determine the relationships displayed between these variables during ICP plateau waves, using an inverse function that was previously theorized to characterize this relationship. Non-linear regression analysis for CPP versus sPI in each individual plateau wave patient is shown in Appendix A of this thesis. Non-linear regression analysis for CPP versus sPI in each unstable MAP patient is shown in Appendix B.

The results of the non-linear regression across the compiled plateau wave patient data for CPP versus sPI are shown in Figure 5.2A. Similarly, the non-linear regression for CPP versus AMP is shown for Figure.5.2B. The corresponding results for the compiled unstable MAP patient data are shown in Figure 5.3A and Figure 5.3B respectively.

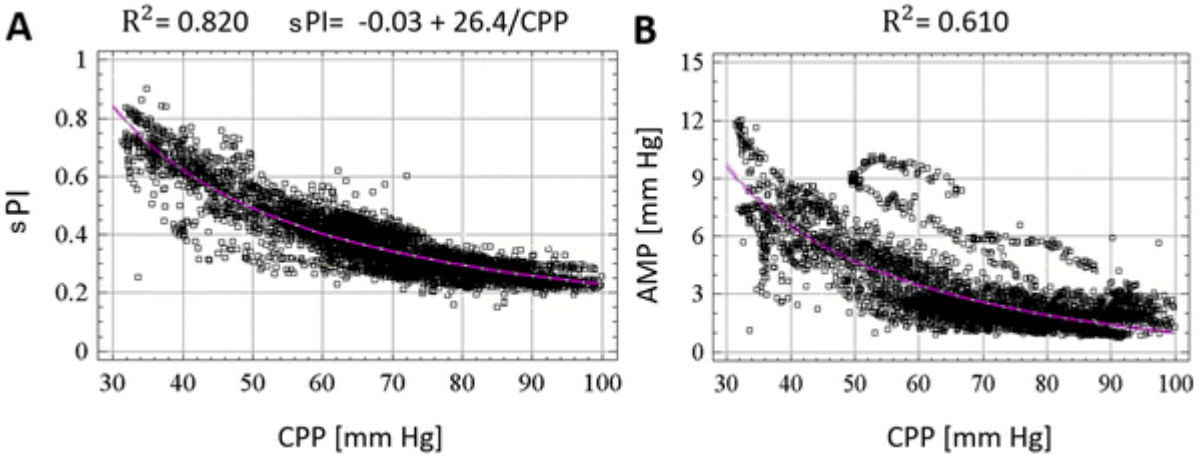

Figure 5.2. **Non-linear Regression Analysis of CPP versus sPI (F1/FV) and CPP versus AMP in the Plateau Waves Cohort.** A) Non-linear regression of CPP versus sPI. B) Non-linear regression of CPP versus AMP.

AMP – ICP pulse amplitude, CPP – cerebral perfusion pressure, F1 – amplitude of the fundamental frequency of FV, FV – mean blood flow velocity in the mean cerebral artery (MCA), mm Hg – millimeters of mercury, and sPI – spectral pulsatility index.

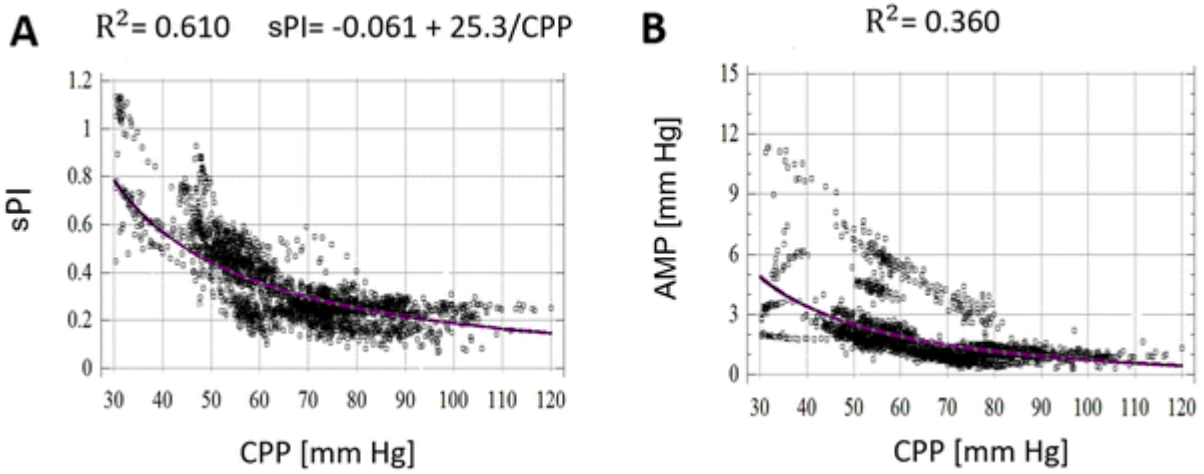

Figure 5.3. **Non-Linear Regression Analysis of CPP versus sPI (F1/FV) and CPP versus AMP in the Unstable MAP Cohort**. A) Non-linear regression of CPP versus sPI. B) Non-linear regression of CPP versus AMP.

AMP – ICP pulse amplitude, CPP – cerebral perfusion pressure, F1 – amplitude of the fundamental frequency of FV, FV – mean blood flow velocity in the mean cerebral artery (MCA), mm Hg – millimeters of mercury, and sPI – spectral pulsatility index.

AMP versus CPP

Non-linear regression analysis of the relationship between CPP and AMP in plateau wave patients produced an inverse relationship between CPP and AMP (R^2=0.610). Non-linear regression analysis of the relationship between CPP and AMP in unstable MAP patients produced an inverse relationship between the two parameters (R^2=0.36).

sPI versus CPP

Similarly, non-linear regression analysis of the relationship between CPP and sPI in the plateau wave cohort produced an inverse relationship (R^2=0.820), best described by the following function:

$$\mathbf{sPI} = a + (b/\mathbf{CPP}) \qquad [5.2]$$

with CPP measured in mm Hg, and the statistical analysis concluding: a=–0.03 and b=26.4. When the individual plateau wave patients were analyzed via non-linear regression, the mean and standard deviation for the values of "a" and "b" were: a=0.005 ±0.061, b=23.61 ±6.33.

Non-linear regression analysis of CPP versus sPI in the unstable MAP cohort also demonstrated an inverse relationship between CPP and sPI (R^2=0.61), as shown in Figure 5.3A. As seen within the plateau cohort's non-linear regression of CPP versus sPI, the model of best fit showed the same function (with CPP measured in mm Hg, a=–0.061 and b=25.3). When the individual unstable MAP patients were analyzed via non-linear regression, the mean and standard deviation for the values of "a" and "b" were: a=–0.144 ±0.391, b=27.43 ± 21.72. Interestingly, both relationships closely resemble and support the inverse non-linear relationship between CPP and PI previously proposed by de Riva et al.[28].

The "a" and "b" values calculated for each patient cohort were compared in a two-tailed independent-samples t-test to evaluate significant differences between the plateau wave versus unstable MAP cohorts. Levene's test for equality of variances was assumed and dictated a nonsignificant difference between both the "a" and the "b" values obtained from the two groups (t[27]=–1.507, p=0.143 and t[27]= 0.670, p=0.509, respectively). The effects of this hypothesis were further examined to determine whether each group's sets of "a" values were statistically different from the test value of 0 via two-tailed one-sample t-tests. There was a nonsignificant difference between 0 and the "a" values in unstable MAP patients as well as in plateau wave patients (t[12]=–1.330, p=0.208 and t[15]=0.300, p=0.768, respectively).

Relationships Between ICP, AMP, and sPI During Plateau Waves and Unstable MAP

Unlike the relationships between CPP versus sPI and AMP (where non-linear relationships were found), linear regression techniques yielded robust relationships of ICP with calculated variables in the plateau waves cohort.

The relationship between ICP and AMP across the compiled patient data for the plateau wave cohort is shown in Figure 5.4A A statistically significant linear relationship was described between ICP and AMP (r= 0.871, R^2=0.758). Similarly, a statistically significant linear relationship was described between ICP and sPI (r= 0.728, R^2=0.530), as displayed in Figure 5.4B. The relationship between AMP and sPI is displayed in Figure 5.4C. Linear regression techniques yielded a significant relationship between AMP and sPI(r=0.700, R^2=0.490).

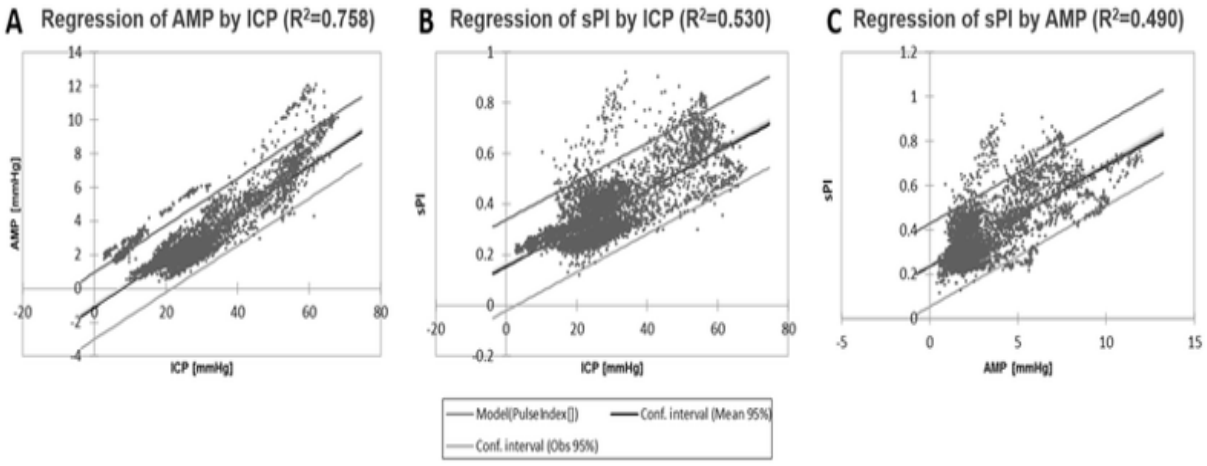

Figure 5.4. **Linear Regression Analysis of ICP versus AMP, ICP versus sPI, and AMP versus sPI in the Plateau Waves Cohort.** A) Linear regression of ICP versus AMP. B) Linear regression of ICP versus sPI. **C)** Linear regression of AMP versus sPI.

AMP– ICP pulse amplitude, ICP– intracranial pressure, mm Hg– millimeters of mercury, sPI– spectral pulsatility index, and R^2 *– the coefficient of determination.*

While linear regression also demonstrated significant relationships between ICP and AMP across the unstable MAP cohort, these relationships were less robust (Figure 5.5A). A statistically significant linear relationship was described between ICP and AMP (R^2=0.470). A very weak linear relationship was described between ICP and sPI (R^2=0.059), as displayed in Figure 5.5B. Finally, the relationship between AMP and sPI was linear (R^2=0.310) (Figure 5.5C).

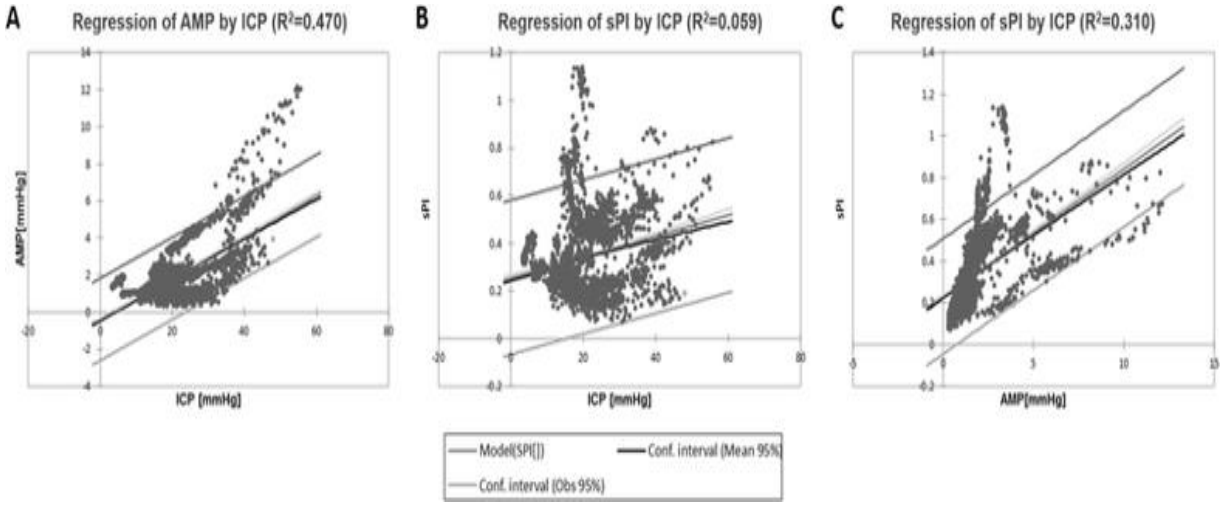

Figure 5.5. **Linear Regression Analysis of ICP versus AMP, ICP versus sPI, and AMP versus sPI in the Unstable MAP Cohort.** A) Linear regression of ICP versus AMP; B) Linear regression of ICP versus sPI; C) Linear regression of AMP versus sPI.

AMP – ICP pulse amplitude, ICP – intracranial pressure, mm Hg – millimeters of mercury, sPI– spectral pulsatility index, and R^2 *– the coefficient of determination.*

5.1.4. Discussion

In the past, observations of brain pulsatility in the context of lowering CPP[206] and increasing ICP[185] were reported, although much mixed methodology was used in those works. In this study, a unified method compared the same relationship in clinical conditions where CPP is affected either by increasing ICP or by the oscillations of unstable MAP.

The application of linear and non-linear regression analysis, has displayed both confirmatory and new results regarding the relationships between TCD-based PI and invasively-measured cerebral hemodynamic indices, ICP and CPP. This is older data harvested from the "Cambridge database" of high-resolution recorded signals from the 1990s, as neuro-intensive care TBI patients at that time were not treated according to a rigorous CPP-/ICP-oriented protocol; therefore, incidences of lowered CPP were recorded more easily. This is a relevant major aspect of these data recordings given that it is uncommon to have high-resolution datasets in the absence of CPP-directed therapy post-TBI.

Here, it has been demonstrated that large fluctuations in CPP, either via changes in ICP or MAP, hold true the inverse non-linear relationship between CPP versus sPI, and this relationship can be best described through the function: PI=a +(b/CPP); with a~0 (i.e., plateau waves, a=−0.03; unstable MAP, a=−0.06) and b almost identical between both cohorts (i.e., plateau waves, b=26.4; unstable MAP, b=25.3). Furthermore, non-linear regression analysis of each individual patient in both cohorts shows that the value for "a" is also close to 0. This was displayed strongly within the plateau waves cohort (mean "a"=0.005; SD= 0.061). The unstable MAP cohort displayed this same relationship, but less substantially (mean "a=−0.144; SD= 0.391). The statement that "a" was no different from 0 was further solidified via t-test analysis demonstrating no statistically significant difference between "a" and 0 in both cohorts. Therefore, if "a" is essentially equal to 0, then the relationship between CPP versus sPI can be approximated by the relation: PI=b/CPP, with b~25. This closely models the relation proposed by de Riva et al.[28] and provides the first evidence in support of this mathematical relationship between CPP and PI in human models.

Secondly, positive linear correlations were demonstrated between ICP versus AMP, ICP versus sPI, and AMP versus sPI in both the plateau waves and unstable MAP cohorts. Linear regression analysis of ICP versus AMP displayed the most robust linear relationship. Although the relationship between ICP versus non-spectral methods of PI calculation had been already described (i.e. that ICP can be well-approximated by TCD-based PI models)[11,207–209], limited literature exists utilizing spectral methods for PI determination. Furthermore, the relationship between ICP versus AMP and AMP versus sPI is seldom described, leaving this study as a clear example of their linear relationships.

Third, it is also remarkable that the relationship between CPP and AMP also followed an inverse non-linear relationship through non-linear regression techniques. Again, this was also confirmed for both the plateau waves and unstable MAP cohorts. In contrast, ICP seems to have a stronger link to intra-cranial/extra-vascular parameters (i.e., AMP, with an R^2=0.758) compared to intra-vascular measurements (i.e., sPI, with an R^2=0.530). Conversely, CPP displays a stronger relationship to intra-vascular parameters (i.e., sPI, with an R^2=0.820) versus extra-vascular intra-cranial measures (i.e., AMP, with an R^2=0.610).

Finally, the fact that sPI is a smooth inverse function of CPP makes it very difficult to prove that the CPP level below which sPI starts to increase could denote the lower limit of autoregulation (where the brain is on the verge of becoming unable to maintain a constant level of blood flow). Chan et al.[206] observed in patients with disturbed autoregulation that at a CPP value of about 40 mm Hg, adequate blood flow perfusion becomes more dependent on MAP than on CPP itself. However, later experimental challenges[210] demonstrated that increases in PI secondary to instances of decreasing CPP do not automatically signify a patient reaching the lower limit of autoregulation[210].

Clinical Implications

The most recent edition of the Brain Trauma Foundation Guidelines recommends that CPP be directed towards the target range of 60–70 mm Hg. Constraining CPP between these values is thought to prevent either the hyper- or hypo-perfusion that could, respectively, increase patient risk of poor outcome. When

considering trends across individual patient data, all sPI versus CPP curves suggest that values of sPI around 0.4 correspond to CPP values around 60 mm Hg. In this manner, sPI can easily be interpreted by clinicians as an indicator of the accepted "safe" lower bound of CPP[182]. Furthermore, the above analysis demonstrated the correlation between TCD-based sPI and CPP. This reinforces previous literature stating that TCD potentially provides the ability for non-invasive estimation of CPP in the absence of invasive ICP monitoring, which could expand the usage of both TCD as a technique and CPP as a metric outside of neurocritical care environments[82]. Finally, this study suggests that the relationship between CPP- and TCD-based sPI is maintained during extremes of physiology (i.e., plateau waves and unstable MAP), and can be theoretically applied to TBI monitoring. Thus, if clinician apply this methodology of non-invasive CPP estimation, this data suggests that the relationship between sPI and CPP should hold true, regardless of the individual clinical situation and extremes of physiology seen at the time of measurement.

Limitations

Several limitations must be acknowledged. First, the analyses are based on observational data, rather than a prospective recording of response to a change in CPP. Consequently, many confounders may have affected critical variables, and the data access (and the relatively small volume of data compatible with ICM+™ during this period) does not allow full accountability for them. Second, results are derived from only 11 sets of patient data containing 18 distinct plateau waves and 9 datasets containing 13 instances of variable MAP. Consequently, extrapolation of this data to all patients with TBI is not possible, and confirmation of the described relationships will need to occur through comparative analysis of larger datasets.

Third, non-linear regression techniques for the relationships between CPP versus AMP and CPP versus sPI described the best fit with an inverse non-linear function. However, with a total of only 20 patients, larger datasets are needed to better delineate and further prove this inverse relationship. Given that this patient population was so small, the next step is to validate these findings within a large TBI cohort to show that the proposed relationship holds. The relation yielded via non-linear regression cannot

be extrapolated and must serve only as a point of interest in the relationship between CPP versus AMP and CPP versus sPI, providing preliminary supporting evidence for the theorized non-linear relation previously described by Czosnyka et al.[202]. Fourth, within the unstable MAP cohort, it is difficult clinically to isolate pure MAP from pure ICP contributions to changes in CPP. These patients exhibit significant fluctuations in various physiologic measures, as shown in Table 5.2. Finally, patients with severe TBI and plateau waves are an extreme cohort of critically ill patients, with injuries that may yield abnormal physiologic brain properties. Therefore, the distinct relationships described in this small study cannot necessarily be applied to all TBI patients.

5.1.5. Conclusions

In severe TBI patients with plateau waves or unstable MAP, the relationships between CPP and pulsatility of brain signals are inversely proportional, irrespective of the mechanism that lowers CPP. ICP versus AMP, ICP versus sPI, and AMP versus sPI display positive linear correlations.

5.2. Estimation of Pulsatile Cerebral Arterial Blood Volume Based on Transcranial Doppler Signals

5.2.1. Introduction

The volume of arterial blood circulating throughout the brain at any one time can be adversely affected by traumatic brain injury (TBI) [211]. Pulsatile cerebral arterial blood volume (CaBV) can now be modeled with different input signals. Although this modeling reflects the inherent nature of blood flow throughout the brain, there is no

consensus on which specific combination of model elements yields a best-fit equation that could be globally applied in neurocritical care. This specific study sought to revisit the extant modeling methods[1,92,212–216] with the following aims: a) to comprehend which method is most suitable for describing patient hemodynamics, and b) to build a function able to monitor changes in cerebral compartmental compliances when considered alongside invasive monitoring and data-driven trend charts.

Fundamentals of Mathematical Modeling

Mathematical models of cerebral circulation must be able to account for pulsatile changes in the vasculature as a result of the cardiac cycle. TCD can both capture and continuously monitor cerebral hemodynamic changes in real time; FV through the MCA can be expressed as a variable that can be further analyzed with ICM+™ software to provide additional descriptors of hemodynamic activity.

With this application, Kim et al.[212] studied the changes in compartmental compliances (pressure/volume ratios expressed as either: Ca – the compliance of the cerebral arterial bed or Ci – the compliance of the cerebrospinal space) during plateau waves of ICP. During this event, the Ca and Ci compartments of the brain vary inversely as a result of dynamic shifts in the vasomotor tone of the cerebral vessels[212]. These authors[212] emphasized the mean arterial inflow curve when computing a comprehensive descriptor of cerebral arterial blood volume and their model below[212] returns the TCD-derived parameter *CaBV*. This parameter can be mathematically transformed through Fourier analysis to yield the fundamental harmonics of pulsatile components of CaBV, allowing a further-detailed expression of cerebral hemodynamics:

$$CaBV(n) = S_a \times \sum_{i=m_1}^{m_n} [CBFVa(i) - mean(CBFVa)]\Delta t\ (i) \qquad [5.3.]$$

where: S_a represents the cross-sectional area of the MCA, m_1 the first sample of the interval, n the number of samples, *CBFVa* the cerebral arterial blood flow velocity, and Δt is the time interval between two consecutive samples[212].

The foundations of this present study are rooted in the outcomes from laboratory modeling research conducted by Uryga et al.[216]. While manipulating arterial blood carbon dioxide concentration in healthy volunteers, the abilities of continuous flow forward (CFF) and pulsatile flow forward (PFF) models of CaBV change were compared as holistic descriptors of various cerebral hemodynamic indices. "Flow forward" refers to the direction of cerebral blood transport from large arteries into resistive arterioles. The CFF modeling approach relies on the balance between the simultaneously-opposing forces of pulsatile cerebral blood inflow and cerebral blood outflow, which influence changes in CaBV. Citing Avezaat and van Eijndhoven[217], Uryga et al. [216] created a time-integrated function of the difference between both inflow and outflow over a single cardiac cycle (Equation 5.4., below).

$$\Delta C_a BV_{CFF}(t) = \int_{t_0}^{t} (CBF_a(s) - meanCBF_a) ds \qquad [5.4.]$$

However, when employing TCD, this simplistic function requires averaging over several cardiac cycles to provide a surrogate measure of the blood inflow and outflow that occur in tandem[184,216]. To counter the effects of the variability of both blood outflow and systemic vascular impedances as a result of pulsatile changes in the ABP waveform, a second modeling approach was necessitated, becoming PFF. CaBV expressed by PFF would be a time-integrated function of the difference between the cerebral blood flow (CBF) signal and the ABP signal divided by CVR. The CVR can be estimated by TCD (i.e. the ratio between mean ABP and CBF, normalized by the unknown cross-sectional area of the MCA, which is presumed constant, see Equation 5.5, below). Uryga et al.[216] reported that each model's virtual signal is able to capture the pulsatile nature of its constituents and is respectively identified by their different waveform shapes and amplitudes.

$$\Delta C_a BV(t)_{PFF} = \int_{t_0}^{t} \left(CBF_a(s) - \frac{ABP(s)}{CVR} \right) ds \qquad [5.5.]$$

where: *s* – the arbitrary time variable of integration, CBF_a – cerebral blood flow velocity, *ABP* –arterial blood pressure, and *CVR* – cerebrovascular resistance[216].

This study modifies the PFF modeling approach in particular to include both ABP and cerebral perfusion pressure (CPP), and to consider both CFF and PFF as potentially useful tools in the determination of clinical outcome. The previous method of CaBV modeling assumed constant outflow of the blood from the modeled compartment (compliance of cerebral arteries and vascular resistance). The proposed modification (PFF) presumes that outflow may be pulsatile, and investigates changes in formulas for the calculation of the amplitude of CaBV estimators. As there is no objective gold standard for the non-invasive calculation of CaBV, the novel CaBV estimator models are further compared against the spectral pulsatility index (sPI)[88] to assess their respective capabilities to approximate the cerebral blood volume component of ICP in extreme pathologies. To current knowledge, this paper is the first of its kind attempting to apply these modeling perspectives to a population of neuro-critically ill patients.

5.2.2. Methods

Patients

52 adult patients were selected from a database of 432 moderately to severely head-injured patients with TCD, ICP, and ABP monitoring, stored between 1992 and 2012 that demonstrated a variety of clinically-extreme scenarios. Of these 52 patient datasets: 16 presented plateau waves of ICP which are difficult to capture during routine TCD monitoring sessions[88], 19 underwent a period of mild, controlled hypocapnia (30-60 minutes' duration), and 17 received vasopressors to stabilize mean ABP that fluctuated at least 15 mm Hg during the recording. All patients were admitted to the Neurosciences Critical Care Unit (NCCU) at Addenbrooke's Hospital, Cambridge,

United Kingdom. All patients were sedated and mechanically ventilated; barring the hypocapnic challenge to assess CO_2 reactivity, all patients were treated in accordance with an ICP/CPP-oriented protocol that constrained ICP below 20-25 mm Hg and maintained CPP between 60-70 mm Hg[218,219]. Table 5.3 describes these patients in detail.

These particular patient groups were chosen in the interest of observing the direction(s) of CaBV changes in response to biophysical "challenges"[218–226] which are thought to mimic physiological responses to hemodynamic disturbances that are provoked, pathological, or pharmacological. Therefore, CaBV can be manipulated by ICP[218,220,221] CO_2[219,222–224], and ABP[225–227], making these parameters important clinical discriminants. Dramatic fluctuations in CaBV can be best studied in patients exhibiting complex clinical profiles, such as plateau waves of ICP, hypocapnia, and unstable ABP; these specific patient cohorts were chosen to test the veritable limits of the mathematical modeling of cerebral hemodynamics, and to provide secondary insight into outcome prediction.

Retrospective data was anonymized and is stored as such in the NCCU Users Group database. TCD recordings were incorporated into standard patient monitoring practices on the NCCU and utilized an anonymized database of physiological monitoring variables in neurocritical care. Demographic data, injury severity, and clinical status at hospital discharge were collected prospectively during the monitoring of these patients; these clinical records were not consulted further to provide additional information for this study. All data retrieved from the database was extracted from these pre-existing patient records, and fully anonymized. Data pertaining to long-term outcome or patient-identifiers was not available, and formal patient or proxy consent to access these items was not sought, with the exception of the vasopressors cohort, which consented for positron emission tomography (PET) under two different blood pressure levels.

ICP Plateau Waves

The observable phenomenon of an ICP plateau wave has been explained as a function of increasing CaBV at the expense of cerebral vasomotor tone and flow

regulatory mechanisms[222]. As cerebral vessels react with maximal dilation and obstruct draining veins, both the velocity and the volume of blood flowing within their walls increases. However, the brain cannot accommodate these alterations as they occur, so ICP rapidly increases. The increased amplitude of the raw ICP waveforms can be attributed to the influx of pulsatile cerebral blood coursing through the cerebral vessels, as opposed to an increase in mean ICP[220,228]. Both the CFF and PFF models can express the heightened magnitude of pulsatile changes in CaBV as a result of ICP plateau waves. It was hypothesized that this cohort in particular would be best-described by the PFF model using CPP as input, as plateau waves increase ICP, and therefore will affect CPP.

Hypocapnia

Data from patients submitted to short-term episodes of hypocapnia (mean $PaCO_2$, the partial pressure of carbon dioxide in arterial blood, was maintained at 4.38±0.34 kPa and deviated on average by 0.72±0.26 kPa during hypocapnia) were also included to test the limits of CaBV modeling in the opposite direction. The vasoconstrictive effects of hypocapnia can be observed in the characteristic reduction of ICP attributed to a "backshift of the working point on [the] pressure-volume curve", in which CaBV circulation is negatively affected by the increasing resistance to arterial inflow[225]. Cerebral autoregulation is thus compromised[229]; prolonged exposure to hypocapnia exacerbates the risk of both disability and mortality, as decreasing ICP at the expense of CPP overreaching its targeted value can lead to ischemia or irreversible damage to brain tissue[224].

Vasopressors

Infusions of vasopressors such as norepinephrine or phenylephrine have been found to increase cerebral perfusion and oxygenation in both human and swine models[25]. Following TBI, they are administered to increase ABP and CPP to prevent secondary ischemia (Meng 2012; Sperna 2017). The selected cohort of patients maintained a mean ABP of 87.31±7.16 mm Hg that was increased to 111.41±6.45 mm Hg following infusion of either phenylephrine (0.5 mcg/kg/min) or norepinephrine (0.05

mcg/kg/min). It was hypothesized that both PFF models, either with ABP or CPP used as input, would be strongly correlated with this cohort.

Monitoring

All patients received both invasive and non-invasive monitoring while under clinical observation. Raw data signals from select monitoring devices were captured and archived electronically through WREC software (Warsaw University of Technology) or ICM+™ (licensed through Cambridge Enterprise, Cambridge, U.K.; http://www.neurosurg.cam.ac.uk/icmplus).

ABP was continuously monitored invasively [from the radial artery using a pressure monitoring kit (Baxter Healthcare C.A., U.S.A.; Sidcup, U.K.)]. ICP was monitored using an intraparenchymal probe with strain gauge sensors (Codman & Shurtleff, M.A., U.S.A.). End-tidal CO_2 ($ETCO_2$) was measured in the patients experiencing periods of mild, controlled hypocapnia via capnograph (Marquette Solar 8000 M, GE Medical Systems, U.K.). Cerebral blood flow velocity (FV) was recorded from both unilateral and bilateral monitoring of the middle cerebral artery (MCA) with a 2 MHz TCD probe (Multi Dop X4, DWL Elektronische Systeme, Sipplingen, Germany). Data were processed through a 16-bit, 100kHz analog-to-digital converter (DT9803 USB Data Acquisition (DAQ) Module, Measurement Computing Corporation, Norton, M.A., U.S.A.).

Raw TCD data sampled from the three types of events (ICP plateau waves, hypocapnia, and vasopressors) included in the study encapsulated the baseline readings, the entirety of the challenge/event, and the post-event recordings. Signal artifact removal was achieved manually. CPP was determined from the difference between raw ABP and ICP signals. The average duration of these TCD recordings was over 108.59±57.56 minutes, with a minimum of 18 minutes and maximum of 177 minutes captured per patient. 18-90 minutes of continuous TCD data recordings were obtained from the plateau waves cohort, with 85-138 and 135-177 minutes each obtained from the hypocapnia and vasopressors cohorts, respectively.

Data Processing

The previous section of this thesis[88,184] allowed the expression of a TCD-based "spectral pulsatility index" (sPI), defined above as sPI = F1/FVm) using the following model presented below in Equation 5.6. This model describes the relationships among several cerebral hemodynamic parameters that would be expected to yield variations in CPP[88]. Here, estimators for Ca and CaBV were chosen, which produce the best agreement between the left and right sides of this equation.

$$sPI = \frac{A_1}{CPP_m} \times \sqrt{(CVR \times Ca)^2 \times HR^2 \times (2\pi)^2 + 1} \qquad [5.6.]$$

where: A_1 represents the fundamental harmonic of the ABP pulse waveform determined using Fourier transformation, Ca the cerebral arterial compliance, CPP_m the calculated mean of recorded CPP values, CVR the cerebrovascular resistance, and HR the heart rate calculated in Hz[184]. All parameters were calculated as averages over a 10-second time window.

Within ICM+™, virtual signals from the invasive monitoring (ABP and ICP) devices and from TCD blood flow velocity monitoring (FV) were sampled at a frequency of 50 Hz to form the backbones of the three CaBV change approximation models. A continuous flow forward model (CFF)[28,92,216,217] was applied as a time-integral of FV to form $CaBV_{CFF}$ ($CaBV_1$; Equation 5.7) sampled at a frequency of 50 Hz (Equation 5.7), whereas the two pulsatile flow forward models (PFF_{ABP} and PFF_{CPP}) were similarly derived using ABP and CPP as input, to form the respective $CaBV_{PFFABP}$ ($CaBV_2$; Equation 5.8) and $CaBV_{PFFCPP}$ ($CaBV_3$; Equation 5.9).

$$\Delta CaBV_{CFF}(t) = \int_{to}^{t} (FV\ \ (i) - FV_m)\, di \qquad [5.7.]$$

$$\Delta CaBV_{PFF_{ABP}}(t) = \int_{to}^{t}(FV(i) - \left(\frac{ABP_{(i)}}{\frac{ABPm}{FVm}}\right) di \quad [5.8.]$$

$$\Delta CaBV_{PFF_{CPP}}(t) = \int_{to}^{t}(FV(i) - \left(\frac{ABP_{(i)} - ICP_{(i)}}{\frac{ABPm - ICPm}{FVm}}\right)) di \quad [5.9.]$$

where: t_o and t are the respective beginning and end of a single cardiac cycle, Δt is the time interval between two consecutive samples, $FV(i), ABP(i), and\ ICP(i)$ are the moving averages of FV, ABP, and ICP over a specified time window including previous cardiac cycles (a moving average filter of 600 seconds was applied), *FVm* is the mean value of FV, *ABPm* is the mean value of ABP, *ICPm* is the mean value of ICP, and *s* is the arbitrary variable of integration.

Primary analysis involved the determination of time-averaged mean values for ABP, CPP, FV, ICP, $\Delta CaBV_1$, $\Delta CaBV_2$, and $\Delta CaBV_3$. Each mean was calculated during 10-second time windows and continuously updated every 10 seconds. For the CFF model, Fourier transformation was employed to determine the fundamental frequencies of each of the above parameters, to use as scaffolds for more extensive evaluation of spectral changes in ΔCaBV, yielding $AmpCaBV_{CFF}$. For the PFF models, the fundamental amplitudes were calculated with Equation 5.10 (see Appendix C); $AmpCaBV_{PFF_{CPP}}$ was obtained with this same formula but required AmpCPP as input rather than AmpABP (see Appendix C). Each of these calculations was similarly sampled and updated over a 10-second time window.

The secondary phase of analysis computed time-averaged mean values of all of the above parameters, sampled and updated over a 10-second time window, with the introduction of time-averaged mean values of $\Delta CABV_1$, $\Delta CABV_2$, and $\Delta CABV_3$ resolved into the spectral domain to yield the respective $CABV_{1S}$, $CABV_{2S}$, and $CABV_{3S}$. These spectral components were included in the final analysis to create nine separate models of CaBV approximation to be validated against the existing sPI model[88,184] describing changes in CPP as a result of extreme pathology that were directly observed by TCD.

Final data processing efforts continued to determine the time-averaged mean values from previous analytic phases, each sampled and updated over a 10-second time window. Several new derived parameters were introduced here, including: sPI as the quotient of the means of F1 and FV, mean $CABV_{1S}$, $CABV_{2S}$, and $CABV_{3S}$, and the time

constant of the cerebral arterial bed (tau, τ). Commonly interpreted as a simplified electronic circuit model consisting of a single resistor and capacitor, τ is evaluated as the relative time period required to fill the cerebral arterial bed[92,216]. τ is the product of Ca and CVR and emphasizes the "mutual interdependence" of these parameters from an absolute value of ABP[210,230]. Additionally, τ is not affected by the surface area of the middle cerebral artery (MCA), so challenges to the long-held assumption of its constant value do not pose a threat to this parameter's applicability to patient data.

Although the calculation of τ was not the primary feature of this report, its inclusion in the final analysis supports its utility for further description of changes in CaBV. τ varies inversely with fluctuations in ABP or CPP, which are crucial components of the interpretation of CFF and PFF models[210,230]. The nine derived estimators of CaBV pulsatility each employ a similar circuit model to τ, with single resistors (Ra1-Ra3) and capacitors represented by manipulated combinations of aspects of either the continuous or pulsatile flow forward models and cerebral hemodynamic parameters (ABP, CPP, FV) sourced through ICM+™. The resistors and capacitors "available" (listed as PI_CxRax) for the creation of each of these models are listed below, with the full formulaic characterizations to be found in Appendix D.

All data post-processing was exported from each patient to separate comma-separated variable (CSV) files for further statistical analysis.

Statistics

All statistical analyses were conducted utilizing R (R Core Team [2017]; R: a language and environment for statistical computing. R Foundation for Statistical Computing, Vienna, Austria. URL https://www.R-project.org/). Post-processing, individual CSV documents containing the data of each patient, were compiled into one CSV document per cohort containing the relevant patients and all of the signals described above. Cerebral hemodynamic trends were separately analyzed for each of the three patient cohorts (as plateau waves, hypocapnia, and vasopressors) to appreciate the physiological differences between clinical profiles. A visual example of the trends exhibited by a patient from each group was exported from ICM+™, and is provided in Figure 5.6 below.

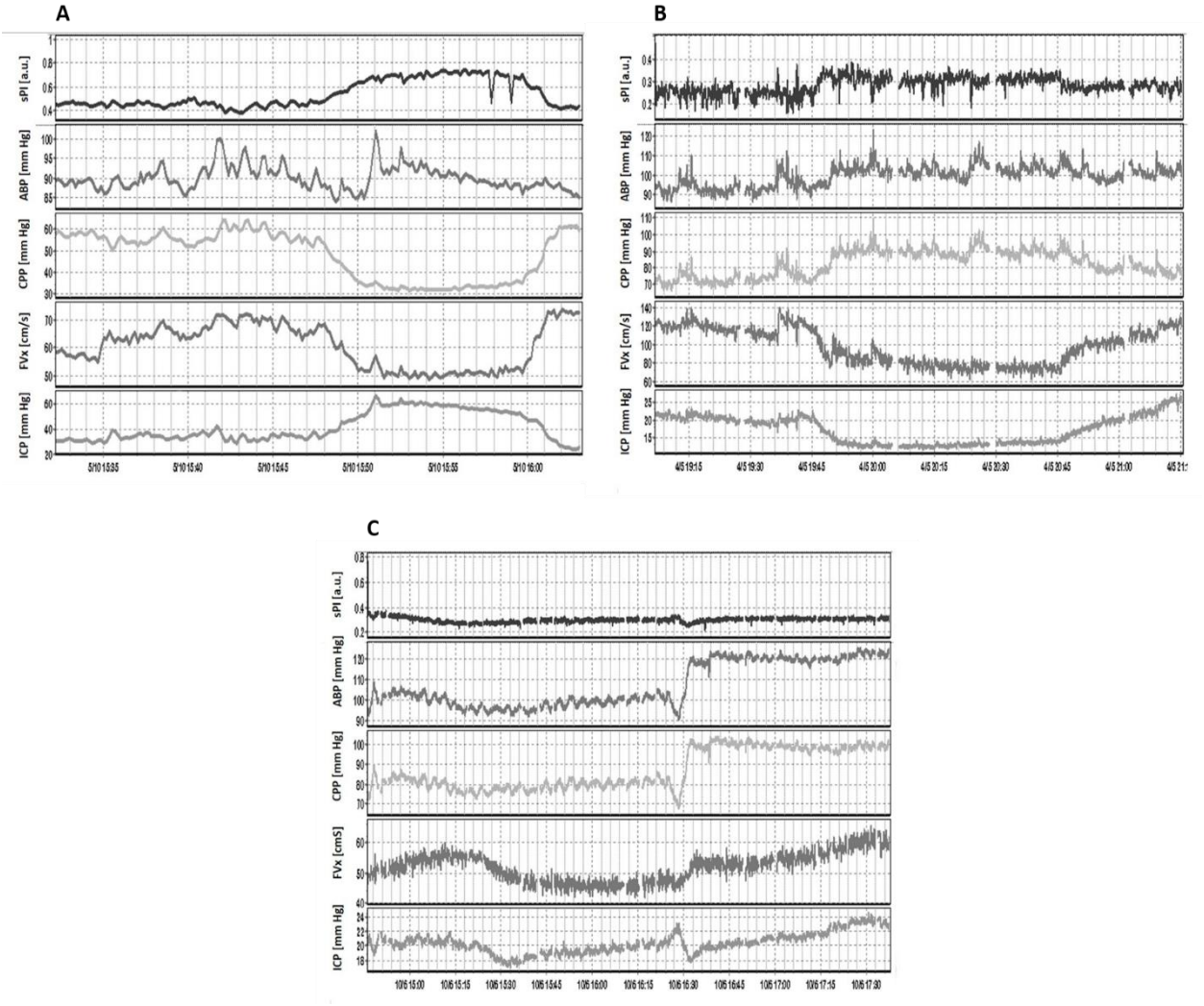

Figure 5.6. **Examples of sPI, ABP, CPP, FV, and ICP dynamic trends exported directly from ICM+™ for a single patient** in the A) plateau waves, B) mild hypocapnia, and C) arterial hypertension cohorts.

sPI- spectral pulsatility index, ABP- arterial blood pressure, CPP- cerebral perfusion pressure, FV- flow velocity, ICP- intracranial pressure, mm Hg- millimeters of mercury.

Various statistical techniques were employed to describe the strength of the following relationships in all three patient cohorts: sPI vs. PI_C1Ra1, PI_C1Ra2, PI_C1Ra3, PI_C2Ra1, PI_C2Ra2, PI_C2Ra3, PI_C3Ra1, PI_C3Ra2, and PI_C3Ra3. Goodness of fit between the metric of sPI and each of the nine CaBV estimator models was assessed via

linear regression in R; this was achieved with the Pearson correlation coefficient (r) and the determination coefficient (R^2).

The Bland Altman method was applied, also in R, to measure the agreement between sPI and each respective estimator model for the purpose of explaining changes in CaBV demonstrated by each pathology. Descriptive statistics for each of the three patient cohorts, along with the results of the linear regression and Bland Altman analyses, are reported in Tables 5.4-5.6.

5.2.3. Results

Relationships between sPI and CaBV Estimators

Tables 5.4 (plateau waves), 5.5 (hypocapnia), and 5.6 (vasopressors) summarize the mean values and standard deviations of sPI and of the estimator models.; they additionally feature summary statistics data for all TCD recordings comprising each of the patient cohorts, and Bland Altman means and critical differences for sPI and each estimator model. To appreciate the agreement between the sPI and each estimator model, the Pearson correlation coefficients (r) were also listed per respective cohort.

The results of the final analyses indicated that irrespective of the patient cohort, each of the nine CaBV estimator models was robustly correlated with sPI. However, the best-fit estimator model that was superior in approximating changes in CaBV throughout the entire recording varied as a result of the distinct clinical profiles of these patients. Tables 5.4-5.6 demonstrate these trends.

Plateau Waves

This cohort demonstrated high agreement between the derived and the "traditional" parameters comprising the electronic circuit-inspired estimator models. The readings from each subgroup were closely approximated to sPI by all of the models (fully detailed in Appendix C) but were most strongly determined by PI_C1Ra3 with an average r-value of 0.915 for the entire recording (Figure 5.7). The strengths of each estimator as measured against sPI are reported in Table 5.4, below.

Table 5.3. Patient Demographics and Outcomes

Patient Cohort	**Number of Patients**	**Mean Age (years)**	**Male:Female Ratio**	**Median Admission GCS**	**Glasgow Outcome Scale at Discharge**	
Plateau Waves	16 (5/16 lost to follow-up)	27.18 (range: 17 to 32)	12:4	5 (range: 1 to 10)	***GOS***	***# of Patients***
					Dead	**0**
					PVS	**4**
					Severe disability	**5**
					Moderate disability	**0**
					Good	**2**
						N.A.: 5
Hypocapnia	19 (4/19 lost to follow-up)	39.1 (range: 17 to 70)	14:5	6 (range: 3 to 12)	***GOS***	***# of Patients***
					Dead	**1**
					PVS	**0**
					Severe disability	**5**
					Moderate disability	**8**
					Good	**1**
						N.A.: 4

Vasopressors	17 (5/17 lost to follow-up)	32.79 (range: 18 to 69)	13:4	5 (range: 3 to 9)	***GOS***	***# of Patients***
					Dead	**2**
					PVS	**0**
					Severe disability	**2**
					Moderate disability	**4**
					Good	**4**
						N.A.: 5

GCS = Glasgow Coma Scale, GOS = Glasgow Outcome Score, # = number, PVS – persistent vegetative state.

Table 5.4. sPI vs. Derived PI Models in the Plateau Waves Cohort

	sPI	**PI_C1Ra1**	**PI_C1Ra2**	**PI_C1Ra3**	**PI_C2Ra1**	**PI_C2Ra2**	**PI_C2Ra3**	**PI_C3Ra1**	**PI_C3Ra2**	**PI_C3Ra3**
Entire Recording										
Mean	0.340	0.639	0.369	0.448	0.459	0.326	0.343	0.428	0.325	0.329
Standard Deviation	0.176	0.392	0.119	0.147	0.311	0.182	0.134	0.281	0.212	0.128
Bland Altman Mean	---	-0.299	-0.028	-0.084	-0.119	0.014	-0.002	-0.088	-0.015	0.012
Bland Altman Critical Difference	---	0.548	0.337	0.17	0.506	0.538	0.306	0.501	0.610	0.333
Pearson Correlation Coefficient	---	0.888	0.843	0.915	0.886	0.888	0.889	0.887	0.882	0.886

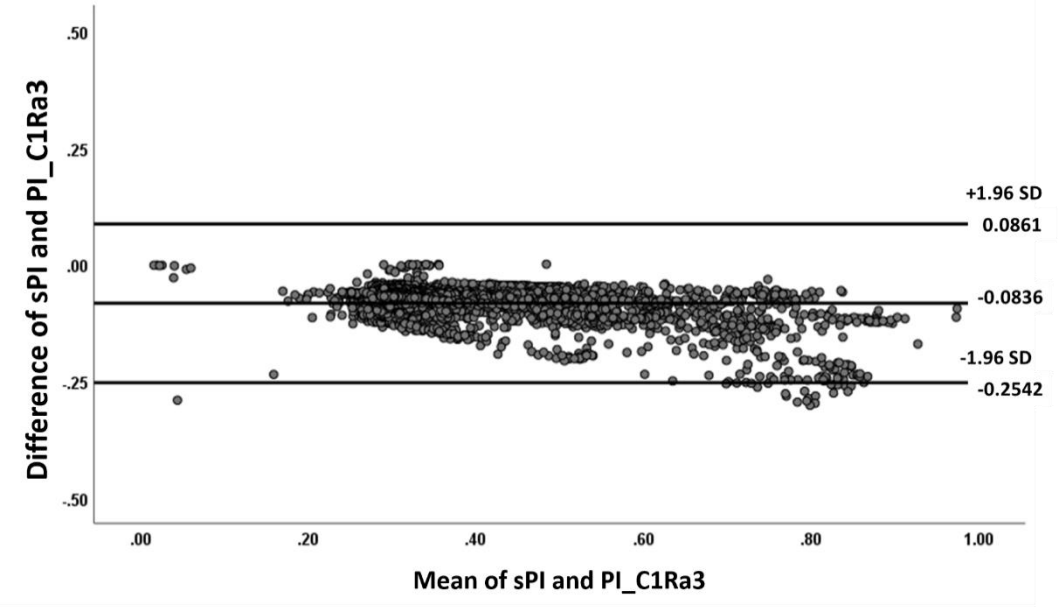

Figure 5.7. **A Bland Altman plot representing the compatibility between sPI and PI_C1Ra3 to estimate changes in CaBV in the plateau waves patient cohort**. The bold lines indicate the limits of agreement as measured with a confidence interval of 95%, yielding a bias of -0.0836.

Hypocapnia Cohort

The hypocapnia patient cohort provided a similar example of high agreement between parameters determined both invasively and non-invasively. In conjunction with the results from the plateau waves cohort, sPI was closely approximated by all of the models, in particular by PI_C1Ra3 with an average *r*-value of 0.955 for the entire recording (see Table 5.5, below). PI_C1Ra3 was overwhelmingly found to be the superior estimator of the volumetric changes in cerebral arterial blood within the hypocapnia patient cohort. As above, complete descriptions of each of the models are contained in Appendix C.

Table 5.5. sPI vs. Derived PI Models in the Hypocapnia Cohort

	sPI	**PI_C1Ra1**	**PI_C1Ra2**	**PI_C1Ra3**	**PI_C2Ra1**	**PI_C2Ra2**	**PI_C2Ra3**	**PI_C3Ra1**	**PI_C3Ra2**	**PI_C3Ra3**
Entire Recording										
Mean	0.301	0.432	0.337	0.385	0.273	0.253	0.262	0.265	0.250	0.257
Standard Deviation	0.102	0.150	0.109	0.124	0.094	0.104	0.086	0.087	0.103	0.082
Bland Altman Mean	---	-0.131	-0.036	-0.084	0.029	0.048	0.039	0.036	0.051	0.044
Bland Altman Critical Difference	---	0.117	0.102	0.061	0.065	0.161	0.065	0.068	0.165	0.072
Pearson Correlation Coefficient	---	0.918	0.588	0.955	0.830	0.600	0.821	0.830	0.613	0.815

Vasopressors Cohort

As observed in both the plateau waves and the hypocapnia patient cohorts, the vasopressors cohort also suggested high agreement with sPI. However, when compared to the previous cohorts, the variability between each of the models as predictors of sPI was significantly greater for each recording subgroup, although PI_C1Ra1 and PI_C1Ra3 were repeatedly closely-matched (see Table 5.6, below). When considering the average *r*-value, the vasopressors patient cohort challenged the notion of PI_C1Ra3 as being considered the "best-fit" for sPI. PI_C1Ra1 and PI_C1Ra3 were nearly identical approximators of sPI, with respective average r-values of 0.938 and 0.931. As above, the construction of each model is outlined in Appendix C.

Table 5.6. sPI vs. Derived PI Models in the Vasopressors Cohort

	sPI	**PI_C1Ra1**	**PI_C1Ra2**	**PI_C1Ra3**	**PI_C2Ra1**	**PI_C2Ra2**	**PI_C2Ra3**	**PI_C3Ra1**	**PI_C3Ra2**	**PI_C3Ra3**
Entire Recording										
Mean	0.299	0.484	0.374	0.434	0.324	0.306	0.312	0.314	0.305	0.305
Standard Deviation	0.647	0.710	0.088	0.628	0.714	0.721	0.631	0.715	0.807	0.631
Bland Altman Mean	---	-0.044	-0.075	-0.134	-0.024	-0.006	-0.023	-0.014	-0.005	-0.005
Bland Altman Critical Difference	---	0.072	1.264	0.987	1.099	1.910	1.025	1.104	2.040	1.029
Pearson Correlation Coefficient	---	0.938	0.621	0.931	0.870	0.687	0.826	0.814	0.652	0.781

5.2.4. Discussion

The first aim of this study was to assess the feasibility of either a CFF or a PFF model to approximate CaBV in physiologically extreme conditions affecting neurocritical care patients. It was hypothesized that a PFF model with CPP as the input signal (PI_C3Ra3) would be the best-fit estimator model because its core parameter contains raw signals from both standard cerebral hemodynamic indices (ABP and ICP) that largely direct patient management. However, the results seem to disprove this hypothesis, suggesting that it is mainly PI_C1Ra3 (closely followed by PI_C1Ra1, but only for the vasopressors cohort – see Tables 5.4-5.6) that is the best fit for these groups of neurocritical patients.

Although inspired by the work of Uryga et al.[216] which concluded that PFF was superior to CFF when measured in healthy volunteers during hypo- and hypercapnia, these results taken from a population of TBI patients contradict this point. This could be related to the fact that the CFF method of CaBV estimation is more "stable" for measurement, as it discards the dependence on ABP for calculation that characterizes both PFF modeling scaffolds. ABP appears to be the most sensitive parameter, as any large fluctuations of ABP in patients would dramatically change the value of the numerators of any one of the three resistors applied to either PFF model (please see Appendix C). Though the TCD-based pulsatility index can describe hemodynamic asymmetry and alert clinicians to low CPP, it cannot reliably explain CVR or be considered a secure measure of risk against intracranial hypertension or dysautoregulation[184]. When plotting sPI against CPP[88], the curve does not exhibit an abrupt breakpoint that would indicate the lower limit of autoregulation when targeting CPP in accordance with neuro-intensive care protocols[184].

This section concentrated on building mathematical models of cerebral circulation able to account for pulsatile changes in the vasculature as a result of the cardiac cycle. TCD can capture continuous monitoring of cerebral hemodynamic changes in real time that can be further analyzed with ICM+™ software to provide additional descriptors of hemodynamic activity, such as the compliance of the cerebral arterial bed (Ca) and the cerebrovascular resistance (CVR). Although the diameter of the MCA has been observed as relatively constant in healthy volunteers[231,232]

(discounting cases of vasospasm), the volume of cerebral arterial blood flowing through it is subject to change, especially when exposed to extreme physiological conditions (i.e. plateau waves of ICP, hypocapnia, or unstable ABP requiring the use of vasopressors for stabilization)[88].

Although the modeled approximation of CaBV without its venous component appears noncompliant with natural circulatory transit cycles, there is a long-standing assumption that venous flow pulsatility is much lower than its arterial counterpart. Regarding the possible influence of the venous component, Carrera et al.[220] reported that during one cardiac cycle, venous outflow carries a low enough pulsatility to be deemed "negligible" when calculating CaBV changes[184,212,217,220,230]. Therefore, ΔCaBV can be represented as the time-integrated difference between the values of current and mean cerebral blood flow velocity[212,220]. In fact, Avezaat & van Eijndhoven[217] had already noted the influence of pulsatile in- and outflow curves in determining the subtle, time-sensitive variations in ΔCaBV that occur over one cardiac cycle. The degree of quantifiable change in pulsatile CaBV would be an effect of the "temporal relationship" between cerebral arterial inflow and venous outflow processes; this is contingent on the impedances of the vascular bed, which can be both actively and passively mediated by either vasomotor tone or compression within the cerebral compartment[217].

Clinical Implications

Improvements in the estimation of CaBV provide various potentially crucial advancements for the monitoring of critically-ill patients. First, in patients suffering from intracranial hypertension, knowledge of which intracranial component is contributing most to ICP elevation is not always clear (i.e. CSF, blood volume, edema, etc.). Optimal models for CaBV estimation, such as those presented here, are required to properly outline the blood volume component of ICP. Such knowledge may allow the implementation of targeted therapies for particular intracranial components contributing to elevated ICP. Second, most clinicians currently manage intracranial hypertension by treating a single number, based on the Brain Trauma Foundation guidelines[182]. It is unknown if targeting particular aspects of ICP, such as standard invasively-measured parameters or estimated CaBV, could provide greater impact on

patient functional outcome. However, adequate, optimized models of CaBV estimation are required prior to investigating therapies directed at continuously/semi-continuously measured CaBV.

Third, it is understood that persistent ICP elevations near, or at, the critical closing pressure (CrCP) are detrimental to sustained cerebral blood flow in the setting of brain injury. As accurate CrCP is predicated on CBV estimation, it becomes theoretically possible to estimate an individual patient's CrCP in a continuous/semi-continuous manner, allowing clinicians real-time knowledge of this critical threshold that can be incorporated into therapeutic interventions. Fourth, to date, the majority of continuously-measured indices of cerebrovascular reactivity are derived based on the notion that the correlation between slow-wave fluctuations in a surrogate measure of cerebral blood flow (such as TCD-based FV) or ΔCaBV (such as ICP) and a driving pressure (such as ABP or CPP), provide information regarding cerebral autoregulatory status. The most widely-employed index, pressure reactivity index (PRx)[92] is based on the correlation between slow-wave fluctuations of ICP (surrogate of CaBV) and mean ABP. In (TBI), PRx has demonstrated a strong association with global outcome[21] and has been validated as a measure of the lower limit of autoregulation in experimental models[18,93]. However, there exists the potential to further optimize the ability to continuously assess cerebrovascular reactivity. With accurate CaBV estimation, instead of evaluating a surrogate measure of ΔCaBV, such as ICP, vasogenic slow-wave fluctuations in CaBV and their association with either ABP or CPP can be evaluated more directly. Such measures may prove superior to existing measures of cerebrovascular reactivity; prior to the evaluation of such measures, one requires optimal models for CBV estimation.

Finally, as both medicine and the critical care management of brain injury patients shift towards a personalized approach, the ability to accurately and continuously assess various aspects of cerebral physiology is of the utmost importance. In TBI care, the emergence of literature on both individualized CPP[5,61,233] and ICP[181] is based on various aspects of physiologic signal measurement, processing, and analysis. It is unknown where continuously measured CaBV or CrCP will provide additional benefit in such care. However, it isn't until accurate estimation of CaBV is provided, that any benefit towards the goal of purely individualized care can be evaluated.

Limitations

Although a single model could be identified as the most robust estimator of CaBV changes when compared against sPI, this study provided only a correlational assessment of model efficacy. Additionally, the proposed model requires numerical integration over sampled signals; this process is prone to errors due to noise. The immediate validity of this study is limited by the common, nearly fundamental assumption that the cross-sectional area of the MCA is of a constant, yet unknown, value. If the MCA is indeed proven variant[234,235], then these calculations would require reconfiguration in order to accommodate for the additional fluctuations in its tone. These calculations would also be discounted if the negligible contribution of the venous outflow to ΔCaBV calculations is found to be just the opposite; the current models are comprised of time-integrated differences between current and mean cerebral blood flow velocity that make no allowance for venous outflow during raw signal collection. Statistical analysis yields such robust agreement among the estimators largely due to their shared parameters with slight mathematical modifications. Further, the patient cohorts selected for this study made up a fraction of the patients within the Cambridge TBI database; these cohorts were specifically chosen because they represent physiological extremes that would test the limits of the models. Therefore, it was presumed that if the models demonstrated such significant effects in these patients, that they should also for the entire database. Finally, of overwhelming significance, is the inability of these TCD-based parameters to provide direct measurements. Despite the power of TCD as a non-invasive predictive tool, each derived parameter contingent on the TCD waveform can only be interpreted as a surrogate descriptor of cerebral hemodynamics. The true value of a TCD-based model (such as PI_C1Ra3) in the determination of pulstile CaBV changes can only be investigated via comparison with invasive measures, such as PET[224,236,237] or a reference method based on plethysmography (electrical impedance) to attempt to validate alternative techniques.

5.2.5. Conclusions

sPI is considered a theoretical explanation of the effects of extreme pathology on CPP^s. Our results indicated that the CFF-based model of sPI using ICP as an input signal (PI_C1Ra3) performed well within all of the three patient cohorts that were examined; however, this cannot be generalized to the entire population receiving neurocritical care. Further investigation of CaBV approximation needs to be conducted in a larger, more heterogenous sample of TBI patients.

Chapter 6

Applications of Non-Invasive Neuromonitoring

The following publications formed the basis of this chapter:

- Calviello LA, Czigler A, Zeiler FA, Smielewski P, Czosnyka M. Validation of non-invasive cerebrovascular pressure reactivity and pulse amplitude reactivity indices in traumatic brain injury. *Acta Neurochirurgica*. 2019 Dec 18:1-8.

- Calviello LA, Cardim DA, Smielewski P, Czosnyka M, Preller J, and Damian MS. Feasibility of Non-Invasive Brain Multi-Modal Monitoring in Intensive Care Patients. *Neurocritical Care. In Submission*.

6.1. Validation of Non-Invasive Cerebrovascular Pressure Reactivity and Pulse Amplitude Reactivity Indices in Traumatic Brain Injury

6.1.1. Introduction

PRx is a common descriptor of cerebrovascular reactivity (CVR) following TBI. PRx quantifies the changes in vascular smooth muscle tone that occur as a result of variations in transmural pressure[1] and is calculated as the moving linear correlation coefficient between MAP and ICP. PRx has become essential to mortality prediction, with negative or zero values of PRx indicative of favorable outcome and positive values indicative of poor outcome[95]. Traditionally relying on the input from invasive, continuous ABP and ICP monitors, PRx is considered to be an invasively-quantified surrogate marker of cerebral autoregulation (CA) that accounts for changes in intracerebral blood volume attributable to either vasodilation or vasoconstriction[239].

The pulse-amplitude index (PAx) is another index of cerebrovascular reactivity, which theoretically can outperform PRx when the compliance of the cranial space is increased (i.e. after craniotomy, with CSF leakages, etc.). It correlates the changes in the pulse amplitude of ICP (AMP) with changes in mean ABP (as the moving correlation coefficient of 30 samples of 10-second averages of AMP and mean ABP). Both PRx and PAx can be only calculated when ICP is monitored. Since ICP monitoring usually provides a clear signal over a few days or even weeks after TBI, PRx and PAx may be used for long-term management of patients (i.e. for example optimal-CPP oriented therapy[23,240–242]

Indices of cerebral autoregulation can be calculated directly with TCD monitoring. The mean flow index (Mx) or the systolic flow index (Sx) show stronger performance than PRx (the moving correlation coefficients of 30 samples of 10-second averages of mean or systolic CBFV and mean CPP)[86,243]. However, TCD monitoring is intermittent (30 minutes to a few hours daily), whereas ICP monitoring is continuous. This is associated with the difficulty to maintain the continuous insonation of cerebral

vessels that is essential to the calculation of TCD indices; Sx and Mx are probably more accurate than PRx and PAx, but the latter indices can be used continuously.

Changes in cerebral arterial blood volume can be calculated in two ways. Equation 6.1 presumes that pulsatile inflow through the basal arteries is equilibrated by non-pulsatile blood outflow through the dural sinuses, creating the continuous flow forward model (CFF). Equation 6.2 presumes that the inflow of arterial blood is equilibrated by pulsatile flow forward through the regulating arterioles (the pulsatile flow forward model, PFF)[216].

$$\Delta C_a BV_{CFF}(t) = \int_{t_0}^{t} (CBF_a(s) - meanCBF_a)ds \quad [6.1]$$

$$\Delta C_a BV_{PFF}(t) = \int_{t_0}^{t} \left(CBF_a(s) - \frac{ABP(s)}{CVR}\right) ds \quad [6.2]$$

where: s – the arbitrary time variable of integration, CBF_a– cerebral blood flow, ABP– arterial blood pressure, and CVR – cerebrovascular resistance[216].

There is great clinical interest in the application of non-invasive metrics (particularly more accurate surrogate measures of PRx and PAx) during the subacute and long-term phases of TBI care, where invasive ICP monitoring is no longer present and is thus unable to influence patient management or contribute to traditional PRx and/or PAx evaluation. Although the established Mx and Sx are TCD metrics of cerebrovascular reactivity, they are in composition not true direct surrogates of PRx and PAx, even if there is a moderate correlation between them. The purpose of nPRx and nPAx is to provide, as closely as possible, non-invasive measures for PRx and PAx by modeling the constituent components of invasively-derived PRx and PAx using non-invasive TCD-based models of pulsatile CaBV as a direct surrogate for ICP. Doing so provides nPRx and nPAx metrics which are more similar in method of derivation and physiologic composition than other TCD metrics (i.e. Mx and Sx).

This retrospective study seeks to explore the utility of the nPRx and nPAx indices (calculated with both the CFF and the PFF models of CaBV) by correlating them with the established cerebrovascular reactivity markers PRx and PAx. As slow waves between ICP and CaBV are well-synchronized (due to ICP pulsatility and CaBV modifications being triggered simultaneously during the cardiac cycle), it was presumed that the CFF and PFF models could evaluate cerebrovascular reactivity in the absence of invasive ICP monitoring. A secondary aim of this work is correlate all of the aforementioned indices with patient outcome according to the Glasgow Outcome Score (GOS).

6.1.2. Methods

Patients

273 severely head-injured patients (218 males and 55 females with an average age of 33 years old [range: 3-77 years]) were admitted to the Neurosciences Critical Care Unit (NCCU) at Addenbrooke's Hospital, Cambridge, United Kingdom between 1992 and 2012. All patients were managed in accordance with an ICP/CPP-oriented protocol designed to maintain ICP below 20 mm Hg. The exact protocol changed several times over the monitoring period, but its essential components were stable[88].

Monitoring

All patients underwent both invasive (ABP and ICP) and daily non-invasive monitoring (TCD) while admitted to NCCU. Raw data signals from select monitoring devices were recorded and electronically stored using WREC software (Warsaw University of Technology) and ICM+™ software (Cambridge Enterprise, Cambridge, United Kingdom; http://www.neurosurg.cam.ac.uk/icmplus).

ABP was continuously monitored both invasively [from the radial artery using a pressure monitoring kit (Baxter Healthcare C.A., U.S.A.; Sidcup, U.K.)] and non-invasively. ICP was monitored using an intraparenchymal probe with strain gauge sensors (Codman & Shurtleff, M.A., U.S.A. or Camino Laboratories, C.A., U.S.A.). Blood

flow velocities were monitored from the middle cerebral artery (MCA) with a 2 MHz probe (Multi Dop X4, DWL Elektronische Systeme, Sipplingen, Germany). Raw TCD data recordings within the entire patient cohort (295 individual recordings) with an average continuous monitoring duration of 35 minutes. Of the patients receiving multiple TCD monitoring sessions, all recordings were utilized where signal quality was adequate. TCD measurements were intermittently performed anywhere between the first 24 hours of admission and before final removal of intraparenchymal ICP sensors. The exact period and availability of TCD monitoring varied on an individual basis.

This study was conducted as a retrospective analysis of a prospectively maintained database cohort, in which high frequency clinical neuromonitoring data had been archived. Monitoring of brain modalities was conducted as a part of standard NCCU patient care using an anonymized database of physiological monitoring variables in neurocritical care. Data on age, injury severity, and clinical status at hospital discharge were recorded at the time of monitoring on this database, and no attempt was made to re-access clinical records for additional information (REC 97/291). Since all data was extracted from the hospital records and fully anonymized, no data on patient identifiers were available, and need for formal patient or proxy consent was waived. Within our institution, patient data may be collected with waiver of formal consent, as long as it remains fully anonymized, with no method of tracing it back to an individual patient. Patient physiologic, demographic, and outcome data was collected by the clinicians involved with patient care, and subsequently recorded in an anonymous format. This anonymous data is then provided for future research purposes. Such data curation remains within compliance for research integrity as outlined in the UK Department of Health - Governance Arrangements for Research Ethics Committees (GAfREC), guidelines, section 6.0.

Data Processing

Processing of raw data signals utilized ICM+™ software (Cambridge Enterprise, Cambridge, United Kingdom; http://www.neurosurg.cam.ac.uk/icmplus). Signal artifact removal was first conducted with signal cropping tools within ICM+™. CPP was determined from the difference between raw ABP and ICP signals.

Primary analysis involved the calculation of time-averaged mean values for ABP, ICP, cerebral blood flow velocity (FV), CPP, CaBV_CFF (according to Equation 6.1, taking the FV signal instead of CBF), and CaBV_PFF (according to Equation 6.2, taking the FV signal instead of CBF). Substituting CBF in Equations 6.1 and 6.2 with blood flow velocities has a consequence; estimators of blood volume are presented as blood volume per 1 cm^2 of cross-sectional area of the vessel. Also, the arbitrary choice of t_0 within the calculation window of each interval containing 10 to 20 heartbeats, produces the effect that only the relative changes of cerebral arterial blood volume can be observed with the CaBV(t) signals. The amplitudes of the fundamental frequencies of CaBV_CFF and CaBV_PFF pulse waveforms (i.e. for a frequency equivalent to a heart rate) were also calculated as AMP_CFF and AMP_PFF, respectively.

Mean values of the listed parameters were calculated during 10-second time windows, and were updated every 10 seconds to emphasize vasogenic slow wave fluctuations and to eliminate overlap. A coherence module was calculated between series of 10-second averages of ICP, CaBV_CFF, and CaBV_PFF in the frequency band ranging from 0.005Hz to 0.05 Hz. The same calculations were applied to time series of AMP, AMP_CFF, and AMP_PFF.

Final data processing involved the calculations from the primary analysis, with the addition of PRx (the correlation between ABP and ICP), nPRx_CFF (the correlation between CaBV_CFF and ABP), and nPRx_PFF (the correlation between CaBV_PFF and ABP). Non-invasive PAx was calculated by correlating ABP with either AMP_CFF or AMP_PFF (nPAx_CFF and nPAx_PFF, respectively). Each of these parameters was calculated utilizing a 300-second time window, updated every 10 seconds.

Post-processing, all 10-second by 10-second data were exported from each patient to separate comma-separated variable (CSV) files for further statistical analysis.

Statistics

All statistical analyses were conducted utilizing R software (R Core Team [2017]; R: a language and environment for statistical computing. R Foundation for Statistical Computing, Vienna, Austria, URL https://www.R-project.org/). Grand means of and descriptive statistics for each parameter were calculated. Data were normally-

distributed. Descriptive analyses were applied to the coherences between ICP slow waves and CaBV and between the AMP and AMP_CaBV series.

Linear regression techniques were employed to describe the following relationships in the entire cohort: PRx vs. nPRx_CFF, PRx vs. nPRx_PFF, PAx vs mPAx_CFF, and PAx vs. nPAx_PFF. Goodness of fit was reported utilizing the Pearson correlation coefficient (R). Agreement between the parameters was assessed with the Bland Altman method.

Each of the above indices were also correlated with dichotomized GOS data (favorable versus unfavorable outcome). Favorable outcome was classified by GOS scores of 4 (moderate disability) and 5 (mild to no disability). Unfavorable outcome was classified by GOS scores of 1 (dead) or 2 (vegetative state), or 3 (severe disability). The strength of the relationship between each index and outcome was reported via area under the receiver operating curve (AUC), with bold AUCs reaching $p<0.05$ (statistical significance identified by the Delong test;. p-values between groups were compared with t- and Mann-U tests.

6.1.3. Results

Table 6.1 summarizes descriptive statistics for the entire cohort of TBI patients. Slow waves of ICP and CaBV in most cases appeared well-synchronized in time (Figure 6.1A, top panel). The same observation can be made for time series of AMP, AMP_CFF, and AMP_PFF (Figure 6.1B, bottom panel). The averages of the modules of coherence functions in low frequency limits (0.005Hz to 0.05 Hz) are presented in Table 6.2.

Table 6.1. Mean Cerebral Hemodynamic Parameters in TBI. *ABP – arterial blood pressure, CaBV_CFF – cerebral arterial blood volume calculated with the continuous flow forward method, CaBV_PFF – cerebral arterial blood volume calculated with the pulsatile flow forward method, cm/s – centimeters per second, CPP – cerebral perfusion pressure, Favorable: Unfavorable Outcome – Glasgow Outcome Score [Favorable: GOS 4-5 (moderate-mild, or no disability); Unfavorable: GOS 1-3 (dead, vegetative state, or severe disability)], FV – cerebral blood flow velocity, Admission GCS – Glasgow Coma Score on admission, mm Hg – millimeters of mercury, IQR – interquartile range, nPAx_CFF – non-invasive PAx calculated with the continuous flow forward method, nPAx_PFF – non-invasive PAx calculated with the pulsatile flow forward method, nPRx_CFF – non-invasive PRx calculated with the continuous flow forward method, nPRx_PFF – non-invasive PRx calculated with the pulsatile flow forward method, PAx – pulse amplitude index, and PRx – pressure reactivity index.*

Parameter	Mean	Range	Standard Deviation
Age [Years]	33.14	3.0-77.0	± 15.96
Favorable: Unfavorable Outcome	132:122	1-5	---
Admission GCS (Median)	6.0	1-15	IQR 4
ABP [mm Hg]	91.36	58.61-147.57	± 12.08
ICP [mm Hg]	18.12	-3.27-75.69	± 9.92
CPP [mm Hg]	73.61	20.63-109.55	± 13.20
FV [cm/s]	63.41	19.67-168.79	± 25.64
PRx	0.02	-0.65-0.96	± 0.27
PAx	-0.10	-0.93-0.76	± 0.20
nPRx_CFF	0.16	-0.41-0.80	± 0.20
nPRx_PFF	-0.21	-0.69-0.45	± 0.19
nPAx_CFF	-0.07	-0.45-0.56	± 0.14
nPAx_PFF	-0.06	-0.44-0.62	± 0.13

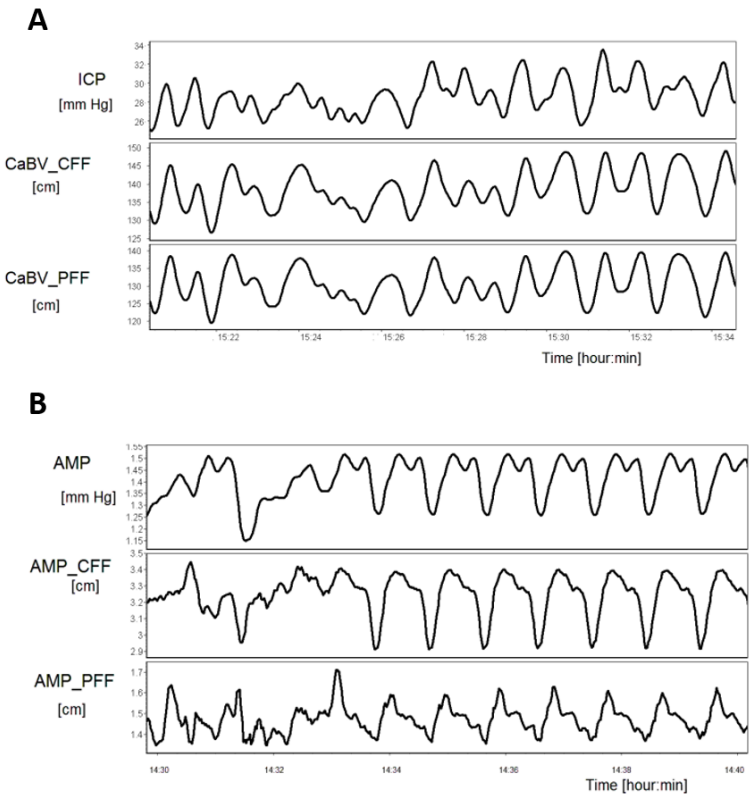

Figure 6.1. **ICP Waveforms and CaBV Modeling.** Examples of good synchronization of mean ICP and CaBV time series in a frequency range of slow waves (Figure 6.1A). Figure 6.1B demonstrates good synchronization of AMP time series with AMP_CFF and AMP_PFF.

Table 6.2. Coherences between variables within the frequency range 0.005-0.05 Hz.

Variables	**Module of Coherence <0.005-0.05 Hz>**	**95% Confidence Intervals**
ICP vs. $CaBV_{CFF}$	0.765	0.748-0.782
ICP vs. $CaBV_{PFF}$	0.758	0.741-0.776
AMP vs. AMP_CFF	0.73	0.718-0.747
AMP vs. AMP_PFF	0.678	0.665-0.692

The correlations between PRx and nPRx and those between PAx and nPAx are only moderately strong (although the *R*-value is significantly non-zero at $p<0.0001$). Scatterplots and correlation coefficients for each model (calculated with either the CFF or PFF methods) are shown in Figure 6.2. Table 6.3 includes the results of Bland-Altman analysis for invasive and non-invasive reactivity indices. The majority of data points were clustered around the mean for each of the modeled pairs with few outliers. It must be noted that the outliers derived from the results shown in Fig. 6.2 are due to the varying blood pressures exhibited by patients in the TBI database.

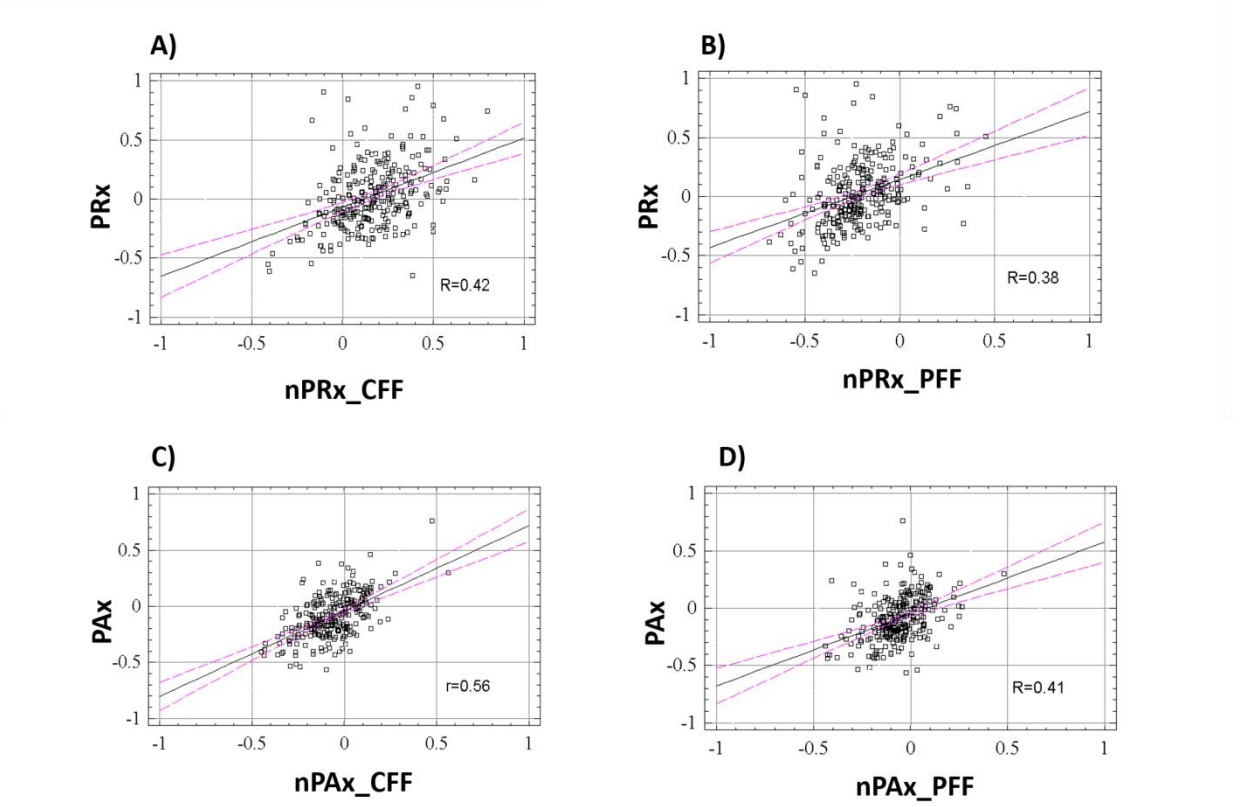

Figure 6.2. **Scatterplots of PRx vs. nPRx and PAx vs. nPAx calculated by the different CaBV models.** Pearson correlation coefficients are given. The correlation between PAx and nPAx_CFF is significantly the strongest (p<0.003). Correlations between traditional parameters and derived parameters based on CFF models are stronger than those based on PFF models (p<0.01 for nPAx and p<0.076 for nPRx).

Table 6.3. Bland Altman Agreement Between PRx-nPRx and PAx-nPAx.

	Critical Difference	**Lower Limit**	**Mean Difference**	**Upper Limit**
PRx vs. nPRx_CFF	0.51	-0.65	-0.13	0.38
PRx vs. nPRx_PFF	0.52	-0.28	0.24	0.76
PAx vs. nPAx_CFF	0.33	-0.36	-0.03	0.30
PAx vs. nPAx_PFF	0.40	-0.44	-0.03	0.37

Finally, all reactivity indices (invasive and non-invasive) were compared in two outcome groups: favorable outcome (n=132) and unfavorable outcome (n=122). 19 patients were not available for follow up. The strongest separation was detected for the nPAx_CFF index (Table 6.4). nPAx_CFF performed the best when compared to outcome, but was not significantly different from the other indices when evaluated with the Delong test.

Table 6.4. Differences between reactivity indices in patients with favorable and unfavorable outcomes at 6 months after TBI. The strength of the relationship between each index and outcome was additionally reported via area under the receiver operating curve (AUC), with bold AUCs reaching $p<0.05$.

Pressure Reactivity Index	**FAVORABLE** **Mean and 95% CI**	**UNFAVORABLE** **Mean and 95% CI**	***p*-value**◊ **t-test**	***p*-value**◊ **Mann-U**	***AUC*** ***95% CI***
PRx	-0.014 [-0.046;0.018]	0.189 [0.165;0.21]	**0.022**	0.078	**0.564** **[0.493-0.635]**
nPRx_CFF	0.137 [0.113;0.161]	0.189 [0.165;0.21]	**0.037**	**0.021**	**0.584** **[0.514-0.654]**
nPRx_PFF	-0.242 [-0.26;-0.22]	-0.018 [-0.21;-0.16]	**0.013**	**0.015**	**0.601** **[0.531-0.671]**
PAx	-0.134 [-0.159;-0.11]	-0.055 [-0.08;-0.028]	**0.018**	**0.002**	**0.615** **[0.546-0.684]**
nPAx_CFF	-0.10 [-0.12;-0.085]	-0.037 [-0.055;-0.019]	**0.0003**	**0.0003**	**0.632** **[0.564-0.701]**
nPAx_PFF	-0.076 [-0.09;-0.059]	-0.052 [-0.069;-0.035]	0.164	0.093	0.561 [0.490-0.632]

◊Statistical significance was determined via both t- and Mann-Whitney U-tests with an alpha of 0.05 assigned to entries with p-values below this threshold.

6.1.4. Discussion

In the evaluated population of TBI patients, nPRx and nPAx calculated with the CFF model were found to better approximate PRx and PAx. It is likely that the PFF model in general is more susceptible to variations in its key components (i.e. unstable ABP in patients would affect the numerators in Equation 6.2) that impact its stability as a calculation method; this effect is consistent with the findings of Eide et al.[244], which discovered weak correlations between ABP and ICP pulse pressure amplitudes and autoregulation indices such as PRx. On the basis of their results[244], as the PFF model is comprised of input from the ABP signal, it is fitting that the nature of the nPRx_PFF index is incompatible with PRx and PAx, which are all "noisy" surrogate markers of cerebral autoregulation to begin with. The CFF and PFF models partially account for total cerebral blood volume change, as they are calculated as the difference between systolic and mean cerebral blood flow integrated over a given period of time. Cerebral blood flow velocity as assessed by TCD is a surrogate measure of cerebral blood flow, as the TCD monitoring technique does not directly quantify cerebral circulation. Thus, current applications of these models can only approximate cerebral blood volume change.

PRx ultimately responds to alterations in cerebral blood volume, and responds to both ICP and ABP fluctuations as vessel diameter changes There is the additional possibility that PRx may be inaccurately represented in TBI patients with either low or high levels of ICP, as the index does not describe cerebrospinal fluid compliance, which influences the direction of cerebral blood volume change, and thus measured ICP[240]. As the nPRx and nPAx indices do not rely on information from invasive ICP sensors but rather ABP, they only moderately correlated with traditional PRx and PAx, which are both more commonly associated with ICP. It is important to note that the determination of nPRx and nPAx with the current TCD-based CFF and PFF models cannot definitively describe the relationships between the "true" input from cerebral blood flow and either the ABP or the ICP signals.

These non-invasive TCD models of PRx and PAx based on CaBV estimates provide information closer to invasively-derived ICP. Further refinement of the nPRx_CFF model in particular will enhance the ability to non-invasively approximate traditional PRx, which has been experimentally-validated as a measure of the lower limit of autoregulation[245]. nPRx can be employed for long-term follow-up using continuous, non-invasive ABP (via finger-cuff). Cerebrovascular reactivity during the subacute phase of care can be correlated with long-term autoregulatory status, inclusive of clinical phenotype and chronic neuroimaging changes (i.e. magnetic resonance imaging (MRI)-based cortical atrophy or diffusion tensor imaging (DTI) white matter tract volume). nPRx can inform clinicians of patient autoregulatory status in the absence of neurosurgical placement of invasive monitors; it can be directly calculated from emergency rooms or in remote hospitals without neurosurgical services. Non-invasive determinations of optimal cerebral perfusion pressure ($nCPP_{OPT}$) can also benefit from nPRx, as PRx is a key component in the visualization of CPP[242].

When comparing both traditional and derived autoregulation indices with outcome, nPAx_CFF trended towards higher AUCs in association with dichotomized 6-month outcomes. It must be acknowledged that TCD-based indices such as Mx and Sx, and both sets of nPRx and nPAx estimators can only be calculated if patients receive TCD monitoring, which is intermittently applied at best; at present, it is difficult to provide continuous measures of nPRx or nPAx in the absence of invasive monitoring. Traditional TCD devices such as the DWL Multi Dop X4 require careful placement of TCD probes that are both fragile and very easily disturbed by small movements. Although emerging TCD technology with robotic-assisted probes allows for longer, uninterrupted TCD monitoring, these newer devices are ultimately less popular and too expensive for the majority of centers to obtain for purely research purposes.

Limitations

The strength of this study is fundamentally limited by the reliance on intermittent TCD recordings that were relatively short in duration, and susceptible to motion artifacts. Additionally, statistical analyses were based on grand mean data, which reduces the natural variability within datasets and can potentially create artificial

effects. The correlation coefficient values are in a weak to moderate range for strength. As such, the definitiveness of conclusions from this current study are limited, and should not be extrapolated to other TBI populations at this time. It is also worth noting that Mx and Sx have been previously validated as having stronger outcome-predictive power than PRx[244], which was not addressed in this study. The rationale for nPRx and nPAx is somewhat artificial at the moment; these indices may become more clinically relevant when the next generation of continuous TCD monitoring devices becomes available. There are differences between TCD-based autoregulation and pressure reactivity[47]; with better technology, it may be useful to explore them jointly.

6.1.5. Conclusions

With TCD, it is possible to derive non-invasive estimators of PRx (nPRx) and PAx (nPAx) based on cerebral blood volume modeling (nPRx_CFF, nPRx_PFF, nPAx_CFF, and nPAx_PFF). Direct clinical application of these non-invasive cerebrovascular reactivity indices is limited by the current state of continuous TCD monitoring, but following further improvements on the autofocusing of TCD probes and waveform visualization, they may become clinically useful.

6.2. Feasibility of Non-Invasive Brain Multi-Modal Neuromonitoring in Intensive Care Patients

6.2.1. Introduction

Secondary neurological complications may occur in patients admitted to general intensive care for a variety of conditions, such as cardiac arrest, metabolic encephalopathies, sepsis, and multi-organ failure[246–249]. Coma is associated with

increased risk of life-threatening events (status epilepticus, stroke, intracranial hemorrhage, etc.). Often, clinicians can no longer obtain critical neurological information before brain injury may be already beyond treatment. Implanted probes that continuously monitor cerebral dynamic functions (i.e. intracranial pressure, brain tissue oxygenation, cerebral metabolism, etc.) have become well-established modalities used during neurocritical treatment protocols; however, they are seldom used outside of neurocritical care. Continuous neuromonitoring is not routinely in place for these patients, and as a result, comatose patients under intensive care do not receive neuromonitoring outside of intermittent clinical assessments, which roughly approximate neurological status at the time of intervention and are commonly influenced by sedative drugs. Neurophysiological tests such as electroencephalography (EEG), somatosensory evoked potentials (SSEP) and brain stem auditory evoked potentials are at best available intermittently; likewise, the information provided by other imaging techniques such as magnetic resonance imaging (MRI) or computed tomography (CT), which require transfer out of the intensive care unit.

TCD is commonly utilized in neurocritical care for brain multi-modal monitoring; it examines the cerebral blood flow velocity (CBFV) of basal cerebral arteries via ultrasound probe(s) placed on the temporal window[32]. TCD is a reliable method of assessing cerebral blood circulation by the bedside with minimal disruption to nursing interventions. The TCD-based CBFV signal, in particular, can be further derived to provide non-invasive assessment of cerebral blood flow autoregulation, estimates of intracranial pressure[250] and cerebral perfusion pressure, which are essential to outcome prediction. Previously, TCD has been applied outside of the neurocritical care environment to evaluate patient risk of secondary neurological complications[251] in non-neurosurgical settings. The combination of TCD and non-invasive ABP monitoring has been utilized in orthopedic[252] surgery to assess position-based changes that could adversely affect cardiac output, or transplant procedures[253] to identify instances of intracranial hypertension and/or post-operative neurological damage.

This study aimed to assess the feasibility and preemptive clinical benefits of a TCD-based non-invasive multi-modal approach for neuromonitoring in critically-ill

patients. Additionally, it attempted to describe the outcome-predictive power of TCD-related indices in a population of general intensive care patients.

6.2.2. Methods

Patient Recruitment and Ethics

Intensive care staff at the Neurosciences Critical Care Unit (NCCU) and the John Farman Intensive Care Unit (JFICU) at Addenbrooke's Hospital, Cambridge, U.K., identified eligible patients and referred them to the research team at the University of Cambridge Brain Physics Laboratory for inclusion in this study conducted between March 2017 and March 2019. The experimental protocol and informed consent were approved by the institutional review board at Addenbrooke's Hospital, Cambridge University Hospitals Foundation Trust (Cerebral Autonomic Regulation in Multi-Modal Monitoring After Cardiac Arrest – A TTM2 Sub-Trial (TTM2-CAR), shortened to "Triple M", IRAS: 165207). Patients who failed to awaken appropriately after resuscitation from cardiac arrest, or were in coma due to a number of medical conditions including meningitis, seizures, sepsis, metabolic encephalopathies, overdose, multi-organ failure, or transplant were eligible for inclusion. Patients were considered eligible for the study if they were at least 18 years of age and comatose following resuscitation from cardiac arrest or any of the above listed conditions. As patients were unable to provide informed consent themselves at the point of inclusion, they were included either by a process of deferred assent by next of kin or of inclusion by professional assent through treating physicians, who were not involved in the trial. Exclusion criteria comprised of patients under the age of 18, a pre-existing lack of mental capacity to consent, express wish to not participate in research, or inability to undergo transcutaneous TCD monitoring safely such as skin infections or known allergies.

Clinical Data

Data was gathered on admission diagnosis, duration of ventilation, length of stay in the ICU, length of stay in the hospital, and discharge status using Cerebral Performance Categories (CPC). A detailed neurological status was obtained on the day

of monitoring. All patients had CT and EEG; individual cases were investigated with MRI, continuous EEG, and SSEP as indicated clinically.

Data Collection

ABP was continuously monitored invasively from the radial artery using a pressure monitoring kit [Baxter Healthcare C.A., U.S.A.; Sidcup, U.K.]). Mean and peak blood flow velocities were non-invasively monitored from the middle cerebral artery (MCA) with a unilateral 2 MHz TCD probe (Rimed Digi-Lite™, Rimed Ltd., Israel). The probe was held in place during the entire recording session using a head frame provided by the TCD device manufacturer. The signals were all sampled at 300 Hz, digitally transferred from the patient monitor (Carescape B850, GE, U.S.A.) or digitized using an analogue to digital converter (DT9801, Data Translation, Marlboro, M.A., U.S.A.), and were recorded using a laptop computer with ICM+™ software (Cambridge Enterprise Ltd., Cambridge, U.K., http://www.icmplus.neurosurg.cam.ac.uk/).

The above monitoring procedures are in compliance with standardized patient care management using an anonymized database of physiological variables (UK Health Departments Governance Arrangements for Research Ethics Committees (GAfREC)). Demographic data such as age, diagnosis and brain dysfunction on admission, and clinical status as hospital discharge were documented at the time of monitoring; clinical records were not further consulted for additional information for this part of the study, as all extracted data were fully anonymized.

Data Processing and Analysis

Signal artifacts were manually removed by internal signal cropping tools within ICM+™. In the primary analysis phase, time-averaged mean values of both FV and ABP were calculated over 10-second time windows, and updated every 10 seconds to eliminate overlap. Heart rate (HR, Hz) was calculated as the fundamental amplitude of the ABP signal, and both F1 and A1, the fundamental frequencies of FV and ABP, respectively, were each calculated over 20-second time windows and updated every 10 seconds. Baroreflex sensitivity (BRS, ms/mm Hg) was calculated using the ABP waveform according to the algorithm described by Nasr et al.[254]. Heart rate variability

in both the low and high frequency ranges (HRV_LFHF, Hz) was calculated over 300-second time windows and updated every 10 seconds, using specialized ICM+™ functions [255].

Non-invasive ICP (nICP, mm Hg) was estimated using the method developed by Schmidt et al.[256], which describes nICP using a "black box" model with the FV and ABP waveforms as input variables that return the nICP waveform as output. Diastolic ABP (ABPd, mm Hg) and FV (FVd, cm/s) were each determined as the minimum values of their respective signals, and calculated over 2-second time windows with a 2-second update. Systolic FV (FVs, cm/s) was determined as the maximum value of the FV signal, and similarly calculated and updated over 2-second time windows. The autoregulation of cerebral blood flow was estimated by the Mx_a index as a running correlation coefficient between 30 consecutive 10-second time averages of the FV and ABP signals. Clinical evaluation of Mx_a has specified a critical threshold for dichotomized outcome at 0.62 (based on the area under the curve [257]).

Critical closing pressure (CrCP, mm Hg) was calculated using mean values and spectral heart rate fundamental components of the ABP and FV signals (Equation 6.3):

$$\text{CrCP (mm Hg)} = Mean\ (ABP) - \frac{Mean(A1)}{Mean(F1)} * Mean(FV) \quad [6.3]$$

The diastolic closing margin was calculated as the difference between diastolic ABP and CrCP (Equation 6.4, below).

$$\text{DCM (mm Hg)} = Mean(ABPd) - Mean(CrCP) \quad [6.4]$$

Non-invasive cerebral perfusion pressure (nCPP) was assessed using ABP and FV signals using a formula adopted from studies of TBI patients (Equation 6.5, below)[258]:

$$\text{nCPP (mm Hg)} = \left(\frac{(Mean\ ABP\ x\ Mean\ FVd)}{Mean\ FV}\right) + 14$$

[6.5]

The cerebrovascular time constant was calculated as the product of cerebrovascular resistance (Ra= Mean (ABP)/Mean (FV)) and compliance, Ca (Equation 6.6, below):

$$Ca = \frac{(\frac{F1 - A1}{Mean\ Ra})}{2\pi \times HR}$$

[6.6]

Finally, two indices describing the shape of the TCD pulse waveform were calculated: Gosling pulsatility index, gPI (gPI = (FVs-FVd)/FVmean), and the waveform index, Waveform, which indicates how much the TCD waveform differs from the "ideal" triangular shape (Waveform = FVmean- ((2(FVd+FVs))/3). gPI has previously been posited as a non-invasive estimator of both ICP and CPP, with gPI thresholds for ICP based on the area under the curve varying from 0.62 (ICP >15 mm Hg) to 0.74 (ICP >35 mm Hg) for ICP, and 0.68 (CPP <70 mm Hg) to 0.81 (CPP <50 mm Hg) for CPP[259]. A summary of calculated secondary indices is given in Table 6.5.

Table 6.5. Summary of Calculated Secondary Parameters.

Parameter	**Description**	**Interpretation**
BRS (ms/mm Hg)	Baroreflex Sensitivity	Index demonstrating how strong changes in baroreflex can regulate systolic blood pressure; normal value: >10.
HRV_LF/HF (Hz)	Heart Rate Variability (Low Frequency to High Frequency Ratio)	Index describing the ratio of sympathetic-derived heart rate variability (low frequency) to parasympathetic variability (high frequency); normal value: >2.
TAU (s)	Cerebrovascular Time Constant	Hypothetically, how fast arterial blood covers the distance between the conducting to regulating brain arteries, normal value: 0.1 seconds.
Mx_a	Cerebral Autoregulation	Index describing the passivity of changes in FV when mean ABP changes. Disturbed autoregulation shows Mx_a >0.3.
CrCP (mm Hg)	Critical Closing Pressure	Index describing the minimal blood pressure value which keeps cerebral arteries open.
DCM (mm Hg)	Diastolic Closing Margin	Index describing the distance between diastolic ABP and CrCP. When DCM reaches 0, there is no diastolic blood flow observed with TCD.
gPI	Gosling Pulsatility Index	Index which shows the proportion of pulsatile to total blood transport. It is an inverse function of cerebral perfusion pressure, $PaCO_2$, and blood pressure pulsatility (A1), normal value: 1.
Waveform	Waveform	Shows how much the shape of the TCD pulse waveform differs from the ideal triangular pattern.
nICP	Non-Invasive Intracranial Pressure	This is an estimator only, real term accuracy ±10 mm Hg.
nCPP	Non-Invasive Cerebral Perfusion Pressure	This is an estimator (but independent of nICP, above), accuracy ±15 mm Hg.

Statistical Analysis

All statistical analyses were conducted using Statgraphics Version 5 (Manugistics, Irvine, C.A., U.S.A,) and R data analysis software ((R Core Team [2017]; R: a language and environment for statistical computing. R Foundation for Statistical Computing, Vienna, Austria. URL https://www.R-project.org/). Post-processing data, exported as CSV files, were compiled into one large CSV document containing all of the above recorded signals for each patient. Summary statistics for each parameter were calculated across the entire patient cohort (Table 6.6). Patient data was further dichotomized into subsets according to available outcome data (Table 6.7). Statistical significance for invasively-monitored variables (ABP) and non-invasively derived variables (based on TCD) was determined both within and between each subset of patients via the Mann-Whitney U-test with an alpha of 0.05 and assigned to entries with *p*-values below this value.

6.2.3. Results

40 patients (27 males: 13 females; age range: 20-69 years with an average age of 53.79 ± 13.11 years) were identified and enrolled in the study. Data from 37 of these 40 patients were included in our analysis, as 3 patient datasets were later excluded due to poor TCD signal acquisition or the absence of invasive ABP monitoring. Patients were admitted for the following conditions: cardiac arrest (14), complications relating to sepsis (6), meningitis (5), organ transplant (5), drug/alcohol overdose (3), encephalopathy (2), sickle cell crisis (1), pancreatitis (1), colitis (1), pneumonia (1), and refractory status epilepticus (1). It is important to note that findings were not discriminated across the different disease categories. The data recording sessions within the entire patient cohort (68 individual recordings) lasted between 19.5 and 171.75 minutes, with an average continuous monitoring duration of 43.68 ± 16.14 minutes. Figure 6.3 (below) illustrates a typical example of the monitored signals and calculated parameters.

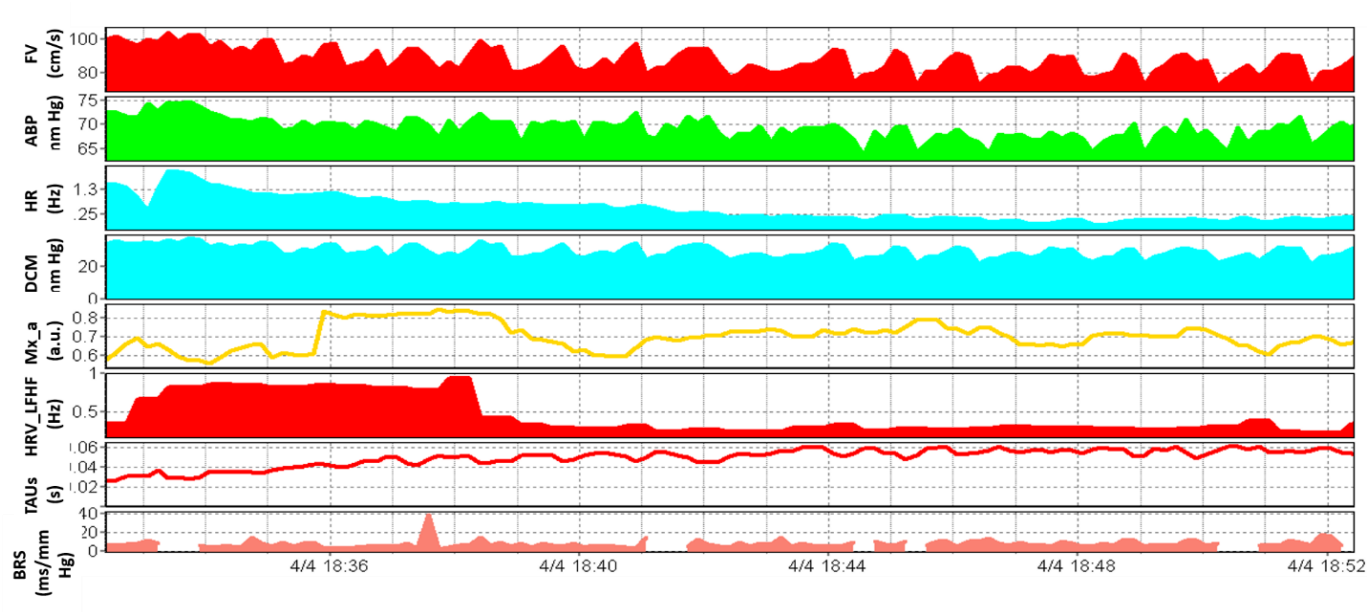

Figure 6.3. **An example of a TCD monitoring session for a 3M patient**, with both standard and derived parameters.

FV – TCD-based flow velocity, ABP – arterial blood pressure (measured invasively), HR – heart rate, DCM – diastolic closing margin, Mx_a – cerebral autoregulation, HRV_LFHF – heart rate variability (low frequency to high frequency ratio), TAUs – cerebrovascular time constant, BRS – baroreflex sensitivity, cm/s – centimeters per second, mm Hg – millimeters of mercury, Hz – Hertz, s – seconds, a.u. – arbitrary units, and ms/mm Hg – milliseconds per millimeter of mercury.

Table 6.6 summarizes the mean values and standard deviations, minimum, maximum, and median values of each parameter across the entire patient cohort. Table 6.7 reports the effects of the measured parameters on patient outcome. Significance levels are highlighted in bold typeface. The results of the presented analyses indicated that irrespective of condition, this population of general intensive care patients had significantly disturbed cerebral autoregulation when comparing survivors to non-survivors (TAUs: p=0.03; Mx_a: p<0.01; and Waveform: p=0.03). Apart from these three parameters that demonstrated a robust relationship with outcome, none of the other metrics reached statistical significance. We further evaluated the differences between those patients who survived according to "good" (CPC 1-2) or "bad" (CPC 3-4) outcome to identify whether there were significant changes in cerebral hemodynamics that predicated poorer recovery. This additional comparison did not present any relationships reaching statistical significance.

Table 6.6. Grand Mean Values of Cerebral Hemodynamic Parameters Across All Patients. *Calculated parameters are explained in Table 6.5.*

	Mean	**Standard Deviation**	**Minimum**	**Maximum**	**Median**
FV (cm/s)	48.40	22.23	16.26	107.90	38.88
ABP (mm Hg)	84.23	15.48	57.25	118.1	78.00
HR (Hz)	1.44	0.31	0.79	2.34	1.41
BRS (ms/mm Hg)	11.06	9.56	1.11	53.5	9.97
TAUs (s)	0.06	0.03	0.002	0.14	0.06
HRV_LFHF (Hz)	1.24	1.10	0.18	5.60	0.91
Mx_a	0.23	0.25	-0.34	0.71	0.22
Waveform	1.49	2.73	-3.45	8.64	1.34
CrCP (mm Hg)	28.37	14.98	-16.90	64.24	27.77
DCM (mm Hg)	32.43	15.03	9.99	72.06	30.88
gPI	1.36	0.40	0.68	2.36	1.30
nICP (mm Hg)	15.74	5.38	5.14	28.78	14.58
nCPP (mm Hg)	57.65	13.75	34.31	87.34	56.25

Table 6.7. Dichotomized Outcomes of Patients. *Calculated parameters are explained in Table 6.5.*

Parameter	Good Outcome (CPC 1-2)	Bad Outcome (CPC 3-5)	*p*-value[◊]
Male:Female Ratio	14:7	12:4	----
Age (Years)	57.50 (±12.20)	49.33 (±12.77)	0.06
Days Ventilated	19.86 (±24.22)	19.81 (±23.35)	0.99
FV (cm/s)	49.28 (±23.13)	47.31 (±21.00)	0.79
ABP (mm Hg)	84.44 (±15.86)	83.96 (±14.98)	0.93
HR (Hz)	1.34 (±0.33)	1.55 (±0.23)	0.46
TAUs (s)	0.07 (±0.03)	0.04 (±0.03)	**0.03**
Mx_a	0.15 (±0.27)	0.37 (±0.17)	**<0.01**
Waveform	0.96 (±2.31)	2.99 (±2.91)	**0.03**
BRS (ms/mm Hg)	12.93 (±12.16)	9.19 (±5.30)	0.26
HRV_LFHF (Hz)	1.32 (±1.27)	1.16 (±0.85)	0.67
CrCP (mm Hg)	29.41 (±12.43)	27.05 (±17.57)	0.64
DCM (mm Hg)	30.86 (±12.43)	34.38 (±17.55)	0.48
gPI	1.39 (±0.37)	1.33 (±0.42)	0.65
nICP (mm Hg)	15.69 (±5.15)	15.81 (±5.65)	0.95
nCPP (mm Hg)	57.39 (±13.55)	57.97 (±13.99)	0.90

[◊]Statistical significance was determined via Mann-Whitney U-tests with an alpha of 0.05 assigned to entries with *p*-values below this threshold.

6.2.4. Discussion

The overall context of this study is to elucidate the feasibility of a multi-modal TCD approach for cerebrovascular assessment in critically-ill, comatose patients. The main findings from these preliminary results from the "Triple-M" trial underscore the importance of utilizing a multi-modal approach to neuromonitoring. Multi-modal monitoring approaches aim to provide a highly-accurate gauge of secondary neurological complications by balancing the shortcomings of individual techniques (i.e. poor probe placement, motion artifacts, intermittent monitoring sessions)[260]. In a 2011 clinical report of advances in neuromonitoring, a focus on the interpretation of combined information from invasive (ICP, ABP, CPP, brain tissue oxygenation, and brain temperature) and non-invasive probes (i.e. TCD to monitor cerebral blood flow) was suggested to have great potential in both the improvement of bedside interventions and of outcome[260]. With the introduction of TCD and the derived indices from the TCD base signal FV to general intensive care, clinicians can gain a more holistic[22,261] understanding of cerebral hemodynamic abnormalities that occur as a result of relatively common conditions such as cardiac arrest, metabolic encephalopathies, sepsis, organ failure, etc. To current knowledge, this study is the first of its kind to extend a multi-modal monitoring approach inclusive of TCD to a mixed population of general intensive care patients in addition to routine EEG[262], and suggests that TCD is able to identify deficient autoregulatory mechanisms[263] in most, if not all, critically-ill patients.

In particular, the highly significant effect of the TCD-based index Mx_a (the correlation coefficient between FV and ABP) on patient outcome prediction in this selected population correlates well with similar studies of Mx_a[21,36,264] in patients suffering from traumatic brain injuries, which defined this index as a robust descriptor of outcome. Mx_a has been cited as an appropriate substitute for quantifying cerebral autoregulation in the absence of invasive ICP, and has been validated against Mx (the index describing the passivity of changes in mean FV when CPP changes) in outcome-predictive power[265]. Sorrentino et al.[21] identified lower and upper boundaries for Mx_a, with a threshold of 0.05 signifying a likelihood for survival and good outcome,

and a threshold of 0.30 signifying a strong association with unfavorable outcome and/or mortality. The observations of differences in Mx_a between our general intensive care patients with CPC 1-2 (0.15) versus those with CPC 3-5 (0.37) are in keeping with these critical thresholds for outcome.

Additionally, although not determined to be significant in the analyses, TCD-derived non-invasive estimators of ICP such as nICP or ICP_FVd have been found to closely approximate traditional invasive ICP monitoring in patients with hypoxic ischemic brain injuries following resuscitation from cardiac arrest[250]. Further, more simplistic descriptors of cerebrovascular resistance such as FVd and gPI have been demonstrated to dichotomize good and bad outcome in patients after cardiac arrest (>1/3 of this cohort), although these parameters did not reach significance[266].

Autoregulation monitoring indices have been utilized to inform personalized treatment following both TBI and cardiac arrest. Non-invasive, multi-modal TCD approaches to autoregulation monitoring integrate the information provided by invasive measurements (i.e. ABP or ICP) with cerebral hemodynamic activity. For instance, the non-invasive identification of potential instances of intracranial hypertension is advantageous for all patients with neurological complications; in contrast to patients with traumatic brain injuries, general intensive care monitoring standards do not routinely incorporate ICP into management protocols. Multi-modal monitoring lends itself to the potential for individualized patient management; a variety of parameters can be evaluated simultaneously in real time and revisited when necessary to redirect and optimize targeted treatment, such as ICP, ABP, or Mx_a. Non-invasive ICP monitoring with TCD poses no risk to patients, and the machines can easily be connected to bedside monitors to provide clinicians with more insight into the dynamic effects of various diseases on the brain that would otherwise be unavailable.

Limitations

It must be acknowledged that the strength of the results, and therefore statistical power, is fundamentally limited by the small sample size of the "Triple-M" trial. With a larger cohort, perhaps more parameters would have reached statistical significance, and further supported the rationale for multi-modal neuromonitoring in general intensive care. However, TCD is primarily viewed as a research tool at the

moment, and is treated as an accessory to standard interventions; thus, recordings are intermittent in nature, and must be coordinated by dedicated operators at the discretion of clinical staff. It is also important to acknowledge that multi-modal monitoring data may not be able to be evaluated in time to provide immediate benefits to patients[260]. However, new state-of-the-art robotic TCD devices are being tested in neurocritical care settings to overcome measurement inaccuracies; these advances in TCD technology have demonstrated stronger FV signal intensity, which enhances the descriptive power of TCD-derived indices such as Mx_a or nICP[267]. This initial foray into more continuous TCD monitoring can improve the reliability of multi-modal TCD parameters in providing personalized treatment targets.

This paper presented preliminary results only, with exclusive focus on TCD-based indices and their relationships with patient outcome. In future communications of this work, it would be useful to correlate TCD and routine EEG findings to compare the two monitoring modalities with respect to outcome. Additionally, patients were not separated by condition, it was impossible to observe any cerebral hemodynamic trends in particular disease states that could, with further study, become viewed as outcome-predictive traits.

6.2.5. Conclusions

Preliminary results from the "Triple-M" trial indicate that multi-modal neuromonitoring increases outcome-predictive power. In particular, TCD-based indices such as Mx_a can be applied to general intensive care monitoring to describe patient outcome as a dynamic function of cerebral autoregulation

Chapter 7

Conclusions and Research Outlook

7.1. Thesis Outcomes in Context

Detailed knowledge and understanding of brain physiology and underlying cerebral hemodynamics are essential to the ongoing management of acute brain injury. Neuromonitoring techniques such as ICP and TCD monitoring provide clinicians with opportunities for the observation and detection of both structural and functional abnormalities that can adversely affect patient outcome. Over time, non-invasive TCD-based parameters have been applied to standard patient monitoring procedures (i.e. FV, Mx) to provide surrogate measures of cerebral autoregulation; increased focus on cerebral blood flow velocity waveform analysis has enabled these new derived parameters to be modified to better approximate their invasive counterparts. The expansion of non-invasive neuromonitoring outside of a strict neurocritical care setting has immense potential for outcome prediction in general intensive care management; these measurement techniques create more holistic patient profiles without any added risks.

7.2. Summary of Main Results

This thesis examined the clinical applications of available neuromonitoring techniques in acute brain injury.

In Chapter 2, the core mechanisms and clinical descriptors of cerebral autoregulation were introduced and evaluated in the context of both invasive and non-invasive neuromonitoring parameters that are used in the prediction of patient

mortality following acute brain injury. Chapter 3 outlined methodologies common to the work presented in this thesis.

In Chapter 4, the clinical indications of elevated intracranial pressure after traumatic brain injury were described in several distinct patient populations. The direction of ICP management is heavily dependent on ICP measurement accuracy. To create the best possible outcomes for patients, "true" ICP should be identified and updated continuously to guide treatment options.

In Chapter 5, new mathematical models were introduced that describe pulsatile cerebral hemodynamics in terms of cerebrovascular resistance and cerebral blood volume in both the time and frequency domains. These models are based on TCD waveform analysis, and expand the ability of TCD monitoring to provide deeper insight into the driving forces behind fluctuations in ICP and CPP that could affect cerebral autoregulation and subsequently, outcome.

In Chapter 6, non-invasive neuromonitoring techniques such as TCD were applied to both create alternatives to invasive monitoring and expand neuromonitoring principles to broader patient populations. In a large cohort of TBI patients, TCD-based non-invasive estimators of PRx and PAx were found to be robust approximators of PRx and PAx, which have been previously demonstrated to correlate with outcome. Additionally, TCD monitoring was extended to general intensive care, and was able to identify underlying hemodynamic differences between patients who survived versus those who did not.

7.2.1. Current Limitations

Several fundamental limitations of all of the clinical research presented in this thesis must be addressed prior to the generalization of the results.

First, the retrospective patient data for the majority of points evaluated here stems from the same large, overlapping clinical monitoring database that is divided into subsets to meet the specifications of the comparative study in question. Additionally, notes on clinical events or nursing interventions are not consistently present in the database, so it is impossible to attribute observable ICP or CPP trends solely to natural fluctuations as a result of brain injury rather than to pharmacological or mechanical

manipulations that occurred with the aim to treat unstable patients. With respect to the prospective data collected from a varied population of general intensive care patients, this sample size was much too small to support a universal claim that differences in specific cerebral hemodynamic parameters predicate the risk of mortality.

Second, TCD monitoring is still largely considered to be a "research tool", and is treated as an accessory to standard patient care management. As a result, continuous FV recordings are unavailable, as any TCD monitoring session must be planned in advance at the discretion of bedside nursing staff and the availability of dedicated research teams to operate the device for data collection and interpretation. TCD recordings are intermittent at best, and not every patient within this "Cambridge database" was able to receive TCD monitoring. Although it is presumed that all of the TCD-based parameters introduced in this thesis are equally sensitive and specific to outcome prediction following acute brain injury, it is difficult to generalize the main results of this thesis to all patients.

Finally, several important monitored variables that could significantly affect neuromonitoring indices have not been considered within the scope of this thesis (i.e. brain tissue oxygenation, mechanical ventilation, and microdialysis). The interaction of these variables with TCD-based parameters and cerebral autoregulation has not been evaluated, although these relationships could inform the further development of outcome-predictive modeling.

7.3. Research Outlook

7.3.1. Non-Invasive Markers of Autoregulation and Individualized Treatment Targets

The advancement of non-invasive approximation of "traditional" invasive estimators of cerebral autoregulation (i.e. nPRx and PRx, or nICP and ICP) offers the potential to

expand neuromonitoring both within and outside of neurocritical care. As these parameters can be calculated on the basis of non-invasive TCD waveform analysis, the incorporation of TCD into broader hospital settings poses no further risk of infection or discomfort to patients, and can quickly provide key information about cerebral hemodynamics in real time. If TCD monitoring can be extended to more patients on a more regular basis, real-time TCD data could potentially detect and track the evolution of hemodynamic or structural asymmetry. Longitudinal FV observation (and that of TCD-derived parameters) could then be revisited to inform and individualize patient care plans, rather than make assumptions about prognostication on the basis of research trends.

7.3.2. Multi-Modal Monitoring

The presentation of preliminary results from the "Triple-M" trial introduced the concept of TCD monitoring into a more mainstream care environment. Joint consideration of cerebral electrical and circulatory activity is presumed to provide more thorough insight into brain health than isolated monitoring modalities. Although not evaluated in the scope of this thesis, the comparative analysis of other non-invasive neuromonitoring modalities in general intensive care, such as routine EEG and near-infrared spectroscopy (NIRS) with TCD-based estimators of cerebral autoregulation are of great interest to future studies of outcome prediction.

Appendix A

Non-Linear Regression Between CPP and PI for Individual Patients with Plateau Waves

*Note:

x-axis = CPP measured in mm Hg

y-axis = PI (F_1/FV); no unit

Coefficients of Determination:

P_1 = 0.93	**P_2 = 0.94**
P_3 = 0.75	**P_4 = 0.81**
P_5 = 0.97	**P_6 = 0.80**
P_7 = 0.87	**P_8 = 0.92**
P_9 = 0.83	**P_{10} = 0.89**
P_{11} = 0.84	**P_{12} = 0.73**
P_{13} = 0.56	**P_{14} = 0.92**
P_{15} = 0.94	**P_{16} = 0.98**

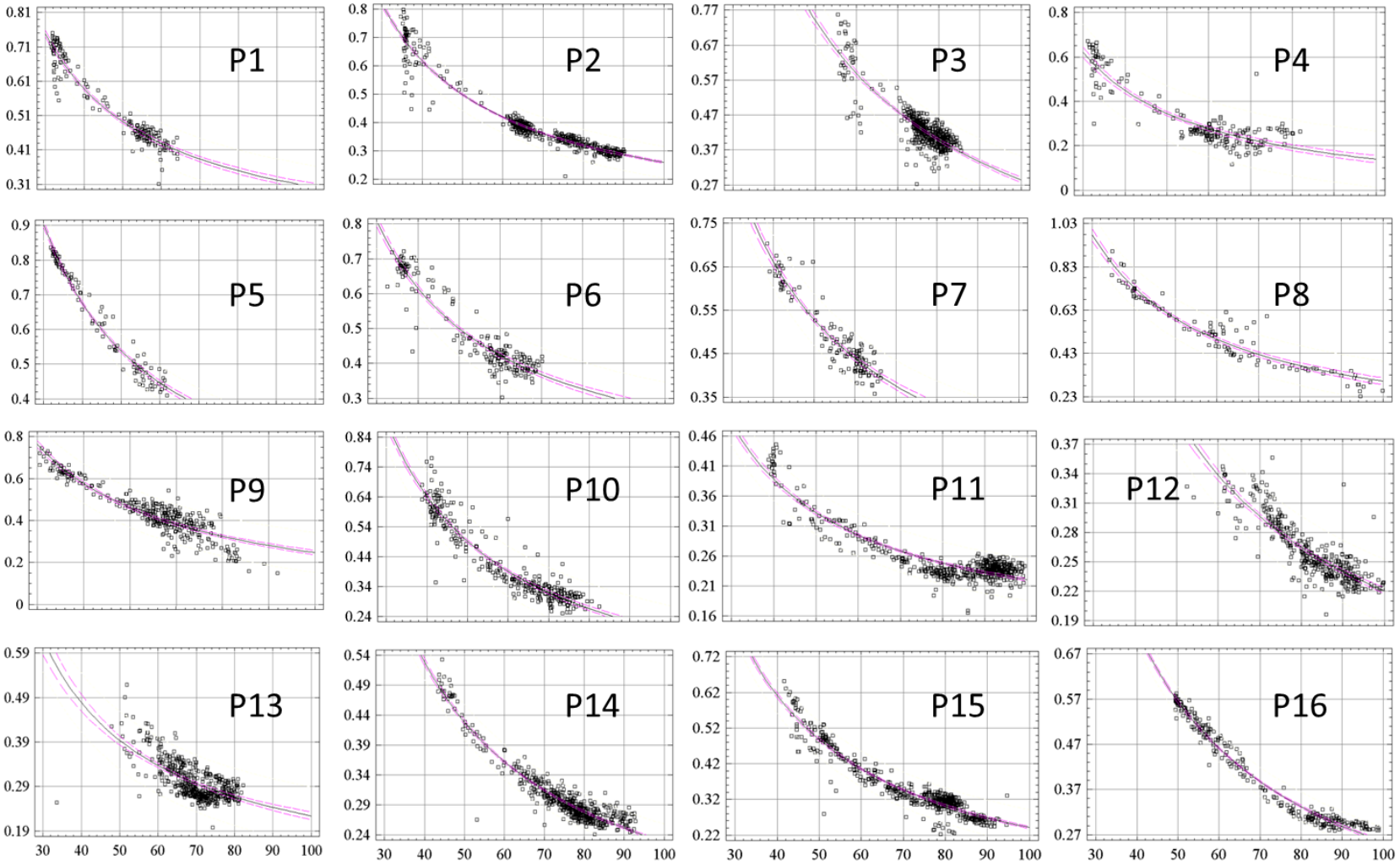
P1
P2
P3
P4
P5
P6
P7
P8
P9
P10
P11
P12
P13
P14
P15
P16

Appendix B

Non-Linear Regression Between CPP and PI for Individual Patients with Unstable MAP

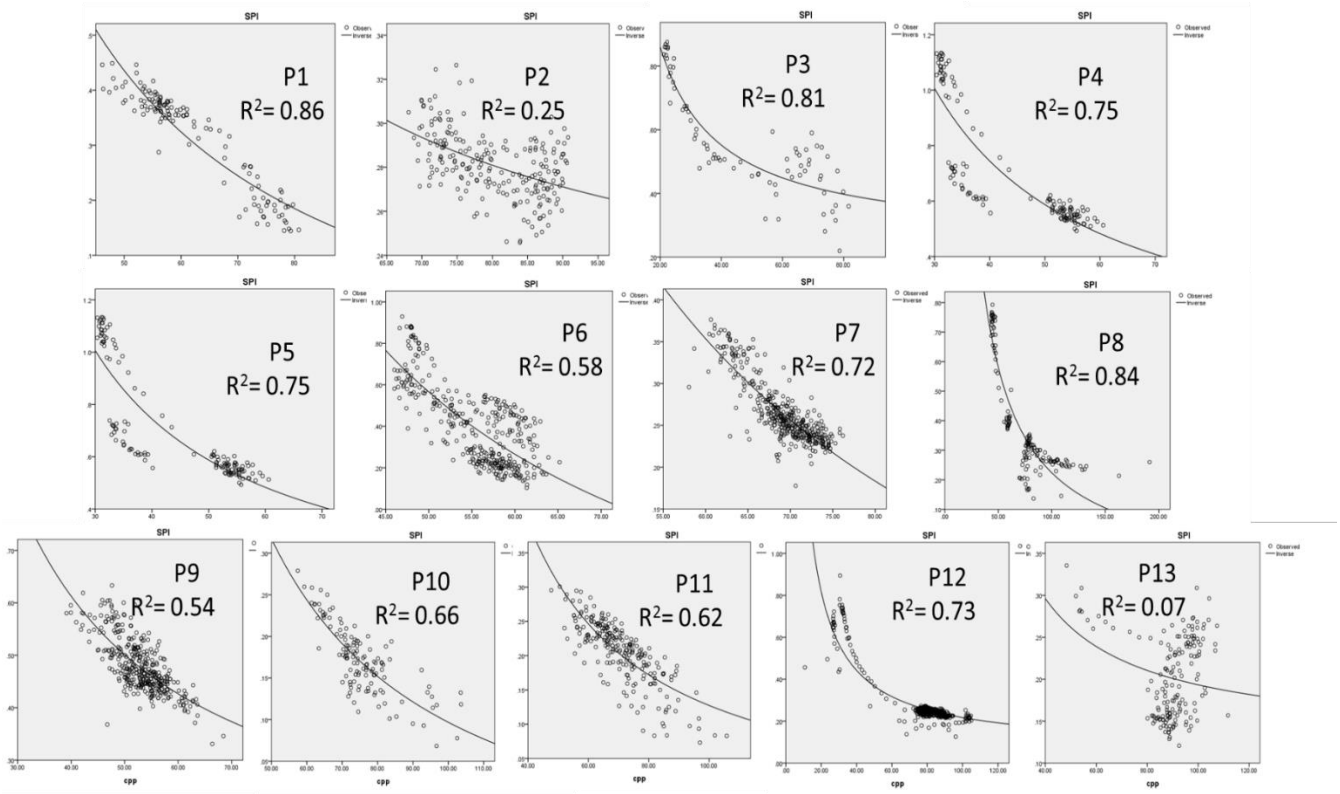

*Note: x-axis = CPP measured in mm Hg, y-axis = PI (F1/FV); no unit

Appendix C

Spectral Models of Cerebral Blood Volume Estimation

$$AmpCaBV_{PFF_{ABP}} = \frac{\left(AmpCBFVa - \left(\frac{AmpABP}{CVR}\right)\right)}{2\pi \times HR} \quad [5.10]$$

$$AmpCaBV_{PFF_{CPP}} = \frac{\left(AmpCBFVa - \left(\frac{AmpABP - AmpICP}{CVR}\right)\right)}{2\pi \times HR} \quad [5.11]$$

where: Amp CBFVa represents the fundamental amplitude of cerebral blood flow velocity (F1), AmpABP – the fundamental amplitude of AMP (A1), AmpCPP – the fundamental amplitude of CPP, AmpCBFVa – the fundamental amplitude of FV, AmpICP – the fundamental amplitude of ICP, CVR – the cerebrovascular resistance, HR – the heart rate, and ICP – intracranial pressure.

Resistors	Capacitors
$Ra1 = \frac{ABP_m}{FV_m}$	$C1 = \frac{AmpCABV_{CFF}}{AmpABP}$
$Ra2 = \frac{A_1}{F_1}$	$C2 = \frac{AmpCABV_{PFF_{ABP}}}{AmpABP}$
$Ra3 = \frac{CPP_m}{FV_m}$	$C3 = \frac{AmpCABV_{PFF_{CPP}}}{AmpABP}$

[5.12]

where: ABP_m, CPP_m, and FV_m each represent the mean value of the respective parameter, A_1 the fundamental harmonic of ABP, and F_1 the fundamental amplitude of the FV waveform.

Appendix D

Formulaic Characterizations of Cerebral Arterial Blood Volume Estimator Models

$$\text{PI\_C1Ra1} = \frac{Mean(A_1)}{CPP_m} \times \sqrt{\left(\frac{Mean\,(CABV_{1S})}{Mean\,(A_1)} \times \frac{ABP_m}{FV_m}\right)^2 \times Mean(HrHz)^2 \times (2\pi)^2 + 1}$$

$$\text{PI\_C1Ra2} = \frac{Mean(A_1)}{CPP_m} \times \sqrt{\left(\frac{Mean\,(CABV_{1S})}{Mean\,(A_1)} \times \frac{Mean\,(A_1)}{Mean(F_1)}\right)^2 \times Mean(HrHz)^2 \times (2\pi)^2 + 1}$$

$$\text{PI\_C1Ra3} = \frac{Mean(A_1)}{CPP_m} \times \sqrt{\left(\frac{Mean\,(CABV_{1S})}{Mean\,(A_1)} \times \frac{CPP_m}{FV_m}\right)^2 \times Mean(HrHz)^2 \times (2\pi)^2 + 1}$$

$$\text{PI\_C2Ra1} = \frac{Mean(A_1)}{CPP_m} \times \sqrt{\left(\frac{Mean\,(CABV_{2S})}{Mean\,(A_1)} \times \frac{ABP_m}{FV_m}\right)^2 \times Mean(HrHz)^2 \times (2\pi)^2 + 1}$$

$$\text{PI\_C2Ra2} = \frac{Mean(A_1)}{CPP_m} \times \sqrt{\left(\frac{Mean\,(CABV_{2S})}{Mean\,(A_1)} \times \frac{Mean\,(A_1)}{Mean(F_1)}\right)^2 \times Mean(HrHz)^2 \times (2\pi)^2 + 1}$$

$$\text{PI\_C2Ra3} = \frac{Mean(A_1)}{CPP_m} \times \sqrt{\left(\frac{Mean\,(CABV_{2S})}{Mean\,(A_1)} \times \frac{CPP_m}{FV_m}\right)^2 \times Mean(HrHz)^2 \times (2\pi)^2 + 1}$$

$$\text{PI\_C3Ra1} = \frac{Mean(A_1)}{CPP_m} \times \sqrt{\left(\frac{Mean\,(CABV_{3S})}{Mean\,(A_1)} \times \frac{ABP_m}{FV_m}\right)^2 \times Mean(HrHz)^2 \times (2\pi)^2 + 1}$$

$$\text{PI\_C3Ra2} = \frac{Mean(A_1)}{CPP_m} \times \sqrt{\left(\frac{Mean\,(CABV_{3S})}{Mean\,(A_1)} \times \frac{Mean\,(A_1)}{Mean(F_1)}\right)^2 \times Mean(HrHz)^2 \times (2\pi)^2 + 1}$$

$$\text{PI\_C3Ra3} = \frac{Mean(A_1)}{CPP_m} \times \sqrt{\left(\frac{Mean\,(CABV_{3S})}{Mean\,(A_1)} \times \frac{CPP_m}{FV_m}\right)^2 \times Mean(HrHz)^2 \times (2\pi)^2 + 1}$$

where: ABP_m, CPP_m, and FV_m each represent the mean value of the respective parameter, A_1 the fundamental harmonic of ABP, F_1 the fundamental amplitude of the FV waveform, $CABV_{1\text{-}3S}$ the time-averaged mean values of each CaBV estimation method resolved into the spectral domain, and *HrHz* the fundamental frequency of FV.

First-Authored Publications

- Calviello LA, de Riva N, Donnelly J, Czosnyka M, Smielewski P, Menon DK, Zeiler FA. Relationship Between Brain Pulsatility and Cerebral Perfusion Pressure: Replicated Validation Using Different Drivers of CPP Change. *Neurocritical Care*. 2017 May 25:1-9.

- Calviello LA, Donnelly J, Zeiler FA, Thelin EP, Smielewski P, Czosnyka M. Cerebral autoregulation monitoring in acute traumatic brain injury: what's the evidence?. *Minerva Anestesiologica.* 2017 Aug;83(8):844

- Calviello LA, Donnelly J, Cardim D, Robba C, Zeiler FA, Smielewski P, Czosnyka M. Compensatory-reserve-weighted Intracranial Pressure and its association with outcome after Traumatic Brain Injury. *Neurocritical Care*. 2018 Apr 1;28(2):212-20.

- Calviello LA, Zeiler FA, Donnelly J, Uryga A, de Riva N, Smielewski P, Czosnyka M. Estimation of pulsatile cerebral arterial blood volume based on transcranial doppler signals. *Medical Engineering & Physics*. 2019 Dec 1;74:23-32.

- Calviello LA and Czosnyka M. Neurocritical Care Monitoring in ICU: Measurement of the Cerebral Autoregulation by TCD. *NESCC Project. 2018 September*.

- Calviello LA, Zeiler FA, Donnelly J, Smielewski P, Czigler A, Lavinio A, Hutchinson PJ, Czosnyka M. Cerebrovascular Consequences of Elevated Intracranial Pressure after Traumatic Brain Injury. *Neurocritical Care. In Review.*

- Calviello LA, Forcht Dagi T, Czosnyka Z, Czosnyka M. Measurement Accuracy for Intracranial Pressure Monitoring. *Neurosurgery. In Review.*

- Calviello LA, Czigler A, Zeiler FA, Smielewski P, Czosnyka M. Validation of non-invasive cerebrovascular pressure reactivity and pulse amplitude reactivity indices in traumatic brain injury. *Acta Neurochirurgica*. 2019 Dec 18:1-8.

- Calviello LA, Cardim D, Smielewski P, Czosnyka M, Preller J, and Damian MS. Feasibility of Non-Invasive Brain Multi-Modal Neuromonitoring in Intensive Care Patients. *Neurocritical Care. In Review*.

Co-Authored Publications

- Kaczmarska K, Kasprowicz M, Uryga A, Calviello L, Varsos G, Czosnyka Z, Czosnyka M. Critical Closing Pressure During Controlled Increase in Intracranial Pressure–Comparison of Three Methods. *IEEE Transactions on Biomedical Engineering*. 2018 Mar;65(3):619-24.

- Zeiler FA, Donnelly J, Calviello L, Smielewski P, Czosnyka M. Pressure Autoregulation Measurement Techniques in Adult TBI, Part I: A Scoping Review of Intermittent Methods. *J Neurotrauma*. 2017 Dec 1;34(23):3207-23.

- Zeiler FA, Donnelly J, Calviello L, Smielewski P, Czosnyka M. Pressure Autoregulation Measurement Techniques in Adult TBI, Part II: A Scoping Review of Continuous Methods. *J Neurotrauma.* 2017 Dec 1;34(23):3224-37.

- Zeiler FA, Donnelly J, Nourallah B, Thelin EP, Calviello L, Smielewski P, Czosnyka M, Ercole A, Menon DK. Intra- and Extra-Cranial Injury Burden as Drivers of Impaired Cerebrovascular Reactivity in Traumatic Brain Injury. *J Neurotrauma*. 2018 Jul 15;35(14):1569-77.

- Czosnyka M., Donnelly J., Calviello L., Smielewski P., Menon D.K., Pickard J.D. (2018) Do ICP-Derived Parameters Differ in Vegetative State from Other Outcome Groups After Traumatic Brain Injury? In: Heldt T. (eds) Intracranial Pressure & Neuromonitoring XVI. *Acta Neurochirurgica Supplement*, vol 126. Springer, Cham. First Online March 1, 2018.

- Liu X, Czosnyka M, Donnelly J, Cardim D, Cabeleira M, Calviello L, Lalou DA, Hutchinson PJ, Smielewski P. Relationship between cerebral autoregulation indices based on transcranial Doppler – a modeling perspective. *Ultrasound in Medicine & Biology*. *In Review*.

- Uryga A, Kasprowicz M, Diehl R, Kaczmarska K, Calviello L, Czosnyka M. Assessment of cerebral hemodynamic parameters using pulsatile versus non-pulsatile blood outflow model. *J Clin Monit Comput.* 2019 Feb 15;33(1):85-94.

- Cardim, D, Varsos, G, Uryga, A, Kaczmarska, K, Robba, C, Calviello, L, Bohdanowicz, M, Kasprowicz, M, Schmidt, B, Smielewski, P, Steiner, L, Czosnyka, Marek. Spectral cerebral blood volume accounting for non-invasive

estimation of changes in cerebral perfusion pressure using transcranial Doppler ultrasonography. *In Submission.*

- Cardim D, Scheeren T, Robba C, Matta B, Tytherleigh-Strong G, Kang N, Schmidt B, Donnelly J, Calviello L, Smielewski P, Czosnyka M. Cerebrovascular assessment of patients undergoing shoulder surgery in beach chair position using a multiparameter transcranial Doppler approach. *J Clin Monit Comp. 2018 Oct 17:1-1.*

- Zeiler FA, Cabeleira M, Calviello L, Smiewlewski P, Czosnyka M. Impaired Cerebral Compensatory Reserve is Associated with Admission Imaging Characteristics of Diffuse Insult in Traumatic Brain Injury. *Acta Neurochir (Wein)*. 2018 Dec 1;160(12):2277-87.

- Nourallah B, Zeiler FA, Calviello L, Smielewski P, Czosnyka M, Menon DK. Critical Thresholds for Intracranial Pressure Vary Over Time in Non-Craniectomized Traumatic Brain Injury Patients. *Acta Neurochirurgica (Wien).* 2018 Jul 1;160(7):1315-24.

- Zeiler FA, Donnelly J, Calviello L, Lee JK, Smielewski P, Brady K, Kim DJ, Czosnyka M. Validation of pressure reactivity and pulse amplitude indices against the lower limit of autoregulation, Part I: experimental intra-cranial hypertension. *J Neurotrauma*. 2018 Nov 12;35(23):2803-11.

- Cardim D, Smielewski P, Sekhon M, Calviello L, Ainslie P, Robba C, Griesdate D, Czosnyka M. A comparison of non-invasive versus invasive measures of intracranial pressure in hypoxic ischaemic brain injury after cardiac arrest. *Resuscitation.* 2019 Jan 7.

- Uryga A, Kasprowicz M, Burzyńska M, Calviello L, Kaczmarska K, Czosnyka M. Cerebral arterial time constant calculated from the middle and posterior cerebral arteries in healthy subjects. *J Clin Monit Compu*. 2018, pp.1-9, https://doi.org/10.1007/s10877-018-0207-3.

- "Kaczmarska K, Uryga A, Placek M, Calviello L, Kasprowicz M, Varsos G, Czosnyka Z, Koźniewska E, Sierzputoskwi T, Koszewski W, Czosnyka M. Critical closing pressure in experimental intracranial hypertension: comparison of three calculation methods. *Neurological Research*. Accepted 2020 Feb 6.

References

1. Calviello LA, Donnelly J, Zeiler FA, Thelin EP, Smielewski P, Czosnyka M. Cerebral autoregulation monitoring in acute traumatic brain injury: What's the evidence? *Minerva Anestesiologica*. 2017.

2. Calviello LA, Czosnyka M. Chapter 1 – Neurocritical Care Monitoring in ICU: Measurement of the Cerebral Autoregulation by TCD. *In: NESCC Course*. 2018.

3. Menon DK, Schwab K, Wright DW, Maas AI. Position statement: Definition of traumatic brain injury. *Archives of Physical Medicine and Rehabilitation*. 2010 Nov 1;91(11):1637-40.

4. Zeiler FA, Donnelly J, Nourallah B, Thelin EP, Calviello L, Smieleweski P, et al. Intra- and Extra-Cranial Injury Burden as Drivers of Impaired Cerebrovascular Reactivity in Traumatic Brain Injury. *J Neurotrauma*. 2018 Jul 15;35(14):1569-77.

5. Needham E, McFadyen C, Newcombe V, Synnot A, Czosnyka M, Menon D. Cerebral Perfusion Pressure Targets Individualized to Pressure-Reactivity Index in Moderate to Severe Traumatic Brain Injury: A Systematic Review. *J Neurotrauma*. 2017 Mar 1;34(5):963-70.

6. Willie CK, Tzeng Y-C, Fisher JA, Ainslie PN. Integrative regulation of human brain blood flow. *J Physiol*. 2014 Mar 1;592(5):841-59.

7. Fog M. Cerebral circulation: The reaction of the pial arteries to a fall in blood pressure. *Arch Neurol Psychiatry*. 1939 Jan 1;41(1):109-18.

8. Lassen NA. Cerebral blood flow and oxygen consumption in man. *Physiol Rev*. 1959 Apr 1;39(2):183-238.

9. Czosnyka M, Smielewski P, Piechnik S, Steiner L a, Pickard JD. Cerebral autoregulation following head injury. *J Neurosurg*. 2001;95(5):756–63.

10. Strandgaard S, Sengupta D, Mackenzie ET, Rowan JO, Olesen J, Skinhøj E, et al. The Lower and Upper Limits for Autoregulation of Cerebral Blood Flow. In:

Cerebral Circulation and Metabolism. 1975 (pp.3-6). Springer, Berlin, Heidelberg.

11. Donnelly J, Czosnyka M, Harland S, Varsos G V., Cardim D, Robba C, et al. Cerebral haemodynamics during experimental intracranial hypertension. *J Cereb Blood Flow Metab* [Internet]. 2017 Feb 21;37(2):694–705. Available from: http://journals.sagepub.com/doi/10.1177/0271678X16639060

12. Mokri B. The Monro–Kellie hypothesis. *Neurology*. 2001 Jun 26;56(12):1746-8.

13. S.A. M, J.Y. C. Critical care management of increased intracranial pressure. J *Intensive Care Med* [Internet]. 2002;17(2):55–67. Available from: http://www.embase.com/search/results?subaction=viewrecord&from=export&id=L34171948%5Cnhttp://dx.doi.org/10.1046/j.1525-1489.2002.17201.x%5Cnhttp://sfx.library.uu.nl/utrecht?sid=EMBASE&issn=08850666&id=doi:10.1046%2Fj.1525-1489.2002.17201.x&atitle=Critical

14. Miller JD, Becker DP, Ward JD, Sullivan HG, Adams WE, Rosner MJ. Significance of intracranial hypertension in severe head injury. *J Neurosurg* [Internet]. 1977;47(4):503–16. Available from: http://www.ncbi.nlm.nih.gov/pubmed/903804

15. Obrist WD, Langfitt TW, Jaggi JL, Cruz J, Gennarelli TA. Cerebral blood flow and metabolism in comatose patients with acute head injury. Relationship to intracranial hypertension. *J Neurosurg*. 1984;61(2):241–53.

16. Youmans J, Winn H. Youmans Neurological Surgery. Vol 4. Ch. 343. 6th ed. Philadelphia, PA: Elsevier/Saunders; 2011.

17. Budohoski KP, Czosnyka M, Kirkpatrick PJ, Smielewski P, Steiner LA, Pickard JD. Clinical relevance of cerebral autoregulation following subarachnoid haemorrhage. *Nature Reviews Neurology*. 2013 Mar;9(3):152.

18. Brady KM, Lee JK, Kibler KK, Easley RB, Koehler RC, Shaffner DH. Continuous measurement of autoregulation by spontaneous fluctuations in cerebral perfusion pressure: comparison of 3 methods. *Stroke*. 2008 Sep 1;39(9):2531-7.

19. Brady KM, Easley RB, Kibler K, Kaczka DW, Andropoulos D, Fraser CD, et al. Positive end-expiratory pressure oscillation facilitates brain vascular reactivity

monitoring. *J Appl Physiol*. 2012 Sep 13;113(9):1362-8.

20. Czosnyka M, Miller C. Monitoring of Cerebral Autoregulation. *Neurocrit Care*. 2014 Dec 1;21(2):95-102.

21. Sorrentino E, Diedler J, Kasprowicz M, Budohoski KP, Haubrich C, Smielewski P, et al. Critical thresholds for cerebrovascular reactivity after traumatic brain injury. *Neurocrit Care*. 2012 Apr 1;16(2):258-66.

22. Cecil S, Chen PM, Callaway SE, Rowland SM, Adler DE, Chen JW. Traumatic brain injury advanced multimodal neuromonitoring from theory to clinical practice. *Crit Care Nurse*. 2011 Apr 1;31(2):25-37.

23. Donnelly J, Aries MJ, Czosnyka M. Further understanding of cerebral autoregulation at the bedside: possible implications for future therapy. *Expert Rev Neurother*. 2015 Feb 1;15(2):169-85.

24. Panerai RB, Jara JL, Saeed NP, Horsfield MA and RT. Dynamic Cerebral Autoregulation Following Acute Ischemic Stroke: Comparison of Transcranial Doppler and Magnetic Resonance Imaging Techniques. *J Cereb Blood Flow Metab*. 2015;1–9.

25. Minciotti P, Ceravolo MG, Provincial L. Inter-examiner variability of Transcranial Doppler procedure and reports: A multicenter survey. *Ital J Neurol Sci*. 1997 Jan 1;18(1):21-30.

26. Lang EW, Lagopoulos J, Griffith J, Yip K, Mudaliar Y, Mehdorn HM, et al. Noninvasive Cerebrovascular Autoregulation Assessment in Traumatic Brain Injury: Validation and Utility. *J Neurotrauma*. 2003 Jan 1;20(1):69-75.

27. Budohoski KP, Reinhard M, Aries MJH, Czosnyka Z, Smielewski P, Pickard JD, et al. Monitoring cerebral autoregulation after head injury. Which component of transcranial Doppler flow velocity is optimal? *Neurocrit Care*. 2012;17(2):211–8.

28. De Riva N, Budohoski KP, Smielewski P, Kasprowicz M, Zweifel C, Steiner LA, et al. Transcranial doppler pulsatility index: What it is and what it isn't. *Neurocrit Care*. 2012;17(1):58–66.

29. Aaslid R, Markwalder TM, Nornes H. Noninvasive transcranial Doppler ultrasound recording of flow velocity in basal cerebral arteries. *J Neurosurg*. 1982 Dec 1;57(6):769-74.

30. Marda M, Prabhakar H. Transcranial Doppler. *J Neuroanaesth Crit Care*. 2015;2(3):215–20.

31. Calviello LA, Donnelly J, Zeiler FA, Thelin EP, Smielewski P, Czosnyka M. Cerebral Autoregulation Monitoring in Acute Traumatic Brain Injury: What's the Evidence? *Minerva Anestesiol*. 2017.

32. Aaslid R, Lindegaard KF, Sorteberg W, Nornes H. Cerebral autoregulation dynamics in humans. *Stroke*. 1989 Jan;20(1):45-52.

33. Tiecks FP, Lam AM, Aaslid R, Newell DW. Comparison of Static and Dynamic Cerebral Autoregulation Measurements. *Stroke*. 1995 Jun;26(6):1014-9.

34. Panerai RB, Haunton VJ, Hanby MF, Salinet ASM, Robinson TG. Statistical criteria for estimation of the cerebral autoregulation index (ARI) at rest. *Physiol Meas* [Internet]. 2016 May 1;37(5):661–72. Available from: http://stacks.iop.org/0967-3334/37/i=5/a=661?key=crossref.182f3f49e669c550fd0f15841536a65e

35. Panerai RB. Assessment of cerebral pressure autoregulation in humans--a review of measurement methods. *Physiol Meas*. 1998 Aug;19(3):305.

36. Liu X, Czosnyka M, Donnelly J, Budohoski KP, Varsos G V, Nasr N, et al. Comparison of Frequency and Time Domain Methods of Assessment of Cerebral Autoregulation in Traumatic Brain Injury. *J Cereb Blood Flow Metab*. 2015 Feb;35(2):248-56.

37. Latka M, Turalska M, Glaubic-Latka M, Kolodziej W, Latka D, West BJ. Phase dynamics in cerebral autoregulation. *Am J Physiol Heart Circ Physiol*. 2005 Nov;289(5):H2272-9.

38. Diehl RR, Linden D, Lucke D, Berlit P. Phase Relationship Between Cerebral Blood Flow Velocity and Blood Pressure : A Clinical Test of Autoregulation. *Stroke*. 1995 Oct;26(10):1801-4.

39. Elting JW, Maurits NM, Aries MJH. Variability of the autoregulation index decreases after removing the effect of the very low frequency band. *Med Eng Phys*. 2014 May 1;36(5):601-6.

40. Czosnyka M, Smielewski P, Kirkpatrick P, Laing RJ, Menon D, Pickard JD. Continuous assessment of the cerebral vasomotor reactivity in head injury. *Neurosurgery*. 1997 Jul 1;41(1):11-9.

41. Hlatky R, Furuya Y, Valadka AB, Gonzalez J, Chacko A, Mizutani Y, et al. Dynamic autoregulatory response after severe head injury. *J Neurosurg*. 2002 Nov 1;97(5):1054-61.

42. Panerai RB, Jara JL, Saeed NP, Horsfield MA, Robinson TG. Dynamic cerebral autoregulation following acute ischaemic stroke: Comparison of transcranial Doppler and magnetic resonance imaging techniques. *J Cereb Blood Flow Metab*. 2016 Dec;36(12):2194-202

43. Schmidt B, Reinhard M, Lezaic V, McLeod DD, Weinhold M, Mattes H, et al. Autoregulation monitoring and outcome prediction in neurocritical care patients: Does one index fit all? *J Clin Monit Comput*. 2016;30(3):367–75.

44. Czosnyka M, Smielewski P, Lavinio A, Pickard JD, Panerai R. An Assessment of Dynamic Autoregulation from Spontaneous Fluctuations of Cerebral Blood Flow Velocity: A Comparison of Two Models, Index of Autoregulation and Mean Flow Index. *Anesth Analg* [Internet]. 2008 Jan;106(1):234–9. Available from: https://insights.ovid.com/crossref?an=00000539-200801000-00041

45. Sánchez-Porras R, Santos E, Czosnyka M, Zheng Z, Unterberg AW, Sakowitz OW. Long pressure reactivity index (L-PRx) as a measure of autoregulation correlates with outcome in traumatic brain injury patients. *Acta Neurochir (Wien)*. 2012 Sep 1;154(9):1575-81.

46. Budohoski KP, Czosnyka M, Smielewski P, Kasprowicz M, Helmy A, Bulters D, et al. Impairment of cerebral autoregulation predicts delayed cerebral ischemia after subarachnoid hemorrhage: A prospective observational study. *Stroke*. 2012 Dec;43(12):3230-7.

47. Budohoski KP, Czosnyka M, De Riva N, Smielewski P, Pickard JD, Menon DK, et al. The relationship between cerebral blood flow autoregulation and cerebrovascular pressure reactivity after traumatic brain injury. *Neurosurgery*. 2012 May 30;71(3):652-61.

48. Sekhon MS, Griesdale DE, Czosnyka M, Donnelly J, Liu X, Aries MJ, et al. The Effect of Red Blood Cell Transfusion on Cerebral Autoregulation in Patients with Severe Traumatic Brain Injury. *Neurocrit Care*. 2015 Oct 1;23(2):210-6.

49. Lavinio A, Menon DK. Intracranial pressure: Why we monitor it, how to monitor it, what to do with the number and what's the future? *Curr Opin Anaesthesiol*. 2011 Apr 1;24(2):117-23.

50. Donnelly J, Czosnyka M, Sudhan N, Varsos G V., Nasr N, Jalloh I, et al. Increased Blood Glucose is Related to Disturbed Cerebrovascular Pressure Reactivity After Traumatic Brain Injury. *Neurocrit Care*. 2015 Feb 1;22(1):20-5.

51. Czosnyka M, Balestreri M, Steiner L, Smielewski P, Hutchinson PJ, Matta B, et al. Age, intracranial pressure, autoregulation, and outcome after brain trauma. *J Neurosurg*. 2005 Mar 1;102(3):450-4.

52. Sykora M, Czosnyka M, Liu X, Donnelly J, Nasr N, Diedler J, et al. Autonomic impairment in severe traumatic brain injury: A multimodal neuromonitoring study. *Crit Care Med*. 2016 Jun 1;44(6):1173-81.

53. Schmidt JM, Kummer BR. Clinical Decision Support for Cerebral Perfusion Optimization After Traumatic Brain Injury*. *Crit Care Med*. 2016 Oct 1;44(10):1958-60.

54. Jaeger M, Dengl M, Meixensberger J, Schuhmann MU. Effects of cerebrovascular pressure reactivity-guided optimization of cerebral perfusion pressure on brain tissue oxygenation after traumatic brain injury. *Crit Care Med*. 2010;38(5):1343–7.

55. Timofeev I, Carpenter KLH, Nortje J, Al-Rawi PG, O'Connell MT, Czosnyka M, et al. Cerebral extracellular chemistry and outcome following traumatic brain injury: A microdialysis study of 223 patients. *Brain*. 2011 Jan 18;134(2):484-94.

56. Steiner LA, Coles JP, Czosnyka M, Minhas PS, Fryer TD, Aigbirhio FI, et al. Cerebrovascular pressure reactivity is related to global cerebral oxygen metabolism after head injury. *J Neurol Neurosurg Psychiatry*. 2003 Jun 1;74(6):765-70.

57. Ang BT, Wong J, Lee KK, Wang E, Ng I. Temporal changes in cerebral tissue oxygenation with cerebrovascular pressure reactivity in severe traumatic brain injury. *J Neurol Neurosurg Psychiatry*. 2007 Mar 1;78(3):298-302.

58. Len TK, Neary JP. Cerebrovascular pathophysiology following mild traumatic brain injury. *Clinical Physiology and Functional Imaging*. 2011 Mar;31(2):85-93.

59. Carney N, Totten AM, O'Reilly C, Ullman JS, Hawryluk GWJ, Bell MJ, et al. Guidelines for the Management of Severe Traumatic Brain Injury, Fourth Edition. *Neurosurgery*. 2017 Jan 1;80(1):6-15.

60. Rosenthal G, Sanchez-Mejia RO, Phan N, Hemphill JC, Martin C, Manley GT. Incorporating a parenchymal thermal diffusion cerebral blood flow probe in bedside assessment of cerebral autoregulation and vasoreactivity in patients with severe traumatic brain injury. *J Neurosurg*. 2011 Jan 1;114(1):62-70.

61. Steiner LA, Czosnyka M, Piechnik SK. Continuous monitoring of cerebrovascular pressure reactivity allows determination of optimal cerebral perfusion pressure in patients with traumatic brain injury. *Crit Care*. 2002 Apr 1;30(4):733-8.

62. Depreitere B, Güiza F, Van den Berghe G, Schuhmann MU, Maier G, Piper I, et al. Pressure autoregulation monitoring and cerebral perfusion pressure target recommendation in patients with severe traumatic brain injury based on minute-by-minute monitoring data. *J Neurosurg* [Internet]. 2014;120(6):1451–7. Available from: http://www.ncbi.nlm.nih.gov/pubmed/24745709

63. Güiza F, Depreitere B, Piper I, Citerio G, Chambers I, Jones PA, et al. Visualizing the pressure and time burden of intracranial hypertension in adult and paediatric traumatic brain injury. *Intensive Care Med*. 2015;41(6):1067–76.

64. Aries MJ, Czosnyka M, Budohoski KP, Kolias AG, Radolovich DK, Lavinio A, et al. Continuous monitoring of cerebrovascular reactivity using pulse waveform of

intracranial pressure. *Neurocrit Care*. 2012 Aug 1;17(1):67-76.

65. Tan CO, Taylor JA. Integrative physiological and computational approaches to understand autonomic control of cerebral autoregulation. *Exp Physiol*. 2014 Jan 1;99(1):3-15.

66. Cabella B, Donnelly J, Cardim D, Liu X, Cabeleira M, Smielewski P, et al. An Association Between ICP-Derived Data and Outcome in TBI Patients: The Role of Sample Size. *Neurocrit Care*. 2017 Aug 1;27(1):103-7.

67. Brady KM, Lee JK, Kibler KK, Smielewski P, Czosnyka M, Easley RB, et al. Continuous time-domain analysis of cerebrovascular autoregulation using near-infrared spectroscopy. *Stroke*. 2007 Oct 1;38(10):2818-25.

68. Bindra J, Pham P, Aneman A, Chuan A, Jaeger M. Non-invasive Monitoring of Dynamic Cerebrovascular Autoregulation Using Near Infrared Spectroscopy and the Finometer Photoplethysmograph. *Neurocrit Care.* 2016 Jun 1;24(3):442-7.

69. Zweifel C, Castellani G, Czosnyka M, Helmy A, Manktelow A, Carrera E, et al. Noninvasive Monitoring of Cerebrovascular Reactivity with Near Infrared Spectroscopy in Head-Injured Patients. *J Neurotrauma*. 2010 Nov 1;27(11):1951-8.

70. Highton D, Ghosh A, Tachtsidis A, Kolyva C, Panovska J, Elwell C, and Smith M. Deoxyhaemoglobin as a biomarker of cerebral autoregulation. *Crit Care*. 2012 Dec;16(1):P295.

71. Weigl W, Milej D, Janusek D, Wojtkiewicz S, Sawosz P, Kacprzak M, et al. Application of optical methods in the monitoring of traumatic brain injury: A review. *Journal of Cerebral Blood Flow and Metabolism*. 2016 Nov;36(11):1825-43.

72. Highton D, Ghosh A, Tachtsidis I, Panovska-Griffiths J, Elwell CE, Smith M. Monitoring cerebral autoregulation after brain injury: Multimodal assessment of cerebral slow-wave oscillations using near-infrared spectroscopy. *Anesth Analg*. 2015 Jul;121(1):198.

73. Diedler J, Zweifel C, Budohoski KP, Kasprowicz M, Sorrentino E, Haubrich C, et al. The limitations of near-infrared spectroscopy to assess cerebrovascular

reactivity: The role of slow frequency oscillations. *Anesth Analg*. 2011 Oct 1;113(4):849-57.

74. Dias C, Silva MJ, Pereira E, Monteiro E, Maia I, Barbosa S, et al. Optimal Cerebral Perfusion Pressure Management at Bedside: A Single-Center Pilot Study. *Neurocrit Care*. 2015 Aug 1;23(1):92-102.

75. Jaeger M, Schuhmann MU, Soehle M, Meixensberger J. Continuous assessment of cerebrovascular autoregulation after traumatic brain injury using brain tissue oxygen pressure reactivity. *Crit Care Med*. 2006 Jun 1;34(6):1783-8.;

76. Adams H, Donnelly J, Kolias AG, Liu X, Newcombe V, Menon DK, et al. Characterising the Temporal Evolution of ICP and Cerebrovascular Reactivity after Severe Traumatic Brain Injury: Best International Abstract Award. *J Neurosurg*. 2016;124:A1195:1196.

77. Zweifel C, Lavinio A, Steiner LA, Radolovich D, Smielewski P, Timofeev I, et al. Continuous monitoring of cerebrovascular pressure reactivity in patients with head injury. *Neurosurg Focus*. 2008 Oct 1;25(4):E2.

78. Soehle M, Jaeger M, Meixensberger J. Online assessment of brain tissue oxygen autoregulation in traumatic brain injury and subarachnoid hemorrhage. *Neurol Res*. 2003 Jun 1; 25(4):411-7.

79. Dias C, Silva MJ, Pereira E, Silva S, Cerejo A, Smielewski P, et al. Post-Traumatic Multimodal Brain Monitoring: Response to Hypertonic Saline. *J Neurotrauma*. 2014 Nov 15;31(22):1872-80.

80. Lang EW, Kasprowicz M, Smielewski P, Pickard J, Czosnyka M. Changes in Cerebral Partial Oxygen Pressure and Cerebrovascular Reactivity During Intracranial Pressure Plateau Waves. *Neurocrit Care*. 2015 Aug 1;23(1):85-91.

81. Bouma GJ, Muizelaar JP, Bandoh K, Marmarou A. Blood pressure and intracranial pressure-volume dynamics in severe head injury: relationship with cerebral blood flow. *J Neurosurg*. 1992 Jul 1;77(1):15-9.

82. Czosnyka M, Matta B, Smielewski P, Kirkpatrick P, Pickard J. Cerebral perfusion

pressure in head-injured patients: a non-invasive assessment using transcranial Doppler ultrasonography. *J Neurosurg*. 1998;88:802–8.

83. Radolovich DK, Aries MJH, Castellani G, Corona A, Lavinio A, Smielewski P, et al. Pulsatile Intracranial Pressure and Cerebral Autoregulation After Traumatic Brain Injury. *Neurocrit Care* [Internet]. 2011 Dec 30;15(3):379–86. Available from: http://link.springer.com/10.1007/s12028-011-9553-4

84. Thees C, Scholz M, Schaller C, Gass A, Pavlidis C, Weyland A, et al. Relationship between Intracranial Pressure and Critical Closing Pressure in Patients with Neurotrauma. *Anesthesiology* [Internet]. 2002 Mar;96(3):595–9. Available from: https://insights.ovid.com/crossref?an=00000542-200203000-00014

85. Varsos G V., Richards HK, Kasprowicz M, Reinhard M, Smielewski P, Brady KM, et al. Cessation of diastolic cerebral blood flow velocity: The role of critical closing pressure. *Neurocrit Care*. 2014;20(1):40–8.

86. Zeiler FA, Donnelly J, Menon DK, Smielewski P, Zweifel C, and Brady K. Continuous Autoregulatory Indices Derived from Multi-Modal Monitoring: Each One Is Not Like the Other. *J Neurotrauma*. 2017 Nov 15;34(22):3070-80.

87. Zeiler FA, Donnelly J, Menon DK, Smielewski P, Hutchinson PJA, Czosnyka M. A Description of a New Continuous Physiological Index in Traumatic Brain Injury Using the Correlation between Pulse Amplitude of Intracranial Pressure and Cerebral Perfusion Pressure. *J Neurotrauma* [Internet]. 2018;974:neu.2017.5241. Available from: http://online.liebertpub.com/doi/10.1089/neu.2017.5241

88. Calviello LA, de Riva N, Donnelly J, Czosnyka M, Smielewski P, Menon DK, et al. Relationship Between Brain Pulsatility and Cerebral Perfusion Pressure: Replicated Validation Using Different Drivers of CPP Change. *Neurocrit Care* [Internet].2017;1–9. https://link.springer.com/article/10.1007/s12028-017-0404-9

89. Czosnyka M, Donnelly J, Liu X, Cardim D, Smielewski P, Lavinio A, et al. ICH-CBF. *In: Presentation at Berlin BRAIN 2017*. 2017.

90. Donnelly J, Czosnyka M, Adams H, Cardim D, Kolias AG, Zeiler FA, et al. Twenty-Five Years of Intracranial Pressure Monitoring After Severe Traumatic Brain

Injury: A Retrospective, Single-Center Analysis. *Neurosurgery*. 2018 Nov 23;85(1):E75-82.

91. Varsos G V, Richards H, Kasprowicz M, Budohoski KP, Brady KM, Reinhard M, et al. Critical closing pressure determined with a model of cerebrovascular impedance. *J Cereb Blood Flow Metab*. 2013;33161(10):235–43.

92. Czosnyka M, Smielewski P, Kirkpatrick P, Piechnik S, Laing R, Pickard JD. Continuous monitoring of cerebrovascular pressure-reactivity in head injury. *Acta Neurochir Suppl*. 1998;71:74–7.

93. Zeiler FA, Donnelly J, Smielewski P, Menon DK, Hutchinson PJ, Czosnyka M. Critical Thresholds of Intracranial Pressure-Derived Continuous Cerebrovascular Reactivity Indices for Outcome Prediction in Noncraniectomized Patients with Traumatic Brain Injury. *J Neurotrauma*. 2018 May 15;35(10):1107-15.

94. Bouma GJ, Muizelaar JP, Bandoh K, Marmarou A. Blood pressure and intracranial pressure-volume dynamics in severe head injury: relationship with cerebral blood flow. *J Neurosurg. 1992*;77(1):15–9.

95. Czosnyka M, Smielewski P, Kirkpatrick P, Laing RJ, Menon D, Pickard JD. Continuous Assessment of the Cerebral Vasomotor Reactivity in Head Injury. *Neurosurgery* [Internet]. 1997 Jul 1;41(1):11–9. Available from: https://academic.oup.com/neurosurgery/article/41/1/11/2859060

96. Czosnyka M, Brady K, Reinhard M, Smielewski P, Steiner LA. Monitoring of cerebrovascular autoregulation: Facts, myths, and missing links. *Neurocritical Care*. 2009 Jun 1;10(3):373-86.

97. Lundberg N. Continuous recording and control of ventricular fluid pressure in neurosurgical practice. *Acta Psychiatr Scand Suppl*. 1960;36(149):1-93.

98. Srinivasan VM, O'Neill BR, Jho D, Whiting DM, Oh MY. The history of external ventricular drainage. *J Neurosurg*. 2014 Jan 1;120(1):228-36.

99. Czosnyka M, Kirollos R, Van Hille P. David Price-Pioneer of digital ICP monitoring, neurosurgeon and teacher. *British Journal of Neurosurgery*. 2015 May

4.;29(3):312-3.

100. Rosner MJ, Becker DP. ICP monitoring: complications and associated factors. *Clin Neurosurg*. 1976; 23:494-519.

101. Price DJ. Digitised ICP over three decades. *In: Acta Neurochirurgica, Supplementum*. 2012.

102. Eide PK, Fremming AD, Sorteberg A. Lack of relationship between resistance to cerebrospinal fluid outflow and intracranial pressure in normal pressure hydrocephalus. *Acta Neurol Scand*. 2003;108(6):381–8.

103. Khan M, Shallwani H, Khan M, Shamim M. Noninvasive monitoring intracranial pressure – A review of available modalities. *Surg Neurol Int*. 2017;8.

104. Akbik OS, Carlson AP, Yonas H. The roles of ventricular and parenchymal intracranial pressure monitoring. *Curr Neurobiol*. 2016.

105. Vries JK, Becker DP, Young HF. A subarachnoid screw for monitoring intracranial pressure. *J Neurosurg*. 1973 Sep 1;39(3):416-9.

106. Swann KW, Cosman ER. Modification of the Richmond subarachnoid screw for monitoring intracranial pressure. *J Neurosurg*. 1984 May 1;60(5):1102-3.

107. North B, Reilly P. Comparison among three methods of intracranial pressure recording. *Neurosurgery*. 1986 Jun 1;18(6):730-2.

108. Weinstabl C, Richling B, Plainer B, Czech T, Spiss CK. Comparative analysis between epidural (Gaeltec) and subboural (Camino) intracranial pressure probes. *J Clin Monit*. 1992 Apr 1;8(2):116-20.

109. Raboel PH, Bartek J, Andresen M, Bellander BM, Romner B. Intracranial pressure monitoring: Invasive versus non-invasive methods-A review. *Crit Care Res Pract*. 2012;2012.

110. Lescot T, Boroli F, Reina V, Chauvet D, Boch AL, Puybasset L. Effect of continuous cerebrospinal fluid drainage on therapeutic intensity in severe traumatic brain injury. *Neurochirurgie*. 2012 Aug 1;58(4):235-40.

111. Harary M, Dolmans RGF, Gormley WB. Intracranial pressure monitoring—review and avenues for development. *Sensors (Switzerland)*. 2018;18(2):465..

112. Czosnyka M, Pickard JD, Steiner LA. Principles of intracranial pressure monitoring and treatment. *In: Handbook of Clinical Neurology*. 2017 Jan 1 (Vol. 140, pp.67-89). Elsevier.

113. Piper I, Dunn L, Contant C, Yau Y, Whittle I, Citerio G, et al. Multi-centre assessment of the Spiegelberg compliance monitor: preliminary results. *In: Brain Edema XI* 2000 (pp.491-494). Springer, Vienna.

114. Cossu G. Intracranial pressure and outcome in critically ill patients with aneurysmal subarachnoid hemorrhage: a systematic review. *(Doctoral dissertation, Université de Lausanne, Faculté de biologie et médecine)*.

115. Han J, Yang S, Zhang C, Zhao M, Li A. Impact of intracranial pressure monitoring on prognosis of patients with severe traumatic brain injury: A PRISMA systematic review and meta-analysis. *Medicine (United States)*. 2016 Feb;95(7).

116. Heuer GG, Smith MJ, Elliott JP, Winn HR, Leroux PD. Relationship between intracranial pressure and other clinical variables in patients with aneurysmal subarachnoid hemorrhage. J Neurosurg. 2004 Sep 1;101(3):408-16.

117. Shen L, Wang Z, Su Z, Qiu S, Xu J, Zhou Y, et al. Effects of intracranial pressure monitoring on mortality in patients with severe traumatic brain injury: A meta-analysis. *PLoS One*. 2016 Dec 28;11(12):e0168901.

118. Treggiari MM, Schutz N, Yanez ND, Romand JA. Role of intracranial pressure values and patterns in predicting outcome in traumatic brain injury: A systematic review. *Neurocritical Care*. 2007 Apr 1;6(2):104-12.

119. Zafar SF, Postma EN, Biswal S, Fleuren L, Boyle EJ, Bechek S, et al. Electronic Health Data Predict Outcomes After Aneurysmal Subarachnoid Hemorrhage. *Neurocrit Care*. 2018 Apr 1;28(2):184-93.

120. Yu L, Kim B, Meng E, Yu L, Kim BJ, Meng E. Chronically Implanted Pressure Sensors: Challenges and State of the Field. *Sensors*. 2014 Nov 1;4(11):20620-44.

121. Bhatia A, Gupta AK. Neuromonitoring in the intensive care unit. Part I. Intracranial pressure and cerebral blood flow monitoring. *In: Applied Physiology in Intensive Care Medicine 1: Physiological Notes - Technical Notes - Seminal Studies in Intensive Care, Third Edition*. 2012 (pp. 135-143). Springer, Berlin Heidelberg.

122. Koskinen LOD, Grayson D, Olivecrona M. The complications and the position of the Codman MicroSensor™ ICP device: An analysis of 549 patients and 650 Sensors. *Acta Neurochir (Wien)*. 2013 Nov 1;55(11):2141-8.

123. Zhong J, Dujovny M, Park HK, Perez E, Perlin AR, Diaz FG. Advances in ICP monitoring techniques. Neurol Res. 2003 Jun 1;25(4):339-50.

124. Norager NH, Lilja-Cyron A, Bjarkam CR, Duus S, Juhler M. Telemetry in intracranial pressure monitoring: sensor survival and drift. *Acta Neurochir (Wien)*. 2018;160(11):2137–44.

125. Stephensen H, Tisell M, Wikkelsö C, Hodge CJ, Gjerris F, Børgesen SE, et al. There is no transmantle pressure gradient in communicating or noncommunicating hydrocephalus. *Neurosurgery*. 2002;50(4):763–71.

126. Bao Y-H, Liang Y-M, Gao G-Y, Pan Y-H, Luo Q-Z, Jiang J-Y. Bilateral Decompressive Craniectomy for Patients with Malignant Diffuse Brain Swelling after Severe Traumatic Brain Injury: A 37-Case Study. *J Neurotrauma*. 2010 Feb 1;27(2):341-7.

127. Yatsushige H, Takasato Y, Masaoka H, Hayakawa T, Otani N, Yoshino Y, et al. Prognosis for severe traumatic brain injury patients treated with bilateral decompressive craniectomy. *In: Brain Edema XIV* 2010 (pp. 265-270). Springer, Vienna.

128. Bor-Seng-Shu E, Figueiredo EG, Amorim RLO, Teixeira MJ, Valbuza JS, de Oliveira MM, et al. Decompressive craniectomy: a meta-analysis of influences on intracranial pressure and cerebral perfusion pressure in the treatment of traumatic brain injury. *J Neurosurg*. 2012 Sep 1;117(3):589-96.

129. Olivecrona M, Rodling-Wahlström M, Naredi S, Koskinen L-OD. Effective ICP

Reduction by Decompressive Craniectomy in Patients with Severe Traumatic Brain Injury Treated by an ICP-Targeted Therapy. *J Neurotrauma*. 2007 Jun 1;24(6):927-35.

130. Hartings JA, Vidgeon S, Strong AJ, Zacko C, Vagal A, Andaluz N, et al. Surgical management of traumatic brain injury: A comparative-effectiveness study of 2 centers: Clinical article. J*ournal of Neurosurgery*. 2014 Feb 1;120(2):434-46.

131. Rossi-Mossuti F, Fisch U, Schoettker P, Gugliotta M, Morard M, Schucht P, et al. Surgical Treatment of Severe Traumatic Brain Injury in Switzerland: Results from a Multicenter Study. *J Neurol Surgery, Part A Cent Eur Neurosurg*. 2016 Jan;77(01):036-45.

132. Reisner A, Chern JJ, Walson K, Tillman N, Petrillo-Albarano T, Sribnick EA, et al. Introduction of severe traumatic brain injury care protocol is associated with reduction in mortality for pediatric patients: a case study of Children's Healthcare of Atlanta's neurotrauma program. *J Neurosurg Pediatr*. 2018 Aug 1;22(2):165-72.

133. Fahlström A, Tobieson L, Redebrandt HN, Zeberg H, Bartek J, Bartley A, et al. Differences in neurosurgical treatment of intracerebral haemorrhage: a nation-wide observational study of 578 consecutive patients. *Acta Neurochir (Wien)*. 2019 May 1; 161(5):955-65.

134. Tariq A, Aguilar-Salinas P, Hanel RA, Naval N, Chmayssani M. The role of ICP monitoring in meningitis. *Neurosurg Focus*. 2017 Nov 1;43(5):E7.

135. Larsen L, Poulsen FR, Nielsen TH, Nordström CH, Schulz MK, Andersen ÅB. Use of intracranial pressure monitoring in bacterial meningitis: a 10-year follow up on outcome and intracranial pressure versus head CT scans. *Infect Dis (Auckl)*. 2017 May 4;49(5):356-64.

136. Tewari MK, Tripathi M, Sharma RR, Mishra GP, Lad SD. Surgical management of moderate sized spontaneous cerebellar hematomas: Role of intracranial pressure monitoring. *Turk Neurosurg*. 2015;25(5):712-720.

137. Perez-Barcena J, Llompart-Pou JA, O'Phelan KH. Intracranial pressure monitoring and management of intracranial hypertension. *Critical Care Clinics*.

2014 Oct 1;30(4):735-50.

138. Messerer M, Daniel RT, Oddo M. Neuromonitoring after major neurosurgical procedures. *Minerva Anestesiologica*. 2012 Jul 1;78(7):810-22.

139. Löfgren J, Zwetnow NN. Cranial and spinal components of the cerebrospinal fluid pressure-volume curve. *Acta Neurol Scand*. 1973 Dec;49(5):575-85.

140. Marmarou A, Shulman K, Rosende RM. A nonlinear analysis of the cerebrospinal fluid system and intracranial pressure dynamics. *J Neurosurg*. 1978 Mar 1;48(3):332-44.

141. Birch AA, Eynon CA, Schley D. Erroneous intracranial pressure measurements from simultaneous pressure monitoring and ventricular drainage catheters. *Neurocrit Care*. 2006;5(1):51–4.

142. Czosnyka M, Czosnyka Z, Pickard JD. Laboratory testing of the Spiegelberg brain pressure monitor: A technical report. *J Neurol Neurosurg Psychiatry*. 1997 Dec 1;63(6):732-5.

143. Allin D, Czosnyka M, Czosnyka Z. Laboratory testing of the pressio intracranial pressure monitor. *Neurosurgery*. 2008;62(5):1158–61.

144. Czosnyka M, Czosnyka Z, Pickard JD. Laboratory Testing of Three Intracranial Pressure Microtransducers: Technical Report. *Neurosurgery*. 1996 Jan 1;38(1):219-24.

145. Al-Tamimi YZ, Helmy A, Bavetta S, Price SJ. Assessment of zero drift in the codman intracranial pressure monitor: A study from 2 neurointensive care units. *Neurosurgery*. 2009;64(1):94–9.

146. Citerio G, Piper I, Cormio M, Galli D, Cazzaniga S, Enblad P, et al. Bench test assessment of the new Raumedic Neurovent-P ICP sensor: A technical report by the BrainIT group. *Acta Neurochir (Wien)*. 2004;146(11):1221–6.

147. Citerio G, Piper I, Chambers IR, Galli D, Enblad P, Kiening K, et al. Multicenter clinical assessment of the raumedic Neurovent-P intracranial pressure sensor: A report by the brainIT group. *Neurosurgery*. 2008 Dec 1;63(6):1152-8.

148. Czosnyka M, Czosnyka Z, Pickard JD. Laboratory Testing of Three Intracranial Pressure Microtransducers: Technical Report. *Neurosurgery*. 1996;38(1):219–24.

149. Gelabert-González M, Ginesta-Galan V, Sernamito-García R, Allut AG, Bandin-Diéguez J, Rumbo RM. The Camino intracranial pressure device in clinical practice. Assessment in a 1000 cases. *Acta Neurochir (Wien)*. 2006;148(4):435–41.

150. Gray WP, Palmer JD, Gill J, Gardner M, Iannotti F. A clinical study of parenchymal and subdural miniature strain-gauge transducers for monitoring intracranial pressure. *Neurosurgery*. 1996;39(5):927–32.

151. Koskinen LOD, Olivecrona M. Clinical experience with the intraparenchymal intracranial pressure monitoring Codman microsensor system. *Neurosurgery*. 2005 Apr 1;56(4):693-8.

152. Lang JM, Beck J, Zimmermann M, Seifert V, Raabe A, Kelly DF, et al. Clinical evaluation of intraparenchymal Spiegelberg pressure sensor. *Neurosurgery*. 2003 Jun 1;52(6):1455-9.

153. Lilja A, Andresen M, Hadi A, Christoffersen D, Juhler M. Clinical experience with telemetric intracranial pressure monitoring in a Danish neurosurgical center. *Clin Neurol Neurosurg*. 2014;120:36–40.

154. Martinez-Mañas RM, Santamarta D, De Campos JM, Ferrer E. Camino® intracranial pressure monitor: Prospective study of accuracy and complications. *J Neurol Neurosurg Psychiatry*. 2000;69(1):82–6.

155. Morgalla MH, Mettenleiter H, Bitzer M, Fretschner R, Grote EH. ICP measurement control: Laboratory test of 7 types of intracranial pressure transducers. *J Med Eng Technol*. 1999 Jan 1;23(4):144-51.

156. Morgalla MH, Dietz K, Deininger M, Grote EH. The problem of long-term ICP drift assessment: Improvement by use of the ICP drift index. *Acta Neurochir (Wien)*. 2002 Jan 1;144(1):57-61.

157. Piper I, Barnes A, Smith D, Dunn L. The Camino intracranial pressure sensor: Is it optimal technology? An internal audit with a review of current intracranial

pressure monitoring technologies. *Neurosurgery*. 2001 Nov 1;49(5):1158-65.

158. Banister K, Chambers IR, Siddique MS, Fernandes HM, Mendelow AD. Intracranial pressure and clinical status: Assessment of two intracranial pressure transducers. *Physiol Meas*. 2000 Nov;21(4):473.

159. Eide PK. Comparison of simultaneous continuous intracranial pressure (ICP) signals from a Codman and a Camino ICP sensor. *Med Eng Phys*. 2006 Jul 1;28(6):542-9.

160. Eide PK, Bakken A. The baseline pressure of intracranial pressure (ICP) sensors can be altered by electrostatic discharges. *Biomed Eng Online* [Internet]. 2011;10(1):75. Available from: http://biomedical-engineering-online.biomedcentral.com/articles/10.1186/1475-925X-10-75

161. Brean A, Eide PK, Stubhaug A. Comparison of intracranial pressure measured simultaneously within the brain parenchyma and cerebral ventricles. *J Clin Monit Comput*. 2006;20(6):411–4.

162. Bruder N, N'Zoghe P, Graziani N, Pelissier D, Grisoli F, François G. A comparison of extradural and intraparenchymatous intracranial pressures in head injured patients. *Intensive Care Med*. 1995 Oct 1;21(10):850-2.

163. Chambers KR, Kane PJ, Choksey MS, Mendelow AD. An evaluation of the camino ventricular bolt system in clinical practice. *Neurosurgery* [Internet]. 1993 Nov;33(5):866–8. http://www.ncbi.nlm.nih.gov/pubmed/8264885

164. Chambers IR, Siddique MS, Banister K, Mendelow AD. Clinical comparison of the Spiegelberg parenchymal transducer and ventricular fluid pressure. *J Neurol Neurosurg Psychiatry*. 2001 Sep 1;71(3):383-5.

165. Childs C, Shen L. Regional pressure and temperature variations across the injured human brain: Comparisons between paired intraparenchymal and ventricular measurements. *Crit Care.* 2015 Dec;19(1):267.

166. Crutchfield JS, Narayan RK, Robertson CS, Michael LH. Evaluation of a fiberoptic intracranial pressure monitor. *J Neurosurg*. 2009 Mar 1;72(3):482-7.

167. Eide PK, Holm S, Sorteberg W. Simultaneous monitoring of static and dynamic intracranial pressure parameters from two separate sensors in patients with cerebral bleeds: comparison of findings. *Biomed Eng Online*. 2012 Dec;11(1):66.

168. Gopinath SP, Robertson CS, Contant CF, Narayan RK, Grossman RG. Clinical evaluation of a miniature strain-gauge transducer for monitoring intracranial pressure. *Neurosurgery*. 1995 Jun 1;36(6):1137-41.

169. Lenfeldt N, Koskinen LOD, Bergenheim AT, Malm J, Eklund A. CSF pressure assessed by lumbar puncture agrees with intracranial pressure. *Neurology*. 2007;68(2):155–8.

170. Schickner DJ, Young RF. Intracranial pressure monitoring: Fiberoptic monitor compared with the ventricular catheter. *Surg Neurol*. 1992 Apr 1;37(4):251-4.

171. Antes S, Tschan CA, Heckelmann M, Breuskin D, Oertel J. Telemetric Intracranial Pressure Monitoring with the Raumedic Neurovent P-tel. *World Neurosurg*. 2016;91:133–48.

172. Lilja-Cyron A, Kelsen J, Andresen M, Fugleholm K, Juhler M. Feasibility of Telemetric Intracranial Pressure Monitoring in the Neuro Intensive Care Unit. *J Neurotrauma*. 2018 Jul 15;35(14):1578-86.

173. Ganslandt O, Mourtzoukos S, Stadlbauer A, Sommer B, Rammensee R. Evaluation of a novel noninvasive ICP monitoring device in patients undergoing invasive ICP monitoring: preliminary results. *J Neurosurg*. 2018 Jun 1;128(6):1653-60.

174. Alberico A, Ward J, Choi S, Marmarou A, Young H. Outcome after severe head injury. Relationship to mass lesions, diffuse injury, and ICP course in pediatric and adult patients. *J Neurosurg*. 1987;67(5):648–56.

175. Chesnut RM, Temkin N, Carney N, Diken S, Rondina C, Videtta W, et al. A trial of intracranial-pressure monitoring in traumatic brain injury. *N Engl J Med*. 2012;367(26):2471–81.

176. Hutchinson PJ, Kolias AG, Czosnyka M, Kirkpatrick PJ, Pickard JD, Menon DK. Intracranial pressure monitoring in severe traumatic brain injury. *Br J Med*.

2013;346:f1000.

177. Cushing H. The third circulation in studies in intracranial physiology and surgery. London: Oxford University Press. 1926.

178. Rosner MJ, Becker DP. Origin and evolution of plateau waves. Experimental observations and a theoretical model. *J Neurosurg*. 1984 Feb 1;60(2):312-24.

179. Kusske JA, Turner PT, Ojemann GA, Harris AB. Ventriculostomy for the treatment of acute hydrocephalus following subarachnoid hemorrhage. *J Neurosurg*. 2009 May 1;38(5):591-5.

180. Burton A. Fundamental instability of the small blood vessels and critical closing pressure in vascular beds. *J Neurosurg*. 1951;164:330–1.

181. Lazaridis C, DeSantis SM, Smielewski P, Menon DK, Hutchinson P, Pickard JD, et al. Patient-specific thresholds of intracranial pressure in severe traumatic brain injury. *J Neurosurg* [Internet]. 2014 Apr;120(4):893–900. Available from: https://thejns.org/view/journals/j-neurosurg/120/4/article-p893.xml

182. Carney N, Totten A, O'Reilly C, Chesnut R, Coplin W, Ghajar J, et al. Brain Trauma Foundation Guidelines for the Management of Severe Traumatic Brain Injury: 4th Edition. [Internet]. 2016 [cited 2017 Feb 16]. Available from: https://braintrauma.org/uploads/03/12/Guidelines_for_Management_of_Severe_TBI_4th_Edition.pdf

183. Miller JD, Pickard JD. Intracranial Volume Pressure Studies in Patients with Head Injury. 1974;5:265–8.

184. Czosnyka M, Guazzo E, Whitehouse M, Smielewski P, Czosnyka Z, Kirkpatrick P, et al. Significance of intracranial pressure waveform analysis after head injury. *Acta Neurochir (Wien)*. 1996;138(5):531–42.

185. Avezaat CJJ, Van Eijndhoven JHM, Wyper DJ. Cerebrospinal fluid pulse pressure and intracranial volume-pressure relationships. *J Neurol Neurosurg Psychiatry*. 1979 Aug 1;42(8):687-700.

186. Czosnyka M, Steiner LA, Balestreri M, Schmidt E, Smielewski P, Hutchinson PJ,

et al. Concept of "weighted ICP" in monitoring and prognostication in head trauma. *Acta Neurochir Suppl*. 2005;95(341–4).

187. Czosnyka M, Whitehouse H, Smielewski P, Kirkpatrick P, Guazzo EP, Pickard JD. Computer supported multimodal bed-side monitoring for neuro intensive care. Int *J Clin Monit Comput*. 1994 Nov 1;11(4):223.

188. Patel HC, Menon DK, Tebbs S, Hawker R, Hutchinson PJ, Kirkpatrick PJ. Specialist neurocritical care and outcome from head injury. *Intensive Care Med*. 2002 May 1;28(5):547-53.

189. Smielewski P, Czosnyka M, Steiner L, Belestri M, Piechnik S, Pickard JD. ICM+: Software for on-line analysis of bedside monitoring data after severe head trauma. *In: Acta Neurochirurgica, Supplementum*. 2005. p. 43–9.

190. Hassler W, Steinmetz H, Gawlowski J. Transcranial Doppler ultrasonography in raised intracranial pressure and in intracranial circulatory arrest. *J Neurosurg*. 1988 May;68(5):745-51.

191. Petty GW, Wiebers DO, Meissner I. Transcranial Doppler Ultrasonography: Clinical Applications in Cerebrovascular Disease. *Mayo Clin Proc*. 1990 Oct 1 (Vol. 65, No.10, pp.1350-1364). Elsevier.

192. Castellani G, Zweifel C, Kim DJ, Carrera E, Radolovich DK, Smielewski P, et al. Plateau waves in head injured patients requiring neurocritical care. *Neurocrit Care*. 2009 Oct 1;11(2):143-50.

193. Hutchinson PJ, Kolias AG, Timofeev I, Al. E. Trial of decompressive craniectomy for traumatic intracranial hypertension. *N Engl J Med*. 2016;375(12):1119–30.

194. Vik A, Nag T, Fredriksli OA, Skandsen T, Moen KG, Schirmer-Mikalsen K, et al. Relationship of "dose" of intracranial hypertension to outcome in severe traumatic brain injury. *J Neurosurg*. 2008 Oct 1;109(4):678-84.

195. Lu CW, Czosnyka M, Shieh JS, Smielewska A, Pickard JD, Smielewski P. Complexity of intracranial pressure correlates with outcome after traumatic brain injury. *Brain*. 2012 Jun 25;135(8):2399-408.

196. Eide PK, Sorteberg W. An intracranial pressure-derived index monitored simultaneously from two separate sensors in patients with cerebral bleeds: Comparison of findings. *Biomed Eng Online*. 2013 Dec;12(1):14.

197. Hall A, O'Kane R. The best marker for guiding the clinical management of patients with raised intracranial pressure—the RAP index or the mean pulse amplitude? *Acta Neurochir (Wien)*. 2016 Oct 1;58(10):1997-2009.

198. Lafrenaye AD, Krahe TE, Povlishock JT. Moderately elevated intracranial pressure after diffuse traumatic brain injury is associated with exacerbated neuronal pathology and behavioral morbidity in the rat. *J Cereb Blood Flow Metab*. 2014 Oct;34(10):1628-36.

199. Le Roux P, Menon DK, Citerio G, Vespa P, Bader MK, Brophy GM, et al. Consensus Summary Statement of the International Multidisciplinary Consensus Conference on Multimodality Monitoring in Neurocritical Care. *Neurocrit Care*. 2014 Dec 1;21(2):1-26.

200. Cardim D, Robba C, Bohdanowicz M, Donnelly J, Cabella B, Liu X, et al. Non-invasive Monitoring of Intracranial Pressure Using Transcranial Doppler Ultrasonography: Is It Possible? *Neurocrit Care*. 2016 Dec 1;25(3):473-91.

201. Czosnyka M, Guazzo E, Iyer V, Kirkpatrick P, Smielewski P, Whitehouse H, et al. Testing of Cerebral Autoregulation in Head Injury by Waveform Analysis of Blood Flow Velocity and Cerebral Perfusion Pressure. *In: Brain Edema IX*. 1994 (pp.468-471). Springer, Vienna.

202. Czosnyka M, Richards H, Kirkpatrick P, Pickard J. Assessment of cerebral autoregulation with ultrasound and laser doppler wave forms--an experimental study in anesthetized rabbits. *Neurosurgery*. 1994 Aug 1;35(2):287-93.

203. Ursino M, Giulioni M, Lodi CA. Relationships among cerebral perfusion pressure, autoregulation, and transcranial Doppler waveform: a modeling study. J Neurosurg. 1998 Aug 1;89(2):255-66.

204. Czosnyka M, Smielewski P, Piechnik S, Schmidt EA, Al-Rawi PG, Kirkpatrick PJ, et al. Hemodynamic characterization of intracranial pressure plateau waves in

head-injured patients. *J Neurosurg*. 1999 Jul 1;91(1):11-9.

205. Varsos G V., De Riva N, Smielewski P, Pickard JD, Brady KM, Reinhard M, et al. Critical closing pressure during intracranial pressure plateau waves. *Neurocrit Care*. 2013 Jun 1;18(3):341-8.

206. Chan K-H, Miller JD, Dearden NM, Andrews PJD, Midrlev S. The effect of changes in cerebral perfusion pressure upon middle cerebral artery blood flow velocity and jugular bulb venous oxygen saturation after severe brain injury. *J Neurosurg*. 1992;77:55–61.

207. Cardim D, Robba C, Donnelly J, Bohdanowicz M, Schmidt B, Damian M, et al. Prospective Study on Noninvasive Assessment of Intracranial Pressure in Traumatic Brain-Injured Patients: Comparison of Four Methods. *J Neurotrauma*. 2016 Apr 15;33(8):792-802.

208. Morgalla MH, Magunia H. Noninvasive measurement of intracranial pressure via the pulsatility index on transcranial doppler sonography: Is improvement possible? *J Clin Ultrasound*. 2016 Jan;44(1):40-5.

209. Bellner J, Romner B, Reinstrup P, Kristiansson KA, Ryding E, Brandt L. Transcranial Doppler sonography pulsatility index (PI) reflects intracranial pressure (ICP). *Surg Neurol*. 2004 Jul 1;62(1):45-51.

210. Richards HK, Czosnyka M, Whitehouse H, Pickard JD. Increase in transcranial Doppler pulsatility index does not indicate the lower limit of cerebral autoregulation. *Acta Neurochir Suppl* [Internet]. 1998;71:229–32. Available from: http://www.ncbi.nlm.nih.gov/entrez/query.fcgi?cmd=Retrieve&db=PubMed&dopt=Citation&list_uids=9779192

211. Marmarou A, Shulman K, Rosende RM. A nonlinear analysis of the cerebrospinal fluid system and intracranial pressure dynamics. *J Neurosurg*. 1978 Mar 1;48(3):332-44.

212. Kim D-J, Kasprowicz M, Carrera E, Castellani G, Zweifel C, Lavinio A, et al. The monitoring of relative changes in compartmental compliances of brain. *Physiol Meas* [Internet]. 2009 Jul 1;30(7):647–59. Available from:

http://stacks.iop.org/0967-3334/30/i=7/a=009?key=crossref.45578e96dd7681da9736200db5e96400

213. Varsos G V., Richards H, Kasprowicz M, Budohoski KP, Brady KM, Reinhard M, et al. Critical closing pressure determined with a model of cerebrovascular impedance. *J Cereb Blood Flow Metab*. 2013;33(2):235–43.

214. Ambarki K, Baledent O, Kongolo G, Bouzerar R, Fall S, Meyer ME. A new lumped-parameter model of cerebrospinal hydrodynamics during the cardiac cycle in healthy volunteers. *IEEE Trans Biomed Eng*. 2007;54(3):483–91.

215. Panerai RB, Salinet ASM, Brodie FG, Robinson TG. The influence of calculation method on estimates of cerebral critical closing pressure. *Physiol Meas* [Internet]. 2011 Apr 1;32(4):467–82. Available from: http://stacks.iop.org/0967-3334/32/i=4/a=007?key=crossref.e5a09afc7939209a064aae0f2debd176

216. Uryga A, Kasprowicz M, Calviello L, Diehl RR, Kaczmarska K, Czosnyka M. Assessment of cerebral hemodynamic parameters using pulsatile versus non-pulsatile cerebral blood outflow models. *J Clin Monit Comput.* 2019 Feb 15;33(1):85-94.

217. Avezaat CJJ, Van Eijndhoven JHM. The role of the pulsatile pressure variations in intracranial pressure monitoring. *Neurosurg Rev*. 1986;9:113–20.

218. Steiner LA, Balestreri M, Johnston AJ, Czosnyka M, Coles JP, Chatfield DA, et al. Sustained moderate reductions in arterial CO2 after brain trauma Time-course of cerebral blood flow velocity and intracranial pressure. *Intensive Care Med* [Internet]. 2004 Dec 12;30(12):2180–7. Available from: http://link.springer.com/10.1007/s00134-004-2463-6

219. Helmy A, Vizcaychipi M, Gupta AK. Traumatic brain injury: Intensive care management. Vol. 99, *British Journal of Anaesthesia*. 2007. p. 32–42.

220. Carrera E, Kim D-J, Castellani G, Zweifel C, Czosnyka Z, Kasprowicz M, et al. What Shapes Pulse Amplitude of Intracranial Pressure? *J Neurotrauma* [Internet]. 2010 Feb;27(2):317–24. http://www.liebertonline.com/doi/abs/10.1089/neu.2009.0951

221. Avezaat C, Eijndhoven J Van. Cerebrospinal fluid pulse pressure and craniospinal dynamics: a theoretical, clinical and experimental study [Internet]. Vol. 5, *Resuscitation*. 1984. 111–26 p. Available from: http://www.ncbi.nlm.nih.gov/pubmed/1028117%5Cnhttp://repub.eur.nl/pub/38457

222. Risberg J, Lundberg N, Ingvar DH. Regional Cerebral Blood Volume During Acute Transient Rises of the Intracranial Pressure (Plateau Waves)*. 1969;31.

223. Grubb RL, Raichle ME, Eichling JO, And MM, Ter-Pogossian J. The Effects of Changes in $Paco_2$ on Cerebral Blood Volume, Blood Flow, and Vascular Mean Transit Time. 1974 Sep;5(5):630-9.

224. Ito H, Kanno I, Ibaraki M, Hatazawa J, Miura S. Changes in Human Cerebral Blood Flow and Cerebral Blood Volume during Hypercapnia and Hypocapnia Measured by Positron Emission Tomography. *J Cereb Blood Flow Metab* [Internet]. 2003 Jun;23(6):665–70. Available from: http://journals.sagepub.com/doi/10.1097/01.WCB.0000067721.64998.F5

225. Haubrich C, Steiner LA, Diehl RR, Kasprowicz M, Smielewski P, Pickard JD, et al. Doppler flow velocity and intra-cranial pressure: Responses to short-term mild hypocapnia help to assess the pressure-volume relationship after head injury. *Ultrasound Med Biol*. 2013 Sep 1;39(9):1521-6.

226. Roberts BW, Karagiannis P, Coletta M, Kilgannon JH, Chansky ME, Trzeciak S. Effects of PaCO2 derangements on clinical outcomes after cerebral injury: A systematic review. *Resuscitation*. 2015;91:32–41.

227. Meng L, Gelb AW, Alexander BS, Cerussi AE, Tromberg BJ, Yu Z, et al. Impact of phenylephrine administration on cerebral tissue oxygen saturation and blood volume is modulated by carbon dioxide in anaesthetized patients. *Br J Anaesth*. 2012 Mar 4;108(5):815-22.

228. Sookplung P, Siriussawakul A, Malakouti A, Sharma D, Wang J, Souter MJ, et al. Vasopressor use and effect on blood pressure after severe adult traumatic brain injury. *Neurocrit Care*. 2011 Aug 1;15(1):46-54.

229. Panerai RB, Deverson ST, Mahony P, Hayes P, Evans DH. Effects of CO2 on dynamic cerebral autoregulation measurement. *Physiol Meas*. 1999;20(3):265–75.

230. Kasprowicz M, Czosnyka M, Soehle M, Smielewski P, Kirkpatrick PJ, Pickard JD, et al. Vasospasm shortens cerebral arterial time constant. *Neurocrit Care*. 2012 Apr 1;16(2):213-8.

231. Brothers RM, Zhang R. CrossTalk opposing view: The middle cerebral artery diameter does not change during alterations in arterial blood gases and blood pressure. Vol. 594, *Journal of Physiology*. 2016. p. 4077–9.

232. Hoiland RL, Ainslie PN. CrossTalk proposal: The middle cerebral artery diameter does change during alterations in arterial blood gases and blood pressure. Vol. 594, *Journal of Physiology*. 2016. p. 4073–5.

233. Aries MJH, Czosnyka M, Budohoski KP, Steiner LA, Lavinio A, Kolias AG, et al. Continuous determination of optimal cerebral perfusion pressure in traumatic brain injury*. *Crit Care Med* [Internet]. 2012 Aug;40(8):2456–63. Available from: https://insights.ovid.com/crossref?an=00003246-201208000-00025

234. Kasprowicz M, Diedler J, Reinhard M, Carrera E, Smielewski P, Budohoski KP, et al. Time constant of the cerebral arterial bed. *In: Acta Neurochirurgica, Supplementum*. 2012. p. 17–21.

235. Horikoshi T, Akiyama I, Yamagata Z, Sugita M, Nukui H. Magnetic resonance angiographic evidence of sex-linked variations in the circle of willis and the occurrence of cerebral aneurysms. *J Neurosurg*. 2002;96(4):697–703.

236. Ito H, Ibaraki M, Kanno I, Fukuda H, Miura S. Changes in the arterial fraction of human cerebral blood volume during hypercapnia and hypocapnia measured by positron emission tomography. *J Cereb Blood Flow Metab* [Internet]. 2005;25(7):852–7. Available from: http://www.ncbi.nlm.nih.gov/entrez/query.fcgi?cmd=Retrieve&db=PubMed&dopt=Citation&list_uids=15716851

237. Steiner LA, Coles JP, Johnston AJ, Chatfield DA, Smielewski P, Fryer TD, et al. Assessment of cerebrovascular autoregulation in head-injured patients: A

validation study. *Stroke*. 2003 Oct 1;34(10):2404-9.

238. Czosnyka M, Smielewski P, Kirkpatrick P, Laing RJ, Menon D, Pickard JD. Continuous assessment of the cerebral vasomotor reactivity in head injury. *Neurosurgery*. 1997 Jul 1;41(1):11-9.

239. Zeiler FA, Donnelly J, Calviello L, Smielewski P, Menon DK, Czosnyka M. Pressure Autoregulation Measurement Techniques in Adult Traumatic Brain Injury, Part II: A Scoping Review of Continuous Methods. *J Neurotrauma*. 2017 Dec 1;34(23):3224-37.

240. Zeiler FA, Lee JK, Smielewski P, Czosnyka M, Brady K. Validation of intracranial pressure-derived cerebrovascular reactivity indices against the lower limit of autoregulation, Part II: Experimental model of arterial hypotension. *J Neurotrauma*. 2018 Nov 12;35(23):2812-9.

241. Dias C, Pereira E, Cerejo A, Paiva J, Czosnyka M. Prx-a tool to evaluate autoregulation and decide the optimal CPP management at bedside in a neurocritical care unit. *Cerebrovasc Dis* [Internet]. 2013;35:20. Available from: http://www.embase.com/search/results?subaction=viewrecord&from=export&id=L71159862%5Cnhttp://dx.doi.org/10.1159/000351748%5Cnhttp://sfx.library.uu.nl/utrecht?sid=EMBASE&issn=10159770&id=doi:10.1159%2F000351748&atitle=Prx-a+tool+to+evaluate+autoregulation+

242. Aries MJH, Czosnyka M, Budohoski KP, Steiner LA, Lavinio A, Kolias AG, et al. Continuous determination of optimal cerebral perfusion pressure in traumatic brain injury. *Crit Care Med*. 2012 Aug 1;40(8):2456-63.

243. Zeiler FA, Cardim D, Donnelly J, Menon DK, Czosnyka M, Smielewski P. Transcranial Doppler Systolic Flow Index and ICP-Derived Cerebrovascular Reactivity Indices in Traumatic Brain Injury. *J Neurotrauma*. 2018 Jan 15;35(2):314-22.

244. Eide PK, Czosnyka M, Sorteberg W, Pickard JD, Smielewski P. Association between intracranial, arterial pulse pressure amplitudes and cerebral autoregulation in head injury patients. *Neurol Res* [Internet]. 2007 Sep

19;29(6):578–82. http://www.tandfonline.com/doi/full/10.1179/016164107X172167

245. Zeiler FA, Donnelly J, Calviello L, Menon DK, Smielewski P, Czosnyka M. Pressure Autoregulation Measurement Techniques in Adult Traumatic Brain Injury, Part I: A Scoping Review of Intermittent/Semi-Intermittent Methods. *J Neurotrauma* [Internet]. 2017 Dec;34(23):3207–23. Available from: http://www.liebertpub.com/doi/10.1089/neu.2017.5085

246. Hoesch RE, Koenig MA, Geocadin RG. Coma After Global Ischemic Brain Injury: Pathophysiology and Emerging Therapies. *Critical Care Clinics*. 2008 Jan 1;24(1):25-44.

247. Bolton CF, Bryan GY, Zochodne DW. The neurological complications of sepsis. *Annals of Neurology*. 1993 Jan;33(1):94-100.

248. Sandroni C, Geocadin RG. Neurological prognostication after cardiac arrest. *Current Opinion in Critical Care*. 2015 Jun;21(3):209.

249. Khot S, Tirschwell DL. Long-term neurological complications after hypoxic-ischemic encephalopathy. *In: Seminars in Neurology*. 2006 Sep (Vol. 26, No. 04, pp. 422-431). Copyright© 2006 by Thieme Medical Publishers, Inc., 333 Seventh Avenue, New York, NY 10001, USA..

250. Cardim D, Griesdale DE, Ainslie PN, Robba C, Calviello L, Czosnyka M, et al. A comparison of non-invasive versus invasive measures of intracranial pressure in hypoxic ischaemic brain injury after cardiac arrest. *Resuscitation*. 2019 Apr 1;137:221-8.

251. Robba C, Goffi A, Geeraerts T, Cardim D, Via G, Czosnyka M, et al. Brain ultrasonography: methodology, basic and advanced principles and clinical applications. A narrative review. *Intensive Care Medicine*. 2019 Apr;25:1-5.

252. Cardim D, Robba C, Matta B, Tytherleigh-Strong G, Kang N, Schmidt B, et al. Cerebrovascular assessment of patients undergoing shoulder surgery in beach chair position using a multiparameter transcranial Doppler approach. *Journal of Clinical Monitoring and Computing*. 2018 Aug 15;33(4):615-25.

253. Cardim D, Robba C, Schmidt E, Schmidt B, Donnelly J, Klinck J, et al. Transcranial Doppler Non-invasive Assessment of Intracranial Pressure, Autoregulation of Cerebral Blood Flow and Critical Closing Pressure during Orthotopic Liver Transplant. *Ultrasound Med Biol.* 2019 Jun 1;45(6):1435-45.

254. Nasr N, Gaio R, Czosnyka M, Budohoski K, Liu X, Donnelly J, et al. Baroreflex Impairment after Subarachnoid Hemorrhage Is Associated with Unfavorable Outcome. *Stroke*. 2018 Jul;49(7):1632-8.

255. Tymko MM, Donnelly J, Smielewski P, Zeiler FA, Sykora M, Haubrich C, et al. Changes in cardiac autonomic activity during intracranial pressure plateau waves in patients with traumatic brain injury. *Clin Auton Res*. 2019 Feb 11;29(1):123-6.

256. Schmidt B, Czosnyka M, Raabe A, Yahya H, Schwarze JJ, Sackerer D, et al. Adaptive noninvasive assessment of intracranial pressure and cerebral autoregulation. *Stroke*. 2003 Jan 1;34(1):84-9.

257. Smielewski P, Donnelly J, Zeiler FA, Menon DK, Czosnyka M, Cardim D. Transcranial Doppler Systolic Flow Index and ICP-Derived Cerebrovascular Reactivity Indices in Traumatic Brain Injury. *J Neurotrauma*. 2018 Jan 15;35(2):314-22.

258. Czosnyka M, Richards HK, Whitehouse HE, Pickard JD. Relationship between transcranial Doppler-determined pulsatility index and cerebrovascular resistance: an experimental study. *J Neurosurg*. 1996 Jan 1;84(1):79-84.

259. Zweifel C, Czosnyka M, Carrera E, De Riva N, Pickard JD, Smielewski P. Reliability of the blood flow velocity pulsatility index for assessment of intracranial and cerebral perfusion pressures in head-injured patients. *Neurosurgery*. 2012 Jul 11;71(4):853-61.

260. Wright WL. Multimodal monitoring in the ICU: When could it be useful? *J Neurol Sci* [Internet]. 2007 Oct;261(1–2):10–5. Available from: https://linkinghub.elsevier.com/retrieve/pii/S0022510X0700295X

261. De Georgia MA, Deogaonkar A. Multimodal monitoring in the neurological intensive care unit. *Neurologist*. 2005 Jan 1;11(1):45-54.

262. Amodio P, Montagnese S. Clinical neurophysiology of hepatic encephalopathy. *Journal of Clinical and Experimental Hepatology*. 2015 Mar 1;5:S60-8.

263. Pierrakos C, Attou R, Decorte L, Kolyviras A, Malinverni S, Gottignies P, et al. Transcranial Doppler to assess sepsis-associated encephalopathy in critically ill patients. *BMC Anesthesiol.* 2014 Dec;14(1):45.

264. Budohoski KP, Reinhard M, Aries MJH, Czosnyka Z, Smielewski P, Pickard JD, et al. Monitoring cerebral autoregulation after head injury. Which component of transcranial Doppler flow velocity is optimal? *Neurocrit Care* [Internet]. 2012 Oct 21;17(2):211–8. Available from: http://link.springer.com/10.1007/s12028-011-9572-1

265. Carrera E, A Steiner L, Brady K, Zweifel C, Castellani G, Hiler M, et al. Integration of Brain Signals in Multimodal Bedside Monitoring After Traumatic Brain Injury. *Open Neurosurg J*. 2010; 2:3.

266. Rafi S, Tadie J marc, Gacouin A, Leurent G, Bedossa M, Le Tulzo Y, et al. Doppler sonography of cerebral blood flow for early prognostication after out-of-hospital cardiac arrest: DOTAC study. *Resuscitation* [Internet]. 2019;1–7. Available from: https://doi.org/10.1016/j.resuscitation.2019.05.024

267. Zeiler FA, Smielewski P. Application of robotic TCD in critically ill TBI patients: first experiences. *J Neurotrauma*. 2018 Aug 1; 35(16): A59.